

Strong disorder RG approach of random systems

Ferenc Iglói

Research Institute for Solid State Physics,
H-1525 Budapest, P.O.Box 49, Hungary
Institute for Theoretical Physics,
Szeged University H-6720 Szeged, Hungary

Cécile Monthus

Service de Physique Théorique,
Unité de recherche associée au CNRS,
DSM/CEA Saclay, 91191 Gif-sur-Yvette, France

November 27, 2019

Abstract

There is a large variety of quantum and classical systems in which the quenched disorder plays a dominant rôle over quantum, thermal, or stochastic fluctuations : these systems display strong spatial heterogeneities, and many averaged observables are actually governed by rare regions. A unifying approach to treat the dynamical and/or static singularities of these systems has emerged recently, following the pioneering RG idea by Ma and Dasgupta and the detailed analysis by Fisher who showed that the Ma-Dasgupta RG rules yield asymptotic exact results if the broadness of the disorder grows indefinitely at large scales. Here we report these new developments by starting with an introduction of the main ingredients of the strong disorder RG method. We describe the basic properties of infinite disorder fixed points, which are realized at critical points, and of strong disorder fixed points, which control the singular behaviors in the Griffiths-phases. We then review in detail applications of the RG method to various disordered models, either (i) quantum models, such as random spin chains, ladders and higher dimensional spin systems, or (ii) classical models, such as diffusion in a random potential, equilibrium at low temperature and coarsening dynamics of classical random spin chains, trap models, delocalization transition of a random polymer from an interface, driven lattice gases and reaction diffusion models in the presence of quenched disorder. For several one-dimensional systems, the Ma-Dasgupta RG rules yields very detailed analytical results, whereas for other, mainly higher dimensional problems, the RG rules have to be implemented numerically. If available, the strong disorder RG results are compared with another, exact or numerical calculations.

Contents

Organization of the review	7
I BASIC IDEAS OF STRONG DISORDER RG	8
1 Motivations for disorder-dependent RG procedures	8
2 Principles of strong disorder RG	12
2.1 The essential idea : Dominance of the disorder over thermal or quantum fluctuations	12
2.2 Notions of Infinite and Strong disorder fixed points	14
2.3 How to know if the disorder dominates at large scale?	15
2.4 Essential features of infinite disorder fixed points	15
3 General features of Ma-Dasgupta RG rules	16
3.1 What is a strong disorder RG rule ?	17
3.2 Iteration and convergence towards a fixed point	19
3.3 The basic Infinite Disorder Fixed Point (Critical point)	19
3.4 The basic Strong Disorder Fixed Point (Griffiths phases)	20
3.5 Auxiliary variables and critical exponents	21
II RG STUDY OF QUANTUM MODELS	22
4 Random Transverse Field Ising Chain	22
4.1 Model	22
4.1.1 Free-fermion representation	23
4.1.2 Surface magnetization, phase diagram and critical exponents	23
4.1.3 Low-energy excitations and dynamics	24
4.2 RG rules	26
4.3 RG flow	27
4.3.1 Renormalization of the distribution functions	27
4.3.2 Fixed-point solution	28
4.3.3 Asymptotic exactness of the results	29
4.3.4 Relation between energy- and length-scale	30
4.4 RG detailed results	30
4.4.1 Renormalization of lengths and magnetic moments	30
4.4.2 Scaling of thermodynamic quantities	33
4.4.3 Renormalization of dynamical correlations	35
4.5 Finite-size systems : RG results and numerical studies	37
4.5.1 RG results for finite-size scaling properties	37
4.5.2 Ensemble dependence of the results	38
4.5.3 Numerical studies based on free-fermions	39
4.6 Relation with Dirac-type equations with random mass	39

5	Random quantum chains with discrete symmetry	39
5.1	Quantum Potts and clock models	39
5.2	Ashkin-Teller model	40
5.3	Decimation equations	40
5.4	Disorder induced cross-over effects	41
6	Random $S = 1/2$ AF Heisenberg chains	45
6.1	Models	45
6.2	RG rules	46
6.3	RG detailed results	47
6.3.1	Renormalization of the random XX chain	47
6.3.2	Renormalization of the random XXX chain	49
6.3.3	Properties of the random-singlet phase	49
6.3.4	Properties of the random dimer phase	51
6.3.5	Renormalization of dynamical correlations	51
7	Random $S = 1$ AF Heisenberg chain	53
7.1	The antiferromagnetic chain $S = 1$ without disorder	53
7.2	Construction of appropriate RG rules	54
7.3	Numerical study of the RG procedure	56
7.4	Exact critical exponents via a soluble effective model	61
7.5	Direct numerical studies	63
7.6	Generalizations : dimerization, dynamics	64
8	Other 1D quantum models	64
8.1	Higher spin AF Heisenberg chains	65
8.2	Heisenberg chain with random ferro- and antiferromagnetic couplings	67
8.3	Disordered spin ladders	69
8.4	Other investigations in 1d	74
9	Quantum models in $d > 1$ dimensions	75
9.1	Random transverse-field Ising model in 2d	75
9.1.1	Scaling at the critical point	76
9.1.2	Disordered phase	77
9.1.3	Ordered phase	78
9.2	Random Heisenberg models	79
9.2.1	Numerical RG results	79
9.2.2	Related numerical studies	80
9.3	Other problems	81
10	Variations : Correlations, disorder Broadness, etc...	81
10.1	Correlated disorder	82
10.2	Broad disorder distribution	83
10.3	Inhomogeneous disorder	83
10.4	Aperiodic systems	84

III	RG STUDY OF CLASSICAL MODELS	86
11	Sinai walk : Random walk in Brownian potential	86
11.1	Model	86
11.1.1	Drift velocity and dynamics	87
11.1.2	Persistence and order	87
11.2	RG rules for the Sinai model : Physical motivations	88
11.3	Notions of effective dynamics and localization	90
11.4	Properties of the effective dynamics	91
11.4.1	Diffusion front	91
11.4.2	Energy distribution	93
11.4.3	Aging properties	93
11.4.4	Statistics of returns to the origin	93
11.5	Localization properties	94
11.5.1	Distribution of the thermal packet	94
11.5.2	Localization parameters	95
11.5.3	Comparison with equilibrium in a Brownian potential	95
11.5.4	Thermal width and rare events	95
11.6	Relations with the general theory of slow dynamics and metastable states	96
11.6.1	Metastable States	96
11.6.2	Decomposition of the diffusion front over metastable states	97
11.7	Eigenfunctions of the Fokker-Planck operator	97
11.7.1	Fokker-Planck eigenfunctions associated to the effective dynamics	97
11.7.2	Spatial Structure of eigenfunctions: 2 peaks and 3 length scales	98
12	Biased Sinai walk and associated directed trap model	99
12.1	Models	99
12.1.1	Biased Sinai walk	99
12.1.2	Directed trap model	100
12.2	Principle of the generalized RG	102
12.3	Results for the associated directed trap model	103
12.4	Quantitative mapping between the biased Sinai model and the directed trap model	103
12.5	Results for the biased Sinai model	104
13	Symmetric Trap model	106
13.1	Model	106
13.2	Principle of the RG procedure	106
13.3	Results for the symmetric trap model	108
13.4	Linear and non-linear responses to an external field	110

14 Classical Spin chains : Equilibrium and Coarsening dynamics	112
14.1 Models : Random-field Ising chain and spin-glass chain in external field	113
14.2 RG construction of the ground state	114
14.3 Low temperature properties from two-level excitations	115
14.4 Coarsening Dynamics	118
15 Localization of a random polymer at an interface	120
15.1 Model	120
15.2 Symmetric case	121
15.2.1 Imry-Ma argument based on typical events	121
15.2.2 Comparison between two strategies	121
15.3 Asymmetric case	122
15.3.1 Imry-Ma argument based on rare events	122
15.3.2 The disorder-dependent strategy based on real space RG	123
15.3.3 Results of the strong disorder RG	124
16 Asymmetric simple exclusion process with disorder	125
16.1 ASEP with particle-wise disorder	126
16.1.1 RG rules	127
16.1.2 Relation with the random XX -chain	128
16.2 ASEP with site-wise disorder	130
17 Reaction-diffusion models with disorder	130
17.1 Phase transition into an absorbing state	130
17.2 Random contact process	131
17.2.1 RG rules	132
17.2.2 Analysis of the RG equations	133
17.2.3 Numerical results and scaling in the weak disorder regime	135
17.3 Other types of reaction-diffusion models with quenched disorder	136
18 Classical models in $d \geq 2$	136
18.1 Random contact process in 2d	136
18.2 Classical systems with layered randomness	137
18.2.1 The McCoy-Wu model and the RTFIC	138
18.2.2 Percolation in a random environment	138
18.3 Random-bond Potts model in the large- q limit	140
18.3.1 Numerical study in three-dimensions	142
19 Summary and perspectives	143
Acknowledgements	145
APPENDICES	146

A	Scaling in random systems	146
A.1	General notions	146
A.2	Conventional random critical scaling	148
A.3	Infinite disorder scaling	150
A.4	Scaling in the Griffiths phases	152
A.4.1	Disordered Griffiths phase	152
A.4.2	Ordered Griffiths phase	153
A.5	Scaling in the large spin phase	154
B	Mapping between different models	154
B.1	The random RW and the RTFIC	155
B.2	The random XY chain and the RTFIC	156
C	Kesten random variables : exact results versus strong disorder	
	RG	156
C.1	Discrete Kesten random variables	156
C.2	Continuous version of Kesten random variables	157
C.3	Meaning of the strong disorder RG	158
D	Extrema of 1D random potentials via RG	159
D.1	RG for Markovian potentials	159
D.2	Results for the Brownian potential with quadratic confinement .	160
D.2.1	Definition and properties of the model	160
D.2.2	Results on the statistics of the minima	161
D.2.3	Results on the statistics of the largest barrier	162
E	Comparison with some growth models without disorder	163
	REFERENCES	165

Organization of the review

This work aims to review the recent developments obtained via strong disorder renormalization group methods in the theory of disordered systems. The strong disorder RG method, which has been introduced by Ma and Dasgupta in 1979, has become a very efficient method with a clear physical status only much later with the works of Daniel Fisher, who showed that the RG method becomes asymptotically exact if the distribution of disorder broadens without limits at large scales, and who computed several exact critical exponents and scaling functions in random quantum spin chains. Following Fisher's results, intensive research started, first in random quantum models and then in classical disordered systems. In all concerned fields the asymptotically exact strong disorder RG results have provided new insights into the physical mechanisms and helped to interpret the existing numerical findings. It is likely that the strong disorder RG methods will give new impulses in the future to the numerical and theoretical research of disordered systems.

Early developments of the strong disorder RG method for random quantum spin chains have been summarized in a conference proceedings [143] and briefly described in [54, 183]. However, a comprehensive review with applications of different fields of research is still lacking and we aim to fill this gap by this work.

The review is organized into three parts :

(i) **The first part is a general introduction to the essential concepts of the strong disorder RG method :**

In sections 1 and 2, we explain the interest of defining disorder-dependent real space RG procedures, and why strong disorder RG rules are an ideal tool to study systems in which disorder dominates at large scales over quantum, thermal, or stochastic fluctuations.

Then in section 3, we present the simplest specific examples of strong disorder RG rules, the associated Infinite and Strong disorder fixed points, and how exact non-trivial critical exponents emerge in this framework. This section 3 being somewhat more technical, it can be skip at the first reading, although it is essential to understand the meaning and the properties of strong disorder RG flows.

(ii) **The second part is devoted to the detailed study of various quantum models**

(ii) **The third part is devoted to the detailed study of various classical models**

The sections of Parts II and III devoted to specific models have been written to be as independent as possible. As a consequence, after the general introduction contained in Part I, the reader interested in a specific model may jump directly to the corresponding section. For readers who wish to learn strong disorder RG methods in details in order to be able to use them, we recommend to read the first sections of each part, devoted respectively to the random transverse-field Ising chain in Sec.4 and to the Sinai walk in Sec.11, because these two sections are the more detailed ones.

(iv) **The Appendices** contain more technical aspects or more specialized

discussions. In particular, Appendix A deals with the scaling concept in disorder systems, making a comprehensive presentation of scaling at different types of singular points (conventional random fixed point, infinite disorder fixed point, Griffiths singularities, large spin fixed point). The various types of scaling are especially important to find the appropriate scaling analysis of numerical data.

(iv) **The References**

Before the references to original articles, we have added a short list of books and reviews that give a more general background on topics or models that we discuss only from the point of view of strong disorder RG.

Part I

BASIC IDEAS OF STRONG DISORDER RG

1 Motivations for disorder-dependent RG procedures

Various descriptions of disordered systems

The presence of disorder in a system can give rise to completely new phenomena, like for instance the Anderson localization[32] in condensed matter physics, or the aging behaviors in statistical physics[12, 13]. The study of disordered systems has thus generated various specific approaches since fifty years, for reviews see[6, 7, 8, 9, 10, 11]. The first example is the Dyson-Schmidt method [129, 322], based on the notion of invariant measure : it yields exact results for the one dimensional systems that can be described by infinite products of random transfer matrices [8, 9]. To understand the interest and the specificity of strong disorder renormalizations, which constitute the subject of this review, it is convenient to classify the various ways of dealing with disordered the systems into two main categories:

- there are on one hand **approaches which start by averaging over the disorder**, because their aim is to compute self-averaging observables, such as for instance the free energy if one is interested into the thermodynamics. There exist a certain number of specific prescriptions to carry out this average over the disorder, such as the replica method [7], the supersymmetric method [130], and the dynamical method [62] (for a parallel presentation of the three methods, see [226]). After this average on the disorder, there are no more spatial heterogeneities, but the homogeneous system that has to be studied contains in counterpart new effective interactions.

- there are on the other hand **approaches which try to describe spatial heterogeneities of the disorder**, like certain famous arguments and various real-space renormalizations : we will now discuss both in some more details,

since these approaches belong to the same ‘family’ of the strong disorder RG.

From scaling arguments on disorder fluctuations...

Among the arguments which have played a great role in the understanding of disordered systems, one may quote

(a) **the Lifshitz argument** [236, 237], which allows to predict the essential singularities of the density of states near spectrum edges. The idea consists in identifying the disorder configurations that support states in this energy region, and in estimating the probabilities of these favorable configurations.

(b) **the Griffiths phases**, in which rare ordered regions induce essential singularities for the statics [158] as well as very slow relaxation behaviors for the dynamics [306, 69].

(c) **the Harris criterion** [165] on the relevance of weak disorder around a pure critical point. It consists in estimating the fluctuations of the critical temperature induced by the disorder spatial fluctuations.

(d) **the theorem of Chayes *et al.*** [96], which shows that the space fluctuations of the disorder imply the bound $\nu \geq 2/d$ for the critical exponent ν for disordered systems in dimension d .

(e) **the Imry-Ma argument** [200], which allows to predict the presence of domain walls at zero temperature in random field systems, by balancing the local energy fluctuations from the random fields with the energy cost of domain walls.

(f) **the theorem by Aizenman and Wehr** [28] about the rounding of first-order phase transitions by quenched disorder. In $2d$, arbitrarily weak (continuous) disorder softens the phase transition to second order.

In fact, these various arguments only involve two different statistical properties. Indeed, the arguments (a) and (b), which are very close [285, 8], are both based on the notion of rare events: in any infinite configuration of disorder, there exist arbitrarily large ordered domains with exponentially small probabilities. On the other hand, the arguments (c), (d), (e) and (f) all refer to the average or typical behavior in \sqrt{N} for the sum of a large number N of (independent) random variables.

These simple probabilistic arguments are well founded and almost “irrefutable”. To the best of our knowledge, the only argument which has given rise to a controversy [201] is the Imry-Ma argument which was in disagreement with the “dimensional reduction” predicted by the field theory approaches, either at all the orders in perturbation theory [26, 348] or in the supersymmetric formalism [298]. The rigorous studies [199, 72] finally gave reason to... the Imry-Ma argument! This example shows that the simple heuristic arguments may have some non-trivial physical content, which is not always easy to obtain by more sophisticated methods.

In conclusion, these probabilistic arguments allow to understand clearly the physics, because they identify the local fluctuations of the disorder which are responsible for such or such phenomenon. On the other hand, it is often difficult to go beyond the qualitative ideas to do more precise computations! To make

some progress while remaining in the same spirit, the most natural idea is of course to consider real space renormalizations.

... to real space renormalizations on the disorder

The choice to work in real space to define a renormalization procedure, which already presents a great interest in pure systems [283, 78], becomes the unique choice in the presence of disorder if one wishes to describe space heterogeneities.

Block Renormalizations The block renormalizations, based on decimation or on Migdal-Kadanoff ideas seem the most frequent procedures for disordered systems. The Migdal-Kadanoff procedures [260, 211] indeed constitute simple approximations to carry out block renormalizations on regular lattices. They also represent exact renormalizations on certain hierarchical lattices [216]. Among the various systems that have been studied in this way, one may quote for instance the Potts model [221], the diluted ferromagnet [204], and especially spin glasses, which gave rise to a large number of works : their aim was either to determine phase diagrams [361, 66, 65], or to study various properties of the spin-glass phase [339, 274, 321], especially the chaotic character [68] of the RG flow trajectories [253, 41, 287, 339] which is a great novelty with respect to pure systems. Also random-field systems are studied by this type of renormalization group method [282].

In addition, various disordered systems have been studied via renormalization procedures on hierarchical networks, in particular the Potts model [119], directed polymers in random media [120, 100, 111], or wetting on disordered substrates [122, 337].

Let us also mention the block renormalization for the trap model [247], for random quantum spin chains [175] and for the random contact process [176]. In this renormalization approach, the lattice, and thus the disorder, is treated in a homogeneous fashion and characterized by a Gaussian distribution the variance of which is renormalized during the transformation. For strongly disordered system, which are spatially heterogeneous the block RG yields only a rather approximative picture of the critical behavior.

Functional Renormalization for interfaces in random media For models of interfaces in random media, there exist a field theoretical functional RG method [136] which studies the flow of the disorder correlator. We refer to the review [354] for the description of the various recent developments, and to the references [40, 234] for comparisons with the replica method.

Renormalization for disordered XY models The introduction of disorder in two-dimensional XY models, in which there exist Kosterlitz-Thouless transitions in the pure case, leads to a Coulomb gas RG describing the flow for the probability distribution for fugacities [88] to take into account the influence of spatial heterogeneities on the topological defects. This approach has also been

used to study the glass transition of a particle in a random potential presenting logarithmic correlations [89], a problem that has otherwise been studied by various methods [93, 223, 90].

Phenomenological RG for spin glasses The “droplet theory” [137] for spin glasses in finite dimensions, originates from a phenomenological renormalization introduced by Mc Millan [251] and developed by Bray and Moore [67]. In the formulation of Bray and Moore [67], the essential idea is that the probability distribution $P_L(J)$ of the effective couplings J at scale L converges towards a fixed form, with a width $J(L) = JL^y$ which depends on the scale L . The exponent y and the limiting distribution, which are calculable exactly in $d = 1$, have been studied numerically in $d = 2$ ($y < 0$) and in $d = 3$ ($y > 0$ strong coupling) [67]. This idea of a strong coupling fixed point (or zero temperature fixed point), described by a scaling form for the probability distribution of a disorder variable, corresponds in fact exactly to the description of strong disorder renormalizations, whenever they can be applied.

Ma-Dasgupta Renormalization for quantum spin chains The renormalization procedure introduced by Ma-Dasgupta-Hu in 1979 [248] to study the quantum spin chain $S = 1/2$ with random antiferromagnetic couplings has for essential property to renormalize space in an inhomogeneous way in order to adapt better to the local disorder fluctuations. Indeed, usual RG methods treat space in a homogeneous way, by replacing for instance each block of spins of a given size by one super-spin. If this homogeneous character is natural for pure systems, one may however question its legitimacy in the presence of disorder which breaks the translation invariance. Ma, Dasgupta and Hu have thus defined a renormalization procedure based on the energy, and not on the size of a spatial cell. The procedure consists in eliminating in an iterative way the degrees of freedom of higher energy, to obtain in the end an effective theory at low energy : this low energy effective theory for the spin chain is nowadays called “the random singlet phase”.

This renormalization procedure has actually remained not well known and not well understood during many years... until the works of Daniel Fisher in 1994-1995 [138, 139] which gave to this method :

(i) a well defined theoretical status, via the notion of “infinite disorder fixed points”

Whereas the method was first considered as an approximate procedure without control, Daniel Fisher showed that the renormalization flow takes a scaling form which converge towards an “infinite disorder fixed point” (this means that the disorder increases indefinitely at large scale), which made the method asymptotically exact [138, 139]. In addition, the application of the method to Random Transverse Field Ising Chain allowed him to explicitly show the exactness of the obtained results via a direct comparison with some observables that had been rigorously computed for the McCoy and Wu model [252, 329]. (This disordered McCoy-Wu model is a two-dimensional Ising model with columnar

disorder, which is equivalent to RTFIC.)

(ii) remarkable possibilities of explicit computations

For the RTFIC [138], the Ma-Dasgupta procedure allows to obtain a lot of new results with respect to the rigorous methods [252, 329, 286], in particular the exact critical exponent $\beta = (3 - \sqrt{5})/2$ for the spontaneous magnetization. More surprisingly, Daniel Fisher even computed observables that are unknown for the corresponding pure model, i.e. for the pure two-dimensional Ising model! (for instance the explicit scaling function describing the magnetization as a function of the external field in the critical region).

These works of Daniel Fisher have thus generated a great interest for these methods in the field of the quantum spins, as we will describe in the following. We will also show that the strong disorder renormalizations are in fact not limited to the quantum disordered spin systems, but are also an ideal tool to study also a large class of disordered systems in statistical physics.

2 Principles of strong disorder RG

In this section, we present the essential physical ideas common to the various strong disorder RG that have been proposed in the different physical contexts.

In all models considered in this review, the various strong disorder RG procedures are based on the same idea: at large scale, the disorder dominates with respect to the thermal or quantum fluctuations. In particular, the strong disorder renormalizations are intrinsically specific to disordered systems and cannot even be defined for the pure systems which do not present space heterogeneities.

2.1 The essential idea : Dominance of the disorder over thermal or quantum fluctuations

In some sense, the pure systems, which are controlled by the thermal or quantum fluctuations are characterized by a large “degeneracy”, since all sites are equivalent, whereas the presence of disorder breaks completely this degeneracy. To be more specific, let us discuss some examples of this idea in the various fields.

Example for the Ground state of a quantum system

In the pure antiferromagnetic quantum chain of spin $S = 1/2$, the ground state can be qualitatively seen as an appropriate linear combination of all the states that correspond to a possible way of pairing the spins two by two to form singulets.

On the contrary, in the presence of disorder, the Ma-Dasgupta renormalization procedure associates to each realization of the disorder a ground state which corresponds to only one way of pairing the spins two by two in singulets. Thus, in a fixed disordered sample, a given spin is completely correlated with only one another spin of the chain, which may be at a rather large distance, but

is almost not correlated with the other spins, even its immediate neighbors on the chain.

Example for the equilibrium of a classical spin chain

In the pure Ising ferromagnetic chain, a domain wall can be found with equal probabilities on all the bonds because they all are equivalent. The usual energy/entropy argument between the cost energy $2J$ of a domain wall and the entropy $S \sim K \ln L$ associated with the arbitrary position of the domain wall in a finite system of length L , allows to understand the absence of long range order at any finite temperature and the behavior of the typical size $L_T \sim e^{2J/T}$ of domains.

On the contrary, the presence of random fields completely destroys this equivalence between all the sites. The Imry-Ma argument [200], which replaces the previous energy/entropy argument is an energy/energy argument : the comparison between the domain wall energy cost $2J$, and the typical energy $\sqrt{\sigma L}$ which can be gained by taking advantage of a favorable fluctuation of the sum $\sum_{i=1}^L h_i$ of the random fields on a domain of size L leads to the absence of long range order even at zero temperature, with a typical domain length $L_{IM} \sim J^2/\sigma$. We will see later that the strong disorder RG allows to construct the positions of the Imry-Ma domain walls in each given sample.

Examples for random walks in random media

For random walks in random media, it is useful to introduce two different characteristic lengths

- the first important length $x(t)$ represents the typical distance traveled during time t . This scales characterizes the anomalous diffusion properties. For instance, in the following, we will encounter both logarithmic $x(t) \sim (\ln t)^2$ and algebraic $x(t) \sim t^a$ behaviors.

- the second important length $y(t) = x_1(t) - x_2(t)$ represents the distance between two independent particles diffusing in the same disordered sample from the same initial condition. In the pure case, this length scale of course coincides with the first one $y(t) \sim \sqrt{t} \sim x(t)$, but this is not the case anymore in disordered samples. The notion of localization, which is the crucial property to apply a strong disorder RG analysis, concerns the behavior of this relative distance $y(t)$: if the variable y remains finite with probability $p = 1$ in the limit of infinite time, the localization is ‘total’, and can be associated with an infinite disorder fixed point; if the variable y remains finite with probability $0 < p < 1$ in the limit of infinite time, the localization is ‘partial’, and can be associated with a finite disorder fixed point. In this review, we will encounter both cases.

For a random walk in a Brownian potential (the so called Sinai walk), there are sample-dependent areas that concentrate almost all the probability weight, and we will see later how to characterize them by a renormalization procedure. In particular, the thermal fluctuations are completely sub-dominant : the distance between two independent particles (i.e. with two independent thermal

histories) which diffuse in the same disordered sample, remains a finite random variable in the limit of infinite time : this phenomenon is known as the Golosov localization [155].

In the unidimensional trap model characterized by a broad distribution of trapping times $p(\tau >) \sim 1/\tau^{1+\mu}$ with $0 < \mu < 1$, the diffusion front in a given sample is concentrated on a finite number of important traps. Again, we will see later how to study the statistical properties of these traps via a strong disorder RG. In contrast, in the phase $\mu > 1$ where the averaged trapping time is finite, there is no localization anymore in the limit of infinite time, and the strong disorder approach loses its meaning.

2.2 Notions of Infinite and Strong disorder fixed points

If one is interested into the behavior of a disordered system at large scale, there are a priori three possibilities for the evolution of the effective disorder compared to the thermal fluctuations. Indeed, when the scale increases, this effective disorder can either become

(i) smaller and smaller without bound : the system then is controlled by a pure fixed point.

(ii) larger and larger without bound : the system is then controlled by an infinite disorder fixed point.

(iii) or it may converge towards a finite level: the system is then controlled by a finite disorder fixed point.

In certain models, any initial disorder, even very small, drives the system towards an infinite disorder fixed point (ii) at large scale : in particular, this is the case for the random antiferromagnetic quantum chain random $S = 1/2$, for the Sinai model, etc....

A finite disorder fixed point (iii) is usually characterized by a parameter which varies continuously, like the parameter μ in the trap model. The fixed point can often be considered as a strong disorder fixed point in a certain region of the parameters. For instance, in the trap model or in the Sinai model in external field, the dynamics is controlled by a strong disorder fixed point in the phase $0 < \mu < 1$ which presents a partial localization of the thermal packet: in this phase, there is a finite probability that two thermal trajectories in the same sample remain at a relative finite distance in the limit of infinite time.

In conclusion, the strong disorder renormalization methods concern:

- the infinite disorder fixed points (ii).
- the finite disorder fixed points (iii) that present strong disorder properties, such as Griffiths phases in quantum models or localization phenomena for random walks in random media.

2.3 How to know if the disorder dominates at large scale?

Via a priori theoretical arguments ?

The relative importance of thermal fluctuations with respect to disorder fluctuations at large scale can not be seen directly on the microscopic model. It is actually not very well-known for the majority of disordered systems. Even for the random field systems, for which there exists at zero temperature an Imry-Ma argument discussed above, there does not exist, to our knowledge, any general argument which would include the thermal fluctuations of the domain walls and which would estimate the the entropy of decomposing a sample into Imry-Ma domains.

Via numerical studies?

In the numerical studies which have a priori direct informations on various thermal configurations for a fixed realization of the disorder, it is actually quite rare to find this information sample by sample, because the published results are in general devoted to the various disorder averaged observables. What is of course a pity from the point of view of the strong disorder approaches, for which the essential information is precisely the importance of the thermal fluctuations in a fixed sample. Indeed, the averages over the samples always present the “risk” to be dominated by rare events and to give a false idea of typical behaviors. For instance, in the Sinai model, the thermal width averaged over the samples, which is a very natural observable in numerical simulations to characterize the spreading of the thermal packet, diverges at large time. This result could be interpreted at first sight as an absence of localization asymptotically, whereas in fact, the distance between two independent particles in the same sample remains a finite random variable at infinite time, which corresponds to a very strong localization in law.

Assumption of strong disorder and its check

As a consequence, the reasoning in strong disorder approaches is usually as follows: one starts by assuming that the disorder dominates at large scale, and one checks at the end the consistency of this assumption. More precisely, the strong disorder renormalization procedures contain their own test of validity : if the probability distributions have a width which grows indefinitely by the RG flow, the obtained results are asymptotically exact, whereas if the width of the probability distributions converge towards a finite value, the obtained results are only approximate, and the order of magnitude of the approximation can be characterized.

2.4 Essential features of infinite disorder fixed points

In several random systems the explicit construction of the strong disorder RG is not evident, in another cases the form of singularities at the critical point

may depend on the strength of disorder. In these cases combined numerical and analytical studies could help to identify the type of the random fixed point. An infinite disorder fixed point is characterized by the following properties.

- Strong dynamical anisotropy
The typical length-scale is related to the logarithm of the typical time-scale, thus the dynamical exponent is formally infinity.
- Ultra-slow dynamics
The dynamical processes, such as autocorrelations for random magnets or diffusion of the random random walk takes place in a very slow, logarithmic time-scale.
- Broad distribution of physical quantities
Distribution of a physical quantity, say the order-parameter, m , is logarithmically broad. Generally, in a finite system of length, L , the appropriate scaling combination is $L^\psi \ln m$. As a consequence typical and average values are different and generally involve different type of singularities.
- Dominant effect of rare regions
The average value of a physical quantity is generally dominated by the rare events (or rare regions of a large sample). In a rare event the physical quantity has a value of $O(1)$ and to obtain the critical singularities it is generally enough to determine the fraction of rare events. Therefore calculations at infinite disorder fixed points are often comparatively easier, than at a conventional random fixed point.

In conclusion, the strong disorder RG approaches have a meaning whenever the disorder heterogeneities determine the dominant state of the system, whereas the thermal or quantum fluctuations only provide subleading corrections. Their goal is then to build the dominant state of the system for each realization of the disorder. To implement this program, it is now necessary to specify the computation methods to carry out the renormalization on the disorder.

3 General features of Ma-Dasgupta RG rules

Whereas renormalizations in pure systems usually involve a finite number of coupling constants, renormalizations in disordered systems involve probability distributions, i.e. functions which belong to an infinite dimensional space. The analysis of the RG flow and of the fixed points obviously become much harder. This difficulty usually leads to completely numerical studies, or, at the analytical level, to additional approximations which consist in projecting on finite spaces, i.e. one chooses a certain analytical form for distributions containing a few parameters whose evolutions are studied. In this section, we will see that the strong disorder RG rules generate, in a certain number of favorable cases, RG flows that are simple enough to be analyzed completely. Moreover, the fixed point distributions have usually an interesting probabilistic interpretation.

3.1 What is a strong disorder RG rule ?

The various strong disorder RG which have been developed in different physical contexts, are characterized by the two essential properties :

- the renormalization concerns the extreme value of a random variable. This extreme value which evolves by renormalization and constitutes the scale of renormalization: it is the “ cut-off” of the renormalized distribution.
- the renormalization is local in space: at each stage, it is only the immediate neighbors of the extreme random variable which is concerned by the RG procedure.

Let us now present the two basic examples, one for a quantum spin chain, one for a dynamical classical model, that actually leads to the same RG rules for appropriate variables.

Quantum Example : RG rule for the Random Transverse field Ising Chain (RTFIC)

In the RTFIC model, there are random couplings $J_i > 0$ and random transverse fields $h_i > 0$, that alternate along the chain. The physics of the model will be discussed in details in Section 4. Here our goal is simply to describe the strong disorder RG rules [138] : at each step, the maximum $\Omega = \max\{J_i, h_j\}$ is chosen. If it is a random transverse field $h_2 = \Omega$, it is eliminated with its two neighbor couplings (J_2, J_3) to produce the new effective coupling

$$J' = \frac{J_2 J_3}{\Omega} \quad (3.1)$$

If the maximum is a coupling $J_2 = \Omega$, it is eliminated with its two neighbor (h_1, h_2) to produce the new effective transverse field

$$h' = \frac{h_1 h_2}{\Omega} \quad (3.2)$$

So the new effective couplings and transverse fields that are introduced are statistically independent from all other disorder variables remaining in the chain. This property is essential to write closed RG equations for the probability distributions $P_\Omega(J)$ et $P_\Omega(h)$ of the couplings and fields at RG scale Ω .

Classical Example : RG rule for the Sinai model

In the Sinai model, the disorder consists in random forces f_i . The strong disorder RG approach (that will be described in details in Section 11) yields that the important degrees of freedom are the extrema of the associated potential $U(i) = \sum_{j=0}^i f_j$ at large scale. To define the extrema of the initial potential, it is thus necessary to start by grouping all the consecutive forces f_i of the same sign together : the landscape then consists in alternating descending (F_i^+, l_i^+) and ascending (F_i^-, l_i^-) bonds. Barriers F and lengths l are now positive random variables which respectively represent the potential differences and the distances

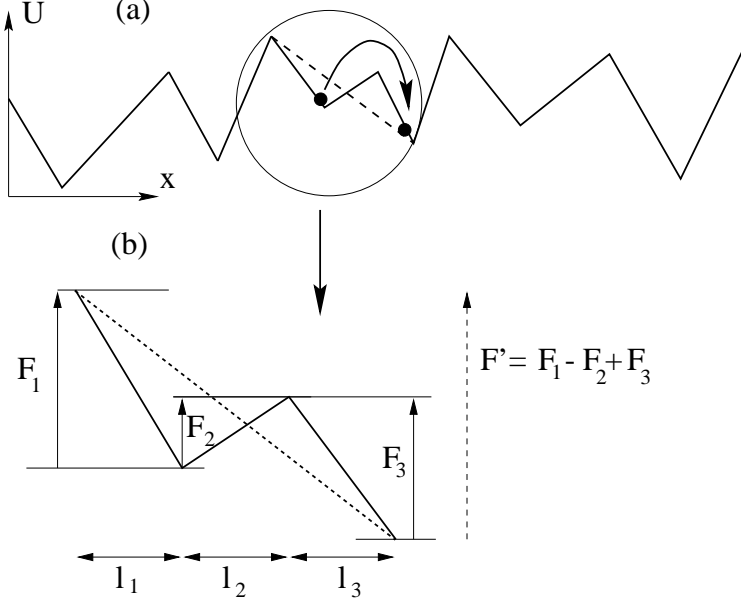


Figure 1: *RG rules for a 1D random potential.*

between two consecutive local extrema of the initial model. The RG rule of the landscape is then the following one [141, 142]: one chooses the smallest barrier $\Gamma = \min\{F_i^+, F_i^-\}$. If the smallest barrier is a descending bond $F_2^+ = \Gamma$, one eliminates it with its two neighboring ascending bonds F_1^- and F_2^- to form a new ascending bond

$$(F^-)' = F_1^- + F_2^- - \Gamma \quad (3.3)$$

If the smallest barrier is an ascending bond $F_1^- = \Gamma$, one eliminates it with its two neighboring descending bonds F_1^+ and F_2^+ to form a new descending bond

$$(F^+)' = F_1^+ + F_2^+ - \Gamma \quad (3.4)$$

These rules are completely equivalent to the decimation rules of the RTFIC (3.1,3.2) by a simple logarithmic transformation of the variables

$$F_i^+ = -\ln J_i \quad (3.5)$$

$$F_i^- = -\ln h_i \quad (3.6)$$

$$\Gamma = -\ln \Omega \quad (3.7)$$

If one wishes to keep in addition the information on the initial distances in physical space, one writes the RG rule for the length during the decimation process: the length of the new renormalized bond is simply equal to the sum of the three eliminated bonds

$$l = l_1 + l_2 + l_3 \quad (3.8)$$

This new length is statistically independent of the other lengths remaining in the system, but is correlated with the barrier F existing on the same bond. Thus, one writes a closed system of two flow equations for the two joint laws $P_{\Gamma}^{\pm}(F, l)$.

3.2 Iteration and convergence towards a fixed point

Once the RG rules have been defined, one has to study the flow upon iteration of the RG rules. This can be done either analytically for a large class of one-dimensional systems, or numerically for more complex systems, in particular models in dimension $d > 1$. In all cases, one is looking for a convergence towards a fixed point, which is generally located at $\Omega^* = 0$, in appropriate rescaled variables. During renormalization, the complementary variables, such as couplings and transverse-fields for the RTFIC or descending and ascending bonds for the Sinai model, can be decimated symmetrically, which corresponds to a critical point, or asymmetrically, which happens in the Griffiths phases. We will now describe the fixed points corresponding to the RG rules described above as examples.

3.3 The basic Infinite Disorder Fixed Point (Critical point)

The symmetric case $\overline{f_i} = 0$ of the Sinai model corresponds to the quantum critical point $\overline{\ln J} = \overline{\ln h}$ of the RTFIC model. At large scale, the descending and ascending bonds become statistically equivalent, and the only relevant parameter at large scale is the variance $\overline{f_i^2} = 2\sigma$ of the initial model, as in the Central Limit theorem. The fixed point is then characterized by a joint distribution $P^*(\eta, \lambda)$ of the scaling variables $\eta = \frac{F-\Gamma}{\Gamma}$ for the barriers and $\lambda = \frac{\sigma l}{\Gamma^2}$ for the lengths. This joined law is defined by its Laplace transform with respect to the length λ [138]

$$\int_0^{+\infty} d\lambda e^{-p\lambda} P^*(\eta, \lambda) = \theta(\eta > 0) \frac{\sqrt{p}}{\sinh \sqrt{p}} e^{-\eta \sqrt{p} \coth \sqrt{p}} \quad (3.9)$$

In particular, the distribution of the barriers alone is simple exponential

$$P^*(\eta) = \theta(\eta > 0) e^{-\eta} \quad (3.10)$$

whereas the distribution of the lengths alone takes the form of an infinite series of exponentials

$$\begin{aligned} P^*(\lambda) &= LT_{p \rightarrow \lambda}^{-1} \left(\frac{1}{\cosh \sqrt{p}} \right) = \sum_{n=-\infty}^{+\infty} \pi(-1)^n \left(n + \frac{1}{2} \right) e^{-\pi^2 (n + \frac{1}{2})^2 \lambda} \quad (3.11) \\ &= \frac{1}{\sqrt{\pi} \lambda^{3/2}} \sum_{m=-\infty}^{+\infty} (-1)^m \left(m + \frac{1}{2} \right) e^{-(m + \frac{1}{2})^2 \frac{1}{\lambda}} \end{aligned}$$

(the two series correspond to each other via a Poisson inversion formula). The convergence towards the fixed point solution (3.9) is of order $1/\Gamma$ for random walk models [138]. For the 1D Brownian motion which already represents the universal scaling limit of random walks, the fixed point (3.9) is an exact result at any scale Γ , as shown by a direct calculation via constrained path integrals [233].

3.4 The basic Strong Disorder Fixed Point (Griffiths phases)

In the biased case $\overline{f_i} = f_0 > 0$, the RG equations lead to a family of solutions depending on one parameter denoted by δ [138]: the two distributions for ascending and descending bonds have for Laplace transforms

$$\int_0^{+\infty} dl e^{-pL} P_\Gamma^{*\pm}(F, l) = \theta(F > \Gamma) \frac{\sqrt{p + \delta^2} e^{\mp \delta \Gamma}}{\sinh \sqrt{p + \delta^2}} e^{-(F-\Gamma) [\sqrt{p+\delta^2} \coth \sqrt{p+\delta^2} \mp \delta]} \quad (3.12)$$

In particular, the distributions of barriers alone have the following exponential forms

$$\begin{aligned} P_\Gamma^{*+}(F) &= \theta(F > \Gamma) \frac{2\delta}{e^{2\delta\Gamma} - 1} e^{-(F-\Gamma) \frac{2\delta}{e^{2\delta\Gamma} - 1}} \underset{\Gamma \rightarrow \infty}{\simeq} \frac{2\delta}{e^{2\delta\Gamma}} e^{-(F-\Gamma) \frac{2\delta}{e^{2\delta\Gamma}}} \\ P_\Gamma^{*-}(F) &= \theta(F > \Gamma) \frac{2\delta}{1 - e^{-2\delta\Gamma}} e^{-(F-\Gamma) \frac{2\delta}{1 - e^{-2\delta\Gamma}}} \underset{\Gamma \rightarrow \infty}{\simeq} \theta(F > \Gamma) 2\delta e^{-(F-\Gamma) 2\delta} \end{aligned} \quad (3.13)$$

From the point of view of the renormalized landscape, the meaning of the parameter 2δ is thus clear: the probability distribution of large barriers against the bias f_0 remains stable at large scale (apart from the presence of the cut-off Γ) and (2δ) is the coefficient of the exponential asymptotic decay of this distribution. It is now necessary to specify the meaning of this parameter δ for the microscopic model. Close to the critical point corresponding to $\delta = 0$, the parameter δ can be developed at the first order in the bias [138]

$$\delta = \frac{f_0}{\sigma} + O(f_0^2) \quad (3.14)$$

However, if one deviates from the immediate vicinity of the critical point, the correct non-perturbative definition of the parameter δ in term of the initial distribution $Q(f)$ of the variables (f_i) of the microscopic model is that δ represents the solution of the equation [142]

$$\overline{e^{-2\delta f_i}} \equiv \int_{-\infty}^{+\infty} df Q(f) e^{-2\delta f} = 1 \quad (3.15)$$

Of course, this definition exactly corresponds, with the change of notation $2\delta = \mu/T$, with the definition of the dimensionless parameter μ representing the exponent of the anomalous diffusion $x \sim t^\mu$ of the biased Sinai model [218, 116, 14]. The development into the two first cumulants yields again the

simple expression (3.14), which is exact at all the orders only for an initial Gaussian distribution. Again, if one directly considers the 1D biased Brownian motion, the solutions (3.12) are exact results on any scale Γ , as shown by a direct calculation by constrained path integrals [233].

Whereas the solution (3.9) of the symmetric case $\delta = 0$ is an infinite disorder fixed point, the solution (3.14) of the asymmetric case $\delta > 0$ is a finite disorder fixed point, because the distribution of large barriers against the bias has a finite width $\frac{1}{2\delta}$ asymptotically. The strong disorder RG thus gives exact results about position dependent quantities only in the limit $\delta \rightarrow 0$. The dynamical quantities, such as the autocorrelation function, however is expected to be exact. We will discuss in Section 12 how to generalize this RG procedure when the parameter δ is small, but non-zero.

3.5 Auxiliary variables and critical exponents

In strong disorder RG, ‘auxiliary variables’ are variables associated with the bonds which will evolve according to rules in parallel with the RG rule of the main variable. The first important example is the length l that we have already met (3.8). It is an auxiliary variable because it is not the length that determines the renormalization, but the associated barrier F : indeed at each stage, one does not choose the minimal length, but the minimal barrier F . Another important auxiliary variable for the RTFIC is the magnetization μ of the spin clusters : this variable exists only in association with the random fields h_i and evolves with the rule [138]

$$\mu = \mu_1 + \mu_3 \quad (3.16)$$

More generally, in the various models discussed in this review, one is led to study various auxiliary variables which evolve according to the general rule

$$\mu = a\mu_1 + b\mu_2 + c\mu_3 \quad (3.17)$$

where (a, b, c) are constants. We have already seen how the joint probability distribution of barriers and lengths characterizes the statics of the renormalized landscape at a given scale (3.9): in particular, in the renormalized landscape at scale Γ , in which there are only barriers $F > \Gamma$, the lengths have for scaling $l \sim \Gamma^2$, which is the usual Brownian scaling as it should. However, apart from this very special case $a = b = c = 1$, the auxiliary variables (3.17) lead to non-trivial exponents $\mu \sim \Gamma^\phi$ who reflect the ‘dynamical’ properties of the RG procedure over all preceding scales $\Gamma' < \Gamma$, and which contain much more information than the landscape at the scale Γ alone. For instance, for the RTFIC, the very simple rule (3.16) corresponding to $a = c = 1$ and $b = 0$ already leads for the magnetization $\mu \sim \Gamma^\phi$ to the irrational exponent equal to the golden mean [138]

$$\phi(a = c = 1, b = 0) = \frac{1 + \sqrt{5}}{2} \quad (3.18)$$

This example already shows that a simple one-dimensional random walk contains non-trivial exponents if one is interested into ‘subtle’ properties involving the dynamics of the renormalized landscape.

More generally, for auxiliary variables of type (3.17), one obtains that, when the condition $a + c = 2$ is satisfied (this happens rather often in practice for the most natural observables), the associated exponent satisfies a quadratic equation and reads

$$\phi(a + c = 2, b) = \frac{1 + \sqrt{5 + 4b}}{2} \quad (3.19)$$

This exponent generalizes the exponent $\phi(a = 1, b = 1, c = 1) = 2$ of the length (3.8). Otherwise, when $a + c \neq 2$, the exponent $\phi(a, b, c)$ satisfies a more complicated equation involving the confluent hypergeometric function $U(A, B, z)$ [142, 232].

As a final remark, let us mention that the strong disorder RG procedures have actually a close relationship with some pure growth models, which were introduced in a completely independent way, as we explain in Appendix E.

Part II

RG STUDY OF QUANTUM MODELS

4 Random Transverse Field Ising Chain

The RTFIC is the paradigmatic example of random quantum spin chains for which the most complete analytic results are known. The early results by McCoy and Wu[252] and others[329] have been greatly extended by Fisher using the strong disorder RG method[138], which has inspired subsequent investigations[327, 276, 108, 198]. These results, in particular at the critical point are of importance for other disordered problems, as well, for which the RG trajectories flow into the infinite disorder fixed point of the RTFIC. Examples are the random quantum Potts, clock and Ashkin-Teller models in Sec.5, the asymmetric simple exclusion process with particle-wise disorder in Sec.16.2, and the random contact process in Sec.17.2.

4.1 Model

The RTFIC is defined by the Hamiltonian:

$$H_I = - \sum_i J_i \sigma_i^x \sigma_{i+1}^x - \sum_i h_i \sigma_i^z. \quad (4.1)$$

Here the σ_i^x , σ_i^z are Pauli matrices at site i and the J_i exchange couplings and the h_i transverse-fields are random variables with distributions $\pi(J)$ and

$\rho(h)$, respectively. The Hamiltonian in eq(4.1) is closely related to the transfer matrix of a classical two-dimensional layered Ising model, as described in details in Sec.18.2.1.

4.1.1 Free-fermion representation

The usual way of study the RTFIC is to map the Hamiltonian in eq(4.1) through a Jordan-Wigner transformation and a following canonical transformation [235] into a free fermion model:

$$H = \sum_{q=1}^L \epsilon_q \left(\eta_q^+ \eta_q - \frac{1}{2} \right), \quad (4.2)$$

where η_q^+ and η_q are fermion creation and annihilation operators, respectively. Here we consider a finite chain of length L with free or fixed boundary conditions, i.e. with $J_L = 0$, when the fermion energies ϵ_q are obtained via the solution of an eigenvalue problem[188], which necessitates the diagonalization of a $2L \times 2L$ tridiagonal matrix \mathbf{T} with non-vanishing matrix-elements $T_{2i-1,2i} = T_{2i,2i-1} = h_i$, $i = 1, 2, \dots, L$ and $T_{2i,2i+1} = T_{2i+1,2i} = J_i$, $i = 1, 2, \dots, L-1$, thus

$$\mathbf{T} = \begin{pmatrix} 0 & h_1 & & & & \\ h_1 & 0 & J_1 & & & \\ & J_1 & 0 & h_2 & & \\ & & h_2 & 0 & \ddots & \\ & & & \ddots & \ddots & J_{L-1} \\ & & & & J_{L-1} & 0 & h_L \\ & & & & & h_L & 0 \end{pmatrix}, \quad (4.3)$$

One is confined to the $\epsilon_q \geq 0$ part of the spectrum. In the free-fermion representation one can also calculate the (local) magnetization and different types of correlation and autocorrelation functions[235, 191]. Here we just quote two simple results, with the help of them we shall illustrate features of scaling of the RTFIC.

4.1.2 Surface magnetization, phase diagram and critical exponents

Fixing the end-spin at site $i = L$, thus taking the transverse field, $h_L = 0$, the magnetization at the other surface, at $i = 1$, can be expressed by the simple exact formula[301, 191]:

$$m_s = \left[1 + \sum_{i=1}^{L-1} \prod_{j=1}^i \left(\frac{h_j}{J_j} \right)^2 \right]^{-1/2}. \quad (4.4)$$

The surface magnetization thus involves a so-called Kesten random variable, whose properties are discussed in more details in Appendix C.

Analyzing Eq.(4.4) in a disordered system in the thermodynamic limit we can define a quantum control-parameter,

$$\delta = \frac{[\ln h]_{av} - [\ln J]_{av}}{\text{var}[\ln h] + \text{var}[\ln J]}, \quad (4.5)$$

so that the system is ferromagnetic, the average surface magnetization is non-zero for $\delta < 0$, and it is paramagnetic with vanishing average surface magnetization for $\delta > 0$.

At the critical point, $\delta = 0$, in a large, finite sample the surface magnetization is determined by the largest term in the sum of Eq.(4.4), which typically grows as $\exp(AL^{1/2})$, which follows from the central limit theorem. Consequently the typical surface magnetization is exponentially small in $L^{1/2}$

$$m_s^{typ}(L) \sim \exp(-\text{cst}L^{1/2}), \quad (4.6)$$

the appropriate scaling combination is $(\ln m_s)/L^{1/2}$ and the distribution of m_s is logarithmically broad. For analytical results about the distribution function of the surface magnetization see[126, 271].

As argued in[191] there are rare realizations, in which the sum of random variables: $\varepsilon_j = \ln \frac{h_j}{J_j}$ have surviving walk character and therefore $m_s^{rare} = O(1)$. The average of m_s at the critical point is dominated by these rare realizations and its value follows from the fraction of surviving walks, $P_{surv}(L) \sim L^{-1/2}$:

$$[m_s]_{av}(L) \sim L^{-x_m^s}, \quad x_m^s = 1/2. \quad (4.7)$$

Here x_m^s is the anomalous dimension of the surface magnetization.

Repeating the analyses[191] in the ferromagnetic phase close to the critical point, we obtain:

$$[m_s]_{av}(\delta) \sim -\delta^{\beta_s}, \quad \beta_s = 1, \quad (4.8)$$

and from the finite-size dependence of $[m_s]_{av}(L, \delta)$ we obtain for the average correlation length,

$$\xi \sim |\delta|^{-\nu}, \quad \nu = 2, \quad (4.9)$$

so that the scaling relation: $\beta_s = x_m^s \nu$ is satisfied. Finally, typical correlations have a faster decay:

$$\xi_{typ} \sim |\delta|^{-\nu_{typ}}, \quad \nu_{typ} = 1. \quad (4.10)$$

The critical exponents of the RTFIC are summarized in table 1, in which we have included the bulk magnetization exponent, β , and scaling dimension, x_m , together with the exponent, ψ , defined in Eq.(4.13). Note, that the scaling relations, $\beta = \nu x_m$ and $\beta_s = \nu x_m^s$ are satisfied.

4.1.3 Low-energy excitations and dynamics

The lowest energy gap of the RTFIC, $\epsilon_1(L)$ in Eq.(4.3), can be estimated for free boundary conditions, provided $\epsilon_1(L)$ goes to zero faster, than $1/L$. It is

Table 1: Critical exponents of the RTFIC

β	β_s	x_m	x_m^s	ν	ν_{typ}	ψ
$(3 - \sqrt{5})/2$	1	$(3 - \sqrt{5})/4$	$1/2$	2	1	$1/2$

given by[189]:

$$\epsilon_1(L) \sim m_s \overline{m_s} \prod_{i=1}^{L-1} \frac{h_i}{J_i} . \quad (4.11)$$

Here m_s and $\overline{m_s}$ denote the finite-size surface magnetizations at both ends of the chain, as defined in eq(4.4) (for $\overline{m_s}$ simply replace h_j/J_j by h_{L-j}/J_{L-j} in this eq.).

Critical point

Here $\epsilon_1(L)$ typically behaves as the surface magnetization, consequently:

$$\epsilon(\delta = 0, L) \sim \exp(-\text{const} \cdot L^{1/2}) . \quad (4.12)$$

Thus time-scale, $t_r \sim \epsilon^{-1}$, and length-scale, $L \sim \xi$, are related as:

$$\ln t_r \sim \xi^\psi, \quad \psi = 1/2, , \quad (4.13)$$

which corresponds to extreme anisotropic scaling with an anisotropy, or dynamical exponent $z = \infty$. We remark that in conventional anisotropic systems the usual relation is: $t_r \sim \xi^z$, with $z < \infty$.

Paramagnetic phase

Here, for $\max\{J\} > \min\{h\}$ there are rare regions of size, $l_{rare} \sim \ln L$, in which the local couplings are stronger than the local transverse fields, which prefers (local) ferromagnetic ordering. The corresponding energy gap is exponentially small in l_{rare} , $\epsilon \sim \exp(-Al_{rare})$, thus between time- and length-scale the relation is:

$$t_r \sim \xi^z . \quad (4.14)$$

This is the usual scaling relation in the Griffiths-phase of the system[158]. In Eq.(4.14) the dynamical exponent, $z = z(\delta)$, depends on the distance of the critical point. Its value can be obtained from a mapping to the random random walk problem, see Sec.B.1 and given by the positive root of the equation:

$$\left[\left(\frac{J}{h} \right)^{1/z} \right]_{\text{av}} = 1 . \quad (4.15)$$

Similarly, there is a Griffiths-phase in the ferromagnetic region, too. Here, the first energy state is exponentially degenerate, and the time-scale is set by the second gap and follows a relation like in Eq.(4.14). To obtain the value of z one should interchange h and J in Eq.(4.15), which also follows from duality[224].

We note that these exact results illustrate the general features of infinite and strong disorder fixed points as summarized in Sec.2.4. In the following we turn to systematically use the strong disorder RG method for the model.

4.2 RG rules

The decimation rules for the model have been announced in Sec.3.1 to illustrate the general features of the Ma-Dasgupta RG method. Here we present a detailed derivation and show the physical picture behind these rules. As already mentioned the strongest term in the Hamiltonian in Eq.(4.1) can be either a bond or a transverse field and different decimation procedure has to be adopted in the two cases.

Strong bond decimation

Here we consider a pair of spins, which are connected by the strongest bond of the system, the strength of which is denoted by $J_2 = \Omega$, where Ω is the energy scale in the system. By definition J_2 is larger than any transverse field, thus typically $J_2 \gg h_2, h_3$, where h_2 and h_3 are the transverse fields acting on the spins of the two-site cluster. Under these circumstances the two spins are strongly correlated so they flip in a longitudinal magnetic field coherently. In a good approximation the two spins can be considered as a composite spin with double momentum in an effective transverse field, \tilde{h}_{23} , which is calculated perturbatively. The first two energy levels of the spectrum of the two-spin cluster with free boundary conditions is given by $E_0 = -\sqrt{J_2^2 + (h_2 + h_3)^2}$ and $E_1 = -\sqrt{J_2^2 + (h_2 - h_3)^2}$, respectively, which are separated by a large gap of $\approx 2J_2$ from the two other levels. With a small error we drop the two highest energy states and keep the two lowest, which are identified as the two states of a composite Ising spin. The renormalized value of the transverse field follows from the relation:

$$\tilde{h}_{23} = \frac{E_1 - E_0}{2} \approx \frac{h_2 h_3}{J_2}, \quad (4.16)$$

where the second equation holds for $J_2 \gg h_2, h_3$.

Strong transverse field decimation

In this case the strongest term is a transverse field, say $h_2 = \Omega$, acting on site $i = 2$. The connecting couplings, J_2 and J_3 are typically much smaller, $h_2 \gg J_2, J_3$. In a small external longitudinal field this spin has a negligible response, consequently in a good approximation it can be considered as "dead", as far as susceptibility and magnetic correlations are concerned. Therefore this spin is decimated out and a new coupling, \tilde{J}_{23} , is generated between the remaining spins, the strength of which is calculated perturbatively. Most easily the result is obtained through the duality properties of the RTFIC[224], which amounts to interchange couplings and transverse fields, $h_i \leftrightarrow J_i$ in Eq.(4.16):

$$\tilde{J}_{23} \approx \frac{J_2 J_3}{h_2}. \quad (4.17)$$

4.3 RG flow

Under the repeated use of the decimation transformations in Eqs.(4.16) and (4.17) the energy scale, Ω , is gradually lowered and at the same time the distribution of the transverse fields, $P_0(h, \Omega)$, and that of the couplings, $R_0(J, \Omega)$, are subject of variation. We are interested in the renormalization of these distribution functions, in particular we want to obtain their scaling behavior around the fixed point of the transformation, which is located at $\Omega^* = 0$.

4.3.1 Renormalization of the distribution functions

Let us denote the energy scale in the initial model by Ω_{in} , which during renormalization is decreased to a value of $\Omega < \Omega_{\text{in}}$. Further infinitesimal decrease of the energy scale as $\Omega \rightarrow \Omega - d\Omega$ amounts to eliminate a fraction of $d\Omega[P_0(\Omega, \Omega) + R_0(\Omega, \Omega)]$ spins, during which the coupling distribution changes as:

$$R_0(J, \Omega - d\Omega) = \left\{ R_0(J, \Omega) + d\Omega P(\Omega, \Omega) \int_0^\Omega dJ_1 \int_0^\Omega dJ_3 R_0(J_1, \Omega) R_0(J_3, \Omega) \times \right. \\ \left. \left[\delta \left(J - \frac{J_1 J_3}{\Omega} \right) - \delta(J - J_1) - \delta(J - J_3) \right] \right\} \{1 - d\Omega[P_0(\Omega, \Omega) + R_0(\Omega, \Omega)]\}^{-1} \quad (4.18)$$

Here in the r.h.s. the three delta functions represent the generated one new coupling and the decimated two old couplings during one RG step and the second factor ensures normalization. A similar equation is obtained for the distribution of the transverse fields, just from duality one should make the interchange $h \leftrightarrow J$ and $P \leftrightarrow R$.

Now expanding $R_0(J, \Omega - d\Omega)$ one arrives to the integral-differential equation:

$$\frac{dR_0}{d\Omega} = R_0(J, \Omega) [P_0(\Omega, \Omega) - R_0(\Omega, \Omega)] \\ - P_0(\Omega, \Omega) \int_J^\Omega dJ' R_0(J', \Omega) R_0\left(\frac{J}{J'} \Omega, \Omega\right) \frac{\Omega}{J'}, \quad (4.19)$$

and similarly for the distribution $P_0(h, \Omega)$:

$$\frac{dP_0}{d\Omega} = P_0(h, \Omega) [R_0(\Omega, \Omega) - P_0(\Omega, \Omega)] \\ - R_0(\Omega, \Omega) \int_h^\Omega dh' P_0(h', \Omega) P_0\left(\frac{h}{h'} \Omega, \Omega\right) \frac{\Omega}{h'}. \quad (4.20)$$

The two integral-differential equations in Eqs.(4.20) and (4.19) have to be supplemented by the initial conditions, represented by the distributions $P_{\text{in}}(h) = P_0(h, \Omega_{\text{in}})$ and $R_{\text{in}}(J) = R_0(J, \Omega_{\text{in}})$.

4.3.2 Fixed-point solution

A special solution to the problem in Eqs.(4.20) and (4.19) is given by the functions:

$$P_0(h, \Omega) = \frac{p_0(\Omega)}{\Omega} \left(\frac{\Omega}{h} \right)^{1-p_0(\Omega)} \quad (4.21)$$

$$R_0(J, \Omega) = \frac{r_0(\Omega)}{\Omega} \left(\frac{\Omega}{J} \right)^{1-r_0(\Omega)}, \quad (4.22)$$

thus they depend only on the values of the distributions at their edges, at $P_0(\Omega, \Omega) = p_0/\Omega$ and at $R_0(\Omega, \Omega) = r_0/\Omega$. It is argued in Refs.[138, 139] and has been checked through the numerical solution of Eqs.(4.19) and (4.20) that this special solution represents the true solution of the problem at the fixed point, i.e. as $\Omega \rightarrow 0$. Later we also show how the parameters of the special solution can be related with the initial distributions, $P_{in}(h)$ and $R_{in}(J)$. Putting Eqs.(4.21) and (4.22) into Eqs.(4.20) and (4.19) one obtains ordinary differential equations for p_0 and r_0 , what can be written as:

$$\frac{dy_0}{d\Gamma} + y_0^2 = \Delta^2. \quad (4.23)$$

in terms of $y_0 = p_0 - \Delta = r_0 + \Delta$. Here $\Gamma = -\ln \Omega$ is the log-energy variable and Δ is the asymmetry parameter, which is related to the relative strengths of the couplings and the transverse fields and can be calculated from the initial distributions. At the critical point, $\Delta = 0$, since the couplings and the transverse-fields have identical distributions. On the other hand for $\Delta > 0$ ($\Delta < 0$) we are in the disordered (ordered) phase.

Critical point solution

At the critical point, $\Delta = 0$, the solution to Eq.(4.23) is given by:

$$y_0 = p_0 = r_0 = \frac{1}{\Gamma - \Gamma_0} = \frac{1}{\ln(\Omega_0/\Omega)}, \quad \delta = \Delta = 0, \quad (4.24)$$

where $\Gamma_0 = -\ln \Omega_0$ is a reference (log)energy scale. It is instructive to consider the distribution of the reduced log-coupling variable $\eta = -(\ln \Omega - \ln h)/\ln \Omega = -(\ln \Omega - \ln J)/\ln \Omega \geq 0$, which is given from Eqs.(4.21) and (4.24) as

$$\rho(\eta)d\eta = \exp(-\eta)d\eta. \quad (4.25)$$

This solution has been obtained by Fisher[138] and corresponds to the distribution of barriers in the Sinai model in Eq.(3.10).

Off-critical solution

The solution to Eq.(4.23) in the off-critical region, $\Delta \neq 0$, is given by:

$$y_0 = \frac{\Delta \bar{y}_0 + \Delta^2 \text{th} [\Delta(\Gamma - \Gamma_0)]}{\Delta + \bar{y}_0 \text{th} [\Delta(\Gamma - \Gamma_0)]} = |\Delta| \left(1 + 2 \frac{\bar{y}_0 - \Delta}{\bar{y}_0 + \Delta} (\Omega/\Omega_0)^{2\Delta} + \dots \right), \quad (4.26)$$

where the solution goes through the point $y_0 = \bar{y}_0$ at the reference (log)energy cut-off, Γ_0 . The second equation in Eq.(4.26) is the approximate form of the solution close to the line of fixed points, where in terms of the original energy-scale variable $\Omega/\Omega_0 \ll 1$.

It is shown in Ref.[198] that there is a conserved quantity, say κ , along the RG trajectory provided $[(J/h)^{2\kappa}]_{\text{av}} = 1$. Evaluating the average with the fixed point solution in Eqs.(4.21) and (4.22) we obtain:

$$\left[\left(\frac{J^2}{h^2} \right)^\Delta \right]_{\text{av}} = 1 . \quad (4.27)$$

Consequently the asymmetry parameter, Δ , does not change during the RG transformation and related to the initial distributions. Close to the critical point $\Delta = \delta + O(\delta^2)$, therefore it is called the non-linear quantum control parameter of the RTFIC.

4.3.3 Asymptotic exactness of the results

Next we show that the RG equations in Eqs.(4.16) and (4.17) become asymptotically exact as the line of fixed points is approached, i.e., as $\Omega/\Omega_0 \rightarrow 0$.

First we consider the disordered Griffiths phase, $\Delta > 0$, but the reasoning holds for $\Delta < 0$ from duality and can be applied at the critical point, too. For $\Delta > 0$ the ratio of decimated bonds, Δn_J , and decimated transverse fields, Δn_h , goes to zero as $\Delta n_J/\Delta n_h = R_0(\Omega, \Omega)/P_0(\Omega, \Omega)r_0/p_0 \sim \Omega^{2\Delta}$, thus close to the fixed point almost exclusively transverse fields are decimated out. Then the probability, $Pr(\alpha)$, that the value of a coupling, J , being neighbor to a decimated transverse field is $\Omega > J > \alpha\Omega$ with $0 < \alpha < 1$ is given by

$$Pr(\alpha) \simeq \int_{\alpha\Omega}^{\Omega} R_0(J, \Omega) dJ = 1 - \alpha^{r_0} \approx r_0 \ln(1/\alpha) , \quad (4.28)$$

which goes to zero during iteration, since according to Eq.(4.26) $r_0 = R_0(\Omega, \Omega)\Omega \rightarrow 0$. At the critical point, where couplings and transverse fields are decimated with the same rate Eq.(4.28) is still valid, and $Pr(\alpha)$ goes to zero as $r_0 = 1/(\Gamma - \Gamma_0)$. Consequently the RG transformation becomes asymptotically exact and the dynamical singularities, which are characterized by the parameter Δ are also exact.

As far as static quantities or spatial correlations are concerned the asymptotic exactness of the RG method is valid only at the critical point, which is controlled by an infinite disorder fixed point. The origin of this is the existence of a diverging correlation length and the infinitely broad distributions of both the couplings and the transverse fields. On the other hand in the disordered Griffiths phase, which is controlled by a line of strong disorder fixed points the correlation length is finite and the distribution of the transverse fields have a finite width. Therefore static quantities calculated by the RG are only exact in the vicinity of the critical point. This phenomena is analogous to that of the biased Sinai walk in Sec.3.4, which is discussed in detail in Section 12.

4.3.4 Relation between energy- and length-scale

The length-scale of the problem, L_Ω , which is the typical distance between remaining spins is related to the fraction of non-decimated spins, n_Ω , as $L_\Omega \sim n_\Omega^{-1}$. When the energy scale is decreased by an amount of $d\Omega$ a fraction of spins, $dn_\Omega = n_\Omega[P_0(\Omega, \Omega) + R_0(\Omega, \Omega)]$, is decimated out, so that we obtain the differential equation:

$$\frac{dn_\Omega}{d\Omega} = n_\Omega[P_0(\Omega, \Omega) + R_0(\Omega, \Omega)] . \quad (4.29)$$

This can be integrated by using the solution in Eq.(4.26) as:

$$n_\Omega = \left\{ \text{ch} \left[\Delta \ln \frac{\Omega_0}{\Omega} \right] + \frac{\bar{y}_0}{\Delta} \text{sh} \left[\Delta \ln \frac{\Omega_0}{\Omega} \right] \right\}^{-2} . \quad (4.30)$$

At the critical point: $\Delta \rightarrow 0$ and $\Gamma = -\ln \Omega \rightarrow \infty$, with however $\Delta \times \Gamma \rightarrow 0$ one obtains:

$$L_\Omega \sim \frac{1}{n_\Omega} \sim \left[\ln \frac{\Omega_0}{\Omega} \right]^2 , \quad \Delta = 0 , \quad (4.31)$$

which is just the relation in Eq.(4.13) as found by Fisher[138].

In the Griffiths phases, $|\Delta| > 0$, one obtains in Eq.(4.30), $n_\Omega \sim \Omega^{2|\Delta|}$, in the limit $\Omega \rightarrow 0$. Consequently the relation between typical distance between remaining spins, $L_\Omega \sim 1/n_\Omega$, and the energy scale is given by:

$$L_\Omega \simeq L_{\Omega_0} (\Delta + y_0)^2 \left(\frac{2}{\Delta} \right)^2 \left(\frac{\Omega_0}{\Omega} \right)^{2|\Delta|} \sim \Omega^{-2|\Delta|} . \quad (4.32)$$

Thus Δ is simply related to the dynamical exponent, z ,

$$z = \frac{1}{2|\Delta|} , \quad (4.33)$$

which is in accordance with the result in Eq.(4.15), which is obtained through a mapping to the random RW.

4.4 RG detailed results

In the following we complete the RG analyses by calculating auxiliary variables (lengths and magnetic moments), dynamical and thermodynamic quantities.

4.4.1 Renormalization of lengths and magnetic moments

During renormalization sites and bonds are decimated out and the distance between the remaining spins as well as the size (moment) of the spin can be expressed with the original variables. To keep track of this process we assign a length to each bond, l_i^b , (connecting sites i and $i+1$) and a moment, μ_i and a length, l_i^s , to each spin. In the initial model $l_i^b = l_i^s = 1/2$ and $\mu_i = 1$. During

a strong bond decimation, see Sec. 4.2, we have the RG rules for the auxiliary variables:

$$\tilde{l}_{23}^b = l_2^s + l_2^b + l_3^s, \quad \tilde{\mu}_{23} = \mu_2 + \mu_3. \quad (4.34)$$

which completes the relation in Eq.(4.16). Similarly, decimating out a strong transverse field, see Sec. 4.2, we obtain for the lengths:

$$\tilde{l}_{23}^s = l_1^b + l_2^s + l_2^b. \quad (4.35)$$

what should be consider together with Eq.(4.17). Note that lengths for the Sinai model is introduced in Eq.(3.8) with analogous definition and renormalization of magnetic moments is announced in Eq.(3.16).

The joint distribution functions are given by: $P(h, l^s, \mu; \Omega)$, and $R_l(J, l^b; \Omega)$, from which we obtain through integration the reduced distribution functions: $P_0(h, \Omega)$, $P_l(h, l^s, \Omega)$, $P_\mu(h, \mu, \Omega)$ and $R_0(J, \Omega)$. Renormalization of $P_0(h, \Omega)$ and $R_0(J, \Omega)$ have already been presented in Sec. 4.3.

Solution of the other reduced distribution functions can be obtained in the following steps[138, 198], what we illustrate in the example of the moment distribution.

- In the first step, one should write down the RG equation for the distribution functions, in this way to generalize the relation in Eqs.(4.19) and (4.20). For the moment distribution we have:

$$\begin{aligned} \frac{dP_\mu(h, \mu, \Omega)}{d\Omega} &= P_\mu(h, \mu, \Omega) [R_0(\Omega, \Omega) - P_0(\Omega, \Omega)] - \\ &R_0(\Omega, \Omega) \int_h^\Omega dh' \frac{\Omega}{h'} \int_0^\mu d\mu' P_\mu(h', \mu', \Omega) P\left(\frac{h}{h'}, \mu - \mu', \Omega\right). \end{aligned} \quad (4.36)$$

- In the second step the solution is searched in the form of a Laplace transform, c.f.:

$$\tilde{P}_\mu(h, s, \Omega) = \int_0^\infty e^{-\mu s} P_\mu(h, \mu, \Omega) d\mu. \quad (4.37)$$

- The third step is to observe that the different s -components of the transformed function are separated, which makes possible to obtain the solution in the fixed point.

- In the fourth step we generalize the solution found in Eq.(4.21) for the component, $s = 0$, and search the solution for general s in the form:

$$\tilde{P}_\mu(h, s, \Omega) = \frac{\pi_\mu(s, \Omega)}{\Omega} \left(\frac{\Omega}{h}\right)^{1-p_\mu(s, \Omega)}. \quad (4.38)$$

- In the fifth step we write ordinary differential equations for the functions, $p_\mu(s, \Omega)$ and $\pi_\mu(s, \Omega)$, which appear in Eq.(4.38).

- The solution, in the sixth step, is found in linear order of s : $p_\mu(s, \Omega) = p_0(\Omega) + s\tilde{p}_1(\Omega)$ and $\pi_\mu(s, \Omega) = p_0(\Omega) + s\tilde{\pi}_1(\Omega)$, where \tilde{p}_1 satisfies the differential equation:

$$(y_0^2 - \Delta^2) \frac{d^2 \tilde{p}_1}{dy_0^2} = \tilde{p}_1, \quad (4.39)$$

where $y_0 = y_0(\Omega)$ is given in Eq.(4.26).

• Finally, in the seventh step the average cluster moment is obtained through the relation:

$$\bar{\mu} = \frac{\tilde{p}_1 - \tilde{\pi}_1}{p_0} - \frac{\int_{\tilde{y}_0}^{y_0} dy_0' \tilde{p}_1(y_0') / (y_0' - \Delta)}{y_0 + \Delta}. \quad (4.40)$$

At the critical point with $\Delta = 0$ the solution of Eq.(4.39) is $\tilde{p}_1 = y_0^{-\tau}$, with $\tau = (\sqrt{5} - 1)/2$, thus the average cluster moment is given by

$$\bar{\mu} = \text{const } y_0^{-(1+\tau)} = \bar{\mu}_0 \left[\ln \left(\frac{\Omega_0}{\Omega} \right) \right]^\phi, \quad \phi = \frac{1}{\tau} = \frac{1 + \sqrt{5}}{2}. \quad (4.41)$$

This result, which is announced in Eq.(3.18) has been first obtained by Fisher[138].

In the Griffiths phases with $\Delta \neq 0$ the solution of the differential equation in Eq.(4.39) in terms of the variable $y = y_0/\Delta$ can be expressed by the hypergeometric function[24], $F(a, b; c; z)$, as

$$\tilde{p}_1 = |\Delta|^{-\tau} y^{-\tau} F\left(\frac{\tau}{2}, \frac{1}{2} + \frac{\tau}{2}; \frac{3}{2} + \tau; \frac{1}{y^2}\right) = |\Delta|^{-\tau} f_1(y). \quad (4.42)$$

We obtain similarly:

$$\begin{aligned} \tilde{\pi}_1 &= -|\Delta|^{-\tau} (y - 1) y^{-(\tau+1)} F\left(\frac{\tau}{2} + 1, \frac{1}{2} + \frac{\tau}{2}; \frac{3}{2} + \tau; \frac{1}{y^2}\right) \\ &= |\Delta|^{-\tau} \phi_1(y), \end{aligned} \quad (4.43)$$

so that the average cluster moment is given by:

$$\bar{\mu} = \text{const} |\Delta|^{-\tau-1} \frac{f(y)}{y + 1} \quad (4.44)$$

where $f(y) = f_1(y) - \phi_1(y)$. Here one should differentiate between the paramagnetic ($\Delta > 0$, $y > 0$) and the ferromagnetic ($\Delta < 0$, $y > 0$) phases. In the former case the average cluster moment grows slowly $\sim \ln |\Omega/\Omega_0|$, as $\Omega/\Omega_0 \rightarrow 0$, whereas in the ferromagnetic phase, where $y \rightarrow 1^-$ in the fixed point, thus $\bar{\mu}$ is divergent, as $\bar{\mu}(\Omega) \sim \Omega^{-2|\Delta|}$.

Before going to deal with the average magnetization defined by: $m = \bar{\mu}/\bar{l}_s$, we quote results about the average lengths, \bar{l}_s and \bar{l}_b , which are calculated from the distribution functions, $P_l(h, l^s; \Omega)$ and $R_l(J, l^b; \Omega)$, in the steps outlined above. The average lengths are given by:

$$\bar{l}_s = \bar{l}_s(\Omega_0) \frac{\bar{y}_0^2 - \Delta^2}{y_0^2 - \Delta^2}, \quad \bar{l}_b = \bar{l}_b(\Omega_0) \frac{\bar{y}_0^2 - \Delta^2}{y_0^2 - \Delta^2}, \quad (4.45)$$

thus at the line of fixed points, $\Omega \rightarrow 0$, we have $\bar{l}_s \sim \bar{l}_b \sim L_\Omega$. Consequently the interpretation of the dynamical exponent, z , in Sec.4.3.4 in Eq.(4.32) is justified also with the average lengths-scales.

The correlation length, ξ , in the paramagnetic phase is measured by the size of non-decimated, i.e. correlated spins in a cluster. This quantity stays constant as the energy scale is lowered and close to the critical point it is given by:

$$\xi \sim \Delta^{-2} \sim \delta^{-2} . \quad (4.46)$$

Thus the correlation length critical exponent is $\nu = 2$, which is Fisher's result[138].

With the results of the average cluster moment in Eq.(4.44) and the average lengths in Eq.(4.45) we can write for the magnetization:

$$m = m_0 \frac{(1-y)f(y)}{(1-\bar{y})f(\bar{y})} , \quad (4.47)$$

where m_0 is the average magnetization at $\Omega = \Omega_0$ and \bar{y} denotes the value of the variable y at the same energy-scale. In the ferromagnetic phase taking $\Omega/\Omega_0 \rightarrow 0$ we obtain close to the critical point: $(1-\bar{y})^{-1} \sim |\Delta|$ and $f(\bar{y}) \sim |\Delta|^\tau$ so that:

$$m = \text{const} |\Delta|^{1-\tau} = \text{const} |\delta|^{1-\tau} . \quad (4.48)$$

From Eq.(4.48) one can read the critical exponent of the average magnetization as:

$$\beta = 1 - \tau = 2 - \phi , \quad (4.49)$$

which has been first derived by Fisher[138].

4.4.2 Scaling of thermodynamic quantities

In this Section we show the scaling form of singular thermodynamic quantities as a function of a small, but finite temperature, $T > 0$, or magnetic field, $H > 0$.

To treat the effect of a small finite temperature in the RG scheme one should first notice that the thermal energy sets in an energy scale, $\Omega_T \sim T$, and the RG decimation should be stopped as Ω is lowered to Ω_T . At that energy scale a fraction of spin clusters, n_{Ω_T} , in Eq.(4.30) is not decimated out and these spins are loosely coupled comparing with the temperature, T . Consequently the entropy per spin, s , is given as the contribution of non-interacting spin clusters:

$$s \simeq n_{\Omega_T} \ln 2 , \quad (4.50)$$

whereas the specific heat can be obtained through derivation: $c_V = T \frac{\partial s}{\partial T}$. From Eqs.(4.50) and (4.30) we obtain for the singular behavior:

$$s(T) \sim c_V(T) \sim T^{1/z} \quad (4.51)$$

with $1/z = 2|\Delta|$, which is valid both in the ordered and in the disordered Griffiths phases.

Next, we consider the effect of a small longitudinal field, $H > 0$, at zero temperature. During renormalization the local longitudinal field, H_l , at site l is transformed as

$$\tilde{H}_l = H \mu_l , \quad (4.52)$$

so that the energy-scale related to the longitudinal field is given by $\Omega_H = H\bar{\mu}(\Omega)$. As Ω is lowered to Ω_H , i.e. when the energy scale satisfies the equation

$$\Omega_H = H\bar{\mu}(\Omega_H) , \quad (4.53)$$

the RG procedure is stopped and the remaining spin clusters are practically uncoupled. Then the average magnetization and the average susceptibility satisfy the equations:

$$m(H) = m(\Omega = \Omega_H), \quad \chi = \frac{\partial m}{\partial H} . \quad (4.54)$$

In the *disordered Griffiths phase*, where $\bar{\mu}(\Omega_H)$ has a Ω_H independent limiting value, we have $\Omega_H \sim H$, consequently from Eq.(4.47) the singular behavior is given by

$$m(H) \sim \left(\frac{H}{H_D} \right)^{1/z} , \quad \Delta > 0 . \quad (4.55)$$

Similarly one obtains for the scaling of the susceptibility in the disordered Griffiths phase:

$$\chi(H) \sim \left(\frac{H}{H_D} \right)^{-1+1/z} , \quad \chi(T) \sim T^{-1+1/z} , \quad \Delta > 0 , \quad (4.56)$$

where the temperature dependence follows from the scaling relation, $\Omega_H \sim \Omega_T$.

In the *ordered Griffiths phase*, where $\bar{\mu}(\Omega_H) \sim \Omega_H^{-1/z}$, as given above Eq.(4.47) we have $\Omega_H \sim H^{1/(1+1/z)}$. Putting this result into Eq.(4.47) and using the asymptotic expansion for the hypergeometric functions[24] in Eqs.(4.42) and (4.43) we obtain for the leading field dependence of the magnetization:

$$m(H) - m(0) \sim \left(\frac{H}{H_D} \right)^{1/(1+z)} \ln \left(\frac{H}{H_D} \right) , \quad \Delta < 0 , \quad (4.57)$$

and similarly for the susceptibility:

$$\chi(H) \sim \left(\frac{H}{H_D} \right)^{-z/(1+z)} \ln \left(\frac{H}{H_D} \right) , \quad \Delta < 0 . \quad (4.58)$$

Note that in the ordered Griffiths phase the singularity exponent is different from that in the disordered Griffiths phase and there is a logarithmic correction term. The temperature dependence of the susceptibility, which follows from the relation $\Omega_H \sim \Omega_T$, is given by:

$$\chi(T) \sim T^{-1+1/z} \ln T , \quad \Delta < 0 . \quad (4.59)$$

We can conclude that all the singularities of different physical quantities, both in the (strongly) ordered and disordered Griffiths phases can be expressed by the non-linear quantum control parameter, Δ , and thus with the dynamical exponent, z .

4.4.3 Renormalization of dynamical correlations

The autocorrelation functions in imaginary time can be obtained by scaling considerations[312, 191, 195], both at the critical point, see Sec..A.3, and in the Griffiths phase, see Sec.A.4. In the framework of the strong disorder RG dynamical correlations have been calculated in Ref.[108, 277].

The basic quantity used in the renormalization is the local dynamical susceptibility:

$$\chi_{jj}^{\alpha\alpha}(\omega) = \sum_k |\langle k | \sigma_j^\alpha | 0 \rangle|^2 \delta(\omega - \epsilon_k) , \quad (4.60)$$

where the sum runs over the excited states, $|k\rangle$, with excitation energy, ϵ_k , and $\alpha = x, z$. $\chi_{jj}^{\alpha\alpha}(\omega)$ is related through a Laplace transform to the imaginary time local autocorrelation function, $G_{jj}^{\alpha\alpha}(t) = [\langle \sigma_j^\alpha(t) \sigma_j^\alpha(0) \rangle]_{\text{av}}$. The low-frequency limit of the local susceptibilities are related to the long time asymptotic of the autocorrelation function. The $\alpha = x$ component is the magnetization, or spin autocorrelation function and for this we shall omit the superscript in the following. The $\alpha = z$ component is generally called the local-energy autocorrelation function, for which we use the notation $G_{jj}^e(t)$. As usual in the calculation we consider the average quantities, which are different at the bulk, in this case the site-index, j , is omitted, or at a boundary site with $j = 1$.

Average magnetization autocorrelation function We start with the average magnetization autocorrelation function in the bulk and in this example we illustrate the method of the strong disorder RG. During renormalization the energy scale is gradually lowered, bonds and sites are removed, new bonds and composite spins of moment, μ , are generated. As a rule of renormalization the matrix-elements in Eq.(4.60) have the same value, both in terms of the original and in the transformed states, which are denoted by $|\tilde{k}\rangle$. In the renormalized model there is a broad distribution of variables and the existing spins are very loosely coupled to each other, thus can be considered as free. Performing the decimation up to the energy-scale: $\Omega = \omega_2$, only spin clusters with a transverse field, $\tilde{h} = \Omega$, contribute to the average spin susceptibility. In this system the matrix-element, $\langle \tilde{k} | \sigma_j^x | \tilde{0} \rangle$, can be easily calculated: it is one, if j belongs to a non-decimated cluster and zero otherwise. The fraction of spin-clusters at this energy is given from Eq.(4.29) as $n_\Omega P_0(\Omega, \Omega) = n_\Omega p_0(\Omega)/\Omega$, each of which contribute by an average moment, $\overline{\mu}(\Omega)$, thus we obtain:

$$[\chi]_{\text{av}}(\omega) \sim \frac{n_\Omega p_0(\omega) \overline{\mu}(\omega)}{\omega} , \quad (4.61)$$

where we wrote ω instead of $\omega/2$, which makes no difference in the asymptotic expressions.

At the critical point using the solution in Eqs.(4.24), (4.31) and (4.41) we obtain:

$$[\chi]_{\text{av}}(\omega) \sim \frac{1}{\omega |\ln \omega|^{3-\phi}} , \quad (4.62)$$

for $\omega \ll \Omega_0$. From this the average magnetization autocorrelation function is given for $t \gg \Omega_0^{-1}$ as:

$$G(t) \sim |\ln t|^{2-\phi}, \quad (4.63)$$

which is just the scaling result in Eq.(A.24), since $x_m/\psi = 2x_m = 2 - \phi$.

In the disordered phase, $\delta > 0$, with the results in Eqs.(4.26), (4.32) and (4.44) we obtain:

$$[\chi]_{\text{av}}(\omega) \sim |\delta|^{4-\phi} \frac{|\ln \omega|}{\omega^{1-1/z}}, \quad (4.64)$$

and

$$G(t) \sim |\delta|^{4-\phi} \frac{|\ln t|}{t^{1/z}}. \quad (4.65)$$

This corresponds to the scaling result in Sec.A.4 and the origin of the logarithmic correction will be discussed, too.

In the ordered phase, $\delta < 0$, the value of p_0 in Eq.(4.26) is different of that in the disordered phase, which leads to a different functional form of the dynamical susceptibility:

$$[\chi]_{\text{av}}(\omega) \sim |\delta|^{4-\phi} \frac{|\ln \omega|}{\omega^{1-2/z}}, \quad (4.66)$$

and the average magnetization autocorrelation function:

$$G(t) \sim |\delta|^{4-\phi} \frac{|\ln t|}{t^{2/z}}. \quad (4.67)$$

Thus the decay of the magnetization autocorrelation function in the ordered phase involves an exponent $2/z$. The origin of this is that in the ordered phase excitations, $|k\rangle$, which contribute to $\chi_{jj}^{xx}(\omega)$ are rare disordered regions, flipping the spin at site j back and forth in a time-interval $\sim t \sim \omega^{-1}$. This type of excitation represents the second gap in the spectrum and involves the scaling exponent, $z/2$, see in Ref.[195].

The local-energy susceptibility and autocorrelation function can be calculated in a similar way, leading to the results[108, 277] at the critical point:

$$[\chi^e]_{\text{av}} \sim \frac{\omega}{|\ln \omega|^{4-\phi}}, \quad (4.68)$$

$$G^e(t) \sim \frac{1}{t^2 |\ln t|^{4-\phi}}, \quad (4.69)$$

and in the ordered and disordered Griffiths phases:

$$[\chi^e]_{\text{av}}(\omega) \sim |\delta|^{5-\phi} \omega^{1+2/z} |\ln \omega|, \quad (4.70)$$

$$G^e(t) \sim |\delta|^{5-\phi} \frac{|\ln t|}{t^{2+2/z}}. \quad (4.71)$$

We note that from scaling considerations and numerical results in Ref.[195] the decay in the Griffiths phase is predicted in a different form as $G(t) \sim t^{-2-1/z}$.

Autocorrelations at a boundary site involve the local scaling dimensions, therefore they generally differ from their bulk counterparts. The surface magnetization autocorrelation at the critical point is given by:

$$G_{(1)}(t) \sim \frac{1}{|\ln t|} , \quad (4.72)$$

and in the ordered and disordered Griffiths phase:

$$G_1^e(t) \sim |\delta|^2 \frac{1}{t^{1/z}} . \quad (4.73)$$

For the surface energy autocorrelations one obtains at the critical point:

$$G_1^e(t) \sim \frac{1}{t^2 |\ln t|^3} , \quad (4.74)$$

in the disordered phase

$$G_1^e(t) \sim \frac{|\delta|^3}{t^{2+2/z}} , \quad (4.75)$$

and in the ordered phase:

$$G_1^e(t) \sim \frac{|\delta|^3}{t^{2+1/z}} . \quad (4.76)$$

4.5 Finite-size systems : RG results and numerical studies

4.5.1 RG results for finite-size scaling properties

Remarkably, the strong disorder RG method does not only give results in the thermodynamic limit, but it yields finite-size properties, as well. We refer the reader to the paper [140], where the strong disorder RG method is used to obtain the statistical properties of the end-to-end spin-spin correlation

$$C(L) \equiv \langle \sigma_1^z \sigma_L^z \rangle \quad (4.77)$$

and of the gap, i.e. the energy difference between the two lowest levels

$$\Delta(L) \equiv E_1 - E_0 \quad (4.78)$$

over the ensemble of random chains of length L .

These results for finite-size systems are important, since they have been tested in details against numerical studies [140, 126]. Moreover, the asymptotic distribution of end-spin magnetization obtained by the RG method [140] is in full agreement with the direct analytical results [271], obtained from the exact formula (4.4).

Finally, the strong disorder RG approach has been further extended in [309] to compute the end-to-end energy-density correlations.

4.5.2 Ensemble dependence of the results

In the study of disordered systems, it is usual to consider that the random variables defining the disorder in a given sample are independent : following [191, 126], this procedure will be called here the “canonical ensemble” (this procedure is also called the “grand-canonical ensemble” in [300, 27, 356, 49]). However, it has been argued in [300] that it is much more interesting in some cases to consider the so called “microcanonical ensemble” as in [191, 126] (this procedure is called the “canonical ensemble” in [300, 27, 356, 49]) : in the microcanonical ensemble, there exists a global constraint on the random variables defining the disorder in a given sample of N sites. On one hand, it has been strongly argued in [300, 49] that the microcanonical ensemble should be preferred to the canonical ensemble, because the latter introduces an “extra noise” that may hid the “intrinsic” properties of the system. On the other hand, if one divides the system of size L into two halves of size $L/2$, each half will present fluctuations of order \sqrt{L} in both ensembles : in the canonical ensemble, these two halves are independent, whereas in the microcanonical ensemble, the two halves are completely correlated, i.e. they have exactly opposite fluctuations. From this point of view, the microcanonical constraint can thus appear to be quite artificial or even biased. Of course, it seems a priori natural to expect that these two ensembles should be equivalent in the thermodynamic limit, as was shown in [27] for the case of a random classical ferromagnet. However, it is clear that their finite-size properties can be very different. But since the finite-size scaling theory of phase transitions relates the thermodynamic exponents to finite-size effects obtained in numerical simulations, the discussion about these two ensembles actually leads to the general problem of the finite-size scaling theory for disordered systems [300, 356, 49].

The finite-size properties of the RTFIC have actually been studied [191, 126, 271] in the canonical ensemble and in the microcanonical ensemble, in which case there is the global constraint on the disorder variables:

$$\sum_{i=1}^L (\ln J_i - \ln h_i) = 0 \quad (4.79)$$

(With one fixed and one free boundary conditions so that there are exactly the same number L of random bonds and random fields). The microcanonical constraint (4.79) has been chosen to impose, in some sense, the criticality condition $[\ln h]_{av} = [\ln J]_{av}$ on finite samples, whereas in the canonical ensemble, the l.h.s. of (4.79) presents fluctuations of order \sqrt{L} around its mean value, zero.

The probability distributions of the appropriate rescaled variables have been analytically computed for the surface magnetization [126, 271], as well as for the gap and the end-to-end correlation via the real space RG method [271] : these distributions are different at criticality in the two ensembles, in particular in their asymptotic behaviors. As a consequence, the size dependences of the averaged observables, are found to be quite different in the two ensembles : these differences can be explained in terms of the rare events that dominate

a given averaged observable, and whose measure can be very sensitive to the microcanonical constraint.

4.5.3 Numerical studies based on free-fermions

Numerical studies of the RTFIC are generally based on the free-fermionic representation, as described in Sec.4.1.1. In this way relatively large systems up to linear size $L \geq 500$ can be studied. Numerical results [362, 190, 191, 195] both at the critical point and in the disordered and ordered Griffiths phases are in good agreement with the strong disorder RG results. Dynamical correlations[312, 363, 195] and their distribution functions[222] as well as thermodynamic quantities[363, 191] have been also investigated.

4.6 Relation with Dirac-type equations with random mass

In a related work the RTFIC and the random XY spin chain is investigated in such a way that the low-energy behavior near the critical point is described by a Dirac-type equation with a random mass for which an exact analytic treatment is possible[254]. Results obtained for the dynamical critical exponent, the specific heat, and transverse susceptibility agree with results of the strong disorder RG. The approach of random Dirac fermions is used also in related problems of quasi-one-dimensional systems[77, 340, 76, 75]

5 Random quantum chains with discrete symmetry

5.1 Quantum Potts and clock models

The Ising model has been generalized for q -state spin variables distinct states: $|s_i\rangle = |1\rangle, |2\rangle, \dots, |q\rangle$ with two different forms of the interaction energy[357]. For the *Potts-model* in 1d it is given by:

$$U_{Potts} = - \sum_i J_i \delta(s_i, s_{i+1}) , \quad (5.1)$$

whereas for the *clock model* it is given in the form of a scalar product

$$U_{clock} = - \sum_l J_l \cos \left[\frac{2\pi}{q} (s_l - s_{l+1}) \right] . \quad (5.2)$$

The two models are equivalent for $q = 2$ (Ising model) and for $q = 3$, but they are different for higher values of q .

The quantum version of the models is obtained analogously to the Ising model (see Sec.18.2.1), by introducing appropriate transverse fields, the corresponding term in the Hamiltonian is denoted by K . K is defined in such a way that the transfer matrix of the classical 2d model, T , and the 1d quantum

Hamiltonian as $H = U + K$ commute at the transition point. In this way the critical properties of the 2d classical and 1d quantum models are isomorph. Explicit way of construction of H and thus K is made in the extreme anisotropic limit[224] of the 2d system, as described for the Ising model in Sec.18.2.1.

The transverse-field term in the Potts model is given by[333]:

$$K_{Potts} = - \sum_l \frac{h_l}{q} \sum_{k=1}^{q-1} M_l^k, \quad (5.3)$$

where $M_l|s_l\rangle = |s_l + 1, \text{mod } q\rangle$. For the clock model one obtains[205]:

$$K_{clock} = - \sum_l \frac{h_l}{2} (M_l + M_l^{-1}). \quad (5.4)$$

Both models are invariant under the duality transformation, $J_i \leftrightarrow h_i$. From this follows that the non-random models with $J_l = J$ and $h_l = h$ have a self-duality point located at $h = J$. In the non-random Potts model there is one phase transition point, which is just the self-duality point, which separates the disordered and the ordered phases. The phase transition is second order for $q \leq 4$ and first order for $q > 4$ [45]. In the non-random clock model there is also one phase transition point for $q \leq 4$. For $q > 4$, however, there are three phases in the system, the ordered and disordered phases are separated by an extended critical region, which is the precursor of the low-temperature phase of the XY-model, obtained in the limit $q \rightarrow \infty$.

5.2 Ashkin-Teller model

The quantum Ashkin-Teller model is defined by the Hamiltonian[37]:

$$\begin{aligned} H_{AT} = & - \sum_l J_l (\sigma_l^z \sigma_{l+1}^z + \tau_l^z \tau_{l+1}^z) - \sum_l h_l (\sigma_l^x + \tau_l^x) \\ & - \epsilon \sum_l (J_l \sigma_l^z \sigma_{l+1}^z \tau_l^z \tau_{l+1}^z + h_l \sigma_l^x \tau_l^x), \end{aligned} \quad (5.5)$$

in terms of two sets of Pauli matrices, $\sigma_l^{x,z}, \tau_l^{x,z}$. Here the couplings, J_l , and the transverse fields, h_l , are independent random variables, while the coupling between the two Ising models, ϵ , is disorder independent. The Hamiltonian in Eq. (5.5) is invariant under the duality transformation $J_l \leftrightarrow h_l$.

The non-random model is critical along the self-duality line, $J = h$, for $-1 < \epsilon \leq 1$ with the critical exponents $x_{AT} = 1/8$, $x_{AT}^s = \arccos(-\epsilon)/\pi$, whereas $\nu_{AT} = 2x_{AT}^s/(4x_{AT}^s - 1)$ for $-1/\sqrt{2} < \epsilon < -1/2$, and, in the *critical fan*[37] for $-1 < \epsilon < -1/\sqrt{2}$, ν_{AT} is formally infinity.

5.3 Decimation equations

In the random models, in which the couplings, J_i , and the transverse fields, h_i , are independent and identically distributed random variables, one can perform

the strong disorder RG transformation. The renormalization equations, which are obtained by decimating a strong coupling, $J_2 = \Omega$, or a strong transverse field, $h_2 = \Omega$, can be obtained analogously to the RTFIC. Repeating the steps described in Sec.4.2 we arrive for all the three models to the same form of equations[327, 86]:

$$\tilde{h}_{23} = \kappa \frac{h_2 h_3}{J_2}, \quad \tilde{J}_{23} = \kappa \frac{J_2 J_3}{h_2}, \quad (5.6)$$

where the first (second) equation refers to the elimination of a strong bond (field). The value of the prefactor, κ , which for the RTFIC is $\kappa = 1$, for the different models are the following:

$$\kappa_{Potts} = \frac{2}{q}, \quad \kappa_{Clock} = \frac{1 + \delta_{2,q}}{1 - \cos(2\pi/q)}, \quad \kappa_{AT} = \frac{1}{1 + \epsilon}. \quad (5.7)$$

For the Potts and clock models q does not renormalize under the transformation, whereas for the Ashkin-Teller model we have $\tilde{\epsilon} = \epsilon^2(1 + \epsilon)/2$. The control-parameter of the random models, δ , can be defined in the same form as for the RTFIC in Eq.(4.5), and the self-dual point of the models is at $\delta = 0$. We note that the decimation equations for the random contact process (directed percolation) in Eq.(17.7) are in the same form as in Eq.(5.6) with $\kappa = \sqrt{2}$, this model, however, does not have the property of self duality.

5.4 Disorder induced cross-over effects

The renormalization equations in Eq.(5.6) have different characteristics for $\kappa \leq 1$ and for $\kappa > 1$, respectively. In the former case, including the RTFIC, the generated new terms in the Hamiltonian are smaller than the decimated ones, thus during renormalization the energy scale is monotonously decreasing. In this case the fixed point of the problem is expected to be strongly attractive, i.e. the critical behavior is the same for any weak disorder. This type of universality has been demonstrated for the RTFIC [138]. On the contrary for $\kappa > 1$ some generated new terms of the Hamiltonian are larger than the decimated one, thus the decrease of the energy scale is non-monotonic. In this case the behavior of the system for sufficiently weak disorder (when the non-monotonic steps in the energy renormalization are frequent) and for sufficiently strong disorder (when the non-monotonic steps are rare and their fraction is vanishing as the renormalization goes on) are expected to be different. The strong disorder RG is valid in this second region, what we will discuss in the following. The weak disorder region will be considered afterwards.

Strong disorder regime

Here we assume that after the starting decimation steps, when the energy scale can behave non-monotonically, we arrive to the stable, attractive part of the RG trajectory, which is controlled by an infinite disorder fixed point. The RG equations of the distribution function are very similar to that of the RTFIC, as described in Sec.4.3.1. Using the same notations as for the RTFIC

the relation in Eq.(4.19) is modified to:

$$\begin{aligned} \frac{dR_0}{d\Omega} &= R_0(J, \Omega) [P_0(\Omega, \Omega) - R_0(\Omega, \Omega)] \\ &- P_0(\Omega, \Omega) \int_{J/\kappa}^{\Omega} dJ' R_0(J', \Omega) R_0\left(\frac{J}{J'\kappa} \Omega, \Omega\right) \frac{\Omega}{J'\kappa}, \end{aligned} \quad (5.8)$$

and similarly for the distribution $P_0(h, \Omega)$. Solution of these equations at the fixed point are still in the form of Eqs.(4.21) and (4.22), however for a finite δ one can not proceed via Eq.(4.23). Thus outside the critical point ($\delta \neq 0$) one can not obtain an asymptotically exact analytical solution, for $\kappa \neq 1$. At the critical point, however, the solution in Eq.(4.25) stays valid. This is due to the fact that the scaling variable in the solution in Eq.(4.25), η , is modified by an additive term, $\ln \kappa / \ln \Omega$, which goes to zero at the fixed point.

As a consequence for strong enough disorder the critical behavior of all these models (together with the random contact process in Sec.17.2) is controlled by the infinite disorder fixed point of the RTFIC, thus they have the same critical exponents, scaling functions, etc. This universality has been numerically checked on different models[85, 86].

In the ordered and disordered Griffiths phases, in which no analytical solution can be found a weak universality hypotheses is suggested[197]. Two (self-dual) models which are described by the same decimation rules, thus they have the same value of κ , have the same value of the dynamical exponent for the same form of disorder. This conjecture is based on scaling theory of rare events and has been numerically checked[197] on the examples of the $q = 4$ state Potts model and the dimerized AF Heisenberg chain (see Sec.6.2, for both $\kappa = 1/2$).

Weak and intermediate disorder regimes

For weak disorder the first question one can pose is the relevance or irrelevance of the perturbation caused by weak disorder at the fixed point of the non-random model. In this respect one generally invokes the Harris criterion [165, 96] according to which weak disorder is irrelevant if:

$$\nu_0 > 2/d, \quad (5.9)$$

where ν_0 is the correlation length critical exponent of the pure system. In the models we consider here having $\kappa < 1$ the correlation length exponent satisfies the relevance criterion, $\nu_0 < 2/d$. Thus the strong disorder fixed point is probably strongly attractive as for the RTFIC.

The behavior is different of systems with $\kappa > 1$, which corresponds to the Potts-model with $q < 2$, such as the classical 2d percolation ($q = 1$) with correlated (layered) disorder, or to the clock-model with $q > 4$, or the Ashkin-Teller model for $\epsilon < 0$. (To this group belongs also the random contact process as described in Sec.17.2.) Now, depending on the sign of $\nu_0 - 2/d$ different scenarios could happen.

For irrelevant weak disorder, $\nu_0 > 2/d$, which is realized in the clock model for $q > 4$ and in the Ashkin-Teller model with $-1 < \epsilon < -1/2$ the critical

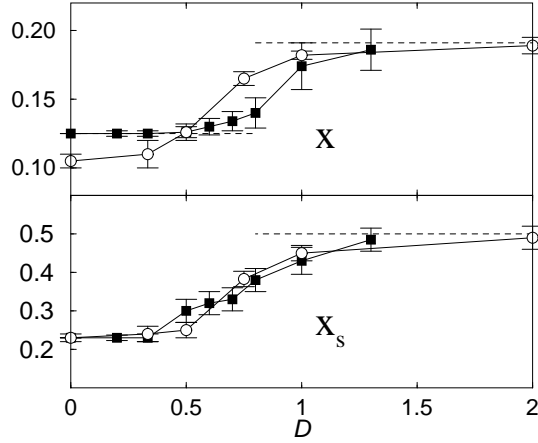


Figure 2: Scaling exponents of the average bulk and surface magnetization as a function of the strength of disorder for the $q = 5$ clock model (\circ) and for the Ashkin-Teller model with $\epsilon = -0.75$ (\blacksquare). The limiting values of the exponents, corresponding to that of the infinite disorder fixed point are denoted by dashed lines.[86]

behavior is expected to be the same as in the pure system if the strength of disorder, D , is smaller than a finite limiting value, D_0 , $0 < D < D_0$. The strength of disorder is characterized by the variance of the initial probability distributions of the couplings and the transverse fields, and directly given by the parameter, D , of a power-law distribution, $P(\lambda) = D^{-1}\lambda^{-1+1/D}$. see in Eq.(A.1). Increasing the strength of disorder over D_0 the critical behavior is controlled by a new fixed point. According to numerical investigations[86] there is a line of conventional random fixed points (see Appendix A.2 in the range of disorder: $D_0 < D < D_\infty$). In this region, which is called the intermediate disorder regime the magnetization critical exponents, such as x_m and x_m^s , are disorder dependent and also the disorder induced dynamical exponent, z' , is a continuous function of D . (The true dynamical exponent is given by $\max(z_0, z')$, where $z_0 = 1$ is the dynamical exponent due to pure quantum fluctuations.) On the other hand the energy density, according to numerical studies[86], is a marginal operator so that the correlation length critical exponent is $\nu = 2$, which is just the borderline case of the Harris-criterion in Eq.(5.9). As the upper critical value of the disorder, D_∞ , is approached the dynamical exponent starts to diverge, $1/z \rightarrow 0$, and at the same time the magnetization exponents reach their value in the infinite disorder fixed point. For $D > D_\infty$ we arrive at the attractive region of the strong disorder fixed point.

For relevant weak disorder (but with $\kappa > 1$), which is realized for 2d percolation with correlated disorder, or in the Ashkin-Teller model with $-1/2 < \epsilon < 0$, first one enters for $0 < D < D_\infty$ into the intermediate disorder regime and for $D > D_\infty$ into the strong disorder regime. This type of scenario is checked nu-

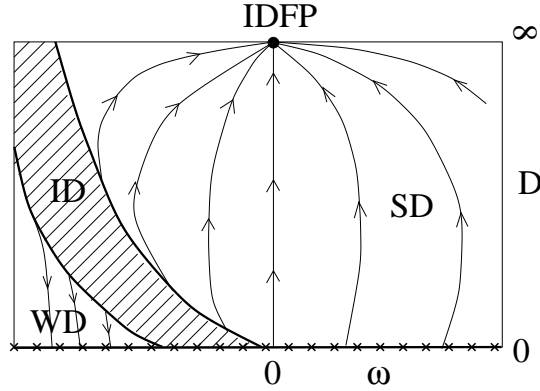


Figure 3: Schematic RG phase diagram of a quantum spin system having a critical line parameterized by ω , in the presence of disorder of strength, D . [86]

merically for the percolation problem [208], see Sec. 18.2.2. Note, however, that the contact process, which has anisotropic scaling behavior in the non-random case, in the intermediate disorder regime show such a scaling behavior which could be of infinite disorder type with varying exponents, see Sec. 17.2.3.

A schematic phase diagram of the disorder induced cross-over effects can be found in Fig. 3. Here the model dependent parameter, ω , is given by: $\omega = \epsilon$ for the Ashkin-Teller model, $\omega = 4 - q$ for the clock model and $\omega = q/2 - 1$ for the quantum Potts model. For $\omega \geq 0$ the system is in the strong disorder (SD) phase, where the infinite disorder fixed point (IDFP) is strongly attractive. In the other part of the phase diagram, for $\omega < 0$, there are two more phases: the weak disorder (WD) and the intermediate disorder (ID) regions. Here the SD part of the phase diagram is attracted by the IDFP, while the critical behavior in the WD regime is governed by the fixed points of the pure system, which are located at $D = 0$. In the ID regime, where there is a competition between quantum fluctuations and disorder effects, dynamical scaling is anisotropic, $1 < z < \infty$, and the static and dynamical critical exponents are disorder dependent. At the boundaries of the ID region there are $1/z = 0$ and $1/z = 1$, respectively, while at $D = 0$, i.e. in the pure system limit they are at $\omega = 0$ and $\omega = \omega_0$. In the latter case for the pure model with a parameter ω_0 the Harris criterion in Eq. (5.9) is saturated, i.e. $\nu_0(\omega_0) = 2/d$.

We note that disorder induced cross-over effects are also present in higher spin random AF Heisenberg chains. The scenario in these systems is, however, somewhat different, see in Sec. 7 and 8.1.

6 Random $S = 1/2$ AF Heisenberg chains

6.1 Models

The Heisenberg model has been introduced to describe the basic features of interacting localized magnetic moments. Most generally, with random couplings and anisotropy, the model is described by the Hamiltonian:

$$H_H = \sum_l (J_l^x S_l^x S_{l+1}^x + J_l^y S_l^y S_{l+1}^y + J_l^z S_l^z S_{l+1}^z) , \quad (6.1)$$

in terms of the spin-1/2 operators, $S_i^{x,y,z}$, at site i . For terminology, the models for different anisotropies are respectively called :

$$\begin{aligned} XYZ\text{-model} : J_l^x &\neq J_l^y \neq J_l^z \\ XXZ\text{-model} : J_l^x &= J_l^y \equiv J_l^\perp \neq J_l^z \\ XXX\text{-model} : J_l^x &= J_l^y = J_l^z \\ XY\text{-model} : J_l^x &\neq J_l^y \text{ and } J_l^z = 0 \text{ for any } l \\ XX\text{-model} : J_l^x &= J_l^y \text{ and } J_l^z = 0 \text{ for any } l \end{aligned}$$

Generally we consider the situation when the sign of the J_l^x couplings is the same, and the same is true for the y and z components, as well. Then rotating spins around the z -axis one can always take $J_l^x > 0$ and $J_l^y > 0$, so that the sign of J_l^z characterizes the model: for $J_l^z > 0$ it is antiferromagnetic and for $J_l^z < 0$ it is ferromagnetic.

The pure system with $J_l^x = J^x, J_l^y = J^y$ and $J_l^z = J^z$ has a reach phase diagram[44] with four ordered phases (z -ferromagnet, z -antiferromagnet, x -antiferromagnet and y -antiferromagnet) which are separated by phase boundaries in which there is quasi-long-range order (QLRO). For example for the XXZ chain with $J^x = J^y = J^\perp$ we have $G^\alpha(r) \sim (-1)^r r^{-\eta_\alpha}$, ($\alpha = x, z$), where the decay exponents are coupling dependent and given by[246]:

$$\eta_x = \frac{1}{\eta_z} = 1 - \frac{1}{\pi} \arccos \Delta . \quad (6.2)$$

with $1 \geq \Delta = J^z/J^\perp \geq -1$.

Dimerization

The isotropic antiferromagnetic chains, i.e. the XXX and XX models are at the phase boundary and they exhibit QLRO. They can be driven out of their critical state, which is gapless, by introducing alternating bond strengths for even (J_e) and odd (J_o) bonds. The corresponding control parameter is the dimerization, which is defined by:

$$d = \frac{J_e - J_o}{J_e + J_o} . \quad (6.3)$$

(For the XXZ -chain one can work similarly by keeping the same J^\perp/J^z on even and odd bonds.) In the dimerized phase we define the *string correlation function*:

$$O^z(r) = -4 \langle S_l^z \exp [i\pi (S_{l+1}^z + S_{l+2}^z + \dots + S_{l+r-1}^z)] S_{l+r}^z \rangle . \quad (6.4)$$

which can be written for spin-1/2 operators and for r odd as:

$$O^z(r) = 2^{r+1} \langle S_l^z S_{l+1}^z \dots S_{l+r}^z \rangle . \quad (6.5)$$

Here we used the identity: $S^z = \exp(i\pi S^z)/2i$, which follows immediately by considering its action on the full basis states $|\uparrow\rangle, |\downarrow\rangle$. The expression in Eq.(6.5) can be simplified further in terms of dual spin operators[196], $\tilde{S}_{l+1/2}^x = S_1^z S_2^z \dots S_{l+1}^z$, and one obtains:

$$O^z(r) = 4 \langle \tilde{S}_{l+1/2}^x \tilde{S}_{l+r+1/2}^x \rangle , \quad (6.6)$$

thus in an obvious notation $O^z(r) = 4\tilde{G}^x(r)$. In a dimerized state $O^z(r)$ is different for l even ($O_e^z(r)$) and l odd ($O_o^z(r)$), and the order is measured as:

$$O_d^z(r) = O_o^z(r) - O_e^z(r) , \quad (6.7)$$

and one should take the limiting value: $\lim_{r \rightarrow \infty} O_d^z(r)$.

6.2 RG rules

The renormalization method of Ma, Dasgupta and Hu[248] is originally developed for the random antiferromagnetic $S = 1/2$ chain. Here we consider the general XYZ -chain, in which a unit of four spins contains the strongest bond of the chain, $J_2 = \Omega$, between the two central ones.

In the limit, $J_1/J_2 = J_3/J_2 = 0$, the ground state for $J_2^z \geq 0$ is a singlet having the energy: $E_0 = -(J_2^x + J_2^y + J_2^z)/4$, which is shifted by $\Delta E_0^{\uparrow\uparrow} \approx -(J_1^z - J_3^z)^2/8(J_2^x + J_2^y)$ if the J_1 and J_2 couplings are switched on and the two edge spins are fixed into parallel, $(\uparrow\uparrow)$, states. For antiparallel states, $(\uparrow\downarrow)$, one obtains $\Delta E_0^{\uparrow\downarrow} \approx -(J_1^z + J_3^z)^2/8(J_2^x + J_2^y)$, which is the consequence of the transformation $J_3^z \rightarrow -J_3^z$. Decimating out the strongest bond, J_2 , in the renormalized Hamiltonian the z -component of the generated new coupling between sites 1 and 4 is given as:

$$\tilde{J}_{14}^z = 2 \left(E_0^{\uparrow\uparrow} - E_0^{\uparrow\downarrow} \right) = \frac{J_1^z J_3^z}{J_2^x + J_2^y} . \quad (6.8)$$

Similarly, by rotating the spins as $S^x \rightarrow S^y$, $S^y \rightarrow S^z$ and $S^z \rightarrow S^x$, etc. we get for the other components of the renormalized coupling as:

$$\tilde{J}_{14}^x = \frac{J_1^x J_3^x}{J_2^y + J_2^z}, \quad \tilde{J}_{14}^y = \frac{J_1^y J_3^y}{J_2^z + J_2^x} . \quad (6.9)$$

In the special case of the XXX -model with $J_l^x = J_l^y = J_l^z = J_l$ we have

$$\tilde{J} = \frac{\tilde{J}_1 \tilde{J}_3}{2\tilde{J}_2}, \quad XXX - \text{model} , \quad (6.10)$$

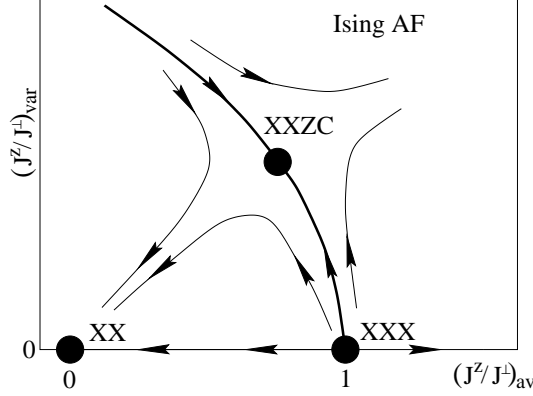


Figure 4: Schematic RG phase diagram of the random XXZ chain as obtained in Ref.[139].

whereas for the XX -model with $J_l^x = J_l^y = J_l$ and $J_l^z = 0$ we obtain:

$$\tilde{J} = \frac{\tilde{J}_1 \tilde{J}_3}{\tilde{J}_2}, \quad \tilde{J}^z = 0, \quad XX - \text{model} . \quad (6.11)$$

Note, that both for the XXX and the XX models the generated new coupling is smaller than the decimated bond, therefore the energy-scale, Ω , gradually decreases during the renormalization process.

6.3 RG detailed results

The phase diagram of the random XXZ chain, as studied in detail in [139], depends on the relative strength of the couplings, J^\perp and J^z . If J^\perp dominates the ground state of the system is composed of singlets (random singlet (RS) phase). On the other hand if J^z dominates in the ground state of the system there is Ising antiferromagnetic (IAF) order, but due to randomness the gap is vanishing, thus the system is in an IAF-ordered Griffiths phase. The schematic RG phase diagram as obtained by Fisher [139] is shown in Fig.4.

It contains three RS fixed points, among which the RG equations have been solved for the random XX and XXX models[139].

6.3.1 Renormalization of the random XX chain

The decimation equation in Eq.(6.11) are in a simple additive form

$$\tilde{\xi} = \tilde{\xi}_1 + \tilde{\xi}_3 , \quad (6.12)$$

in terms of the logarithmic variables: $\xi = \ln(\Omega/J)$, $0 < \xi < \infty$. Here we have used that $\tilde{\xi}_2 = 0$, since $J_2 = \Omega$ being the strongest coupling of the chain. We are looking for the probability distribution $\rho(\xi, \Gamma)$ of the variable ξ at a log-energy

scale $\Gamma = -\ln \Omega$. By decimating out bonds we change the scale as $\Gamma \rightarrow \Gamma + d\Gamma$, which amounts of a change as $\xi \rightarrow \xi - d\Gamma$, thus

$$\rho(\xi, \Gamma)|_{\Gamma=\Gamma+d\Gamma} = \rho(\xi, \Gamma) + \frac{\partial \rho}{\partial \Gamma} d\Gamma - \frac{\partial \rho}{\partial \xi} d\Gamma. \quad (6.13)$$

This variation can also be written into the form of a rate equation: the distribution function $\rho(\xi, \Gamma)$ is reduced due to the eliminated couplings ξ_1 and ξ_3 , but is increased due to the generated one with $\xi_1 + \xi_3$:

$$\begin{aligned} \rho(\xi, \Gamma)|_{\Gamma=\Gamma+d\Gamma} = & \left\{ \rho(\xi, \Gamma) + d\Gamma \rho(0, \Gamma) \int_0^\infty d\xi_1 \int_0^\infty d\xi_3 \rho(\xi_1, \Gamma) \rho(\xi_3, \Gamma) \right. \\ & \times [\delta(\xi - \xi_1 - \xi_3) - \delta(\xi - \xi_1) - \delta(\xi - \xi_3)] \left. \right\} [1 - 2d\Gamma \rho(0, \Gamma)]^{-1}. \end{aligned} \quad (6.14)$$

Here the last factor in the r.h.s. is to ensure normalization since the total number of bonds is reduced by a fraction of $2d\Gamma \rho(0, \Gamma)$ during renormalization. Comparing Eq.(6.13) with Eq.(6.14) and changing the notation as $\xi_1 \rightarrow \xi_-$ and $\xi_3 \rightarrow \xi_+$ we arrive to the integral-differential equation:

$$\frac{\partial \rho(\xi, \Gamma)}{\partial \Gamma} = \frac{\partial \rho(\xi, \Gamma)}{\partial \xi} + \rho(0, \Gamma) \int_0^\infty d\xi_- \int_0^\infty d\xi_+ \rho(\xi_-, \Gamma) \rho(\xi_+, \Gamma) \delta(\xi - \xi_- - \xi_+). \quad (6.15)$$

The solution of Eq.(6.15) is tried in the form:

$$\rho(\xi, \Gamma) = \frac{1}{\Gamma} Q(\xi/\Gamma, \Gamma), \quad (6.16)$$

which leads to the equation in terms of the variable $\eta = \xi/\Gamma$ as:

$$\Gamma \frac{\partial Q(\eta, \Gamma)}{\partial \Gamma} = \frac{\partial Q(\eta, \Gamma)}{\partial \eta} (1 + \eta) + Q(\eta, \Gamma) + Q(0, \Gamma) \int_0^\eta d\eta' Q(\eta', \Gamma) Q(\eta - \eta', \Gamma), \quad (6.17)$$

We are looking for the fixed point solution of this equation, $Q^*(\eta)$, which does not depend on Γ , thus the l.h.s. of Eq.(6.17) is zero. After Fisher[139], for non-singular initial distributions the fixed point solution is characterized by the initial value $Q^*(0) = 1$, when it is given as:

$$Q^*(\eta) = \Theta(\eta) e^{-\eta}, \quad (6.18)$$

where $\Theta(\eta)$ is the Heaviside step-function: $\Theta(\eta) = 0$, for $\eta < 0$ and 1 for $\eta \geq 0$. Note that the fixed point distribution of the couplings is identical to that of the RTFIC in Eq.(4.25), which is due to an exact mapping between the two models, as described in Sec.B.2.

Transforming the solution in Eq.(6.18) in terms of the original variables J and Ω we obtain:

$$P(J, \Omega) = \frac{1}{\Omega \Gamma} \left(\frac{\Omega}{J} \right)^{1-1/\Gamma} \Theta(\Omega - J), \quad \Gamma = -\ln \Omega, \quad (6.19)$$

which becomes singular at the fixed point, as $\Gamma \rightarrow \infty$. Due to this singularity the decimation transformation in Eq.(6.11) becomes exact at the fixed point. This can be shown by calculating the probability that one of the neighboring couplings, beside the strongest bond with $\tilde{J} = \Omega$, has a value of $J > \alpha\Omega$, with $\alpha < 1$:

$$P(\alpha) \simeq \int_{\alpha\Omega}^{\Omega} P(J, \Omega) dJ = \frac{1}{\Gamma} \int_{\alpha}^1 x^{-1+1/\Gamma} dx = 1 - \alpha^{1/\Gamma} \approx \frac{1}{\Gamma} \ln(1/\alpha), \quad (6.20)$$

which indeed goes to zero as the iteration proceeds, since $\Gamma \rightarrow \infty$. Consequently the RG transformation becomes asymptotically exact in a similar way as shown for the RTFIC in Sec.4.3.3.

6.3.2 Renormalization of the random XXX chain

The decimation transformations of the XX and the XXX models in Eqs.(6.10) and (6.11), respectively differ by a constant factor of 2. As a consequence the derivation of the probability distribution in the previous Section is changed at the following points:

- i) the decimation transformation in Eq.(6.12) is extended by a term $\ln 2$ at the r.h.s.,
- ii) the argument of the first delta-function on the r.h.s. of Eq.(6.14) is extended by a term $-\ln 2$,
- iii) the integral in the r.h.s. of Eq.(6.17) is modified as

$$\int_0^{\eta-\Delta} d\eta' Q(\eta', \Gamma) Q(\eta - \Delta - \eta', \Gamma), \quad (6.21)$$

where $\Delta = \ln 2/\Gamma$.

As the renormalization proceeds $\Gamma \rightarrow \infty$ and so $\Delta \rightarrow 0$, thus the RG equation in Eq.(6.17) becomes identical to that of the XX model and consequently the limiting distributions of the two models are the same. Note that the reasoning used here is analogous to that presented in Sec.5.4 for quantum spin models with discrete symmetry.

6.3.3 Properties of the random-singlet phase

The ground state of the random XX (and XXX) models by construction of the strong disorder RG method is composed of singlet pairs. The two spins of a pair can be arbitrarily remote and the effective interaction between them is rapidly decreasing with the distance. In this random-singlet phase relation between energy-scale, $\Omega = e^{-\Gamma}$, and length-scale, $L_\Gamma \sim 1/n_\Gamma$, where n_Γ is the fraction of non-decimated spins, can be obtained along the lines of Sec.4.3.4. As Γ is increased by an amount of $d\Gamma$ (i.e. $\Omega \rightarrow \Omega(1 - d\Gamma)$) a fraction of spins $2d\Gamma\rho(0, \Gamma)$ is decimated out, thus $dn_\Gamma = -2d\Gamma\rho(0, \Gamma)n_\Gamma$. Now using Eq.(6.16) and with the fixed-point solution in Eq.(6.18) we arrive to the differential equation:

$$\frac{dn_\Gamma}{d\Gamma} = -2 \frac{Q^*(0)}{\Gamma} n_\Gamma, \quad (6.22)$$

with the solution, $n_\Gamma = \Gamma^{-2Q^*(0)} = \Gamma^{-2}$, at the fixed point. Consequently the typical distance between remaining spins is

$$L_\Gamma \sim \frac{1}{n_\Gamma} \sim \Gamma^2 \sim \left[\ln \frac{\Omega_0}{\Omega} \right]^2, \quad (6.23)$$

where Ω_0 is some reference energy cut-off. This is the usual form of dynamical scaling at an infinite disorder fixed point, see in Sec.A.3.

The *low-temperature susceptibility* can be estimated by studying the response of the system on external fields for different ratios of the thermal energy, $\sim T$, and the energy scale, Ω . In the low-temperature case, $\Omega \gg T$, the strongly coupled singlet pairs are very weakly excited by thermal fluctuations. In the opposite limit, $\Omega \ll T$, the remaining non-decimated spins are very weakly coupled, since $\tilde{J} \ll T$, and therefore they are essentially free and contribute to a Curie susceptibility, which goes as $\sim 1/T$. Then one should stop the renormalization at $\Omega = T$, when the remaining spins with a density of, $n_{\Gamma_T} \sim [\ln(\Omega_0/T)]^2$, all contribute by a Curie susceptibility leading to the result:

$$\chi_\perp \sim \chi_z \sim \frac{n_{\Gamma_T}}{T} \sim \frac{1}{T [\ln \frac{\Omega_0}{T}]^2}. \quad (6.24)$$

Note that the transverse and longitudinal susceptibilities have the same singular behavior where the Curie-type susceptibility is modified by logarithmic corrections. Since these corrections are very strong they usually lead in measurements effective, temperature dependent critical exponents.

The *average pair correlation function* between two spins at a distance, $r \sim L$, is dominated by those spins which have not been decimated out at a length-scale, L . The decimated spins already form singlets and correlation between two spins which belong to different singlets is negligible. The probability to have a free spin at this length-scale is $n_{\Gamma_L} \sim 1/L$, for two spins it is $(n_{\Gamma_L})^2 \sim 1/L^2$. Then, under further decimation, there is a finite probability that these two spins form a singlet, thus will have a correlation $C(r) = O(1)$. Averaging the correlations over the spin-pairs with a mutual distance, r , we obtain:

$$[C(r)]_{\text{av}} \sim \frac{(-1)^r}{r^2}. \quad (6.25)$$

If we consider two randomly chosen spins at a distance r they typically belong to different singlet pairs and the correlations between them, the *typical correlations* are very weak. If during decimation the length-scale is $L = r$, then the two spins becomes nearest neighbors with an effective coupling, $\tilde{J}_L \sim \Omega_L$, which measures the size of correlations. Thus we have

$$-\ln C^{\text{typ}}(r) \sim \ln \Omega_L \sim \Gamma_L^{-1} \sim \frac{1}{L^{1/2}} \sim \frac{1}{r^{1/2}}, \quad (6.26)$$

which is completely different from its average value in Eq.(6.25). Thus the correlation function in the RS phase is non-self-averaging.

6.3.4 Properties of the random dimer phase

Here we consider the random XX and XXX chains with enforced dimerization, see Sec. 6.1, when couplings at odd, J_o , and even, J_e , sites are taken from different distributions. For the random model the control parameter is defined as:

$$\delta = \frac{[\ln J_o]_{av} - [\ln J_e]_{av}}{\text{var}[\ln J_o] + \text{var}[\ln J_e]} , \quad (6.27)$$

thus for $\delta > 0$ ($\delta < 0$) the odd (even) bonds are stronger in average. Outside the quantum critical point we are in the random dimer phase, which is a Griffiths phase of the system[185].

For the random XX chain the distribution of the odd and even couplings at the fixed point can be exactly obtained[196] through the mapping to the RTFIC in Sec.B.2. With this help results in Sec. 4.3.2 can be translated to the random dimer phase, too. In particular the dynamical exponent, z , is given from Eq.(4.15) as

$$\left[\left(\frac{J_o}{J_e} \right)^{1/z} \right]_{av} = 1 . \quad (6.28)$$

which is related to δ , as $z \approx 1/2|\delta|$ in linear order.

For the random XXX model the dynamical exponent in the random dimer phase is not known exactly. Here there is a conjecture[197] that dynamical exponents for the random dimerized XXX chain and for the random $q = 4$ state quantum Potts models with the same disorder distribution are identical. This is based on the same form of the decimation equations see in Sec. 5.4 and on scaling theory, which has been checked by numerical calculations[197].

Scaling of the thermodynamic quantities can be obtained along the lines as described for the RTFIC in Sec.4.4.2. In this respect the random dimer phase of the random AF Heisenberg chain corresponds to the disordered Griffiths phase of the RTFIC. For example the same reasoning as for Eq.(4.56) leads to the low-temperature susceptibility:

$$\chi(T) \sim T^{-1+1/z} , \quad (6.29)$$

whereas the singularity of the specific heat from Eq.(4.51) follows as:

$$c_V(T) \sim T^{1/z} . \quad (6.30)$$

6.3.5 Renormalization of dynamical correlations

The average autocorrelation functions both in the random singlet and in the random dimer phases are obtained by the strong disorder RG method[108, 277] in the same way as for the RTFIC in Sec.4.4.3. One calculates the local dynamical susceptibilities,

$$\chi_{jj}^{\alpha\alpha}(\omega) = \sum_k |\langle k | S_j^\alpha | 0 \rangle|^2 \delta(\omega - \epsilon_k) , \quad (6.31)$$

with $\alpha = x, z$. The low-frequency behavior of $\chi_{jj}^{\alpha\alpha}(\omega)$ is related to the long-time limit of the corresponding autocorrelation function:

$$G_{jj}^{\alpha\alpha}(t) = \langle S_j^\alpha(t) S_j^\alpha(0) \rangle . \quad (6.32)$$

Repeating the steps of the calculation for the RTFIC in Sec.4.4.3 we obtain for the local dynamical susceptibilities:

$$[\chi]_{\text{av}}(\omega) \sim \frac{n_\omega(p_0^o(\omega) + p_0^e(\omega))(\omega)}{\omega} , \quad (6.33)$$

which is valid in leading order both for $\alpha = x$ and $\alpha = z$. Here $p_0^o(\omega)$ and $p_0^e(\omega)$ (“o” and “e” for odd and even bonds, respectively) are parameters of the fixed-point solution of the RG equations, which corresponds to $p_0(\omega)$ and $r_0(\omega)$, respectively, in the solution of the RTFIC in Sec.4.3.2. see the mapping in Sec.B.2.

In RS phase with $p_0^o(\omega) = p_0^e(\omega)$ we obtain:

$$[\chi]_{\text{av}}(\omega) \sim \frac{1}{\omega |\ln \omega|^3} , \quad (6.34)$$

and

$$G(t) \sim |\ln t|^2 . \quad (6.35)$$

This corresponds to the scaling result in Eq.(A.24) with $x_m/\psi = 2x_m = 2$, where we have used Eq.(6.25) for the average correlation function.

In the random dimer phase the results are:

$$[\chi]_{\text{av}}(\omega) \sim \text{frac}|\delta|^3 \omega^{1-1/z} , \quad (6.36)$$

and

$$G(t) \sim |\delta|^{4-\phi} \frac{|\ln t|}{t^{1/z}} , \quad (6.37)$$

in agreement with the scaling results in Sec.A.4. Dynamical correlations at the boundary spin can be calculated similarly, see Ref.[108, 277].

Another investigations and numerical studies The random XX and XY chains can be transformed into free fermion models, from which some exact results have been obtained[196]. Identifying the rare events the scaling behavior of the bulk and boundary order parameter has been obtained from which the asymptotic decay of the bulk and the end-to-end correlations follows.

Numerical study of the XX and XY models based on the free fermion mapping has given support to the validity of the strong disorder RG results[166, 196]. On the other hand numerical investigation of the random XXZ -chains, which has been done by the DMRG method and thus restricted to comparatively smaller sizes, has found some discrepancies with the strong disorder RG results[163]. These are debated in[227] and attributed to the presence of possible logarithmic corrections[196] or to cross-over effects[227]. Scaling of the spin stiffness in random-1/2 chains has been studied recently[228].

The scaling behavior of typical autocorrelations and their distribution function have been studied in Ref.[196]. In the random singlet phase typical autocorrelations decay algebraically, $G^{typ}(t) \sim t^{-\gamma}$, with a varying parameter, γ . The appropriate scaling combination is thus $\gamma = -\ln G(t)/\ln t$, which has a small γ behavior as $P(\gamma) = A + B\gamma + O(\gamma^2)$. On the other hand in the random singlet phase typical autocorrelations are in a stretched exponential form: $G^{typ}(t) \sim \exp(-\gamma' t^{1/(z+1)})$, thus the appropriate scaling combination is $\gamma' = -\ln G(t)/t^{1/(z+1)}$. The distribution function $P'(\gamma')$ is analyzed in Ref.[196], by making use of similar results about the RTFIC[222].

7 Random $S = 1$ AF Heisenberg chain

7.1 The antiferromagnetic chain $S = 1$ without disorder

Differences between half-integer and integer spin chains

Whereas the pure antiferromagnetic chain $S = 1/2$ presents power-law correlations and excitations without gap, the antiferromagnetic chain $S = 1$ is characterized by exponential correlations and a gap for excitations. A simple way to understand these differences which more generally exist between half-integer and integer spin chains is related to the “Valence-Bond-Solid” (VBS) wavefunction, which allows to highlight a long range order for a topological order parameter which is non-local in terms of the spins.

The VBS wavefunction

If one represents each spin $S = 1$ like the symmetrization of two elementary spins $S = 1/2$, the VBS wavefunction [25] is the state where there exists a singlet on each bond between two constitutive spins $1/2$ (see Figure 5). This wave function is the exact ground state of the Hamiltonian [25]

$$H_{AKLT} = \sum_i P_2(\vec{S}_i + \vec{S}_{i+1}) = \sum_i \left[\frac{1}{2} \vec{S}_i \vec{S}_{i+1} + \frac{1}{6} (\vec{S}_i \vec{S}_{i+1})^2 + \frac{1}{3} \right] \quad (7.1)$$

where P_2 is the projector on the subspace $s = 2$.

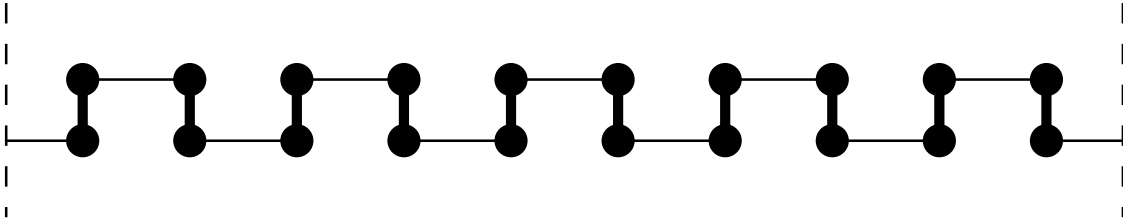


Figure 5: VBS wavefunction: each spin $S = 1$ is represented by the symmetrization of 2 spins $S = 1/2$ (black balls connected by a fat vertical bond); the horizontal lines which connect two spins $1/2$ represent the singlets between constitutive spins $S = 1/2$.

The String Order Parameter

The so called ‘String Order Parameter’ [288] which allows to characterize the topological order of the VBS wave function is non local in the spins

$$t_{ij} = -\langle \psi_0 | S_i^z \exp \left[i\pi \sum_{i < k < j} S_k^z \right] S_j^z | \psi_0 \rangle \quad (7.2)$$

(Note that this definition corresponds to Eq.(6.4), which was analyzed for the $S = 1/2$ model in Sec.6.)

For the pure VBS state on a ring of N spins, one obtains $t_{ij} = 4/9 + O(3^{-N})$. For the ground state of the pure antiferromagnetic $S = 1$ chain, this order parameter also converges towards a finite value, which indicates a relationship with the VBS wave function.

7.2 Construction of appropriate RG rules

Renormalization of an antiferromagnetic bond

The Hamiltonian of an antiferromagnetic bond between two spins $S = 1$

$$h_0 = J_1 \vec{S}_1 \cdot \vec{S}_2 = \frac{J_1}{2} \left[(\vec{S}_1 + \vec{S}_2)^2 - \vec{S}_1^2 - \vec{S}_2^2 \right] = \frac{J_1}{2} \left[(\vec{S}_1 + \vec{S}_2)^2 - 4 \right] \quad (7.3)$$

has three energy levels indexed by the value $s = 0, 1, 2$ of the total spin

$$e_s = \frac{J_1}{2} [s(s+1) - 4] \quad (7.4)$$

the singlet $e_0 = -2J_1$, the triplet $e_1 = -J_1$ and the quintuplet $e_2 = J_1$. If one naively generalizes the Ma-Dasgupta rule for the $S = 1/2$ case by projecting onto the singlet, the new effective coupling is

$$J'_0 = \frac{4}{3} \frac{J_0 J_2}{J_1} \quad (7.5)$$

Since the coefficient $\frac{4}{3}$ is larger than 1, this rule is not automatically consistent, and the procedure can be justified only if one starts from a rather broad disorder.

To avoid this problem, Hyman and Yang [186] have proposed an effective $S = 1/2$ model, containing both Ferromagnetic and Antiferromagnetic bonds to mimic the physics of the weak disorder spin-1 chain. This effective model has the advantage of being consistent and soluble via real-space RG.

Since the mapping between the spin-1 chain and the Hyman-Yang effective model is heuristic and not quantitative, various propositions have been made to define consistent RG rules for arbitrary disorder directly on the spin-1 chain, in particular :

- Monthus, Golinelli and Jolicœur [263] have proposed the following principle : instead of projecting onto the lowest level of h_0 , the correct generalization of the Ma-Dasgupta principle consists in *projecting out the highest level*. Thus,

for the Hamiltonian h_0 , one eliminates the quintuplet, but one should keep the singlet and the triplet, by replacing the two spins $S = 1$ by two spins $S = 1/2$. This partial decimation of course enlarges the initial space of random chains, but it is nevertheless possible to define a closed RG procedure with 4 types of bonds.

- Saguia, Boechat and Contineto [316] have more recently proposed a procedure where the rule (7.5) is applied only if $\max(J_0, J_2) < (3/4)\Omega$, whereas otherwise the 3 spins coupled by $\max(J_0, J_2)$ and Ω are replaced by a new spin with two new couplings.

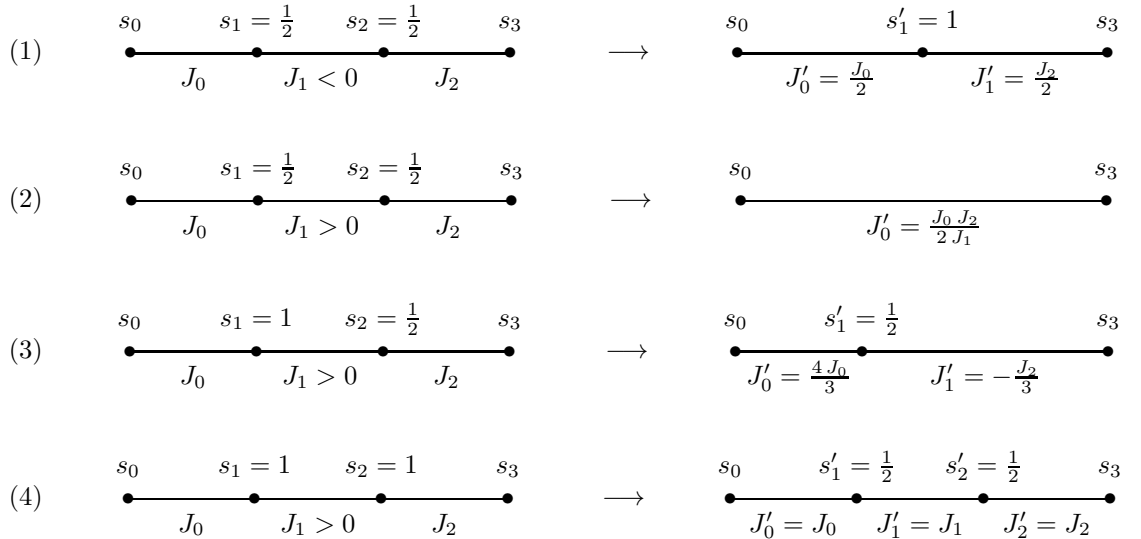
In the following, we will describe the RG procedure with 4 types of bonds [263], the numerical study of the RG flow, and we will finally describe how the numerical estimates of the critical exponents are in full agreement with the analytic critical exponents that can be computed [263] for the Hyman-Yang effective model. Finally we will describe the controversy between various direct numerical studies.

RG procedure with 4 types of bonds

This RG procedure is defined for the enlarged set of chains made of spins of size $S = 1/2$ and $S = 1$, in which the couplings $\{J_i\}$ are either ferromagnetic (F) or antiferromagnetic (AF), with the following constraint: for any segment $\{i, j\}$, the classical magnetization has to satisfy $|m_{i,j}| \leq 1$. This condition for two neighbors $j = i + 1$ shows that there are 4 types of possible bonds:

- 1) F Bond between two $S=1/2$ spins,
- 2) AF Bond between two $S=1/2$ spins,
- 3) AF Bond between a $S=1$ spin and a $S=1/2$ spin,
- 4) AF Bond between two $S=1$ spins.

The four corresponding rules of renormalization are as follows [263] :



Interpretation of the renormalization in terms of VBS clusters

If one represents each spin initial $S = 1$ like the symmetrization of two spins $S = 1/2$, the rules 2, 3, and 4 for AF bonds can be interpret as the formation of a singlet between two constitutive spins $S = 1/2$. Rule 1 for a F bond between two $S = 1/2$ spins corresponds to their symmetrization. At the end of the RG procedure, when there is no free spin anymore, the chain is broken into a set of disjointed clusters which have a VBS structure (see Figure 6).

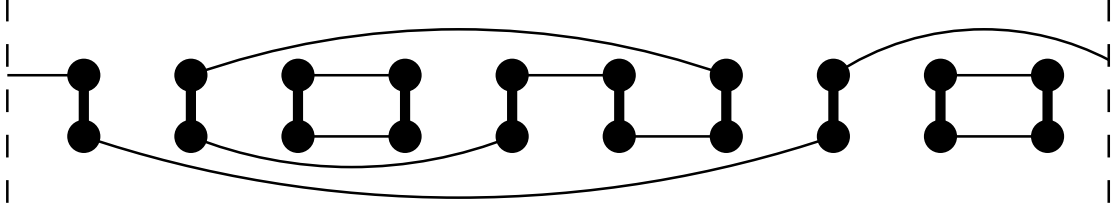


Figure 6: *The ground state obtained by renormalization, in terms of VBS cluster : each spin $S = 1$ is represented by the symmetrization of 2 spins $1/2$ (black balls connected by a fat vertical bond); the lines which connect two spins $1/2$ represent singlets. Initial spins 1 are thus gathered in clusters: here, for example, there are two clusters of size 2, a cluster of size 4, and a larger cluster which exceeds the limits of the figure. [263]*

For the disordered chain, the string order parameter (7.2) takes the value $t_{ij} = 4/9$ if the two sites belong to the same cluster and $t_{ij} = 0$ if not. For a chain of size N , the space average $\sum_{i,j} t_{ij}/N^2$ of the order parameter t_{ij} is proportional to the probability T that two spins belong to the same cluster

$$T \equiv \sum_c \frac{n_c^2}{N^2} = \frac{9}{4} \frac{1}{N^2} \sum_{i,j} t_{ij} + O(1/N) \quad (7.6)$$

where n_c is the number of spins in a cluster C , which is not directly related to its space extension. This order parameter T can be non-zero in the thermodynamic limit only if there exists a VBS cluster containing a finite fraction of the spins of the chain.

7.3 Numerical study of the RG procedure

The numerical study of the RG procedure with 4 types of bonds on the basis has been made for cyclic chains of N spins (for instance $N = 2^{22} \sim 4.10^6$), with initial couplings J_i uniformly distributed in the interval $[1, 1 + d]$. The parameter d thus represents the width of the initial disorder. For each size, the results are averaged over a certain number of samples (typically 100). The flow of the following quantities according as a function of the RG scale Γ has been computed :

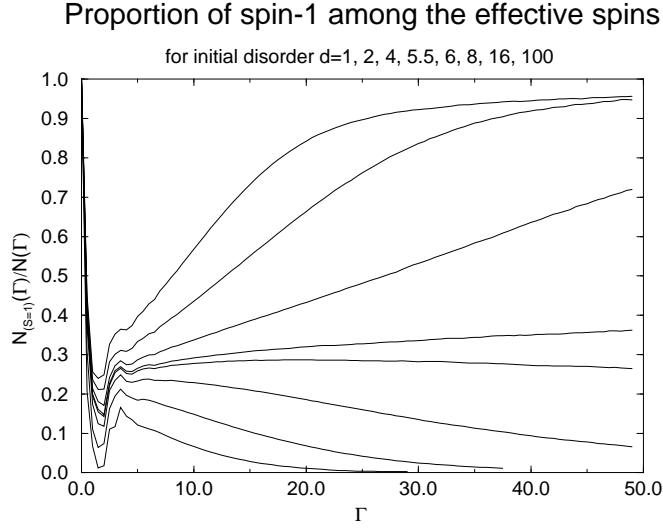


Figure 7: *Proportion of $S = 1$ spins among the effective spins at scale Γ for various values of the initial disorder $d = 1, 2, 3, 4, 5.5, 6, 8, 16, 100$: this proportion converges towards 0 for weak initial disorder, and towards 1 for strong initial disorder. At the point $d \simeq d_c = 5.75(5)$ the proportion remains stationary around the intermediate critical value $0.315(5)$. [263]*

(i) the number $N(\Gamma)$ of effective spins $S = 1/2$ and $S = 1$ still present at the scale Γ

(ii) the proportion $\{N_{(S=1)}(\Gamma)/N(\Gamma)\}$ of spins $S = 1$ among the effective spins still present.

(iii) the proportions $\rho_i(\Gamma) = \{N_i(\Gamma)/N(\Gamma)\}$ of the bonds of the type $i = 1, 2, 3, 4$

(iv) the probability distributions $P_i(J, \Gamma)$ of the remaining effective couplings J for the four types of bonds $i = 1, 2, 3, 4$.

The results of the RG procedure present a qualitative change for a certain critical value $d_c \simeq 5.75(5)$ of the initial disorder. Figure 7 represents the flow of the proportion $\frac{N_{(S=1)}(\Gamma)}{N(\Gamma)}$ of spins $S = 1$ for various values of the initial disorder: there are two attracting values, namely 0 for weak initial disorder and 1 for strong initial disorder.

Results for strong initial disorder

In the phase of strong disorder $d > d_c$, the number $N(\Gamma)$ of effective spins decreases as in the “ Random Singlet Phase ” of the chain $S = 1/2$ chain:

$$N(\Gamma) \underset{\Gamma \rightarrow \infty}{\propto} \frac{1}{\Gamma^2}. \quad (7.7)$$

and the proportions $\rho_i(\Gamma)$ of the four types of bonds converge towards the following asymptotic regime (Fig 8)

$$\rho_1(\Gamma) \sim 0 \quad \rho_2(\Gamma) \sim \epsilon(\Gamma) \quad \rho_3(\Gamma) \sim 2\epsilon(\Gamma) \quad \rho_4(\Gamma) \sim 1 - 3\epsilon(\Gamma) \quad (7.8)$$

where $\epsilon(\Gamma)$ slowly converges towards 0 as $\Gamma \rightarrow \infty$. The chain contains almost everywhere bonds of the type 4, with some defects of the type (bond of the type 3, bond of the type 2, bond of the type 3) which come from the temporary partial decimation of the bonds of the type 4. For strong initial disorder, the renormalization thus converges towards the Random Singlet Phase.

Results for weak initial disorder

In the weak disorder phase $d < d_c$, the number $N(\Gamma)$ of effective spins decreases exponentially

$$N(\Gamma) \underset{\Gamma \rightarrow \infty}{\propto} e^{-\alpha(d)\Gamma} \quad (7.9)$$

with a coefficient $\alpha(d)$ which decreases towards 0 as $d \rightarrow d_c^-$. The proportions $\rho_i(\Gamma)$ of the four types of bonds converge towards the asymptotic regime (Figure 9)

$$\rho_1(\Gamma) \simeq 0.25 \quad \rho_2(\Gamma) \simeq 0.75 \quad \rho_3(\Gamma) \simeq 0 \quad \rho_4(\Gamma) \simeq 0 \quad (7.10)$$

Results at the critical point

At the critical point $d = d_c$, the number of effective spins decrease algebraically as

$$N(\Gamma) \underset{\Gamma \rightarrow \infty}{\propto} \frac{1}{\Gamma^3}. \quad (7.11)$$

and the proportions $\rho_i(\gamma)$ of the four types of bond converge towards the asymptotic regime (Figure 10)

$$\rho_1(\Gamma) \sim 0.17, \quad \rho_2(\Gamma) \sim 0.35, \quad \rho_3(\Gamma) \sim 0.33, \quad \rho_4(\Gamma) \sim 0.15 \quad (7.12)$$

Numerical study of the percolation transition from the VBS clusters

From the point of view of VBS clusters, the quantum phase transition corresponds to a percolation transition : in the strong disorder phase, there are only finite clusters, whereas in the weak disorder phase, there exists a macroscopic cluster which contains a finite fraction of the spins.

String Order Parameter

Let β be the exponent describing the vanishing of the fraction n_1/N of spins in the macroscopic cluster at the transition. The string order parameter then vanishes as $T \sim (d_c - d)^{2\beta}$ for $d < d_c$. The finite size scaling study of Figure (11) leads to the numerical estimate

$$2\beta = 1.0(1). \quad (7.13)$$

Susceptibility

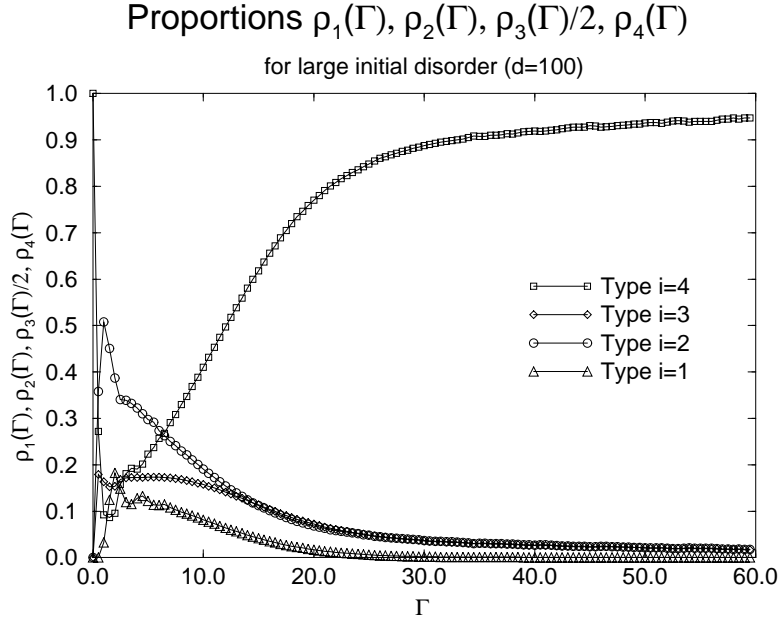


Figure 8: The proportions $\rho_i(\Gamma)$ of the 4 types of bonds $i = 1, 2, 3, 4$ as functions of the RG scale Γ for a very strong initial disorder $d = 100$. [263]

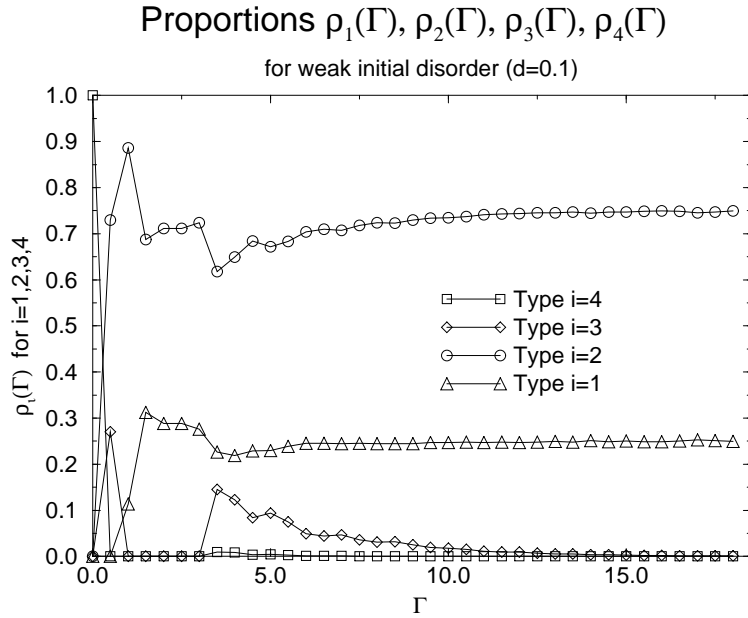


Figure 9: The proportions $\rho_i(\Gamma)$ of the 4 types of bonds $i = 1, 2, 3, 4$ as functions of the scale Γ for a weak initial disorder $d = 0.1$ [263]

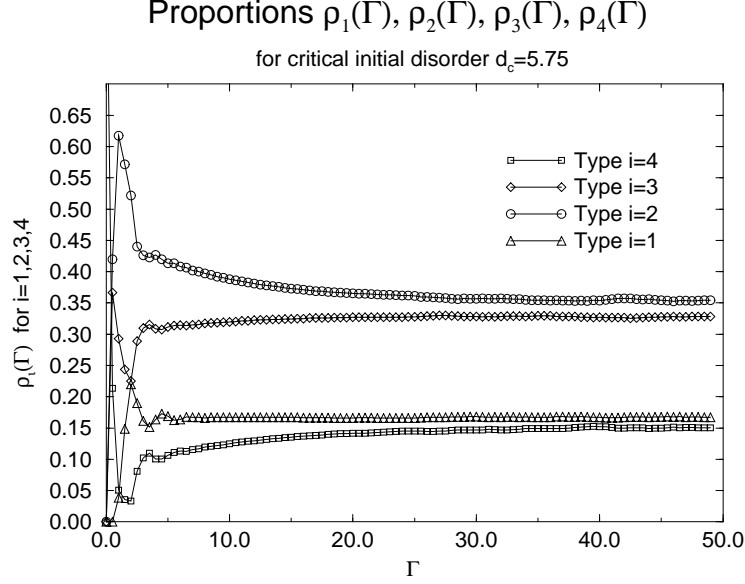


Figure 10: The proportions $\rho_i(\Gamma)$ of the 4 types of bonds $i = 1, 2, 3, 4$ as functions of the RG scale Γ for a critical initial disorder $d_c = 5.75$. [263]

The Figure (12) represents the average size of the finite clusters, which plays the role of a susceptibility

$$\chi \equiv \sum_{c>1} \frac{n_c^2}{N}. \quad (7.14)$$

($c=1$ is the largest cluster). The critical exponent γ controlling the divergence $\chi \sim |d_c - d|^{-\gamma}$ has been measured to be

$$\gamma = 1.2(1). \quad (7.15)$$

Distribution of the cluster sizes at the critical point

At the critical point, the distribution $m_c(s)$ of the size s of the clusters presents an algebraic decay (Figure 13)

$$m_c(s) \sim \frac{1}{s^\tau} \quad (7.16)$$

with the exponent

$$\tau = 2.2(1). \quad (7.17)$$

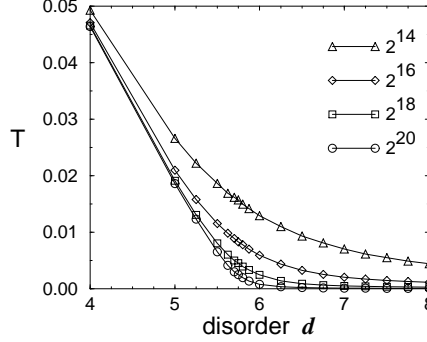


Figure 11: *The string order parameter as a function of the initial disorder d for chains of sizes $N = 2^{14} - 2^{20}$. The critical point is located at $d_c = 5.76(2)$ [263]*

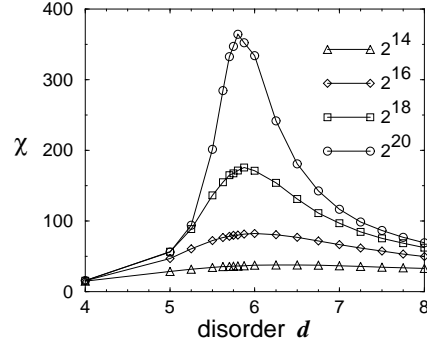


Figure 12: *The susceptibility χ as a function of the initial disorder d for chains of sizes $N = 2^{14} - 2^{20}$. [263]*

7.4 Exact critical exponents via a soluble effective model

The effective model introduced by Hyman and Yang [186] to describe the physics of the random $S = 1$ AF chain is a *random dimerized spin-1/2 chain* containing both Ferromagnetic and Antiferromagnetic bonds. More precisely, this model is defined as follows : all even bonds are AF, whereas the odd bonds are either F or AF. The physical motivation for this last point is that in finite open pure $S = 1$ chains, the low energy physics corresponds to two effective $S = 1/2$ spins at the two ends coupled via a weak coupling $J_{eff}(L) \sim (-1)^{L+1}e^{-cL}$ that can be either Ferro or Antiferro.

The renormalization procedure is then defined as follows [186] : the energy scale Ω is given by the strongest AF bond of the system, so that the odd bonds separate into two groups : *group A* contains F bonds weaker than Ω and all AF bonds, while *group B* contains all F bonds stronger than Ω . In this effective

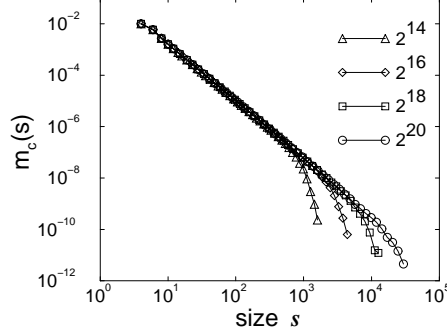


Figure 13: *Distribution $m_c(s)$ of the size s of the clusters at the critical point: the measure of the slope leads to the estimate $\tau = 2.2(1)$ [263]*

model, perfect VBS order means singlets over all even bonds of the initial chain. Indeed, at the stable fixed point of the Haldane phase found in [186] by solving the renormalization flow equations, all odd bonds are much weaker than even bonds so that only singlets over even bonds are generated by decimation. At the critical point between the Haldane phase and the strong disorder phase, the length scale is $l \sim \Gamma^3$, in agreement with the behavior (7.11) found in the 4-bond model.

To compute how the VBS order parameter vanishes at the transition, one needs to introduce an *auxiliary variable* μ for each odd bond still surviving at scale Ω . The variable μ is by definition the number of singlets already made over even bonds of the initial chain that are contained in this odd bond. This μ evolves as follows : when an odd bond of variable (μ) is decimated, a finite cluster of size $(\mu+1)$ is terminated; when an even bond surrounded by two B-odd bonds of variables μ_1 and μ_2 respectively, a finite cluster of size $(\mu_1 + \mu_2 + 2)$ is terminated; when an even bond surrounded by two A-odd bonds, or surrounded by one A-odd bond and one B-odd bond, with respective variables μ_1 and μ_2 , the new odd bond generated by this decimation inherits the variable ($\mu = \mu_1 + \mu_2 + 1$). At the fixed point describing the transition of the effective model, one finds that μ scales as :

$$\mu \propto \Gamma^\varphi \quad \text{with } \varphi = \sqrt{5}. \quad (7.18)$$

This has to be compared with the scaling $l \propto \Gamma^3$ of the auxiliary variable l that counts the number of initial bonds in a surviving bond at scale Γ . Deviations from the critical point are driven by a relevant perturbation[186] that scales as Γ^{λ_+} with $\lambda_+ = (\sqrt{13} - 1)/2$. As a consequence, the exact exponent for the string topological order parameter (7.13) is [263]

$$2\beta = \frac{2(3 - \varphi)}{\lambda_+} = \frac{4(3 - \sqrt{5})}{\sqrt{13} - 1} = 1.17278..., \quad (7.19)$$

the exponent of the percolation susceptibility is

$$\gamma = \frac{(2\varphi - 3)}{\lambda_+} = \frac{2(2\sqrt{5} - 3)}{\sqrt{13} - 1} = 1.13000..., \quad (7.20)$$

and the exponent τ of the scaling form (7.16) for the distribution of cluster sizes :

$$\tau = 1 + \frac{3}{\varphi} = 1 + \frac{3}{\sqrt{5}} = 2.34164..., \quad (7.21)$$

which are in very good agreement with the numerical estimates (7.13), (7.15), (7.17) obtained in the 4-bond RG analysis. It is thus believed that the soluble effective Hyman-Yang model correctly describes the disorder-induced phase transition of the random AF spin-1 chain.

7.5 Direct numerical studies

We now have to discuss results of various direct numerical studies on the existence of the various phases of the random $S = 1$ chain, which are controversial. Generally, one uses here a square-type distribution of the initial couplings, which is uniform in the interval $[1 - W/2, 1 + W/2]$. The correspondence with the flat distribution on the interval $[1, 1 + d]$ used for the previous numerical RG approach can be obtained from the matching for J_{max}/J_{min} leading to

$$W = \frac{2d}{1 + d} \quad (7.22)$$

The limit of strongest disorder of this form, $d \rightarrow \infty$ corresponds to $W \rightarrow 2$, whereas the critical initial disorder $d_c \sim 5.75$ found in the numerical RG study of the four-bond model corresponds to $W_c \sim 1.48$. Note that the power-law distribution, $P(J) = D^{-1}J^{-1+1/D}$ as given in Eq.(A.1) for $D = 1$ corresponds to $W = 2$ and represents more strong disorder for $D > 1$.

- on one hand, the following direct numerical studies have concluded that there was no random singlet phase even for the limiting disorder $W \rightarrow 2$:

- (i) Nishiyama via exact diagonalization for sizes $N \leq 14$ [289],
- (ii) Nishiyama via quantum Monte-Carlo method for sizes $N \leq 32$ [290],
- (iii) Hida via Density-Matrix-RG for sizes $N \leq 42$ [169]

- on the other hand, more recent studies have found the random singlet phase for $W_c < 2$:

- (iv) Todo *et al* via quantum Monte-Carlo method with the continuous-time loop algorithm for sizes $N \leq 256$ [341]

- (v) Bergkvist *et al* via stochastic series expansion quantum Monte-Carlo for sizes $N \leq 64$ [48]

- there were new claims of the theoretical side :

- (vi) in their Comment [358] on the work of Hida [169], Yang and Hyman argue that the random singlet phase appears only for a power-law distribution with stronger disorder, $D > D_c \sim 1.5$.

(vii) Sagia *et al.* [316] claim from the numerical study of their alternative Ma-Dasgupta RG procedure for sizes $N \leq 9000$ that the random singlet phase appears for flat initial distributions only at the point $W_c = 2$.

We believe that the discrepancies in the numerical results are due to strong finite-size effects : the initial flat distribution for the couplings is very far from the RG asymptotic power-law distributions for the remaining effective couplings at low energy. As a consequence, there is a long transient regime to converge towards the asymptotic regime, and this is why the RG for the four-bond model was studied numerically on very large chains to obtain satisfying results.

Also one has to note that the transition point between the gapless Haldane and the RS phases is a tricritical point, if dimerization is included[109]. Therefore the influence of the critical RS fixed point results in strong cross-over effects. On the side of the numerical RG studies there are a number of initial approximative decimation steps until the system approaches sufficiently close the correct asymptotic RG trajectory. Due to these initial steps the position of the transition in the physical model can be somewhat shifted.

To summarize the basic features of the disorder induced phase transitions in the random $S = 1$ AF Heisenberg chain are verified by direct numerical studies, but still further work is necessary to locate the precise position of the tricritical point, as well as to verify the values of the (tri)critical exponents.

7.6 Generalizations : dimerization, dynamics

The effects of enforced dimerization on random $S = 1$ chains have also been studied via real space RG in [109], and numerically in [35] : in the phase diagram in the plane (dimerization δ , randomness R), the critical point at $(\delta = 0, R_c)$ now becomes multicritical. This kind of multicritical point has been further discussed in [110].

Finally let us mention that dynamical properties of the $S = 1$ chain (as well as other random spin chains) have also been studied via strong disorder RG in [108, 277].

8 Other 1D quantum models

Besides the random AF $S = 1/2$ and $S = 1$ Heisenberg models there are another problems of interacting Heisenberg spins in one (and quasi-one) dimension which have been intensively studied. Here we review recent developments obtained for higher spin, $S \geq 3/2$, AF chains, for $S = 1/2$ chains with mixed ferro- and antiferromagnetic couplings and for random spin ladders. These theoretical investigations are often initiated by experimental work.

8.1 Higher spin AF Heisenberg chains

The spin- S random antiferromagnetic Heisenberg chain is defined by the Hamiltonian:

$$H = \sum_i J_i \vec{S}_i \cdot \vec{S}_{i+1} \quad (8.1)$$

where the $J_i > 0$ are quenched random variables. As before we introduce enforced dimerization of strength, δ , so that the couplings are in the form:

$$J_i = J(1 + \delta(-1)^i) \exp(D\eta_i) \quad (8.2)$$

where η_i are random numbers of mean zero and variance unity. Thus the strength of disorder is measured by D , see Eq.(A.1). The properties of this model for $S = 1/2$ and for $S = 1$ have already been presented in Sec.6 and 7, respectively. Here we consider higher values of $S \geq 3/2$.

Non-random models

As already discussed at the beginning of Sec.7 the non-random models with $\delta = 0$ have different low-energy properties for half-integer and integer values of the spin, respectively[161]. Half-integer spin chains, as the $S = 1/2$ model, have a gapless spectrum and quasi long range order. It is believed that they all belong to the same (bulk) universality class independently on S [325]. This was explicitly verified numerically for the $S = 3/2$ chain [162], which was found to have the same bulk decay exponent as for the $S = 1/2$ chain. In the presence of dimerization a gap opens in the spectrum, which behaves for small δ as

$$\epsilon_1(\delta) \sim |\delta|^\nu. \quad (8.3)$$

Here the gap (or correlation-length) exponent for the $S = 1/2$ model is given from a bosonization study[101] as $\nu = 2/3$, for recent numerical work see Ref.[297].

Integer spin chains are instead gapped and have a hidden topological order [288], as defined for the $S = 1$ model in Eq.(7.2). The topological order stays even for a small finite dimerization. If, however, $|\delta|$ exceeds a limiting value, δ , there is a quantum phase transition in the system and for $|\delta| > \delta$ there is dimer order in the ground state.

Effect of disorder

Weak disorder is expected to have different effect of the two types of chains. The Haldane gap for integer spin chains is robust against weak disorder, whereas the behavior of half-integer spin chains can be predicted by the Harris relevance-irrelevance criterion in Eq.(5.9). Since the value of $\nu = 2/3$ seems to be universal for all half-integer chains weak disorder is predicted to be a relevant perturbation. This is indeed the case for the $S = 1/2$ chain, however, for the $S = 3/2$ chain numerical investigations show[87] that weak disorder is irrelevant and the properties of the quasi-long-range order are the same as in the non-random system. We shall come back later to discuss this point.

For stronger disorder one can use the strong disorder RG method. If in the decimation procedure two S spins with the strongest bond, $J_2 = \Omega$, are replaced

by a singlet, the new coupling generated between the remaining sites is given by:

$$\tilde{J} = \frac{2}{3}S(S+1)\frac{J_1J_3}{J_2}. \quad (8.4)$$

Thus for $S > 1$ we encounter the same problem as for $S = 1$: some of the generated couplings are larger than the decimated one, therefore this RG works only for strong enough disorder. The larger the spin the larger the disorder needed for the procedure. In order to obtain the behavior of the system for weaker disorder the strategy used for the random $S = 1$ chain in Sec-7 is generalized in Ref.[308]. In this case each spin- S is represented by the maximally symmetrized multiplet of $2S$ identical $S = 1/2$ spins. Renormalizing a strong term, $J_2\vec{S}_1 \cdot \vec{S}_2$, is equivalent to eliminate the highest spin combination in the spectrum of the two site cluster, thus replacing $S_1 \rightarrow S_1 - 1/2$ and $S_2 \rightarrow S_2 - 1/2$. In other words one $S = 1/2$ singlet bond is eliminated. In this way, during renormalization we obtain an effective model in which at each site there are spin S , $S - 1/2, \dots, 1/2$ degrees of freedom with effective couplings, which can be ferro- or antiferromagnetic. However during renormalization no spin larger than S can be generated. The ground state at an energy scale, Ω , is represented by singlets (valence bonds) formed between spin $S = 1/2$'s.

If the disorder is very strong all the $2S$ valence bonds between the original spins are formed, thus the random singlet phase is given in terms of S spins and called as RS_S phase. For somewhat weaker disorder the valence bonds form two different structures: i) there is a valence bond solid which involves two spin $S = 1/2$ at each site, and ii) there is a random singlet phase of effective $S - 1$ spins. The low-energy excitations are given by this RS_{S-1} phase. Continuing this reasoning by decreasing disorder, D , there is a sequence of RS_S , RS_{S-1} , RS_{S-2} , ... phases, and there are multicritical points which separate these strong disorder phases. Within the different RS phases the singular behavior follows the same rules as in the traditional $RS_{1/2}$ phase, as described in Sec.6. At the multicritical points, however, there are new exponents, which are calculated in Ref.[110]. For example the exponent, ψ , describing the relation between the size- and the log-time-scale in Eq.(A.16) is given by: $\psi = 1/N$, where N is the number of Griffiths phases in the $D - \delta$ phase diagram, which meet at the multicritical point. At the principal multicritical point, separating the RS_S and RS_{S-1} phases we have $N = 2S + 1$. Similarly, the correlation length exponent in the multicritical point is given by: $\nu = (1 + (4N + 1)^{1/2})/2$. Note, that this latter result formally corresponds to Eq.(3.19) with $b = N - 1$. For the $S = 1$ model these results are previously calculated, see in Sec.7.4.

Among the higher-spin AF Heisenberg chains, the random $S = 3/2$ model is investigated in more detail. The phase diagram and the singular properties of the system is studied by a numerical implementation of the strong disorder RG method[308], as outlined above. The two random singlet phases ($RS_{3/2}$ and $RS_{1/2}$) are identified and the properties of the multicritical point are numerically calculated. These are generally in good agreement with the analytical results in Ref.[110], although there are larger deviations for the correlation length ex-

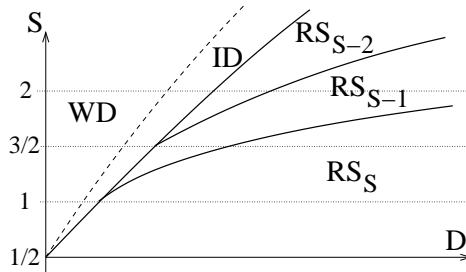


Figure 14: Schematic phase diagram of the spin S AFH chain as function of the strength of disorder D . The RS_S denotes a random singlet phase where the relevant degrees of freedom are effective S -spins. The WD and ID are the region at weak and intermediate disorder.

ponent, ν .

Another type of decimation scheme in the strong disorder RG method is used by Saguia *et al.* [317]. In their work the renormalization flow indicates that the weak disorder is an irrelevant perturbation of the system. This is in agreement with the numerical, DMRG results[87], as mentioned above. The possible origin of the irrelevance of weak disorder, as argued in Ref[87], is due to localized edge states in the $S = 3/2$ (and higher half-integer spin) chains. The correlation length associated to surface excitations is shown to diverge with a larger exponent, $\nu' \approx 2$. This type of excitation could be relevant in the present of bond disorder, thus, according to the Harris criterion in Eq.(5.9) it is a (marginally) irrelevant perturbation.

We close this part by presenting a possible phase diagram[110, 87] for higher S in Fig. 14. The transition lines between the different random singlet phases for the time being cannot be supported by numerical results. The weak disorder (WD) region may be separated from the RS phase(s) by an intermediate disorder (ID) region where exponents vary continuously with D , as observed in other models[86] in Sec.5. For the gapped (integer S) case this would correspond to a region of Griffiths singularities.

8.2 Heisenberg chain with random ferro- and antiferromagnetic couplings

Heisenberg spin chain with randomly mixed ferromagnetic and antiferromagnetic couplings can be realized in the system $Sr_3CuPt_{1-x}Ir_xO_6$. Here the pure compounds, Sr_3CuPtO_6 and Sr_3CuIrO_6 , are antiferromagnetic and ferromagnetic spin chains, respectively, the mixed compound contains randomly both types of couplings[355]. Examples of another experimental realizations can be found, c.f. in[353, 256].

Generalized RG rules

For a theoretical investigation of the low-energy and low-temperature prop-

erties of the system the strong disorder RG method by Ma and Dasgupta have to be generalized. If, during renormalization, the strongest term in the Hamiltonian in Eq.(8.1) is, $J_2 \vec{S}_2 \cdot \vec{S}_3$, with a ferromagnetic coupling, $J_2 < 0$, then the two spins form a spin cluster of effective size, $\tilde{S} = 1$. Repeating the RG procedure the system transforms into a chain of spins of arbitrary size with mixed antiferromagnetic and ferromagnetic couplings. One term of the renormalized Hamiltonian is given in the form: $J \vec{S}_L \cdot \vec{S}_R$, where \vec{S}_L (\vec{S}_R) denotes the effective spin variable at the left (right) of the two-site cluster. During renormalization the two-site cluster with a very strong bond is projected into its ground state multiplet, thus replaced by a single effective spin, S , with $S = |S_L \pm S_R|$, where the $+$ ($-$) sign refers to ferromagnetic (antiferromagnetic) coupling. The energy-scale of the two-site cluster is measured by the energy gap, Δ , defined by: $\Delta = |J|(S_L + S_R)$ for $J < 0$ and $\Delta = J(|S_L - S_R| + 1)$ for $J > 0$, respectively.

During renormalization spin clusters with $\Delta = \Omega$ are transformed by two basic decimation processes. If $S_L = S_R$ and the coupling is antiferromagnetic one performs standard singlet formation, when the effective coupling generated between the remaining sites is given in Eq.(8.4). If $S \neq 0$ there is effective spin (cluster) formation, when the interaction to the neighboring site of spin S_L and coupling J_L is renormalized as $\tilde{J}_L = J_L c_L$ with [353, 255]:

$$c_L = \frac{S(S+1) + S_L(S_L+1) - S_R(S_R+1)}{2S(S+1)}. \quad (8.5)$$

Properties of the fixed point

As renormalization goes on the energy scale, Ω , is lowered and the number of non-decimated sites, n_Ω is decreased. At the same time the length-scale, $L_\Omega \sim 1/n_\Omega$ and the size of the effective spin, $S_{eff} \approx S_L, S_R$ is increased. This latter follows the asymptotic relation:

$$S_{eff} \sim L_\Omega^\zeta, \quad (8.6)$$

where ζ is called the spin moment exponent. The following random walk argument [353] gives $\zeta = 1/2$: The total moment of a typical cluster of size L can be expressed as $S_{eff} = |\sum_{i=1}^L \pm S_i|$, where neighboring spins with ferromagnetic (antiferromagnetic) couplings enter the sum with the same (different) sign. If the position of the two types of bonds are uncorrelated and if their distribution is symmetrical, one has $S_{eff} \propto L^{1/2}$, i.e. Eq.(8.6) with $\zeta = 1/2$.

A non-trivial relation constitutes the connection between the energy scale Ω and the size of the effective spin:

$$S_{eff} \sim \Omega^{-\kappa}. \quad (8.7)$$

For not singular initial disorder in numerical calculation the exponent is found independent of the disorder distribution, as $\kappa = 0.22(1)$ [353]. Comparing Eq.(8.6) with Eq.(8.7), the relation between the length scale and the energy scale is:

$$\Omega \sim L^{-z}, \quad z = \frac{\zeta}{\kappa} = \frac{1}{2\kappa}, \quad (8.8)$$

where z is the dynamical exponent.

The average spatial correlations function, $C(r)$, is studied by numerical application of the RG procedure and by DMRG calculations[172] leading to a very slow, probably logarithmic dependence:

$$C(r) \sim \frac{1}{\ln(r/r_0)} . \quad (8.9)$$

Thus we can conclude that the low-energy fixed point of the $S = 1/2$ Heisenberg chain with mixed ferromagnetic and antiferromagnetic couplings has special characteristics: there is a large spin formation, the dynamical exponent is finite and the average correlation function is logarithmically slow. This type of fixed point is generally called a *large spin fixed point*.

Thermodynamic quantities

From the strong disorder RG calculation one can obtain the singularities of the thermodynamic quantities similarly as for the RTFIC in Sec.4.4.2. At finite, but small temperature, T , the renormalization stops at the energy scale, $\Omega = T$, when the existing spin clusters of size, S_{eff} , are practically independent, since couplings between them are extremely weak. The entropy per site, S/N , is simply the contribution of non-interacting clusters:

$$\frac{S}{N} \sim \left. \frac{\ln(2S_{eff} + 1)}{n_\Omega} \right|_{\Omega=T} \sim T^{1/z} |\ln T| . \quad (8.10)$$

and similarly for the specific heat:

$$\frac{C}{N} \sim T^{1/z} |\ln T| . \quad (8.11)$$

The magnetic susceptibility is given by the Curie-type contribution of large, independent effective spins:

$$\frac{\chi}{N} \sim \left. \frac{[S_{eff}]^2}{T} n_\Omega \right|_{\Omega=T} \sim \frac{1}{T} . \quad (8.12)$$

In a small, finite magnetic field, h , the energy scale is set by the Zeeman-energy, $E_{ZM} \sim hS_{eff} \sim \Omega$. Thus the RG stops at $\Omega \sim h^{1/(1+1/2z)}$, and the existing spin clusters align parallel with the magnetic field. Consequently the magnetization per site, m , is given by

$$m \sim \left. \frac{S_{eff}}{n_\Omega} \right|_{\Omega=E_{ZM}} \sim h^{1/(1+2z)} . \quad (8.13)$$

8.3 Disordered spin ladders

Spin ladders are quasi-one-dimensional Heisenberg systems, in which two or more spin chains are coupled together by interchain bonds. Experimentally they have been realized in different compounds, for a review, see[107]. According to

theoretical investigations spin ladders with even number of legs have a gapped spectrum, whereas the spectrum of odd-leg ladders is gapless[106]. For two-leg ladders, which are analogous objects to $S = 1$ spin chains, the ground state structure can be related to nearest-neighbor valence bonds and a topological hidden order parameter, similar to that in Eq.(7.2) can be defined [220].

More recently, ladder models with competing interactions, such as with staggered dimerization[250] and with rung and diagonal couplings[220], have been introduced and studied. In these models, depending on the relative strength of the couplings, there are several gapped phases with different topological order, which are separated by first- or second-order phase transition lines.

Disorder in a spin ladder material is realized in $\text{Sr}(\text{Cu}_{1-x}\text{Zn}_x)_2\text{O}_3$, which is a two-leg ladder, and can be doped by Zn, a non magnetic ion[39]. The specific heat and spin susceptibility experiments indicate that the doped system is gapless even with low doping concentrations. We note that the experimentally found phase diagram of this compound, as well as other quantities, such as staggered susceptibility have been obtained by quantum Monte Carlo simulations[261].

Spin ladder models

To model a two-leg ladder with different types of interactions one starts with the Hamiltonians of the $\tau = 1, 2$ spin chains:

$$H_\tau = \sum_{l=1}^L J_{l,\tau} \mathbf{S}_{l,\tau} \mathbf{S}_{l+1,\tau} , \quad (8.14)$$

in which dimerization is introduced in the couplings as:

$$J_{l,\tau} = J \left[1 + \gamma(-1)^{l+n(\tau)} \right] , \quad 0 \leq \gamma < 1 , \quad (8.15)$$

with $n(\tau) = 0, 1$. The interchain interactions are

- rung couplings:

$$H_R = \sum_{l=1}^L J_l^R \mathbf{S}_{l,1} \mathbf{S}_{l,2} , \quad (8.16)$$

- one type of diagonal coupling, generating the zig-zag ladder:

$$H_Z = \sum_{l=1}^L J_l^Z \mathbf{S}_{l,2} \mathbf{S}_{l+1,1} . \quad (8.17)$$

- two types of diagonal couplings:

$$H_D = \sum_{l=1}^L J_l^D (\mathbf{S}_{l,1} \mathbf{S}_{l+1,2} + \mathbf{S}_{l,2} \mathbf{S}_{l+1,1}) . \quad (8.18)$$

The different type of ladder models, which can be obtained from these ingredients are shown in Fig.15.

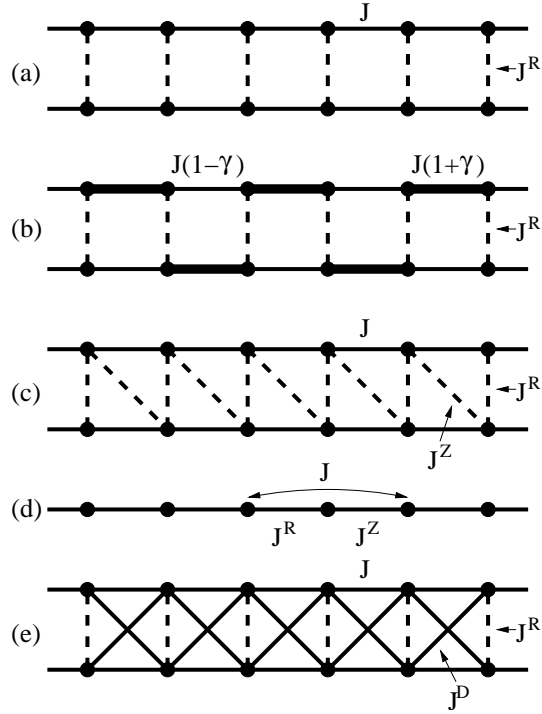


Figure 15: Spin-ladder models: a) conventional two-leg ladder, $H = H_1 + H_2 + H_R$, (b) with staggered dimerization in the chain couplings, (c) zig-zag ladder, $H = H_1 + H_2 + H_R + H_Z$, (d) its representation as a chain with first and second neighbor couplings, (e) full ladder with rung and diagonal couplings, $H = H_1 + H_2 + H_R + H_D$.

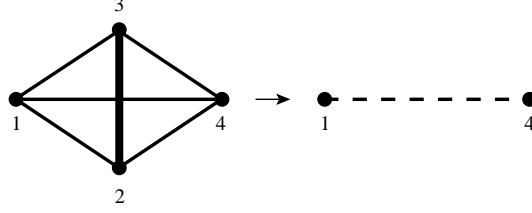


Figure 16: Singlet formation and decimation in the ladder geometry.

Strong disorder RG rules

With a ladder geometry, spins are more interconnected than in a chain, which leads to a modification of the decimation procedure used for a single chain in Sec.6.1. As shown in Fig. 16 both spins of a strongly coupled pair, say (2, 3), are generally connected to the nearest neighbor spins, denoted by 1 and 4. After decimating out the singlet pair the new, effective coupling between 1 and 4 is of the form:

$$\tilde{J}_{14}^{eff} = \kappa \frac{(J_{12} - J_{13})(J_{43} - J_{42})}{\Omega}. \quad \kappa(S = 1/2) = 1/2, \quad (8.19)$$

With the rule in Eq.(8.19) ferromagnetic couplings are also generated. Repeating the reasoning used for the random Heisenberg chain with mixed ferromagnetic and antiferromagnetic bonds in Sec.8.2, the ladder Hamiltonian will renormalize into a set of effective spin clusters having different moments and connected by both antiferromagnetic and ferromagnetic bonds. The renormalization rules are similar to that in Sec.8.2 and consists of i) singlet formation and ii) cluster formation. In the latter case the renormalization rule in Eq.(8.5) has to be modified, since the two-site cluster with spins S_L and S_R has generally two couplings, denoted by J_L and J_R , to a neighboring spin, S_1 . During renormalization the term in the Hamiltonian: $J_L \vec{S}_1 \cdot \vec{S}_L + J_R \vec{S}_1 \cdot \vec{S}_R$ is transformed to $\tilde{J}_1 \vec{S}_1 \cdot \vec{S}$ with: $\tilde{J}_1 = c_L J_L + c_R J_R$. Here c_L is given in Eq.(8.5), whereas c_R can be obtained from Eq.(8.5) by interchanging S_L and S_R .

Numerical renormalization methods

Due to the ladder topology and the complicated renormalization rules the RG equations can not be treated analytically and one resorts to numerical implementations of the renormalization procedure, during which one keeps information about the spin moments, S_{eff} , the gaps of a two-site cluster, Δ , and the energy scale, $\Omega = \max\{\Delta\}$. The numerical RG calculations are generally made in two different forms.

- In the infinite lattice method a few very large ("infinite") samples are decimated and the critical exponents are deduced from the scaling form of the distribution function:

$$P(\Delta, S_{eff}, \Omega) = \Omega^\omega \tilde{P}(\Delta/\Omega, S_{eff} \Omega^{\zeta/z}), \quad (8.20)$$

which is characterized by the gap exponent, ω , by the spin moment or cluster exponent, ζ , and by the dynamical exponent, z .

- In finite lattice method one starts with a finite system of L sites (and with periodic boundary conditions) and perform the decimation procedure until the last remaining spin or singlet pair. The distribution of the gap in the last step, $P_L(\Delta)$ obeys the scaling relation:

$$P_L(\Delta) = L^z \tilde{P}(L^z \Delta) \sim L^{z(1+\omega)} \Delta^\omega . \quad (8.21)$$

from which ω and z can be deduced. In this case the cluster exponent is obtained from the size dependence of the average effective spin, $S_{eff} \sim L^\zeta$, which corresponds to Eq.(8.6).

If the low-energy excitations are localized there is a simple relation between the dynamical exponent, z , and the gap exponent, ω [338, 191, 195]. In this case the gap distribution should be proportional to the volume of the system, $P_L(\Delta) \sim L^d$, and for a ladder the dimension is $d = 1$. From Eq.(8.21) then follows:

$$z = \frac{d}{1 + \omega} , \quad (8.22)$$

In the Griffiths phase with localized rare events (8.22) is expected to hold.

The infinite disorder fixed point is signaled by a diverging z , or more precisely the $P_L(\Delta)d\Delta$ distributions have strong L dependence, so that the appropriate scaling combination is

$$\ln (L^\psi P_L(\Delta)) \simeq f (L^{-\psi} \ln \Delta) . \quad (8.23)$$

Renormalization of spin ladders

Results of numerical renormalization group method can be summarized as follows.

- Random conventional ladders ((a) in Fig.15) are in the random rung singlet phase, which is controlled by a Griffiths-type fixed point having a dynamical exponent which depends on the strength of the initial disorder, D [256, 364].

- Random ladders with staggered dimerization ((b) in Fig.15) have two different phases: random rung singlet and random dimer, both are controlled by Griffiths-type fixed points with finite value of the dynamical exponent[256]. At the phase transition point the transition is controlled by an infinite disorder fixed point with an exponent, $\psi = 1/2$.

- In random zig-zag ladders ((c) and (d) in Fig.15) there is a very narrow region for small second neighbor interaction with infinite disorder characteristics[366, 178]. For larger second neighbor interaction the fixed point is a large spin fixed point with varying dynamical exponent[256].

- In random J_1 - J_2 ladders ((e) in Fig.15) there are two topologically distinct phases with Griffiths-type singular behavior. In between there is a quantum phase transition with infinite disorder scaling properties[256].

- Random conventional ladders with site-dilution or doped with non-magnetic impurities are found to have a large spin fixed point[365].

For related studies of disordered spin ladders we mention Refs.[36, 295, 153, 178].

8.4 Other investigations in 1d

Dissipative random quantum spin chains

The RTFIC coupled to an Ohmic bath of quantum harmonic oscillators is studied by Monte-Carlo simulations using the two-dimensional classical counterpart of the coupled system[104] (see Sec.18.2.1). For small, finite chains this problem constitutes a generalization of the Caldeira-Leggett localization transition[81]. In the thermodynamic limit the coupling to the dissipative bath is found to enhance the extent of the ordered phase. However, from the numerical data it was not possible to distinguish between infinite disorder and strong disorder scaling at the transition point.

AF Heisenberg chains with alternating bonds

$S = 1/2$ antiferromagnetic Heisenberg chains with alternating bonds and quenched disorder is introduced in Ref[170] as a theoretical model of the compound[29] $\text{CuCl}_{2x}\text{Br}_{2(1-x)}(\gamma - \text{pic})_2$. The low-energy properties of the system as a function of the concentration, x , and the type of correlation of disorder is studied in Ref.[240] by the numerical implementation of the strong disorder RG method. For perfect correlation of disorder the system is in the random dimer (Griffiths) phase having a concentration dependent dynamical exponent. On the contrary for weak or vanishing disorder correlations the system is in the random singlet phase. These results are compared with the experimentally measured low-temperature susceptibility[29] of $\text{CuCl}_{2x}\text{Br}_{2(1-x)}(\gamma - \text{pic})_2$.

Random AF $S = 1$ chains with quadratic and biquadratic interactions

Spin-1 chains with random nearest neighbor couplings that are rotationally invariant, but include both Heisenberg and biquadratic exchange, are studied in Ref.[359], see also Ref.[60]. Under renormalization also ferromagnetic couplings are generated, which leads to formation of large magnetic moments.

Weakly coupled AF spin chains

Weakly coupled $S = 1/2$ spin chains with random antiferromagnetic bonds are studied in Ref.[206, 367]. Here the strong disorder RG is used to treat intrachain coupling and combined it with mean-field/random-phase approximation treatment of interchain coupling to obtain the phase diagram and collective modes of such systems.

Random isotropic AF $\text{SU}(N)$ spin chains

Random isotropic antiferromagnetic $\text{SU}(N)$ spin chains are studied by the strong disorder RG[179] and an infinite disorder fixed point with $\psi = 1/N$ is found. The mean correlation function involves the exponent, $\eta = 4/N$, compare with Eq.(6.25).

Kondo necklace model

Griffiths phases in the strongly disordered Kondo necklace model is studied in Ref.[307] by the numerical strong disorder RG method and coupling dependent dynamical exponents are found.

Dirty superconductors

The strong disorder RG approach is used to study Griffiths effects and quantum critical point in dirty superconductors without spin-rotation invariance[278]. In the one-dimensional problem the critical point is found to belong to the same infinite disorder universality class as the particle-hole symmetric Anderson localization. Note that in quasi-one-dimensional systems similar results can be obtained by the use of random Dirac fermions[76, 340].

Bosons in 1D

One-dimensional disordered bosons with large commensurate filling, which is described by a random $O(2)$ rotor model is studied by the strong disorder RG method[31]. A strong disorder fixed point is found to control the phase transition between an incompressible-Mott glass and a superfluid phase. The phase transition is in the Kosterlitz-Thouless universality class with $z = 1$.

9 Quantum models in $d > 1$ dimensions

The infinite disorder fixed point scenario is first observed in one-dimensional systems, in which case several independent exact and numerical results support the validity of the scaling picture in Sec.A.3. It is an interesting and important question if infinite disorder fixed points do exist also in higher dimensional systems. This question can be decided only by numerical investigations, which have been done first for the random transverse-field Ising model by Motrunich *et al*[276] and later for the Heisenberg model by Lin *et al* [239]. These results indicate that systems with discrete and continuous symmetry have different types of random fixed points in $d > 1$, in contrast with the similarities observed in $d = 1$. Systems with discrete symmetry, such as the random transverse-field Ising model, have an infinite disorder fixed point, at least for strong enough disorder[276]. On the other hand models with a continuous symmetry, c.f. the random Heisenberg model, have a low-energy fixed point which is either a Griffiths-type fixed point or a large spin fixed point[239]. In these systems no infinite disorder fixed point is observed, even at a quantum critical point. In the following we review the known numerical results.

9.1 Random transverse-field Ising model in 2d

In the strong disorder RG method the elementary decimation steps are the same as in one-dimension as described in Sec.4.2. The main difference, however, is

that during renormalization, the topology of the lattice is not preserved and the renormalized lattice contains bonds between remote sites, too. In this lattice the decimation of a strong transverse field, $h_i = \Omega$, will generate a new coupling between nearest neighbors, $J'_{jk} = J_{ji}J_{ik}/h_i$, as in Eq.(4.17). Since between sites j and k there could be already an interaction, J_{jk} , after renormalization the new coupling is given by:

$$\tilde{J}_{jk} = \max(J_{jk}, J'_{jk}) . \quad (9.1)$$

Here to use the maximum is justified in the infinite disorder fixed point since the couplings are of very different magnitude.

Similarly, after a strong bond, $J_{ij} = \Omega$, decimation a new spin cluster of moment, $\tilde{\mu}_i = \mu_i + \mu_j$ is created in a transverse field, $\tilde{h}_i = h_i h_j / J_{ij}$, see Eq.(4.16). The interaction of the spin cluster to a remaining spin, k , is given by the maximum rule:

$$\tilde{J}_{ik} = \max(J_{ik}, J_{jk}) . \quad (9.2)$$

Numerical analysis of the RG trajectories shows a disordered phase, when the ratio of average log-fields and average log-couplings exceeds a critical value, $[\ln h]_{\text{av}}/[\ln J]_{\text{av}} = \rho > \rho_c$, and an ordered phase in the opposite limit, $\rho < \rho_c$. The control parameter is then defined by $\delta = \rho - \rho_c$.

9.1.1 Scaling at the critical point

At the critical point infinite disorder scaling (see Sec.A.3) is observed[276], which is manifested by a logarithmic relation between the energy (time) and the length-scale, $L \sim \ln(\Omega_0/\Omega)^{1/\psi}$, as in Eq.(A.16). Also the effective cluster moment follows the relation, $\mu \sim \ln(\Omega_0/\Omega)^\phi$, as in Eq.(4.41). At the critical point the largest spin cluster is a fractal, with a fractal dimension, $d_f = \phi\psi$, thus random quantum criticality has a geometrical, percolative interpretation, see also in Sec.7. The scaling dimension of the magnetization, x_m , in Eq.(A.19) is given by:

$$x_m = d - d_f = d - \phi\psi . \quad (9.3)$$

Finally, infinite disorder scaling theory involves the correlation length exponent, ν . These critical exponents have been numerically calculated by the infinite system algorithm[276] and independently by the finite system algorithm[238, 213], using different type of initial disorder distributions. These results are summarized in Table2.

We note that results by quantum Monte Carlo simulations about the 2d system in Ref.[303] are: $\psi \simeq .4$ and $x_m \simeq 1.$, which are consistent with that obtained by strong disorder renormalization.

One important consequence of the fact that the critical point of the random transverse-field Ising model in 2d is controlled by an infinite disorder fixed point is that here frustration does not matter. In any elementary plaquette the couplings and transverse fields have different magnitudes and the renormalization is not affected if the plaquette is frustrated or not. Therefore the quantum Ising spin-glass (i.e. in which there are positive and negative couplings) belongs to the

Table 2: Critical exponents of the two-dimensional random transverse-field Ising model obtained by numerical strong disorder RG calculations: ⁽ⁱ⁾ Ref.[276], ⁽ⁱⁱ⁾ Ref.[238], ⁽ⁱⁱⁱ⁾ Ref.[213].

ψ	ϕ	ν	x_m
0.42 ⁽ⁱ⁾	2.5 ⁽ⁱ⁾	1.072 ⁽ⁱ⁾	1.0 ⁽ⁱ⁾
0.5 ⁽ⁱⁱ⁾	2.0 ⁽ⁱⁱ⁾		0.94 ⁽ⁱⁱ⁾
0.6 ⁽ⁱⁱⁱ⁾	1.7 ⁽ⁱⁱⁱ⁾	1.25 ⁽ⁱⁱⁱ⁾	0.97 ⁽ⁱⁱⁱ⁾

universality class of the random (ferromagnetic) transverse-field Ising model, at least for strong enough disorder. In this respect the quantum Monte Carlo results in Refs.[311, 160], which predict a conventional random fixed point, could be due to the fact that the original disorder is not sufficiently strong. (In the generic phase diagram of disorder induced cross-over effects in Fig.31 it could be in the ID region.)

9.1.2 Disordered phase

In the disordered phase, $\delta > 0$, during renormalization the transverse fields are more frequently decimated. However, until the spin clusters reach a characteristic size, $\xi \sim \ln \Omega_\xi^{1/\psi} \sim \delta^{-\nu}$, also some couplings are decimated. The characteristic size of clusters, ξ , corresponds to the correlation length associated to the average spin correlation function, which is dominated by spin pairs located in the same cluster. For further decrease of the energy scale, $\Omega < \Omega_\xi$, almost exclusively transverse fields are decimated and the typical distance between existing spin clusters: $L_\Omega \sim \Omega^{-1/z}$ is divergent as the fixed point, $\Omega^* = 0$ is approached. (For the similar quantity in 1d see Eq.(4.32)). A third length-scale can be defined through the typical correlation function, $C_{typ}(r)$, which is measured between spins which are in different clusters. We have asymptotically the relation:

$$\ln C_{typ}(r) \sim r/\xi_{typ}, \quad \xi_{typ} \sim \xi^{1-\psi} \sim \delta^{-\nu(1-\psi)}, \quad (9.4)$$

where the value of the typical correlation length, ξ_{typ} , follows from the following argument. Let us consider typical correlations between two sites of distance, $r \sim \xi$. Performing the decimation up to the log-energy-scale, $\ln \Omega_\xi \sim \xi^\psi$, the system renormalizes into isolated single spin clusters with a typical distance L_{Ω_ξ} among them. The typical correlation function at this distance is given by: $C_{typ}(r = \xi) \sim n_{\Omega_\xi}^2 \sim L_{\Omega_\xi}^{-2d}$. Now making use the relation between $\ln \Omega_\xi$ and ξ we arrive to the result in Eq.(9.4).

The value of the dynamical exponent, z , close to the critical point can be obtained from the consideration, that up to the log-energy scale, $-\ln \Omega_\xi \sim \xi^\psi(\delta)$ the RG trajectory is close to the critical trajectory and the distribution function of the couplings and the transverse fields can be approximated by that at the

critical point. From this follows, that $z(\delta) \sim \ln \Omega_\xi$ and therefore:

$$z \sim \xi^\psi \sim \delta^{-\nu\psi} . \quad (9.5)$$

Singularities in the disordered Griffiths phase can be analyzed similarly as for the 1d case in Sec.4.4.2. The only difference, that in d-dimensions the density, n_Ω , is related to the length-scale as, $n_\Omega \sim L_\Omega^{-d}$. Consequently in the singularities in Eqs.(4.51), (4.55) and (4.56) z should be replaced by z/d . In phenomenological scaling theory in Sec.A.4 in the scaling relation in Eq.(A.31) we have the scaling factor in the r.h.s. as b^{-d} .

9.1.3 Ordered phase

Properties of the ordered phase, $\delta < 0$, are qualitatively different in $d > 1$ and in $d = 1$, due to different topology in the two cases. In the RG procedure as the energy scale is lowered the typical cluster size reaches the correlation length, $\xi \sim |\delta|^{-\nu}$, at Ω_ξ , with $\ln \Omega_\xi \sim \xi^\psi$. At this point the existing renormalized sites becomes nearest neighbors, almost exclusively couplings are decimated and a giant, infinite cluster is formed. The formation of the infinite cluster, as argued in Ref.[276], is a classical percolation process, which should be observed also in finite temperature ordering as the temperature is lowered below $T_\xi \sim \Omega_\xi$. At $T = T_c$, however, at which point the classical d -dimensional random bond Ising model has a phase transition the RG-approach breaks down, since close enough to T_c the quantum fluctuations are irrelevant. In this respect as the temperature is lowered there is a double cross-over effect in the critical behavior.

Next we turn to analyze the properties of quantum Griffiths effects, when the energy and temperature scales are much lower than T_c . As in 1d, singularities in the dynamical quantities are due to rare domains, however, in $d > 1$ these events are much more rare and as a consequence singularities are weaker, than in 1d. To see this we consider the system at the percolation point $\Omega = \Omega_\xi$ and see for a large sub-cluster composed of n effective spins, which has an effective field of $\tilde{h} \sim \Omega_\xi^n$. During further renormalization this sub-cluster will generally either be decimated or be connected to the infinite cluster, unless it is sufficiently isolated from the giant cluster. For an efficient isolation the droplet should be at a linear distance of $l \sim \ln \tilde{h} \sim n\xi^\psi$ from the infinite cluster, which has a very low probability of $\exp(-cn^d)$. Note, that the probability of existence of such droplet in the disordered phase, when there is no infinite cluster, is $\exp(-cn)$. As a consequence the low-energy tail of the excitation energies, which are proportional to \tilde{h} , is given by:

$$P(|\ln \tilde{h}|) \sim \exp\left(-\tilde{c}|\ln \tilde{h}|^d\right) , \quad (9.6)$$

which is less singular than the power-low tail in the disordered phase or in the ordered phase in 1d. Therefore the autocorrelation function assumes an enhanced power-low form:

$$G(t) \sim \exp(-A|\ln t|^d) , \quad (9.7)$$

and also the thermodynamic quantities have weaker singularities.

9.2 Random Heisenberg models

Random antiferromagnetic Heisenberg (and XY) models in one dimension constitute the simplest realization of infinite disorder scaling, as described in Sec.6. In the presence of chain-chain interaction between two or more chains, i.e. for random spin ladders infinite disorder scaling is restricted to quantum critical points, otherwise the low energy behavior is controlled by conventional Griffiths or by large spin fixed points, see Sec.8.3. For two- and three-dimensional systems, in which infinite number of chains are coupled together the strong disorder RG approach has been first applied numerically by Bhatt and Lee[55]. Later investigations[276] and scaling considerations[196] indicate that the low energy fixed point of $d \geq 2$ random Heisenberg antiferromagnets is not an infinite disorder fixed point. A comprehensive numerical analysis of the problem, in which non-frustrated and frustrated lattices, as well as models with competing interactions are considered can be found in Ref.[239].

Numerical renormalization rules

During renormalization higher dimensional random Heisenberg models transform in the same way, as random spin ladders, as described in Sec.8.3. Thus clusters with various value of the spin are formed and the couplings between them are antiferromagnetic or ferromagnetic. The decimation rules are described in Sec.8.3 and if more than one coupling is present between two sites the maximum rule in Eq.(9.2) is applied. In the actual calculation the finite lattice method of Sec.8.3 is used, and one has monitored the distribution of the gaps as well as the size of typical effective spins, S_{eff} .

9.2.1 Numerical RG results

Non-frustrated models

Random antiferromagnetic Heisenberg models on the square and on the simple cubic lattices exhibit conventional Griffiths-type behavior, see Sec.A.4. There is no large spin formation and the dynamical exponent, z , is finite. In the square lattice, in which case qualitative estimate was possible, the gap exponent and the dynamical exponent are found, $\omega = 0.7$ and $z = 1.2$, respectively, which satisfy the relation in Eq.(8.22).

Frustrated models

Frustration in the Heisenberg model can be of different origin. i) In the case of spin glass models there are random antiferromagnetic and ferromagnetic couplings. ii) Frustration of geometrical origin is found in random antiferromagnetic models on the triangular and kagomé lattices. iii) Finally, frustration can be a result of competition between first-, J_1 , and second-neighbor, J_2 , couplings. In two-dimensional problems all frustrated models have the same, so called spin glass (SG) fixed point. This is a large spin fixed point with the special properties:

$$\omega_{SG} = 0, \quad z_{SG} = 2, \quad \zeta_{SG} = 1/2, \quad d = 2. \quad (9.8)$$

Note that in 2d relation in Eq.(8.22) is satisfied, thus the excitations seem to be

localized. Also the quantum phase transitions present in the non-random J_1 - J_2 models are washed out by the disorder.

In three-dimensional frustrated problems, such as the spin glass and the J_1 - J_2 models the gap exponent is found, $\omega \approx 0$, which is consistent with the 2d results in Eq.(9.8). The dynamical exponent is practically universal, $z \approx 3/2$, but the relation in Eq.(8.22) is not valid, thus the excitations are not localized. The moment exponent, ζ , is disorder and parameter dependent and generally larger than $1/2$, found in one- and two-dimensions.

9.2.2 Related numerical studies

Quantum Monte Carlo studies of the Heisenberg antiferromagnet on a diluted square lattice show that Néel-type long-range-order disappears at the classical percolation point[215]. While in earlier investigations a novel, S -dependent critical behavior was found[215], recent studies identify the transition as an S -independent classical percolation transition with the well known exponents[318]. The Heisenberg model on the square lattice with random antiferromagnetic bonds is studied by large scale quantum Monte Carlo simulations, as well as by L nczos exact diadonalization and modified spin-wave theory[230]. In agreement with the numerical strong disorder RG results no infinite disorder fixed point is observed, but rather some Griffiths singularities (for sufficiently strong disorder) with a disorder-dependent dynamical exponent. Moreover, the antiferromagnetic order parameter is found surprisingly very robust against bond randomness and a "coexistence" between an antiferromagnetically ordered backbone with some localized region with easily flipable spins (contributing to a divergent uniform susceptibility) is observed. Another work studied the $\pm J$ Heisenberg (quantum) spin glass and found that for a concentration of ferromagnetic bonds $p > p_c \approx 0.11$ the Néel-type long-range-order in the ground state vanishes and is replaced by a so-called spin glass phase[292]. Within the spin-glass phase, the average ground state spin, S_{tot} , scales as $S_{\text{tot}} \sim \sqrt{N}$, and the gap as $\Delta E \sim 1/N$, where N is the number of spins.[293] This is in accordance with the strong disorder RG results in Eq.(9.8).

A 2d bilayer Heisenberg antiferromagnet with random dimer dilution is studied by quantum Monte Carlo simulations in Ref.[319, 345] and its 3d classical counterpart in Refs.[331]. In this system as the ratio of inter-layer and intra-layer couplings is varied a quantum phase transition takes place, which is governed by a conventional random fixed point. This problem with random antiferromagnetic couplings is studied by a numerical implementation of the strong disorder RG method[241]. For strong enough disorder the antiferromagnetic order and thus the phase transition is found to be destroyed so that the system is in the quantum Griffiths phase. A somewhat related problem, a single layer Heisenberg antiferromagnet with staggered dimers and dimer dilution has been studied recently by quantum Monte Carlo simulations[320]. Surprising critical properties are found, among others at the percolation point there is a whole critical line with varying exponents, including a dynamic exponent that appears to diverge continuously in one limit.

Ground state and finite temperature properties of a system of coupled frustrated and/or dimerized spin-1/2 chains modeling e.g. the CuGeO_3 compound are studied in Ref[229]. This system is mapped into a low-energy effective model, which describes a two-dimensional system of effective spin-1/2 local moments interacting by spatially anisotropic long range spin exchange interactions. By a strong disorder RG analysis large spin formation is observed.

9.3 Other problems

Here we list some higher dimensional problems in which (a variant of) the strong disorder RG method has been successfully used.

Doped spin-Peierls model The problem of antiferromagnetism in a two-dimensional Heisenberg model of doped spin-Peierls system is studied by a numerical application of the strong disorder RG method. The low-energy fixed point of the problem is of finite randomness type[133, 255].

Random tight-binding models The problem of particle-hole symmetric localization in two dimensions is studied in terms of a bipartite hopping Hamiltonian with random hopping rates by the strong disorder RG method[279]. The low-energy fixed point of this model is infinite disorder type, the energy- and length-scales are expected to related as: $|\ln \Omega| \sim |\ln L|^x$, where the conjectured values: $x = 2$ in Ref.[148] or $x = 3/2$ in Ref.[279] (see also Ref.[280]). Note, that this singularity formally corresponds to a divergent z or to a vanishing ψ in Eq.(A.16). Introducing two types of hopping amplitudes with a ratio of e^δ in the brick-wall (honeycomb) lattice the system is found delocalized for $\delta < \delta_c$ and localized for $\delta > \delta_c$.

Random Heisenberg and tight-binding models on fractal lattices Numerical implementation of the strong disorder RG method is used to study the low-energy fixed points of random Heisenberg and tight-binding models on different types of fractal lattices[257]. For the Heisenberg model new types of infinite disorder and strong disorder fixed points are found. For the tight-binding model an orbital magnetic field is added and both diagonal and off-diagonal disorder is considered. For the latter model, besides the gap spectra also the fraction of frozen sites, the correlation function, the diamagnetic response and the two-terminal current is studied. The magnetoresistive effects are found qualitatively different for the bipartite and non bipartite lattices..

10 Variations : Correlations, disorder Broadness, etc...

In the random systems we considered till now the random variables (couplings, transverse fields) are independent and identically distributed, furthermore their

distribution is not too broad, generally we assume that the second moment exists. In some problems, however, these assumptions are not satisfied. Disorder is often correlated or broadly distributed and the strength of disorder can be spatially inhomogeneous. Finally, a somewhat related problem when the variables follow non-random, but aperiodic or quasiperiodic sequences. Here we shortly review these developments.

10.1 Correlated disorder

Here we consider the effect of (isotropic) spatial correlations in the disorder that can be modeled with a disorder correlator $G_d(\mathbf{r})$:

$$[\delta(\mathbf{r})\delta(\mathbf{r}')]_{\text{av}} = G_d(\mathbf{r} - \mathbf{r}') . \quad (10.1)$$

For uncorrelated disorder $G_d(\mathbf{r})$ is a delta-function. Regarding the recent experiments on f -electron systems there is evidence [92] that the spatial correlations in the metallic compound $\text{U}_{1-x}\text{Th}_x\text{Pd}_3$ decay like $G_d(\mathbf{r}) \sim r^{-3}$.

The Harris criterion for correlated disorder [352] shows that any disorder correlator that falls off faster than $r^{-2/\nu}$ (i.e. $G(\mathbf{r}) \sim O(r^{-\rho})$ with $\rho > 2/\nu$, where ν is the correlation length exponent for uncorrelated disorder) does not change the universality class of a model with uncorrelated disorder. On the other hand for

$$G(\mathbf{r}) \sim r^{-\rho} \quad \text{with} \quad 0 < \rho \leq 2/\nu \quad (\leq d) , \quad (10.2)$$

where the last inequality holds generally for disordered system with uncorrelated disorder [96], the disorder correlations are relevant, the critical exponents become different from the uncorrelated case and the critical point constitutes a new universality class.

Detailed study of the RTFIC with correlated disorder[314] has lead to the following exact results for relevant correlations, i.e. with a decay of $0 < \rho < 1$. The strength of singularities at the infinite disorder fixed are enhanced and the critical exponents are ρ dependent:

$$\psi(\rho) = 1 - \rho/2, \quad x_s(\rho) = \rho/2, \quad \nu(\rho) = 2/\rho. \quad (10.3)$$

The bulk magnetization exponent, $x_m(\rho)$, according to numerical studies is a decreasing function of ρ , which behaves for small ρ as $x_m(\rho) \approx \rho/2$.

In the disordered phase the strength of Griffiths singularities are also enhanced, this means that the dynamical exponent, $z(\delta, \rho)$, is larger than for uncorrelated disorder, as given in Eq.(4.15). Close to the transition point z is given by: $z(\delta, \rho) \propto \delta^{1-2/\rho}$, what should be compared with $z(\delta) = (2\delta)^{-1}$, for uncorrelated disorder, see Eq.(4.33).

In higher dimensions one still has the result $\nu = 2/\rho$ for $\rho < 2/\nu_{\text{unc}}$, according to a general argument given in [352]. Moreover, ψ increases with increasing disorder correlations, since its value is connected to the geometric compactness of strongly coupled clusters. Thus, the dynamical exponent $z \sim \delta^{-\nu\psi}$ grows, again enhancing the Griffiths singularities.

10.2 Broad disorder distribution

Here we consider the effect of broad disorder distributions of parameters on the critical properties of random quantum magnets, similar investigations for random random walks have been reviewed in [14]. Keeping in mind that in the infinite disorder fixed point of the RTFIC (and also for the 2d model) the logarithm of the couplings and the transverse fields follows a smooth probability distribution, see Eq.(4.24) the appropriate parameterization is:

$$J_{ij} = \Lambda^{\Theta_{ij}} . \quad (10.4)$$

whereas $h_i = h_0$. The exponents, Θ_{ij} are independent random variables, which are taken from a broad distribution, $\pi(\Theta)$, such that for large arguments they decrease as, $\pi(\Theta) \sim |\Theta|^{-1-\alpha}$ (“Lévy flight”). The Lévy index, $\alpha > 1$, and the κ -th moment of the distribution exists for $\kappa < \alpha$.

The random transverse-field Ising model in one- and two-dimensions is studied by numerical strong disorder RG method, and in 1d several exact results are also obtained [213]. The broadness of the disorder distribution is found relevant, if the Lévy index is lowered below a critical value, α_c . In the region of $1 < \alpha < \alpha_c$ the critical points of the systems are governed by infinite disorder fixed points, in which the critical exponents are continuous functions of α and for $\alpha > \alpha_c$ they are the same as in the model with normal (i.e. non-broad) disorder.

In 1d, for the RTFIC $\alpha_c = 2$, in close analogy with random walks, where the central limit theorem is valid for $\alpha > 2$. This analogy is due to the exact mapping, which is shown in Sec.B.1. For the RTFIC several critical exponents are exactly calculated for $\alpha < 2$:

$$\psi(\alpha) = 1/\alpha, \quad x_s(\alpha) = 1/2, \quad \nu(\alpha) = \alpha/(\alpha - 1). \quad (10.5)$$

In 2d numerical results indicate that $\alpha_c \approx 4.5$, thus in the region of $2 < \alpha < \alpha_c$ the broadness of disorder is relevant for the random transverse-field Ising model, whereas it is irrelevant for the random random walk.

In the off-critical region the strength of Griffiths singularities are also enhanced for $1 < \alpha < \alpha_c$. In 1d the low-energy excitations have a typical size-dependence:

$$\ln \epsilon(L) \sim L^{1/(1+\alpha)}, \quad \delta > 0 . \quad (10.6)$$

Thus the dynamical exponent is formally infinite in the whole Griffiths region.

10.3 Inhomogeneous disorder

Here we consider the critical and off-critical properties at the boundary of the RTFIC when the distribution of the couplings, and/or transverse fields, at a distance l from the surface, deviates from its uniform bulk value by terms of order $l^{-\kappa}$:

$$\pi_l(J) - \pi(J) \simeq Al^{-\kappa}, \quad \text{and/or} \quad \rho_l(h) - \rho(h) \sim Al^{-\kappa} . \quad (10.7)$$

Table 3: Summary of the surface critical properties of the inhomogeneous RTFIC.

	$\ln t_r$	$[m_s(\delta)]_{\text{av}}$	$[G_s(t)]_{\text{av}}$
$\kappa > 1/2$	$\sim \xi^{1/2}$	$\sim \delta $	$\sim (\ln t)^{-1}$
$\kappa = 1/2$	$\sim \xi^{1/2}$	$\sim \delta ^{\beta_s(A)}$	$\sim (\ln t)^{-\beta_s(A)}$
$\kappa < 1/2$	$\sim \xi^{1-\kappa}$	—	—
$A > 0$	—	$\sim A ^{\frac{1}{1-2\kappa}}, \delta = 0$	$\sim \text{const}$
$A < 0$	—	$\sim \exp[-\text{const} \delta ^{-(1-2\kappa)/\kappa}]$	$\sim \exp[-\text{const} (\ln t)^{\frac{1-2\kappa}{1-\kappa}}]$

Exact results are obtained[212] using the correspondence between the surface magnetization of the RTFIC and the surviving probability of a random walk with time-dependent absorbing boundary conditions, see Sec.4.1.2. For slow enough decay, $\kappa < 1/2$, the inhomogeneity is relevant: Either the surface stays ordered at the bulk critical point or the average surface magnetization displays an essential singularity, depending on the sign of A . In the marginal situation, $\kappa = 1/2$, the average surface magnetization decays as a power law with a continuously varying, A -dependent, critical exponent which is analytically known. The surface critical behavior of the model is summarized in Table 3.

In the off-critical region the properties of the Griffiths singularities are not affected by the inhomogeneity. A somewhat different form of the inhomogeneity in the RTFIC is studied in Ref.[344].

10.4 Aperiodic systems

Quasiperiodic, or more generally aperiodic sequences have several similarities with random systems. In both cases i) the systems are inhomogeneous, ii) the perturbations have non-periodic character, i.e. there is no finite length-scale associated with the spatial modulation of the couplings and iii) the fluctuations in the energy generally grow with the size of the system (see Eq.(10.8)). To clarify the possible similarities and differences in the critical behavior of random and aperiodic systems several investigations have been performed, both for the diffusion process[194] and in more details for quantum spin systems[245]. Recently, the analysis is extended by the use of the strong disorder RG method[171, 346].

An aperiodic or quasiperiodic sequence is generated through substitutional rules[304]. For example the Fibonacci sequence is built on two letters, **A** and **B**, following the rules: **A** \rightarrow **AB** and **B** \rightarrow **A**. Putting a transverse-field Ising spin chain in this lattice (see Eq.(4.1) the coupling at bond i is $J_i = J_A$ ($J_i = J_B$) if the letter at this position is **A** (**B**), whereas the transverse fields are chosen constant, $h_i = h_0$. Relevance or irrelevance of aperiodic perturbations are related to the value of the wandering exponent, ω , defined through the

fluctuations of the couplings[128]:

$$\Delta(L) = \sum_{i=1}^L (J_i - [J]_{\text{av}}) \sim L^\omega , \quad (10.8)$$

for large size, L . Note, that for the Fibonacci sequence, $\omega = -1$, thus the fluctuations are bounded, whereas for a random system, $\omega = 1/2$. According to an extension of the Harris criterion due to Luck[244] the aperiodic perturbation is irrelevant for:

$$\nu_0 > 1/(1 - \omega) , \quad (10.9)$$

what should be compared with the Harris criterion in Eq.(5.9).

For the transverse-field Ising chain with uniform couplings $\nu_0 = 1$, thus the border-line value is $\omega = 0$. Therefore with bounded fluctuations, $\omega < 0$, the critical behavior of the aperiodic chain is the same as that of the homogeneous one, whereas for $\omega \geq 0$, there is a new type of fixed point of the system. Calculations on specific sequences are in accordance with the above criterion[343]. For marginal perturbations, $\omega = 0$, coupling dependent critical behavior is found with a varying dynamical exponent, z . These calculations are based on an exact RG method, which is proposed in Ref.[188], applied in Ref.[189] and generalized in Ref.[167]. Similar calculations are made for the aperiodic XY model[168] and for the diffusion process[194]. This aperiodic RG method is equivalent to the strong disorder RG method in Sec.4.2 and 4.2 in the limit of $J_A \gg J_B$, or vice versa.

Aperiodic sequences with unbounded fluctuations, $\omega > 0$, are in close analogy with random systems. In particular the Rudin-Shapiro sequence[304], which is built on four letters, **A**, **B**, **C** and **D** with the substitutional rule:

$$\mathbf{A} \rightarrow \mathbf{AB} , \quad \mathbf{B} \rightarrow \mathbf{AC} , \quad \mathbf{C} \rightarrow \mathbf{DB} , \quad \mathbf{D} \rightarrow \mathbf{DC} , \quad (10.10)$$

have the same wandering exponent, $\omega = 1/2$, as the random system. A comparison of the singular behavior of the two systems is performed in Ref.[192], here we summarize the main findings.

In an aperiodic system the energy-, ΔE , and length-scale, L , are related as:

$$|\ln \Delta E| \sim L^\omega , \quad (10.11)$$

and the energy has a logarithmically broad distribution, as for random chains, see Eq.(4.12). Typical and average values of physical quantities at the critical point are very different and the average is dominated by rare realizations, as observed at an infinite disorder fixed point, see Sec.A.3. For example the surface magnetization in the Rudin-Shapiro chain is typically[187], $m_s^{typ}(L) \sim \exp(-\text{const} \times \sqrt{L})$, whereas the average, which is obtained by averaging over all chains, when the starting $l = 0, 1, \dots$ letters from the sequence are omitted, has a power low dependence, $[m_s(L)]_{\text{av}} \sim L^{-x_m^s}$, with $x_m^s = 1/2$. Another singularities at the critical point are different for the Rudin-Shapiro and the random model. For example the correlation length exponent is $\nu = 4/3$, what should be compared with $\nu = 2$ for the random chain in Eq.(4.9).

In the off-critical region aperiodic and random chains behave very differently. In an aperiodic chain the low-energy excitations are bounded[192], therefore there are no Griffiths-singularities in this case.

Part III

RG STUDY OF CLASSICAL MODELS

11 Sinai walk : Random walk in Brownian potential

11.1 Model

The so called ‘Sinai model’, describing a random walk in a random Brownian potential, has interested both the mathematicians since the works of Solomon [332], Kesten *et al.* [218], Sinai [328]..., and the physicists since the works of Alexander *et al.*[30], Derrida-Pomeau [116]... There have been many developments in the two communities for the last thirty years: we refer the reader to the recent review [330] for the mathematical side and to the reviews [15, 16, 14] for the various physicists’s approaches. For the physicists, the interest of the Sinai model is double. On one hand, the Sinai walk represents a simple dynamical model containing quenched disorder, in which many properties that exist in more complex systems can be studied exactly. On the other hand, the Sinai model naturally appears in various contexts, for instance in the dynamics of a domain wall in the random field Ising chain (see section 14) or in the unzipping of DNA in the presence of an external force [242].

The continuous version of the Sinai model corresponds to the Langevin equation [14]

$$\frac{dx}{dt} = -U'(x(t)) + \eta(t) \quad (11.1)$$

where $\eta(t)$ represents the usual thermal noise

$$\langle \eta(t)\eta(t') \rangle = 2T\delta(t - t') \quad (11.2)$$

and where $U(x)$ is the quenched Brownian potential

$$\overline{(U(x) - U(y))^2} = 2\sigma|x - y| \quad (11.3)$$

More generally, in the whole review, thermal averages of observables are denoted by $\langle f \rangle$, whereas disorder averages are denoted by \overline{f} .

In the discrete Sinai model on the 1D lattice, the particle which is on site i has a probability $\omega_i \equiv w_{i,i+1}$ of jumping to the right and a probability $(1 - \omega_i) \equiv$

$w_{i,i-1}$ of jumping to the left. The ω_i are independent random variables in $]0, 1[$. The random walk is recurrent only if $\overline{\ln \omega_i} = \overline{\ln(1 - \omega_i)}$, which corresponds to the absence of bias of the random potential $U(x)$ (11.3) of the continuous version.

The time evolution of $P_i(t)$, the probability for the particle to be on site i at time t , is governed by the Master equation:

$$\frac{dP_i}{dt} = w_{i-1,i}P_{i-1} - (w_{i,i-1} + w_{i,i+1})P_i + w_{i+1,i}P_{i+1}, \quad (11.4)$$

from the solution of which one can obtain different physical quantities. Here we present the drift velocity, v_d , and the persistence, P_{pr} , which is useful to define the phase diagram and an appropriate order parameter of the model.

11.1.1 Drift velocity and dynamics

For a given sample of length, L , i.e. for a given set of the forward ($w_{i,i+1}$) and the backward ($w_{i+1,i}$) transition rates the drift velocity has been calculated by Derrida[116], as:

$$v_d = \frac{L}{\sum_{i=1}^L r_i} \left[1 - \prod_{i=1}^L \frac{w_{i,i+1}}{w_{i+1,i}} \right], \quad (11.5)$$

where the r_i stands for:

$$r_i = \frac{1}{w_{i+1,i}} \left[1 + \sum_{n=1}^{L-1} \prod_{j=1}^n \frac{w_{i+j-1,i+j}}{w_{i+j+1,i+j}} \right]. \quad (11.6)$$

As for the surface magnetization (4.4) in the random transverse field Ising chain, we recognize again Kesten random variables, whose properties are discussed in more details in Appendix C.

In the thermodynamic limit, $L \rightarrow \infty$, and for asymmetric transition rates, $w_{i,i+1} \neq w_{i+1,i}$, one can define a control parameter:

$$\delta = \frac{[\ln w_{\leftarrow}]_{\text{av}} - [\ln w_{\rightarrow}]_{\text{av}}}{\text{var}[\ln w_{\leftarrow}] + \text{var}[\ln w_{\rightarrow}]}, \quad (11.7)$$

where w_{\rightarrow} (w_{\leftarrow}) stands for transition probabilities to the right (left), i.e. $w_{i,i+1}$ ($w_{i,i-1}$). For the biased Sinai walk, considered in Section 12, $\delta > 0$ or $\delta < 0$ and the particle moves to the right or to the left, respectively. The critical situation, $\delta = 0$, is called the Sinai walk, when ultra-slow diffusion takes place[328]:

$$\overline{\langle x^2 \rangle} \sim (\ln t)^4. \quad (11.8)$$

11.1.2 Persistence and order

For a random walk persistence, $P_{pr}(t, L)$, is the probability that the walker has not crossed the starting position at $i = 1$ until time, t [18]. In a finite

system one has an absorbing wall at $i = L + 1$ and the probability: $p_{pr}(L) = \lim_{t \rightarrow \infty} P_{pr}(t, L)$ plays an analogous role to the order parameter in magnetic systems. For a given sample it is given by the expression[193]:

$$p_{pr}(L) = \left(1 + \sum_{i=1}^L \prod_{j=1}^i \frac{w_{j,j-1}}{w_{j,j+1}} \right)^{-1}, \quad (11.9)$$

and in the thermodynamic limit $[p_{pr}]_{av} > 0$, for $\delta > 0$, whereas $[p_{pr}]_{av} = 0$, for $\delta \leq 0$, which explains analogy with the order parameter.

At the critical point, $\delta = 0$, the average persistence is vanishing, its size dependence, however, can be obtained by simple arguments analogous to those used in Sec.4.1.2 for the surface magnetization of the RTFIC. In a *typical sample* the largest term of the sum in Eq.(11.9) grows as $\sim \exp(\text{cst}L^{1/2})$, which follows from the central limit theorem. Consequently,

$$p_{pr}^{typ}(L) \sim \exp(-\text{cst}L^{1/2}), \quad (11.10)$$

which goes to zero very fast with L . The *average behavior* is dominated by *rare events*, in which the persistence is of $O(1)$. It is easy to see that in a rare event: i) non of the L products in Eq.(11.9) are larger than $O(1)$, and ii) a typical product goes to zero fast enough with L . In such a sample the transition rates are distributed in such a way, that the quantity: $\varepsilon_j = \ln \frac{w_{j,j+1}}{w_{j,j-1}}$, satisfies the relation: $\sum_{j=1}^i \varepsilon_j \leq 0$, $i = 1, 2, \dots, L$. This problem is equivalent to a random walk having a length, ε_j , at step j , and which never crosses the origin, thus has a surviving character. The fraction of the rare events is just the survival probability of an L -step random walk:

$$P^{rare}(L) \sim P_{\text{surv}}(L) \sim L^{-1/2}. \quad (11.11)$$

At this point it is evident that the average of the persistence is dominated by the rare events and the contribution of the typical samples is totally negligible. We obtain finally:

$$p_{pr}^{av}(L) \sim P^{rare}(L) \sim L^{-\theta}, \quad (11.12)$$

thus the persistence exponent is $\theta = 1/2$. (See also the RG derivation in Eq.(11.22)).

The singular behavior of the random random walk has many similarities with that of the RTFIC, which is due to an exact mapping, as described in Appendix B.1.

11.2 RG rules for the Sinai model : Physical motivations

The aim of this Section is to justify in details the physical origin of the RG rules that we have given in Eqs (3.3,3.4) as an example of a strong RG rule.

As we have seen before in this review, the strong disorder RG for quantum spin models corresponds to an elimination of degrees of freedom in the Hamiltonian: it is thus rather close to usual renormalizations, the only difference being

that the decimation is done in an iterative way on the extremal coupling, instead of being done in a homogeneous way on the whole chain at each stage. On the contrary, in the strong disorder RG for statistical physics models, the way of thinking deviates much more from the usual procedures. Indeed, the starting point is usually not an exact or approximate integration on the degrees of freedom in the microscopic model, i.e. on the partition function for static problems or on the master equation for dynamic problems. The starting point is rather a heuristic physical argument, which allows to identify the degrees of freedom which will be important at large scale. One then defines the renormalization directly on these important degrees of freedom, and one obtains in the end, in favorable cases, results that become exact in the asymptotic limit where the RG procedure is applied a large number of times. As this mixture between heuristic arguments at the beginning and exact results at the end can appear disconcerting at first sight, and even often meets a certain incomprehension, it seems useful to analyze in details the various stages of the reasoning on the case of the Sinai model.

Identification of the degrees of freedom which will be important at large scale

There exists for a long time a simple qualitative argument [14] to predict the typical displacement $x \sim (\ln t)^2$ in the Sinai model, instead of the usual behavior $x \sim \sqrt{t}$ of the pure diffusion. It can be summarized as follows: the time $t(x)$ necessary to reach the point $x > 0$ will be dominated by the Arrhenius factor of $e^{\beta B_x}$ associated to the largest barrier B_x which should be passed by thermal activation to go from the starting point $x = 0$ to the point x (This approximation by the Arrhenius factor amounts to apply a saddle-point method on the exact expression for the first passage time). In a Brownian potential, the typical behavior of the barrier $B_x \sim \sqrt{x}$ leads to an Arrhenius time $t \sim e^{\beta \sqrt{x}}$, which indeed corresponds to the scaling $x \sim (\ln t)^2$ after inversion.

This heuristic argument suggests that the degrees of freedom which will be important at large scale are the large barriers which exist in the random potential. More precisely, at a given time t , the particle will not have been able to cross by thermal activation any barrier larger than the scale $(T \ln t)$.

Definition of the RG rules directly on the important degrees of freedom of the disorder

The RG procedure is defined directly on the barriers of the random potential. It simply consists in the iterative elimination of the smallest barrier. This smallest barrier remaining in the system defines the RG scale Γ . The renormalized landscape at scale Γ only contains barriers larger than Γ , all the smaller barriers having already been eliminated. As the scale Γ increases, the probability distribution of barriers F in the landscape at scale Γ converges towards a scaling form $\theta(f \geq \Gamma)P^*\left(\frac{F-\Gamma}{\Gamma}\right)$, where the stationary distribution P^* that characterizes the infinite disorder fixed point has been given in Eq (3.10).

Correspondence with the initial model

To each time t of the initial model, one associates the renormalized landscape at scale $\Gamma = T \ln t$. One defines an effective dynamics without thermal fluctuations, in which the particle is at time t near the minimum of the renormalized valley at scale $\Gamma = T \ln t$ that contains the initial position at $t = 0$. More generally, the various observables of the initial model can be associated to the various properties, either static or dynamic, of the renormalized landscape.

Check of the consistency in the asymptotic limit and study of first corrections

The probability that the particle is not in the renormalized valley of the effective dynamics, is of order $1/(\ln t)$ and thus tends towards zero in the limit of infinite time. This shows the consistency of the RG procedure and its asymptotic exactness. One can then study the thermal fluctuations around the effective dynamics, by considering on the one hand the probability distribution inside the renormalized valley, and on the other hand the rare events of order $1/(\ln t)$ where the particle is not in the renormalized valley of effective dynamics.

Discussion

This example shows very well how this way of reasoning allows to obtain a very detailed description of the asymptotic dynamics at large time. It also shows the interest of this inhomogeneous RG to fully adapt to the local extrema of disorder on various scales, compared to the usual renormalizations based on identical cells at each stage. In a certain sense, the way of reasoning we have just described uses to the maximum the qualitative ideas contained in the concept of renormalization, like the irrelevance of the details of the microscopic model on the behaviors at large scale, and the convergence towards simpler theories representing universality classes, *before* the definition of a quantitative procedure. As a consequence, one should not criticize the strong disorder RG approaches for taking as starting point some qualitative physical arguments, because it is precisely from there that all their effectiveness comes! Indeed, for many statistical physics models that we will consider, whereas a usual renormalization on the disordered microscopic model would have no hope to be closed and to lead to exact results, the strong disorder approach allows to obtain a closed renormalization directly on the degrees of freedom which are really important at large scale, and to obtain in the end asymptotic exact results.

11.3 Notions of effective dynamics and localization

In the strong disorder RG approach of the Sinai model, the essential idea is to decompose the process $x_{U,\eta}(t)$, representing the position of the random walk generated by the thermal noise $\eta(t)$ in the random potential Brownian $U(x)$,

into a sum of two terms

$$x_{\{U,\eta\}}(t) = m_{\{U\}}(t) + y_{\{U,\eta\}}(t) \quad (11.13)$$

- the process $m_{\{U\}}(t)$ called the “effective dynamics” depends only on the disorder but not on the thermal noise : it represents the most probable position of the particle at the moment t . It simply corresponds to the best local minimum of the random potential $U(x)$ that the particle has been able to reach at time t . As the escape over a potential barrier F requires an Arrhénus time of order $t_F = \tau_0 e^{\beta F}$, one can study in detail this effective dynamics by using a strong disorder RG which consists in the iterative decimation of the smallest barriers remaining in the system. One then associates to time t the renormalized landscape in which only barriers larger than the RG scale $\Gamma = T \ln t$ have been kept. The position $m_{\{U\}}(t) \sim \Gamma^2 = (T \ln t)^2$ then corresponds at the bottom of the renormalized valley at scale $\Gamma = T \ln t$ which contains the initial condition at $t = 0$.

- the process $y_{\{U,\eta\}}(t)$ represents the thermal fluctuation with respect to effective dynamics. In the limit of infinite time, it remains a finite random variable. This very strong result is the Golosov localization phenomenon [155] : all the particles which diffuse in the same sample starting from the same starting point with different thermal noises η are asymptotically concentrated in the same renormalized valley of minimum $m_{\{U\}}(t)$. More precisely, if one considers the first corrections at large time, the probability that a particle is not in the valley corresponding to effective dynamics $m_{\{U\}}(t)$ is of order $1/(\ln t)$, in which case the particle is at a distance of order $(\ln t)^2$ from $m_U(t)$. These events are thus rare (their probability tends towards zero to large time) but they nevertheless dominate certain observables, such as the thermal width $\overline{\Delta x^2(t)} \sim < y^2(t) > \sim (\ln t)^3$ which diverges.

11.4 Properties of the effective dynamics

11.4.1 Diffusion front

As a consequence of the Golosov localization, the distribution of the rescaled variable $X = \frac{x_{\{U,\eta\}}}{(T \ln t)^2}$, with respect to the thermal noise η in a given sample is asymptotically a Dirac delta distribution $\delta(X - M)$ where $M = \frac{m_{\{U\}}(t)}{(T \ln t)^2}$ is the rescaled variable of the effective dynamics. To compute the averaged diffusion front over the samples (or equivalently over the initial conditions), it is then enough to study the distribution of M over the samples [141, 142]. This leads to the Kesten law [219, 154, 156]

$$P(X) = LT_{p \rightarrow |X|}^{-1} \left[\frac{1}{p} \left(1 - \frac{1}{\cosh \sqrt{p}} \right) \right] = \frac{4}{\pi} \sum_{n=0}^{+\infty} \frac{(-1)^n}{2n+1} e^{-\frac{\pi^2}{4}(2n+1)|X|} \quad (11.14)$$

which is an exact result of mathematicians [219, 156]. This example explicitly shows how the strong disorder RG allows to obtain asymptotic exact results, and gives confidence in the new results of the method concerning finer properties.

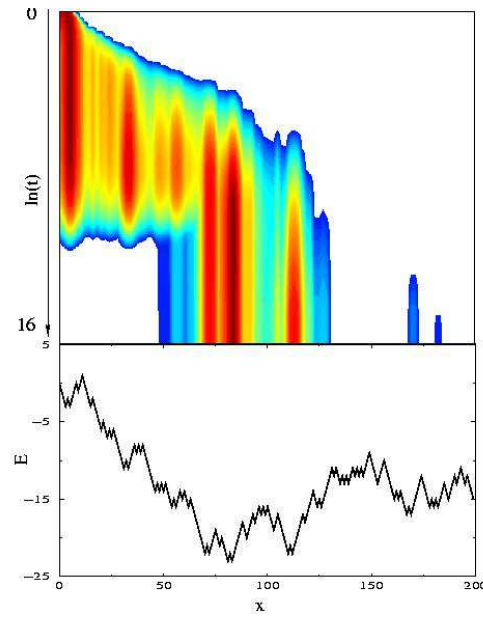


Figure 17: *Example of diffusion front in a given sample, obtained by J. Chave and E. Guitter [95] “Evolution with time (in logarithmic scale) of the distribution $P(x, t)$ in a given energy landscape (drawn below). The evolution runs over 10^7 iterations. The intensity in the grey scale is proportional to $(-\ln P(x, t))$, i.e. darker regions correspond to higher values of $P(x, t)$.”*

11.4.2 Energy distribution

Similarly, the rescaled variable for the energy

$$w = \frac{U(x(0)) - U(x(t))}{(T \ln t)} \simeq \frac{U(m(0)) - U(m(t))}{(T \ln t)} \quad (11.15)$$

is entirely given at large time by the effective dynamics. The reduced variable w has the following limit law as $t \rightarrow \infty$:

$$D(w) = \theta(w < 1) (4 - 2w - 4e^{-w}) + \theta(w \geq 1) (2e - 4) e^{-w} \quad (11.16)$$

This law is continuous, like its derivative at $w = 1$, but the second derivative is discontinuous at $w = 1$, which can seem surprising at first sight. Indeed, for any finite time, the energy distribution is analytic, and it is only in the limit of infinite time that the discontinuity appears for the rescaled variable. It is interesting to note that in the recent mathematical work [181] over the return time to the origin after time t , another not-analytical asymptotic distribution for a rescaled variable also appears. The joint limit distribution of the position $X = \frac{x(t) - x(0)}{(T \ln t)^2}$ and the energy $w = \frac{U(x(0)) - U(x(t))}{(T \ln t)}$ may also be computed in Laplace transform [266]

$$\begin{aligned} \int_0^{+\infty} dX e^{-sX} P(X, w > 1) &= \frac{\sinh \sqrt{s}}{\sqrt{s}} \left(e^{\sqrt{s} \coth \sqrt{s}} - 2 \cosh \sqrt{s} \right) e^{-w \sqrt{s} \coth \sqrt{s}} \\ \int_0^{+\infty} dX e^{-sX} P(X, w < 1) &= \frac{\sinh \sqrt{s} (2 - w)}{\sqrt{s}} - \frac{\sinh 2\sqrt{s}}{\sqrt{s}} e^{-w \sqrt{s} \coth \sqrt{s}} \end{aligned} \quad (11.17)$$

11.4.3 Aging properties

The two-time diffusion front $\overline{P(x, t; x', 0, 0)}$ presents an aging regime in $(\ln t / \ln t')$. In the rescaled variables $X = (x / \ln^2 t)$ and $X' = (x' / \ln^2 t)$, the diffusion front is again determined by the effective dynamics. The RG procedure allows to compute the joint law of the positions $\{m(t), m(t_w)\}$ at two successive times $t \geq t_w$ [142]. In particular, this two time diffusion front presents a Dirac delta function $\delta(X - X')$, which means that the particle can be trapped in a valley from which it cannot escape between t' and t . The weight $D(t, t_w)$ of this delta function thus represents the probability of having $m(t) = m(t_w)$

$$D(t, t_w) = \frac{1}{3} \left(\frac{\ln t_w}{\ln t} \right)^2 \left(5 - 2e^{1(\frac{\ln t}{\ln t_w})} \right) \quad (11.18)$$

11.4.4 Statistics of returns to the origin

The strong disorder RG also yields that the distribution of the sequence $\Gamma_1 = T \ln t_1$, $\Gamma_2 = T \ln t_2 \dots$ of the successive return times to the origin of effective dynamics $m(t)$ has a simple structure [142]: it is a Markovian multiplicative

process defined by the recurrence $\Gamma_{k+1} = \alpha_k \Gamma_k$, in which the coefficients $\{\alpha_i\}$ are independent random variables, distributed with the law

$$\rho(\alpha) = \frac{1}{\sqrt{5}} \left(\frac{1}{\alpha^{1+\lambda_-}} - \frac{1}{\alpha^{1+\lambda_+}} \right) \text{ with } \lambda_{\pm} = \frac{3 \pm \sqrt{5}}{2} \quad (11.19)$$

Here are two important consequences:

- the total number $R(t)$ of returns to the origin during $[0, t]$ behaves as

$$R(t) \sim \frac{1}{3} \ln(T \ln t) \quad (11.20)$$

whereas the total number $S(t)$ of jumps during $[0, t]$ behaves as

$$S(t) \sim \frac{4}{3} \ln(T \ln t) \quad (11.21)$$

(but here there are correlations between times of jumps.)

- the probability that $m(\tau) > 0$ for $\tau \in]0, t]$ involves an irrational persistence exponent [142]

$$\Pi(t) \sim \left[\frac{1}{(T \ln t)^2} \right]^{\bar{\theta}} \text{ with } \bar{\theta} = \frac{3 - \sqrt{5}}{4} = 0.19...$$

whereas the probability that a given walker $x(t)$ does cross the origin during $]0, t]$ has the simpler persistence exponent

$$\Pi_1(t) \sim \left[\frac{1}{(T \ln t)^2} \right]^{\theta} \text{ with } \theta = \frac{1}{2} \quad (11.22)$$

The number of returns to the origin for the effective dynamics translate for quantum spin chain models into the number of decimations above a given point, a quantity which has been recently used to characterize the entanglement properties of these random quantum spin chains [310].

11.5 Localization properties

11.5.1 Distribution of the thermal packet

The asymptotic distribution of the relative position $y = x(t) - m(t)$ with respect to the effective dynamics $m(t)$ corresponds to the Boltzmann distribution in an infinite Brownian valley

$$P(y) = \left\langle \frac{e^{-\beta U_1(|y|)}}{\int_0^\infty dx e^{-\beta U_1(x)} + \int_0^\infty dx e^{-\beta U_2(x)}} \right\rangle_{\{U_1, U_2\}} \quad (11.23)$$

where the average is over two Brownian trajectories $\{U_1, U_2\}$ forming an infinite valley. This formulation is equivalent to the Golosov theorem [155]. The law

can be explicitly computed in Laplace transform in terms of Bessel functions [265], and presents in particular the algebraic decay

$$P(y) \underset{y \rightarrow \infty}{\sim} \frac{1}{y^{3/2}} \quad (11.24)$$

This can be understood as follows: whereas the Brownian potential $U(y)$ yields a typical decay of order $e^{-\beta\sqrt{\sigma y}}$ for the Boltzmann factor, there are rare configurations which return close to $U \sim 0$ at a long distance y , with a probability of order $1/(y^{3/2})$. The correlation of two independent particles in the same sample computed in [265]

$$C(l) = \lim_{t \rightarrow \infty} 2 \int_{-\infty}^{+\infty} dx \overline{P(x, t|x_0, 0)P(x+l, t|x_0, 0)} \quad (11.25)$$

presents the same algebraic decay in $1/l^{3/2}$.

11.5.2 Localization parameters

The localization parameters, which measure the average probabilities to find k particles at the same point at infinite time [265]

$$Y_k = \lim_{t \rightarrow \infty} \int_{-\infty}^{+\infty} dx \overline{[P(x, t|x_0, 0)]^k} = \frac{\Gamma^3(k)}{\Gamma(2K)} (\sigma\beta^2)^{k-1} \quad (11.26)$$

are dominated for large k by the very narrow valleys having a small partition function.

11.5.3 Comparison with equilibrium in a Brownian potential

These various observables which characterize the asymptotic statistics of the thermal packet in the Sinai diffusion actually coincide with their static analogs defined as the thermodynamic limit of the Boltzmann distribution in a Brownian potential on a finite interval [265]. This convergence towards equilibrium of the thermal packet (whereas the effective dynamics remains forever out of equilibrium) is not true any more as soon as one adds a bias (cf section 12)

11.5.4 Thermal width and rare events

The algebraic decay (11.24) for the limit law of the relative position y implies that the second moment $\langle y^2 \rangle$ diverges at infinite time. To obtain its leading behavior at large time, it is in fact necessary to take into account the following rare events [142]: (a) a renormalized valley can have two minima which are almost degenerated in energy; (b) two neighboring barriers can be almost degenerated; (c) a barrier can be near the decimation threshold $(\Gamma + \epsilon)$. These rare events appear with a weak probability of order $1/\Gamma$, but they give rise to

a splitting of the thermal packet into two sub-packets, separated by a long distance of order Γ^2 . As a consequence, these rare events dominate the thermal width [142]

$$\overline{< x^2(t) > - < x(t) >^2} \underset{t \rightarrow \infty}{\propto} \frac{T}{\Gamma} (\Gamma^2)^2 = T(T \ln t)^3 \quad (11.27)$$

This behavior of the thermal width has been measured numerically [95]. More generally, all divergent moments of order $k > 1/2$ have for leading behavior

$$\overline{|x(t) - < x(t) >|^k} \underset{t \rightarrow \infty}{\simeq} c_k T (T \ln t)^{2k-1} \quad (11.28)$$

where the constants c_k can be calculated from the statistical properties of the rare events (a,b,c) described above [142].

11.6 Relations with the general theory of slow dynamics and metastable states

11.6.1 Metastable States

In the usual qualitative description of slow dynamics, the idea of metastable states plays an important role. As the true metastable states only exist in the mean-field approximation or in the zero temperature limit, if one wishes to use this concept for systems in finite dimension at finite temperature, it is necessary to consider metastable states of finite lifetime [56], by decomposing the dynamics into two parts. There are on the one hand fast degrees of freedom, which convergence quickly towards a local quasi-equilibrium : they correspond to the “ metastable states ”. On the other hand, there is a slow out-of-equilibrium dynamics which corresponds to the evolution of the metastable states. In this language, the strong disorder RG description of the Sinai random walk can be reformulated as follows:

- the metastable states at time t are the valleys of the renormalized landscape at scale $\Gamma = T \ln t$: indeed, the walkers who were at $t = 0$ inside this valley have not been able to escape from this valley before time t .
- In each renormalized valley, there is a quasi-equilibrium described by a Boltzmann distribution inside the valley.
- the slow dynamics corresponds to the evolution of the renormalized landscape with the scale $\Gamma = T \ln t$: some metastable states disappear and are absorbed by a neighbor.

One-time observables and Edwards Conjecture

As the ‘ Edwards Conjecture’, which proposes to calculate dynamical quantities via a flat average over all metastable states, has given rise to many recent works [43, 125], it is interesting to reconsider from this point of view the strong disorder RG. In the RG approach, all one-time observables are indeed computed via averages over the renormalized valleys (which are the metastable states), but with a measure which is not flat, but is proportional to the length of the valleys. Indeed, for a uniform initial condition, the length of a renormalized valley represents the size of the attraction basin of the valley.

11.6.2 Decomposition of the diffusion front over metastable states

If one wishes to describe at the same time the effective dynamics of the renormalized valleys and the Boltzmann equilibrium in each renormalized valley, one can write the diffusion front in a sample as

$$P(xt|x_00) \simeq \sum_{V_\Gamma} \frac{1}{Z_{V_\Gamma}} e^{-\beta U(x)} \theta_{V_\Gamma}(x) \theta_{V_\Gamma}(x_0) \quad (11.29)$$

where the sum is over all renormalized valleys V_Γ existing at scale $\Gamma = T \ln t$. The notation $\theta_V(x)$ indicates the characteristic function of the valley V , i.e. $\theta_V(x) = 1$ if x belongs to the valley and $\theta_V(x) = 0$ if not. Finally $Z_V = \int_V dx e^{-\beta U(x)}$ represents the partition function of the valley V . This expression of the diffusion front (11.29) exactly corresponds to the general construction in the presence of metastable states (see [56, 336] and references therein), in which the evolution operator $e^{-tH_{FP}}$ is replaced by a projector on the states (i) of energy $E_i < 1/t$

$$e^{-tH_{FP}} \sim \sum_i |P_i\rangle\langle Q_i| \quad (11.30)$$

whose interpretation is clear: “ everything fast has happened and everything slow has not taken place ” [336]. For the Sinai model, the explicit expressions are as follows: the right eigenvectors

$$P_i(x) = \frac{e^{-\beta U(x)}}{\int_{V_\Gamma^{(i)}} dx' e^{-\beta U(x')}} \theta(x \in V_\Gamma^{(i)}) \quad (11.31)$$

are positive, normalized, and their supports do not overlap, whereas the left eigenvectors

$$Q_i(x) = \theta(x \in V_\Gamma^{(i)}) \quad (11.32)$$

are simply equal to 1 on the support of their corresponding right eigenvector, and zero elsewhere. In the Sinai model, one can in fact go beyond this one-time description by considering the dynamics of the metastable states to obtain information on the spectral properties of the Fokker-Planck operator.

11.7 Eigenfunctions of the Fokker-Planck operator

11.7.1 Fokker-Planck eigenfunctions associated to the effective dynamics

It is interesting to see how the one-time expression (11.29) changes upon the decimation of a renormalized valley, i.e. when a metastable state disappears. The decomposition of the evolution operator on the eigenvalues $E_n \geq 0$ and the right Φ_n^r and left Φ_n^l eigenfunctions of the Fokker-Planck operator H_{FP} reads

$$P(xt|x_00) = \langle X | e^{-tH_{FP}} | x_0 \rangle = \sum_n e^{-E_n t} \Phi_n^R(x) \Phi_n^L(x_0) \quad (11.33)$$

Apart from the ground state $n = 0$ of zero energy $E_0 = 0$ which corresponds to the Boltzmann equilibrium on the full sample

$$\Phi_0^L(x) = 1/\sqrt{Z_{tot}} \quad (11.34)$$

$$\Phi_0^R(x) = e^{-U(x)/T}/\sqrt{Z_{tot}} \quad (11.35)$$

the comparison with equation (11.29) leads to the following identifications for the excited states $n \geq 1$: the energies E_n are determined by the RG scales $\Gamma_n = T \ln t_n = -T \ln E_n$ corresponding to barrier decimations. When a decimation takes place, two valleys V_1 and V_2 merge into one new renormalized valley V' , and the associated eigenfunctions read [265]

$$\Phi_n^L(x) = \sqrt{\frac{Z_{V_1} Z_{V_2}}{Z_{V_1} + Z_{V_2}}} \left(\frac{1}{Z_{V_1}} \theta_{V_1}(x) - \frac{1}{Z_{V_2}} \theta_{V_2}(x) \right) \quad (11.36)$$

$$\Phi_n^R(x) = e^{-U(x)/T} \Phi_n^L(x) \quad (11.37)$$

One can check that these eigenfunctions satisfy all the necessary properties of orthonormalization

$$\int dx \Phi_n^L(x) \Phi_m^R(x) = \delta_{n,m} \quad (11.38)$$

and of the normalization of the thermal packet

$$\int dx \Phi_n^R(x) = 0 \quad (11.39)$$

Beyond the Sinai model, the structure (11.37) in terms of partial partition functions seems more generally to describe the eigenfunctions of the Fokker-Planck operator for slow dynamics in which metastable states disappear in a hierarchical way.

11.7.2 Spatial Structure of eigenfunctions: 2 peaks and 3 length scales

The eigenfunction (11.37) presents two peaks which correspond to the minima of the valleys V_1 and V_2 . Each of the two peaks has a finite width, which represents the characteristic length associated to the Boltzmann weight around the valley minimum. The distance between the two peaks is of order $l(E) \sim \Gamma^2 \sim (\ln E)^2$. Far from the minima, but inside the renormalized valley $r \leq \Gamma^2$, the decay of the eigenfunction $\Phi_n^r(x)$ is controlled by the Boltzmann weight $e^{-\beta U(r)}$ of behavior typical $e^{-c\sqrt{r}}$. In particular at the edge of the valley $r \sim \Gamma^2$, the typical amplitude is of order $e^{-c'\Gamma}$. Beyond the two valleys concerned, the simple approximation (11.37) with theta functions becomes insufficient. To estimate the decay of the eigenfunction at a distance $r \geq \Gamma^2$, one has to consider [277] that the two points are separated by a number of renormalized valleys of order $\frac{r}{\Gamma^2}$ and that the overlap between two neighboring valleys is not zero, but of order $e^{-c''\Gamma}$.

A perturbation theory then leads to an exponential decay of order $e^{-C'' \frac{1}{E}}$, which indeed corresponds to the localization length $\lambda(E) \sim \Gamma \sim (-T \ln E)$ that has been computed for the associated Schrödinger problem via the exact Dyson-Schmidt method [14]. In conclusion, the properties of the eigenfunctions involve three length scales which coexist:

- the finite scale $l \sim 1$ which characterizes the width of a peak, and which is connected to the Golosov localization of the thermal packet.
- the scale $l(E) \sim (\ln E)^2$ which represents the distance between the two peaks and which is connected to the total distance reached by the random walk at time $t \sim 1/E$.
- the scale $\lambda(E) \sim (-\ln E)$ which characterizes the asymptotic exponential decay of the eigenfunction, and which corresponds to the localization length of the associated Schrödinger problem.

Discussion

The Sinai model is thus a perfect ‘infinite disorder fixed point’. The RG procedure gives a very complete picture of the asymptotic dynamics : it allows to obtain many explicit exact results on the effective dynamics of a particle, on the aging properties, on the localization properties of the thermal packet, and on the rare events which control the thermal width. In addition, the description of the Sinai model in terms of renormalized valleys is an explicit example of metastable states of finite life time, and allows to understand the spatial structure of the Fokker-Planck eigenfunctions.

Let us mention to finish that various results obtained via the strong disorder RG have now been confirmed by mathematicians, in particular the results concerning the weight of the singular part of the two time diffusion front [114] and the statistics of the returns at the origin of effective dynamics [97].

12 Biased Sinai walk and associated directed trap model

12.1 Models

12.1.1 Biased Sinai walk

The introduction of a constant force F_0 into the Langevin equation (11.1) of the Sinai model is very natural. This biased model has even more interested mathematicians and physicists for a long time, because it presents a series of dynamic phase transitions [218, 116, 14] in terms of the dimensionless parameter $\mu = F_0 T / \sigma$. In particular, there exists an anomalous diffusion phase for $0 < \mu < 1$, which is characterized by the asymptotic behavior

$$\overline{\langle x(t) \rangle} \underset{t \rightarrow \infty}{\simeq} t^\mu \quad (12.1)$$

whereas for $\mu > 1$, the velocity becomes finite: $\overline{\langle x(t) \rangle} \sim V(\mu)t$ with $V(\mu) = F_0(1 - 1/\mu)$. In the anomalous diffusion phase, the exact diffusion front is given in terms of Lévy stable distributions [218, 14, 180]

The discrete Sinai model corresponds to the Master equation (11.4) with asymmetric rates. The dynamical exponent μ is then defined by the positive root of the equation[116]:

$$\left[\left(\frac{w_{\rightarrow}}{w_{\leftarrow}} \right)^{\mu} \right]_{\text{av}} = 1 . \quad (12.2)$$

The anomalous diffusion phase $0 < \mu < 1$ is analogous to the Griffiths phase of a random magnet.

12.1.2 Directed trap model

It has been proposed for a long time [134, 14, 58] that the biased Sinai model should be asymptotically equivalent to a directed trap model defined by the master equation

$$\frac{dP_t(n)}{dt} = -\frac{P_t(n)}{\tau_n} + \frac{P_t(n-1)}{\tau_{n-1}} \quad (12.3)$$

in which the τ_n are independent random variables distributed with the algebraic law

$$q(\tau) \underset{\tau \rightarrow \infty}{\simeq} \frac{\mu}{\tau^{1+\mu}} \quad (12.4)$$

The anomalous diffusion phase $0 < \mu < 1$ then corresponds to the case where the averaged trapping time is infinite. For a given trap τ , the distribution of the escape time t is exponential

$$f_{\tau}(t) = \frac{1}{\tau} e^{-\frac{t}{\tau}} \quad (12.5)$$

which yields after averaging over τ (12.4)

$$\overline{f_{\tau}}(t) = \int_0^{+\infty} d\tau q(\tau) f_{\tau}(t) = \int_0^{+\infty} \frac{dv}{v} q\left(\frac{t}{v}\right) e^{-v} \underset{t \rightarrow \infty}{\simeq} \frac{\mu \Gamma(1+\mu)}{t^{1+\mu}} \quad (12.6)$$

For a given sample (τ_0, τ_1, \dots) , the probability $P_t(n)$ for the particle to be in the trap n at time t reads

$$P_t(n) = \int \prod_{i=0}^{+\infty} dt_i f_{\tau_i}(t_i) \theta(t_0 + t_1 \dots + t_{n-1} < t < t_0 + t_1 + \dots + t_n) \quad (12.7)$$

and it is thus directly related to the sum of a large number n of independent variables t_i distributed with the law (12.6) presenting an algebraic decay. The diffusion front can be thus expressed in terms of Lévy stable laws [14].

The directed character of this trap model allows to obtain many exact results, since the particle visit sites only once in a fixed order, from left to right. In particular, the thermal width has been exactly computed in [38]

$$\overline{\langle \Delta n^2(t) \rangle} \equiv \overline{\sum_{n=0}^{+\infty} n^2 P_t(n) - \left[\sum_{n=0}^{+\infty} n P_t(n) \right]^2} = \frac{1}{\Gamma(2\mu)} \left(\frac{\sin \pi \mu}{\pi \mu} \right)^3 I(\mu) t^{2\mu} \quad (12.8)$$

where the integral $I(\mu)$ [38] can be rewritten after a change of variables as

$$I(\mu) = \int_0^1 dz \frac{(1+z)z^\mu(1-z)^{2\mu}}{z^{2\mu+2} + 2 \cos \pi\mu z^{\mu+1} + 1} \quad (12.9)$$

The result (12.8) shows that the thermal packet is spread over a length of order t^μ .

On the other hand, the infinite-time limit of the localization parameter for $k = 2$ has been exactly in [98] : their result (24) may be rewritten after a deformation of the contour in the complex plane as

$$Y_2(\mu) \equiv \lim_{t \rightarrow \infty} \sum_{n=0}^{+\infty} \overline{[P_t(n)]^2} = \int_{-\pi}^{+\pi} \frac{d\theta}{2\pi} \frac{e^{i\theta\mu} - e^{i\theta}}{1 - e^{i\theta(\mu+1)}} \quad (12.10)$$

This expression shows that Y_2 is finite in the full phase $0 \leq \mu < 1$ and vanishes in the limit $\mu = 1$. How can this property coexist with the result [38] for the thermal width ? The numerical simulations of [98] show that for a single sample at fixed t , the probability distribution $P_t(n)$ is made out of a few sharp peaks that have a finite weight but that are at a distance of order t^μ (see Figure 18). This explains why at the same time, there is a finite probability to find two particles at the same site even at infinite time, even if the thermal width diverges as $t^{2\mu}$ at large time.

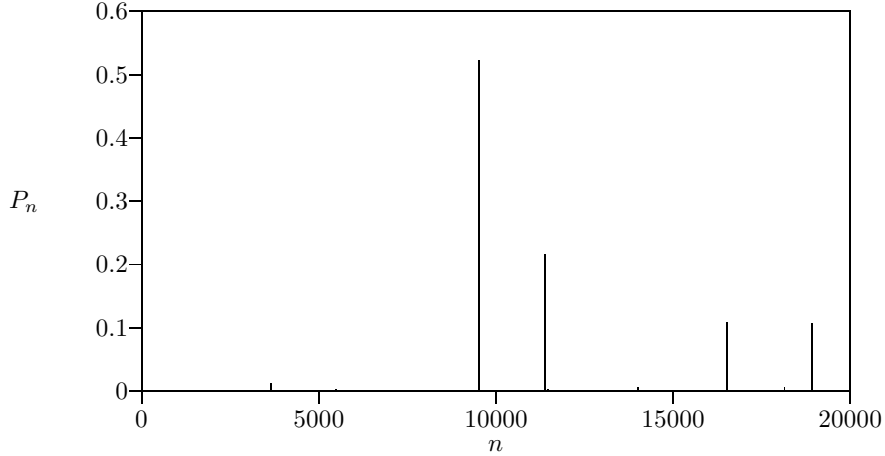


Figure 18: *Figure from Compte and Bouchaud [98] with its caption : “Distribution of probability after a time $t = 7 \times 10^{10}$ for a particular sample of disorder in our 1D directed random walk model with $\mu = 0.4$. The simulation was done with 1,000 particles in a lattice of 20,000 sites. One sees that this probability distribution is made of several sharp peaks that gather a finite fraction of the particles. The position of these peaks is scattered on a region of space of width t^μ .”*

12.2 Principle of the generalized RG

The strong disorder RG presented in the previous section 11 for the symmetric Sinai model can be extended to the biased case, but the obtained results are exact in the limit of infinite time $t \rightarrow \infty$ only if the bias is very small $\mu \rightarrow 0$ [142]: for instance, the RG yields an exponential diffusion front for the rescaled variable $X = \frac{x(t)}{t^\mu}$ that coincide with the exact result involving a Lévy distribution [218, 14] only in the limit $\mu \rightarrow 0$. The reason why the effective dynamics is not exact any more when μ is finite is that the distribution of the barriers F_- against the bias (3.14) converges towards an exponential distribution of finite width proportional to $1/(2\delta) = T/\mu$. This shows that the localization of the full thermal packet in a single renormalized valley at large time, which is valid in the limit $\mu \rightarrow 0$, is not exact any more for finite μ . It is thus necessary to generalize the strong disorder RG approach to include the spreading of the thermal packet into several renormalized valleys [267]. Let us first describe this generalized procedure for the directed trap model (12.3) : in a given sample, the diffusion front is a sum of delta functions with the hierarchic structure explained on the figure (19).

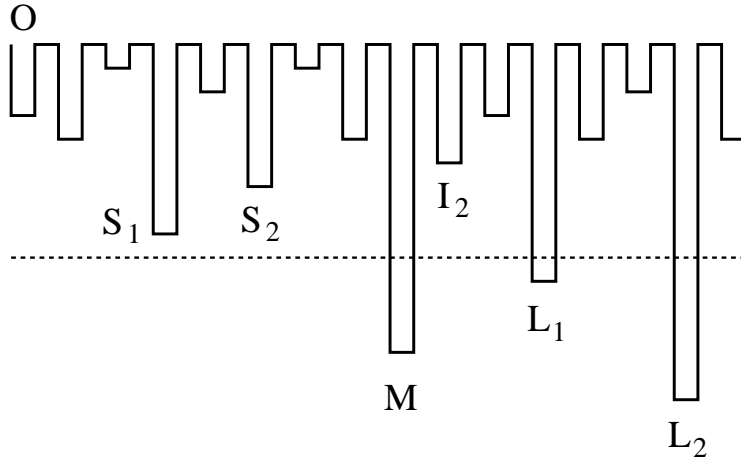


Figure 19: *Hierarchical structure of the important traps for a particle starting at the origin. The dashed line separates the “small” traps (that have a trapping time smaller than t) from the “big” traps (that have a trapping time bigger than t). The first big trap called M is occupied with a weight of order $O(\mu^0)$. The next big trap L_1 and the biggest small trap S_1 before M are occupied with weights of order $O(\mu)$. The third big trap L_2 , the biggest small trap I_2 between M and L_1 , and the second biggest small trap S_2 before M are occupied with weights of order $O(\mu^2)$.*

[267]

12.3 Results for the associated directed trap model

From this description of the diffusion front in each sample, one can compute exact series expansion in μ for all observables. In particular, the explicit computations up to order μ^2 [267] of the diffusion front for the rescaled variable $X = \frac{x}{t^\mu}$, of the thermal width

$$\lim_{t \rightarrow \infty} \frac{\overline{\Delta x^2(t)}}{t^{2\mu}} = \mu(2 \ln 2) + \mu^2 \left[-\frac{\pi^2}{6} + 2 \ln 2 (\ln 2 - 2 + 2\gamma_E) \right] + O(\mu^3) \quad (12.11)$$

and of the localization parameter

$$Y_2(\mu) = 1 - \mu(2 \ln 2) + \mu^2 \left(4 \ln 2 \frac{\pi^2}{6} \right) + O(\mu^3) \quad (12.12)$$

coincide with the series expansions of the corresponding results, for the diffusion front [218, 14], for the thermal width given in Eq 12.8 and for the localization parameter given in Eq 12.10. These comparisons with exact results obtained independently shows that the generalized RG procedure is exact order by order in μ . More generally, to compute observables at order μ^n , it is enough to consider that the diffusion front is spread over $(1+n)$ traps and to average over the samples with the appropriate measure [267].

This approach allows to understand how the anomalous diffusion phase $0 < \mu < 1$ presents at the same time a diverging thermal width as $t^{2\mu}$ (12.11) together with a finite probability $Y_2(\mu)$ (12.12) of finding two particles in the same trap at large time. The qualitative structure of the diffusion front in a given sample is in full agreement with the numerical simulations of A. Compte and J.P. Bouchaud (see Fig 18).

12.4 Quantitative mapping between the biased Sinai model and the directed trap model

The saddle point analysis of the mean thermal exit time from a given renormalized valley of barrier Γ shows that this time is exponentially distributed as in the trap model, with trapping time given by

$$\tau_{\Gamma \rightarrow \infty} \simeq \beta Z_B Z_V e^{\beta \Gamma} \quad (12.13)$$

which mostly depend on the barrier Γ via the usual Arrhénius factor $e^{\beta \Gamma}$, but also on some details of the valley via the prefactor that involves two partition functions Z_V and Z_B of Brownian valleys (see Figure 20).

The probability distribution of the trapping time over the renormalized valleys at scale Γ can be computed from the probability distribution of the barriers and prefactors [267] : the result takes the same form as in the directed trap model

$$q_t(\tau) = \theta(t < \tau) \frac{\mu}{\tau} \left(\frac{t}{\tau} \right)^\mu \quad (12.14)$$

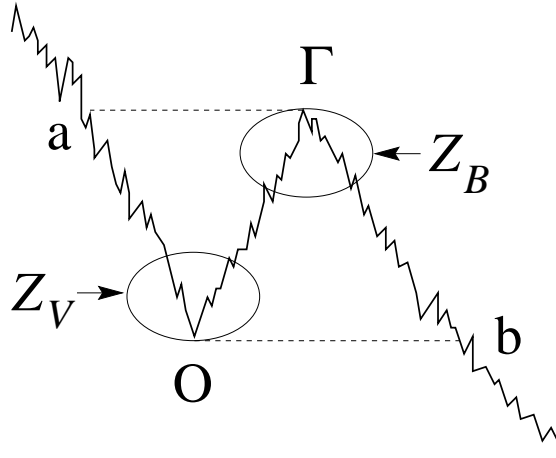


Figure 20: *Computation of the escape time from a renormalized valley of barrier Γ : the first-passage-time at b for a particle starting at 0 is dominated by the Arrhenius factor $e^{\beta\Gamma}$, and the prefactor is the product of two partition functions : Z_V represents the partition function of the bottom of the valley and Z_B represents the partition function of the inverse potential $(-V)$ near the top of the barrier Γ . [267]*

with the following quantitative prescription for the renormalization scale Γ as a function of time

$$\Gamma(t) = T \ln \left[t \sigma^2 \beta^3 \left(\Gamma^2 (1 + \mu) \right)^{\frac{1}{\mu}} \right] \quad (12.15)$$

The corresponding length scale

$$b(t) = \frac{\Gamma^2(\mu)}{\sigma \beta^2} \left[t \sigma^2 \beta^3 \right]^\mu \quad (12.16)$$

is then in full agreement with the constant that has been recently computed by mathematicians for the diffusion front [180].

In conclusion, the generalized strong disorder RG approach allows to establish that the biased Sinai model and the directed trap model are asymptotically equivalent from the point of view of their renormalized descriptions, up to a length scale that can be also exactly computed.

12.5 Results for the biased Sinai model

All the results for the directed trap model can be translated for the biased Sinai model, one simply has to replace traps by renormalized valleys. The diffusion front in a given sample has a hierarchic structure sketched on the Figure 21 which is the analog of Figure 19. For the quantitative results, we just need to replace the rescaled variable $X = \frac{\eta}{t^\mu}$ of the trap model by the rescaled variable

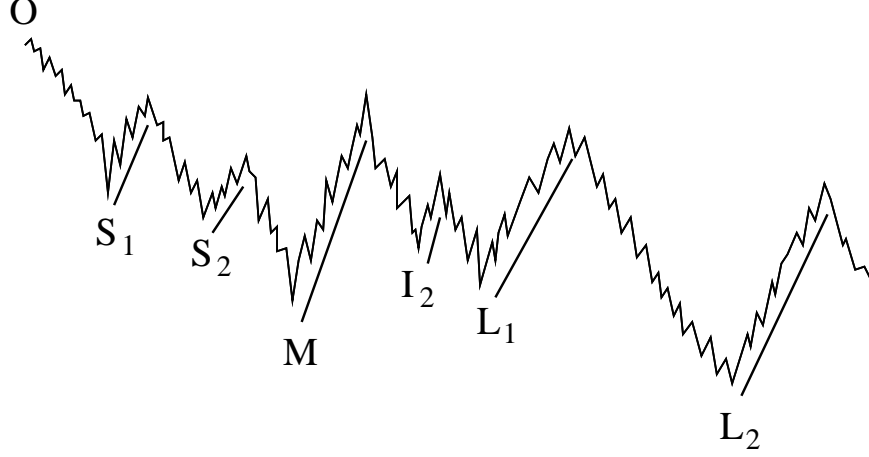


Figure 21: *Hierarchical structure of the important valleys for a particle starting at the origin. The barriers against the bias that are emphasized by the straight lines correspond to the depths of the trap model represented on Figure 19. The bottom M of the renormalized valley that contains the origin at scale Γ is occupied with a weight of order $O(\mu^0)$. The bottom L_1 of the next renormalized valley and the bottom S_1 of the biggest sub-valley before M are occupied with weights of order $O(\mu)$. The next-nearest renormalized valley L_2 , the biggest sub-valley I_2 between M and L_1 , and the second biggest sub-valley S_2 before M are occupied with weights of order $O(\mu^2)$.*

$X = \frac{x(t)}{b(t)}$ of the biased Sinai model (12.16). In particular, the thermal width has for expansion

$$\frac{\overline{\langle \Delta x^2(t) \rangle}}{t^{2\mu}} = \frac{(\sigma^2 \beta^3)^{2\mu}}{\sigma^2 \beta^4} \left[\frac{(2 \ln 2)}{\mu^3} + \left[-\frac{\pi^2}{6} + 2 \ln 2 (\ln 2 - 2 - 2\gamma_E) \right] \frac{1}{\mu^2} + O\left(\frac{1}{\mu}\right) \right] \quad (12.17)$$

And if one translates the exact result of the directed trap model [38], one even obtains the thermal width in the whole phase $0 < \mu < 1$ of anomalous diffusion

$$\frac{\overline{\langle \Delta x^2(t) \rangle}}{t^{2\mu}} = \frac{(\sigma^2 \beta^3)^{2\mu}}{\sigma^2 \beta^4} \frac{\Gamma^4(\mu)}{\Gamma(2\mu)} \left(\frac{\sin \pi \mu}{\pi \mu} \right)^3 I(\mu) \quad (12.18)$$

In conclusion, the anomalous diffusion phase $x \sim t^\mu$ with $0 < \mu < 1$ of the biased Sinai model is characterized by a localization on several renormalized valleys, whose positions and weights can be described sample by sample. The generalized strong disorder RG allows to compute all observables via series expansions in μ . From the strong disorder RG method, this shows that the usual procedure which is exact for infinite disorder fixed point, is an approximation which is already very interesting for finite disorder fixed point : the usual procedure corresponds to the leading term in a systematic expansion.

13 Symmetric Trap model

13.1 Model

Trap models propose a very simple mechanism for aging [59]. A particle performs a random walk in a landscape made of traps, according to the master equation

$$\frac{dP_t(n)}{dt} = -\frac{P_t(n)}{\tau_n} + \frac{P_t(n-1)}{2\tau_{n-1}} + \frac{P_t(n+1)}{2\tau_{n+1}} \quad (13.1)$$

The trapping times $\tau_n = e^{\beta E_n}$ are defined in terms of random energies E_n distributed with the following exponential distribution

$$\rho(E) = \theta(E) \frac{1}{T_g} e^{-\frac{E}{T_g}} \quad (13.2)$$

This choice of exponential distribution comes from the statistics of low energy states in the Random Energy Model [115], in the replica theory [7], and more generally from the exponential tail of the Gumbel distribution which represents an important universality class for extreme statistics. The exponential distribution of energies (13.2) translates for the trapping time $\tau = e^{\beta E}$ into the algebraic law

$$q(\tau) = \theta(\tau > 1) \frac{\mu}{\tau^{1+\mu}} \quad (13.3)$$

with exponent

$$\mu = \frac{T}{T_g} \quad (13.4)$$

At low temperature $T < T_g$, the average trapping time $\int d\tau \tau q(\tau)$ diverges, and this directly leads to aging effects. The aging properties of trap models have been much studied, either in the mean field version [59, 46, 135, 210], or in the 1D version [146, 51, 53], which naturally appears in various physical contexts [30, 14, 184], and which presents two characteristic time scales for aging, in contrast with the mean field case. The aim of this section is to understand this phenomenon via an appropriate strong disorder RG.

13.2 Principle of the RG procedure

We have already described the strong disorder RG for the *directed* trap model in the previous section 12. Here, in the *symmetric* model, each site can be visited several times, which leads to an essential change [268] : a trap of the renormalized landscape will be characterized by two important times, namely (i) its trapping time τ_i , which represents the typical time of exit towards its immediate neighbors (ii) its escape time, which represents the time needed to reach a deeper trap.

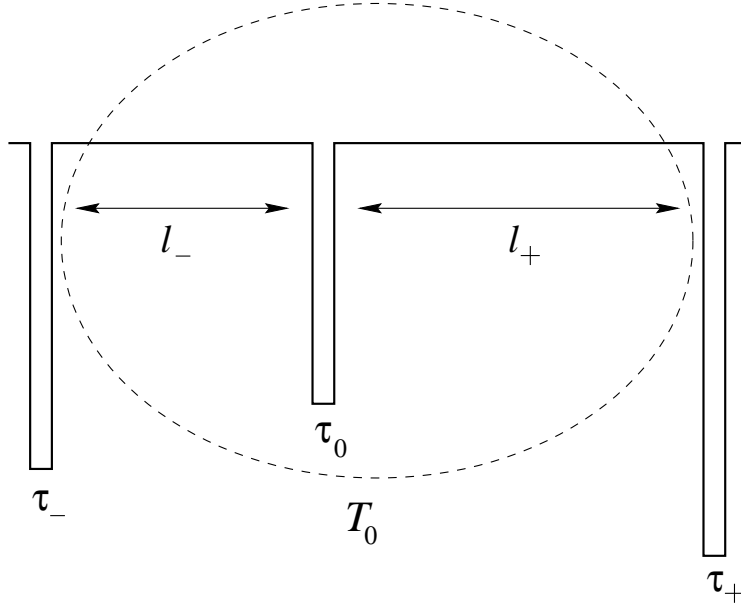


Figure 22: *Definition of the escape time in the renormalized landscape: the trap of trapping time τ_0 is surrounded by two traps, the trap τ_+ at distance l_+ and the trap τ_- at the distance l_- . The escape time is the characteristic time necessary to reach τ_+ or τ_- when one starts from τ_0 . [268]*

The renormalized landscape at scale R is defined as follows: all the traps $\tau_i < R$ are replaced by a flat landscape, whereas all traps $\tau_i > R$ are kept. In the renormalized landscape (see Figure 22), when the particle leaves the trap τ_0 , it escapes to the right or to the left with probability $1/2$. If it escapes to the left, it will succeed to reach the next trap τ_- with probability $1/l_-$. If it escapes to the right, it will succeed to reach the next trap τ_+ with probability $1/l_+$. If not, it will be re-absorbed by the trap τ_0 . Asymptotically, the number of returns to the trap τ_0 before the escape will thus be large, of order R^μ . One can show that the time spent inside τ_0 during these multiple visits dominates over the time spent in the multiple unfruitful excursions and the final successful excursion [268]. The final result is that the escape time t_{esc} from the trap τ_0 has an exponential distribution

$$P(t_{esc}) \underset{R \rightarrow \infty}{\simeq} \frac{1}{T_0} e^{-\frac{t_{esc}}{T_0}} \quad (13.5)$$

with the characteristic time

$$T_0 = \frac{2}{\frac{1}{l_+} + \frac{1}{l_-}} \tau_0 \quad (13.6)$$

To describe the dynamics at time t , one has to keep the traps whose escape time $t_{esc} > t$ (from which particle have not been able to escape at time t). This leads to the following choice for the RG scale $R(t)$ of the landscape as a function of time

$$R(t) \simeq t^{\frac{1}{1+\mu}} \quad (13.7)$$

Moreover, within the limit $\mu \rightarrow 0$, the following effective dynamics becomes exact: at time t , the particle starting from the origin at $t = 0$ will be at time t either on the first renormalized trap M_+ at distance l_+ on the right or on the first renormalized trap M_- at distance l_- on the left. The weight of the trap M_+ is simply the probability $l_-/(l_+ + l_-)$ of reaching M_+ before M_- in a flat landscape

$$P_{eff}(x, t) \sim \frac{l_+}{l_+ + l_-} \delta(x + l_-) + \frac{l_-}{l_+ + l_-} \delta(x - l_+) \quad (13.8)$$

This shows that the dynamics always remains out-of-equilibrium : the weights of the two traps are not given by Boltzmann factors, they do not even depend on the energies of the traps, but only on their distances to the origin.

13.3 Results for the symmetric trap model

Distance between traps in the renormalized landscape

The distances between successive traps in the renormalized landscape are independent random variables and the reduced variable $\lambda = l/\xi(t)$ is exponentially distributed

$$P(\lambda) = e^{-\lambda} \quad (13.9)$$

with the characteristic length scale at time t

$$\xi(t) = \xi_0(\mu) t^{\frac{\mu}{1+\mu}} \quad (13.10)$$

with the prefactor

$$\xi_0(\mu) = 1 + O(\mu) \quad (13.11)$$

Diffusion front

In the rescaled variable $X = x/\xi(t)$, the average of the diffusion front (13.8) over the samples reads [268]

$$g_\mu(X) = e^{-|X|} \int_0^{+\infty} du e^{-u} \frac{u}{|X| + u} + O(\mu) \quad (13.12)$$

Localization parameters

The localization parameters, which represents the averages over the samples of the probabilities to find k independent particles on the same site, are given by [268]

$$Y_k(\mu) \equiv \lim_{t \rightarrow \infty} \overline{\sum_{n=0}^{+\infty} P^k(n, t|0, 0)} = \frac{2}{(k+1)} + O(\mu) \quad (13.13)$$

This result is in agreement with the numerical simulations of Bertin and Bouchaud [51] who have obtained $Y_2 \rightarrow 2/3$ and $Y_3 \rightarrow 1/2$ in the limit $\mu \rightarrow 0$.

Generating function of thermal cumulants

The thermal width reads

$$c_2(\mu) \equiv \lim_{t \rightarrow \infty} \frac{\overline{\langle n^2 \rangle - \langle n \rangle^2}}{\xi^2(t)} = 1 + O(\mu) \quad (13.14)$$

and more generally, the others thermal cumulants can be derived from the generating function

$$Z_\mu(s) \equiv \overline{\ln \langle e^{-s \frac{n}{\xi(t)}} \rangle} = \int_0^{+\infty} d\lambda e^{-\lambda} \lambda \left(\frac{s\lambda}{2} \coth \frac{s\lambda}{2} - 1 \right) + O(\mu) \quad (13.15)$$

Two-particle correlation function

The two-particle correlation function reads

$$C(l, t) \equiv \overline{\sum_{n=0}^{+\infty} \sum_{m=0}^{+\infty} P(n, t|0, 0) P(m, t|0, 0) \delta_{l, |n-m|}} \underset{t \rightarrow \infty}{\simeq} Y_2(\mu) \delta_{l, 0} + \frac{1}{\xi(t)} C_\mu \left(\frac{l}{\xi(t)} \right)$$

The weight of the δ peak at the origin correspond as it should to the localization parameter $Y_2 = 2/3 + O(\mu)$ (13.13), whereas the second term involves the following scaling function

$$C_\mu(\lambda) = e^{-\lambda} \frac{\lambda}{3} + O(\mu) \quad (13.16)$$

The two aging correlations

The probability $\Pi(t + t_w, t_w)$ of no jump during the time interval $[t_w, t_w + t]$ presents a sub-aging scaling form

$$\Pi(t + t_w, t_w) = \tilde{\Pi}_\mu \left(g = \frac{t}{R(t_w)} \right) = \tilde{\Pi}_\mu \left(g = [\tilde{T}_0(\mu)]^{\frac{1}{1+\mu}} \frac{t}{t_w^{\frac{1}{1+\mu}}} \right) \quad (13.17)$$

with

$$\tilde{\Pi}_\mu^{(0)}(g) = \int_0^1 dz \mu z^{\mu-1} e^{-zg} \quad (13.18)$$

In particular, the asymptotic behavior reads

$$\Pi(t + t_w, t_w) \underset{\frac{t}{t_w^{\frac{1}{1+\mu}}} \rightarrow +\infty}{\simeq} \left(\frac{t}{t_w^{\frac{1}{1+\mu}}} \right)^{-\mu} [\mu + O(\mu^2)] \quad (13.19)$$

In contrast, the probability $C(t + t_w, t_w)$ of being at time $(t + t_w)$ in the trap where it was at time t_w presents the aging scaling form

$$C(t + t_w, t_w) = \tilde{C}_\mu \left(h = \frac{t}{R^{1+\mu}(t_w)} \right) = \tilde{C}_\mu \left(h = \tilde{T}_0(\mu) \frac{t}{t_w} \right) \quad (13.20)$$

with

$$\tilde{C}_\mu^{(0)}(h) = \tilde{C}_\mu(h) = \frac{2\mu}{(2h)^\mu} \int_0^{\sqrt{2h}} dz z^{1+2\mu} K_1^2(z) \quad (13.21)$$

In particular, the asymptotic behavior reads

$$C(t + t_w, t_w) \underset{\frac{t}{t_w} \rightarrow \infty}{\simeq} \left(\frac{t}{t_w} \right)^{-\mu} [\mu + O(\mu^2)] \quad (13.22)$$

So these two time correlation present different aging scalings because they involve the two different time scales, the trapping time and the escape time of typical traps reached at time t .

13.4 Linear and non-linear responses to an external field

In the presence of an external field f , the master equation of the trap model becomes [14]

$$\frac{dP_t^{(f)}(n)}{dt} = P_t^{(f)}(n+1) \frac{e^{-\beta \frac{f}{2}}}{2\tau_{n+1}} + P_t^{(f)}(n-1) \frac{e^{+\beta \frac{f}{2}}}{2\tau_{n-1}} - P_t^{(f)}(n) \frac{e^{+\beta \frac{f}{2}} + e^{-\beta \frac{f}{2}}}{2\tau_n} \quad (13.23)$$

in which the transition rates satisfy the detailed balance condition

$$e^{-\beta U(n)} W_{\{n \rightarrow n+1\}}^{(f)} = e^{-\beta U_{n+1}} W_{\{n+1 \rightarrow n\}}^{(f)} \quad (13.24)$$

in terms of the total energy U_n containing the trap random energy $(-E_n)$ trap and the linear potential energy $(-fn)$ associated the external field f

$$U_n = -E_n - fn \quad (13.25)$$

The response has been recently studied by E Bertin and J.P. Bouchaud [52, 53] with scaling arguments and numerical simulations. Their main result is as follows: the Fluctuation-Dissipation theorem for the linear response is valid even in the aging sector, but the response becomes non-linear asymptotically. Here we will generalize the previous RG procedure for the unbiased trap model to take into account the presence of an external field.

Explicit Results for $t_w = 0$

The RG procedure in external field involves a scale length $\xi(t, f)$ which represents the average distance between two traps in the renormalized landscape associated to time t and field f . This scale interpolates between the two behaviors [270]

$$\xi(t, f) \underset{t \ll t_\mu(f)}{\simeq} t^{\frac{\mu}{1+\mu}} [1 + O(\mu)] \quad (13.26)$$

$$\xi(t, f) \underset{t \gg t_\mu(f)}{\simeq} (\beta f t)^\mu [1 + O(\mu)] \quad (13.27)$$

The average of the diffusion front over the samples takes the scaling form

$$\overline{P_t(n, f)} = \frac{1}{\xi(t, f)} g_\mu \left(X = \frac{n}{\xi(t, f)}, F = \beta f \xi(t, f) \right) \quad (13.28)$$

where the scaling function g_μ has the following expression in the limit $\mu \rightarrow 0$ [270]

$$\begin{aligned} g_0(X, F) &= e^{-|X|} \left[\theta(X > 0) + \theta(X < 0) e^{-F|X|} \right] \int_0^{+\infty} d\lambda e^{-\lambda} \frac{1 - e^{-F\lambda}}{1 - e^{-F(|X| + \lambda)}} \\ &= e^{-|X|} \left[\theta(X > 0) + \theta(X < 0) e^{-F|X|} \right] \sum_{n=0}^{+\infty} \frac{F}{(1 + FN)(1 + F + FN)} e^{-nF|X|} \end{aligned}$$

The average position takes the scaling form

$$\overline{\langle x(t, f) \rangle} \equiv \sum_{x=-\infty}^{+\infty} x \overline{P_t(x, f)} = \xi(t, f) X_\mu(F = \beta f \xi(t, f)) \quad (13.29)$$

with the following scaling function X_μ in the $\mu \rightarrow 0$ limit [270]

$$X_0(F) = \int_0^{+\infty} d\lambda \lambda e^{-\lambda} \frac{\frac{F\lambda}{2} \coth \frac{F\lambda}{2} - 1}{F} = 1 - \frac{1}{F} - \frac{1}{F^3} \psi'' \left(1 + \frac{1}{F} \right) \quad (13.30)$$

The thermal width reads

$$\overline{\langle \Delta x^2(t, f) \rangle} = \xi^2(t, f) \Delta_\mu(F = \beta F \xi(t, f)) \quad (13.31)$$

where the scaling function Δ_0 is in fact directly connected to the function X_0 [270]

$$\Delta_0(F) = \left[\frac{1}{F} + \frac{d}{dF} \right] X_0(F) \quad (13.32)$$

Explicit results for $t_w > 0$

The state reached at time t_w in the absence of field must be regarded as an initial condition for the dynamics in field with time $(t - t_w)$. Since at time t_w , the particle is typically in a trap $\tau > R(t_w, f = 0)$, the effective dynamics starts again only when the decimation procedure becomes again activate, i.e. for $R(t - t_w, f) > R(t_w, f = 0)$. It is thus useful to introduce the parameter

$$\alpha(t, t_w, f) \equiv \frac{\xi(t - t_w, f)}{\xi(t_w, f = 0)} = \frac{R^\mu(t - t_w, f)}{R^\mu(t_w, f = 0)} \quad (13.33)$$

which measures the ratio of the length scales for the two renormalized landscapes at t_w and t . In the sector $\alpha < 1$, the response is dominated by rare events, whereas in the sector $\alpha(t, t_w, f) > 1$, the answer is dominated by the effective dynamics. The time domain $(t - t_w)$ corresponding to the sector $\alpha > 1$ depends on the relative values of t_w and time $t_\mu(f)$.

(i) For $t_w \ll t_\mu(f)$, the sector $\alpha > 1$ corresponds to the time domain $(t - t_w) > t_w$, and the parameter α behaves according to

$$\alpha(t, t_w, f) = \left(\frac{t - t_w}{t_w} \right)^{\frac{\mu}{1+\mu}} \quad \text{for } t_w < t - t_w \ll t_\mu(f) \quad (13.34)$$

and

$$\alpha(t, t_w, f) = \left(\frac{\frac{\beta f}{2}(t - t_w)}{t_w^{\frac{1}{1+\mu}}} \right)^\mu \quad \text{for } t - t_w \gg t_\mu(f) \quad (13.35)$$

(ii) For $t_w \gg t_\mu(f)$, the sector $\alpha > 1$ corresponds to the time domain $(t - t_w) > \frac{2}{\beta f} t_w^{\frac{1}{1+\mu}}$, and the parameter α behaves like (13.35) everywhere.

By studying the statistics of the renormalized landscape at two successive RG scales, one obtains explicit results in all the sector $\alpha > 1$ within the limit $\mu \rightarrow 0$. In terms of the rescaled variables $Y = \frac{x(t) - x(t_w)}{\xi(t - t_w, f)}$, $F = \beta F \xi(t - t_w, f)$ and $\alpha = \xi(t - t_w, f) / \xi(t_w, f = 0)$, the averaged distribution of Y takes the form

$$P(Y; F, \alpha) = \frac{1}{\alpha} \delta(Y) + \left[\theta(Y \geq 0) + e^{-F|Y|} \theta(Y \leq 0) \right] G_{ns}(|Y|, F, \alpha) \quad (13.36)$$

The singular part in δ represents the particles which have not been able to escape towards another renormalized trap between t_w and t . The regular part is defined in terms of the function [270]

$$G_{ns}(Y, F, \alpha) = \frac{e^{-Y}}{2} \int_0^{+\infty} du \frac{1 - e^{-Fu}}{1 - e^{-F(Y+u)}} \left[(2 - e^{-(\alpha-1)Y}) e^{-u} - e^{-\alpha u} \right] \quad (13.37)$$

Complementary results concerning in particular the average position and the thermal width are given in [270].

The diffusion front (13.36) presents a very simple asymmetry in $Y \rightarrow -Y$ that implies that the Fluctuation-Dissipation theorem for the linear response is always satisfied. This simple asymmetry of the two-time diffusion front is actually valid for any μ as a consequence of a special dynamical symmetry of the master equation [269] : so the validity of the Fluctuation-Dissipation theorem does not mean that there is some local equilibrium, but is a consequence of this special symmetry of the Master Equation that prevents any FDT violation.

14 Classical Spin chains : Equilibrium and Coarsening dynamics

The thermodynamics of classical disordered spin chains can be studied via product of random 2×2 transfer matrices. In particular, the free energy corresponds to the Lyapunov exponent and can be studied via the Dyson-Schmidt method: the book [8] summarizes the many results obtained within this framework. Here we will instead analyze the equilibrium at low temperature in terms of Imry-Ma domains.

14.1 Models : Random-field Ising chain and spin-glass chain in external field

The random field Ising chain is defined by the following Hamiltonian for classical spins $S_i = \pm 1$

$$H = -J \sum_{i=1}^{N-1} S_i S_{i+1} - \sum_{i=1}^{i=N} h_i S_i \quad (14.1)$$

where the fields $\{h_i\}$ are independent random variables, of zero average $\overline{h_i} = 0$ (see [144] for the non-zero case) and of variance

$$g \equiv \overline{h_i^2} \quad (14.2)$$

According to the Imry-Ma argument [200], the ground state at zero temperature is disordered: there are (+) and (-) domains which alternate, the typical size of a domain being the Imry-Ma length

$$L_{IM} = \frac{4J^2}{g} \quad (14.3)$$

The Imry-Ma argument is based on the competition between the energy cost $4J$ of two domain walls, with the typical energy gain $|\sum_{i=x}^{x+L} h_i|_{\text{typ}} \sim 2\sqrt{gL}$ of a favorable disorder fluctuation on an interval of length L . As a consequence, for $L > L_{IM}$, it becomes favorable to create domains to benefit from the favorable fluctuations of the random fields.

The spin glass chain in external field is defined by the following Hamiltonian for classical spins $\sigma_i = \pm 1$

$$H = - \sum_{i=1}^{N-1} J_i \sigma_i \sigma_{i+1} - \sum_{i=1}^N h \sigma_i \quad (14.4)$$

where the couplings $\{J_i\}$ are independent random variables. In the particular case where $J_i = \pm J$ with probability $(1/2, 1/2)$, there is an equivalence with the random field chain (14.1) with $h_i = \pm h$ via a direct gauge transformation. The physical interpretation of this correspondence between the two models is as follows. In zero field $h = 0$, the two ground states of the spin glass correspond to the two ferromagnetic states of the pure Ising chain. In the presence of $h > 0$, the domain walls of the random field chain correspond to the frustrated bonds $J_i \sigma_i \sigma_{i+1} = J S_i S_{i+1} < 0$ of the spin glass. In the following, we will thus describe the results only in the language of the random field chain, because it is immediate to translate them for the spin glass in external field. For the spin-glass chain in external field with continuous distribution $\rho(J)$ of the couplings J_i , the mapping to the ferromagnetic chain in random fields breaks down, and we refer to the reference [273] for the statistical properties of the ground state and low energy excitations.

14.2 RG construction of the ground state

The Hamiltonian (14.1) for the spins corresponds to the following Hamiltonian for the domain walls $A_\alpha(+|-)$ and $B_\alpha(-|+)$ that appear in the alternate fashion $A_1 B_1 A_2 B_2 \dots$:

$$H = 2J(N_A + N_B) + \sum_{\alpha=1}^{N_A} V(a_\alpha) - \sum_{\alpha=1}^{N_B} V(b_\alpha) \quad (14.5)$$

in term of the Brownian potential seen by the domain walls

$$V(x) = -2 \sum_{i=1}^x h_i \quad (14.6)$$

So each domain wall (A or B) costs an energy $2J$, all domain walls of type $A_\alpha(+|-)$ see the potential $V(x)$ whereas all domain walls of type $B_\alpha(-|+)$ see the opposite potential $(-V(x))$.

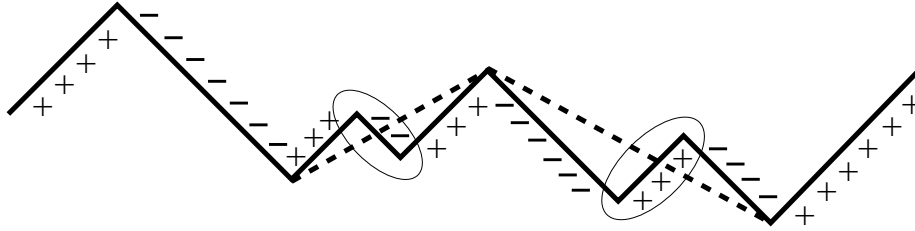


Figure 23: *Illustration of the RG procedure to construct the ground state in a given sample (see text for more details)*

The ground state may now be constructed via the following RG procedure (see Fig 23). We start from the state where each spin is aligned with its local field $S_i = \text{sgn}(h_i)$, i.e. each local extremum of the Brownian potential $V(x) = 2 \sum_{i=1}^x h_i$ is occupied by a domain wall. Then we iteratively eliminate the pair of domain walls that are separated by the smallest potential difference $\Delta V = \Gamma$, as long as it corresponds to a decrease of the total energy $\Delta E = -4J + \Gamma < 0$. So the RG procedure has to be stopped at scale $\Gamma_{eq} = 4J$, the final state giving the structure of the ground state into Imry-Ma domains, as shown on Fig. 24.

In the limit where the Imry-Ma length L_{IM} is large, the statistical properties of the ground state can be obtained from the fixed point associated to the RG rules [144]. In particular, the lengths of Imry-Ma domains are independent variables, distributed with the law

$$P^*(\lambda) = \pi \sum_{n=-\infty}^{\infty} \left(n + \frac{1}{2} \right) (-1)^n e^{-\pi^2 \lambda (n + \frac{1}{2})^2} \quad (14.7)$$

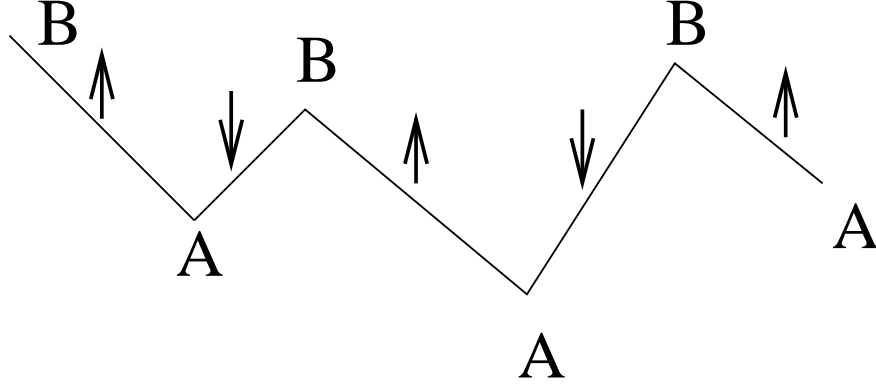


Figure 24: *Picture of the ground-state : the zig-zag line represents the renormalization of the random potential $V(x) = 2 \sum_{i=1}^x h_i$ seen by the domain walls, where only extrema separated by $\Delta V > 4J$ have been kept. Then all maxima are occupied by a domain wall $B(-|+)$, and all minima are occupied by a domain wall $A(+|-)$. So descending bonds are domains of $+$ spins, whereas ascending bonds are domains of $-$ spins. [144]*

for the rescaled variable $\lambda = \frac{l}{2L_{IM}}$. The two-point correlation function then reads [144]

$$\overline{\langle S_0 S_x \rangle} = \sum_{n=-\infty}^{\infty} \frac{48 + 64(2n+1)^2 \pi^2 g \frac{|x|}{\Gamma^2}}{(2n+1)^4 \pi^4} e^{-(2n+1)^2 \pi^2 2g \frac{|x|}{\Gamma^2}} \quad (14.8)$$

with $\Gamma = \Gamma_{eq} = 4J$. In particular, the $n = 0$ term yields the correlation length

$$\xi(T=0) = \frac{8J^2}{\pi^2 g} \quad (14.9)$$

in agreement with the exact solution via the Dyson-Schmidt method [8].

14.3 Low temperature properties from two-level excitations

The thermal fluctuations that exist at very low temperature in disordered systems are often attributed to the existence of some two-level excitations. For the random field Ising chain, these thermal excitations above the ground-state have been numerically studied in [323] via transfer matrix. In this section, we describe how the strong disorder RG approach allows to identify precisely the ‘two-level’ excitations the random field Ising chain and to compute their statistical properties [272].

The excitations of nearly vanishing energy above the ground state are rare events of two kinds, which have been called rare events of type (a) and of type (c) [144, 272] :

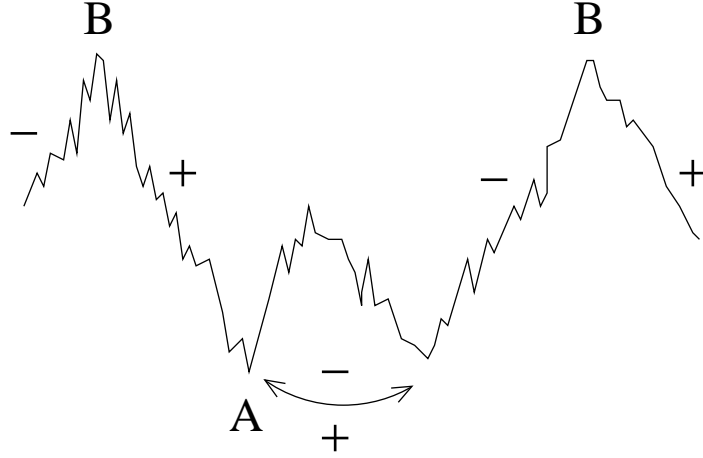


Figure 25: *Representation of a two-level excitation of type (a) : a domain wall A of the ground state may have two nearly degenerate optimal positions, separated by a distance l if $\Delta V = 2 \sum_{i=1}^l h_i \sim 0$. [272]*

(i) The excitations of type (a) involve a single domain wall which has two almost degenerate optimal positions (see Figure 25). These excitations have a length of order $l \sim L_{IM}$, but concerns only a small fraction of order $1/\Gamma_J$ of the domain walls. Their density reads

$$\rho_a^{large}(E=0, l) dl = \frac{\pi^2}{\Gamma_J L_{IM}^2} \sum_{n=1}^{+\infty} n^2 e^{-n^2 \pi^2 \frac{l}{2L_{IM}}} \quad (14.10)$$

The normalization diverges at small l as a result of the continuum limit, but is regularized by the lattice (see [272] for more details). Indeed, nearly degenerate excitations of small length $l \sim 1$ also exist. They are not described by the universal scaling regime (14.10), but depend on specific properties of the initial distribution $P(h_i)$. For instance, the excitations of length $l = 1$ correspond to the domain walls that have a neighbor with a small random field $h_i < T \rightarrow 0$. The density of such excitations is simply proportional to the density $n = 1/L_{IM}$ of domain-walls in the ground-state, and to the weight $P(h_i = 0)$ of the initial distribution at the origin

$$\rho_a(E=0, l=1) = \frac{1}{L_{IM}} 2P(h_i = 0) \quad (14.11)$$

More generally, the statistics of small excitations $l = 2, 3, \dots$ is governed by the probabilities of returns to the origin for a constrained sum of l of random variables.

(ii) The excitations of type (c) involve a pair of domain walls which can appear or annihilate with almost no energy cost (see Figure 26). These excitation

have by definition a large length $l \sim L_{IM} \gg 1$, but they concern only a small fraction of order $1/\Gamma_J$ of the domain walls. Their density reads [272]

$$\rho_c(E=0, l) = \frac{\pi^2}{\Gamma_J L_{IM}^2} \sum_{n=1}^{+\infty} (-1)^{n+1} n^2 e^{-n^2 \pi^2 \frac{l}{2L_{IM}}} \quad (14.12)$$

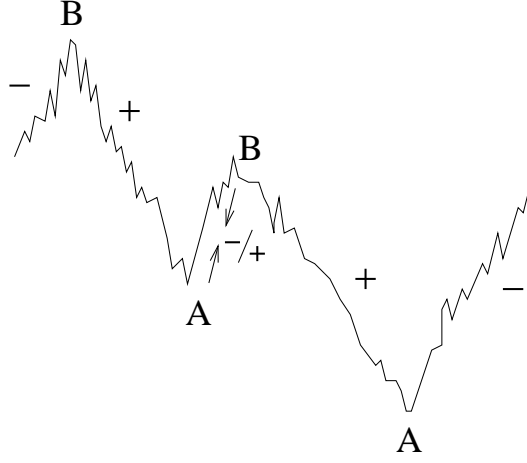


Figure 26: Representation of a two-level excitation of type (c) : a pair (A, B) of neighboring domain walls separated by a distance l may appear or annihilate with almost no energy cost if $\Delta V = 2 \sum_{i=1}^l h_i \sim 4J$. [272]

So there exist on one hand large excitations of length $l \sim L_{IM} \gg 1$, whose universal probability densities are given by the explicit expressions (14.10, 14.12), and there are on the other hand small excitations of length $l \sim 1, 2, \dots$, whose statistics depend on the initial random field distribution.

To compare with the existing rigorous results [284], we now consider that the initial distribution $P(h_i)$ of the random fields has the following scaling form

$$P(h_i) = \frac{1}{H} P\left(\frac{|h_i|}{H}\right) \quad (14.13)$$

where $P(x)$ is a continuous function, such as for instance the exponential distribution $P(x) = e^{-x}/2$ considered in [284] among other cases. In the regime where the Imry-Ma length is large, the results obtained are in agreement (see [272] for more details) with the exact results of the Dyson-Schmidt method [284]. In addition, the RG approach shed light on the influence of small/large excitations on various observables : indeed, the specific heat

$$C(T) = T \frac{\pi^2}{6} \int dl \rho(E=0, l) + O(T^2) \quad (14.14)$$

is dominated by the small non-universal excitations of length $l \sim 1$, that depend on the details of the disorder distribution, whereas the Edwards-Anderson order parameter

$$q_{EA} = \overline{\langle S_i \rangle^2} = 1 - 2T \int_0^{+\infty} dl \, l \rho(E=0, l) + O(T^2) \quad (14.15)$$

and the magnetic susceptibility

$$\bar{\chi} \equiv \frac{N}{T} \left(\overline{\langle m^2 \rangle} - \langle m \rangle^2 \right) = 2 \int_0^{+\infty} dl \, l^2 \rho(E=0, l) + O(T) \quad (14.16)$$

are dominated by the large excitations whose length l is of order of the Imry-Ma length L_{IM} , and whose properties are universal with respect to the initial disorder distribution, since they only depend upon its variance. These excitations are rarer than the small ones, but involve a larger number of spins.

14.4 Coarsening Dynamics

The RG procedure that we have described above to construct the ground state sample by sample has in fact an interesting dynamical interpretation : it corresponds to the coarsening dynamics at low temperature from a random initial configuration with typical domain size $l \sim 1$ towards the equilibrium state with typical domain size $l \sim L_{IM}$. Indeed, the Glauber dynamics involves the transition rate $W(S_j \rightarrow -S_j) = \frac{e^{-\beta \Delta E}}{e^{\beta \Delta E} + e^{-\beta \Delta E}}$ with $\Delta E = 2JS_j(S_{j-1} + S_{j+1}) + 2h_j S_j$, i.e. more explicitly in terms of domain walls

$$\begin{aligned} \Delta E \{ \text{creation of 2 walls} \} &= 4J \pm 2h_j \\ \Delta E \{ \text{diffusion of a wall} \} &= \pm 2h_j \\ \Delta E \{ \text{annihilation of 2 walls} \} &= -4J \pm 2h_j \end{aligned} \quad (14.17)$$

So in the regime $\{h_i\} \sim T \ll J$ on which we will concentrate in this section, the coarsening is described by the following reaction-diffusion model in the Brownian potential

- the domain walls A diffuse towards the minima
- the domain walls B diffuse towards the maxima
- Annihilation when meeting $A + B \rightarrow \emptyset$

One can moreover show [144] that at large time, all maxima and minima are occupied by domain walls, as on the Figure (24), which allows to derive directly the properties of the reaction-diffusion process at time t from the landscape RG at scale $\Gamma = T \ln t$.

In particular, the lengths of Imry-Ma domains are independent variables during the coarsening (this is not true for the pure Ising case [123]), and are distributed with the law (14.7) for the rescaled variable $\lambda = \frac{2gl}{(T \ln t)^2}$. The two

spin correlation also take the same form as in the ground state (14.8) with the RG scale $\Gamma = T \ln t$.

The two-time autocorrelation reads [144]

$$\overline{\langle S_i(t) S_i(t') \rangle} = \frac{4}{3} \left(\frac{\ln t'}{\ln t} \right) - \frac{1}{3} \left(\frac{\ln t'}{\ln t} \right)^2 \quad (14.18)$$

Taking into account the coarsening length scale $L(t) \sim (\ln t)^2$, the non-equilibrium autocorrelation exponent defined by the asymptotic behavior [182]

$$\overline{\langle S_i(t) S_i(t') \rangle} \sim \left(\frac{L(t')}{L(t)} \right)^\lambda \quad (14.19)$$

has thus for value $\lambda = 1/2$ here.

Various persistence exponents can be also obtained [144]

- The probability that a spin does not flip during the time interval $[0, t]$ decays as $\left(\frac{1}{(T \ln t)^2} \right)^\theta$ with $\theta = 1$.
- The probability that the thermal average $\langle S_i(t) \rangle$ keeps the same sign during $[0, t]$ decays as $\left(\frac{1}{(T \ln t)^2} \right)^{\bar{\theta}}$ with $\bar{\theta} = \frac{3-\sqrt{5}}{4}$.
- The probability that an initial domain has not disappeared at time t decays as $\left(\frac{1}{(T \ln t)^2} \right)^\psi$ with $\psi = \frac{3-\sqrt{5}}{4}$.

We now turn to the question of the fluctuation-dissipation violation, which is quantified via the ratio X defined by [102]

$$T R(t, t_w) = X(t, t_w) \partial_{t_w} C(t, t_w) \quad (14.20)$$

where $C(t, t_w)$ represents the connected thermal correlation

$$C(t, t_w) = \sum_x \overline{\langle S_0(t) S_x(t_w) \rangle - \langle S_0(t) \rangle \langle S_x(t_w) \rangle} \quad (14.21)$$

and where $R(t, t_w)$ represents the linear response to a uniform external field H applied from t_w

$$\overline{\langle S_0(t) \rangle} = H \int_{t_w}^t du R(t, u) \quad (14.22)$$

For the coarsening of the random field Ising chain, three regimes have been found [144]

- (i) quasi-equilibrium of the domain walls in renormalized valleys

$$X(t, t_w) = 1 \quad \text{for } 0 < \frac{\ln(t - t_w)}{\ln t_w} < 1 \quad (14.23)$$

- (ii) a nontrivial ratio X when the effective dynamics of the valleys takes place again

$$X(t, t_w) = \frac{t + t_w}{t} \quad \text{for } \frac{t - t_w}{t_w} \text{ fixed} \quad (14.24)$$

(iii) a final aging regime

$$X(t, t_w) = \frac{t}{t_w \ln t_w} \left(1 + \frac{24 \ln^2 t_w}{7 \ln^2 T} \right) \text{ for } \frac{\ln t}{\ln t_w} > 1 \quad (14.25)$$

In particular, X grows towards $+\infty$, because the truncated thermal correlations are very weak with respect to the response.

In comparison with mean field models, the ratio X is not a function of the correlation $C(t, t_w)$ alone : it is because of the two scales (t, t_w) and $(\ln t, \ln t_w)$. In addition, in mean field the ratio X belongs to the interval $[0, 1]$ and is interpreted as an inverse effective temperature $X = 1/T_{eff}$ [103]. Here, the final regime corresponds to $T_{eff} \rightarrow 0$, which can be interpreted as a fixed point of zero temperature. It is also interesting to compare with what is known on the coarsening in pure ferromagnets. At the critical point T_c , there exists a non trivial ratio $X(\frac{t}{t_w})$ which can be identified as an amplitude ratio [152]. For instance, in the pure 1D Ising chain at zero temperature, the amplitude ratio [151] is $X(t, t_w) = \frac{t+t_w}{2t}$: it decreases from $X(t = t_w, t_w) = 1$ to $X(t \rightarrow \infty, t_w) = \frac{1}{2}$.

For $T < T_c$, the ratio X vanishes $X = 0$ [42, 50], which is understood in the following way: the domain walls respond with a factor $O(1)$ but they occupy only a small fraction $1/L(t_w)$ of the volume. By comparison, for the random field chain, only a small fraction $1/\Gamma_w$ of domain walls respond, but with a very large response, since it corresponds to the flipping of an entire domain with length scale Γ_w^2 .

In this section, we have described how the formulation of Glauber dynamics of the random field Ising chain in terms of a reaction-diffusion process in a Brownian potential for the domain walls allows to obtain very detailed results as a consequence of the very strong localization of the domain walls by the disorder. Similarly, more general reaction-diffusion processes in a Brownian potential have also been studied in details [232].

15 Localization of a random polymer at an interface

15.1 Model

This section is devoted to the following random polymer model introduced by Garel, Huse, Leibler and Orland [150]. An heteropolymer made of monomers carrying random charges q_i is near an interface located at $z = 0$. The medium $z > 0$ is favorable for positive charges $q > 0$ whereas the medium $z < 0$ is favorable for negative charges $q < 0$. More precisely, the model is defined by the following partition function on Random Walks $\{z_i\}$ [150]

$$Z_L(\beta; \{q_i\}) = \sum_{RW\{z_i\}} \exp \left(\beta \sum_{i=1}^L q_i \text{sgn}(z_i) \right) \quad . \quad (15.1)$$

At high temperature, Imry-Ma arguments have been proposed [150] for the symmetric case $\overline{q_i} = 0$ as well as for the asymmetric case $\overline{q_i} > 0$: these arguments are based on energy/entropy balances, unlike the usual Imry-Ma arguments which are based on an energy/energy balance. Since the localization mechanism is different in the symmetric and asymmetric cases, we will now discuss them separately.

15.2 Symmetric case

15.2.1 Imry-Ma argument based on typical events

The Imry-Ma argument for the symmetric case [150] is as follows. The chain is assumed to be localized around the interface, with a typical loop length l in each solvent:

- the typical energy gain per loop is of order $\sum_i^{i+l} q_i \sim \sqrt{\sigma l}$, i.e. of order $\sqrt{\sigma/l}$ per site.
- the entropy loss due to the confinement in a band of width $r \sim \sqrt{l}$ around the interface is of order $1/r^2 \sim 1/l$ per site.

The optimization of the free energy by monomer

$$f(l) \sim -\sqrt{\frac{\sigma}{l}} + \frac{T}{l} \quad (15.2)$$

with respect to the length l leads to the characteristic length

$$l \sim \frac{T^2}{\sigma} \quad (15.3)$$

and to the following behavior for the free energy

$$f(T) \sim -\frac{\sigma}{T} \quad (15.4)$$

This argument for the symmetric polymer thus predicts a localization at any temperature, with the above behaviors at high temperature.

15.2.2 Comparison between two strategies

To go beyond the above Imry-Ma argument, two extreme strategies have been proposed for the polymer configurations adapted to a given random sequence :

(a) a sequence-dependent strategy based on a real space RG procedure [264], where only the conformations corresponding to the optimal loop configuration are taken into account.

(b) a sequence-independent strategy, where all configurations compatible with a fixed loop distribution $K(l)$ are considered [57].

The recent mathematical work [57] (and references therein) indicates that the strategy (b) is better for the symmetric case : this means that the disorder

is not able to dominate over the random walk fluctuations. On the contrary, the strategy (a) seems better for the asymmetric case. We will thus describe the sequence-dependent strategy based on a real space RG procedure [264] only for the asymmetric case.

15.3 Asymmetric case

15.3.1 Imry-Ma argument based on rare events

The Imry-Ma argument proposed for the asymmetric case [150] is in fact much more subtle than the argument for the symmetric case, because the correct description of the loops in the minority solvent $(-)$ requires the consideration of the “rare events” where the sum of l_- random variables q_i , of positive average $\overline{q_i} = q_0 > 0$, turns out to be negative enough to make favorable an excursion in the solvent $(-)$. More precisely, the argument is as follows [150] : the polymer is expected to be in its preferred solvent $(+)$, except when a loop of length l^- in the solvent $(-)$ becomes energetically favorable with a sufficient charge $Q_- = -\sum_{i=j}^{j+l^-} q_i > 0$. As the probability of having $\sum_{i=j}^{j+l^-} q_i = -Q^-$

$$\text{Prob}(Q^-) = \frac{1}{\sqrt{4\pi\sigma l^-}} e^{-\frac{(Q^- + q_0 l^-)^2}{4\sigma l^-}} \quad (15.5)$$

is weak, the typical distance l^+ between two such events behaves like the inverse of this probability

$$l^+ \sim e^{\frac{(Q^- + q_0 l^-)^2}{4\sigma l^-}} \quad (15.6)$$

This rare event argument gives that the energy gained Q^- in a loop of the solvent $(-)$ behaves as

$$Q^- \sim \sqrt{4\sigma l^- \ln l^+} - q_0 l^- \quad (15.7)$$

whereas the corresponding entropy loss is of order $(\ln l^+)$. The difference in free energy per monomer between this localized state with loops (l_+, l_-) and the delocalized state in the preferred solvent $(+)$ is of order

$$f(T, l^+, l^-) - f_{deloc}(T) \sim \frac{1}{l^+} (-Q^- + T \ln l^+) \sim \frac{1}{l^+} (q_0 l^- - \sqrt{4\sigma l^- \ln l^+} + T \ln l^+) \quad (15.8)$$

The optimization with respect to the length l^- gives the relation

$$l^- \sim \frac{\sigma}{q_0^2} \ln l^+ \quad (15.9)$$

and thus finally

$$Q^- \sim \frac{\sigma}{q_0} \ln l^+ \quad (15.10)$$

This argument thus predicts that both the energy gain Q^- and the entropy cost have the same dependence in $(\ln l^+)$: the difference in free energy factorizes into

$$f(T, l^+) - f_{deloc}(T) \sim (T - T_c) \frac{\ln l_+}{l_+} \quad (15.11)$$

This argument predicts a transition at a critical temperature

$$T_c \sim \frac{\sigma}{q_0} \quad (15.12)$$

between the localized phase and the delocalized phase. In contrast with the symmetric case, the behaviors of the free energy and length l_+ in terms of the temperature are not determined by the argument.

15.3.2 The disorder-dependent strategy based on real space RG

The aim of the strong disorder RG is to construct the optimal loop structure around the interface for a given disorder realization.

At zero temperature, each monomer is in its preferred solvent $\text{sgn}(z_i) = \text{sgn}(q_i)$: the polymer is broken into loops α containing l_α consecutive monomers of the same sign, and carrying some absolute charge Q_α . When the temperature increases, we consider the configurations which can be obtained from the ground state loop structure by the iterative transfer in opposite solvent of the loop presenting the smaller absolute charge $Q_{min} \equiv \Gamma$. When a loop $(Q_2 = \Gamma, l_2)$ surrounded by two loops (Q_1, l_1) and (Q_3, l_3) is transferred, one obtains a new large loop whose length l and absolute charge Q are given by the rules by the rules (see Fig. 27)

$$\begin{aligned} Q &= q_1 + q_3 - q_2 \\ l &= l_1 + l_2 + l_3 \end{aligned} \quad (15.13)$$

These rules correspond to the RG rules for the Brownian extrema described in Eqs (3.3,3.4) : here the corresponding random walk is the sum of the charges $\sum_0^i q_j$ up to the running monomer i , and the RG procedure builds the best loop structure with the constraint that only loops with absolute charges larger than Γ are allowed. To establish the correspondence between the RG scale Γ and the temperature, we now have to determine under which conditions the transfer of a loop (Q_2, l_2) in opposite solvent is indeed favorable from the free energy point of view. The energy cost is

$$\Delta E^{flip} = 2Q_2 \quad (15.14)$$

whereas the entropy gain is

$$\Delta S^{flip} = \ln(M(l_1 + l_2 + l_3)) - \ln[M(l_1)M(l_2)M(l_3)] \quad (15.15)$$

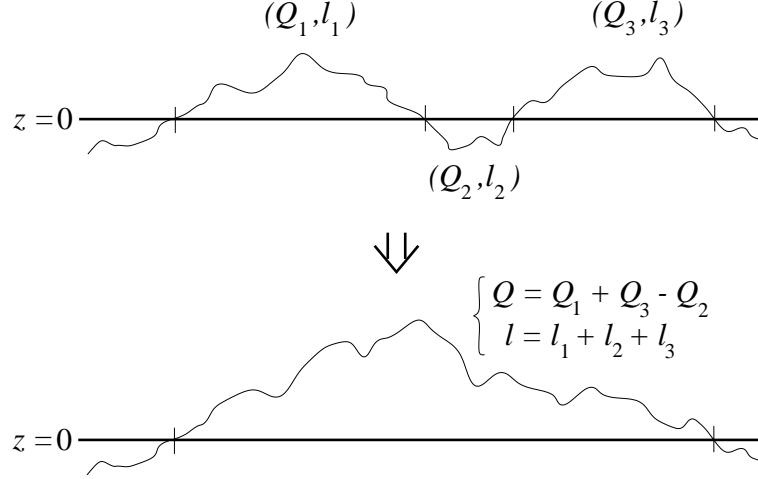


Figure 27: *Illustration of the real space RG procedure : the transfer of a loop $(Q_2 = \gamma, l_2)$ surrounded by the neighboring loops (Q_1, l_1) and (Q_3, l_3) gives rise to a new loop (Q, l) with the RG rules (15.14). [264]*

where $M(l) = c^l/l^{3/2}$ represents the number of random walks of l steps going from $z = 0$ to $z = 0$ in the presence of an absorbing condition at $z = 0^-$. This leads to the following free energy balance

$$\Delta F^{flip} = \Delta E^{flip} - T \Delta S^{flip} = 2Q_2 - T \ln \left(\frac{M(l_1 + l_2 + l_3)}{M(l_1)M(l_2)M(l_3)} \right) \quad (15.16)$$

To obtain the optimal structure at temperature T , the RG procedure has to be implemented as long as it lowers the free energy ($\Delta F^{flip} < 0$), and it should be stopped before the first iteration which would increase the free energy ($\Delta F^{flip} > 0$).

15.3.3 Results of the strong disorder RG

The results of the strong disorder RG for the asymmetric case are the following [264] :

- in the limit $\sigma \gg q_0$, the delocalization transition takes place at high temperature when the loops are large, and the critical temperature reads

$$T_c = \frac{4\sigma}{3q_0} \quad (15.17)$$

- the free energy presents the following essential singularity

$$f(T) - f(T_c) \underset{T \rightarrow T_c^-}{\simeq} -2q_0 \left(\ln \frac{4\sigma}{q_0} \right) \exp \left[-\frac{\ln \frac{4\sigma}{q_0}}{\left(1 - \frac{T}{T_c}\right)} \right] \quad (15.18)$$

i.e. the transition is of infinite order in this scenario.

- the typical loop length $l_{blob}^+(T)$ in the preferred solvent diverges with an essential singularity at the transition, whereas the typical blob length $l_{blob}^-(T)$ in the unfavorable solvent diverges algebraically

$$l_{blob}^+(T) \underset{T \rightarrow T_c^-}{\simeq} \frac{\sigma}{q_0^2} \exp \left[+\frac{\ln \frac{4\sigma}{q_0}}{\left(1 - \frac{T}{T_c}\right)} \right] \quad (15.19)$$

$$l_{blob}^-(T) \underset{T \rightarrow T_c^-}{\simeq} \frac{\sigma}{q_0^2} \frac{\ln \frac{4\sigma}{q_0}}{\left(1 - \frac{T}{T_c}\right)} \quad (15.20)$$

- the scaling variable $\lambda_+ = l_+/l_{blob}^+(T)$ for the loops in the preferred solvent is distributed with the exponential distribution $e^{-\lambda_+}$.

- For a large chain of length L , the distribution of the delocalization temperature can be computed [264]. In particular the typical value presents a logarithmic correction of order $(1/\ln L)$ with respect to the critical temperature of the thermodynamic limit

$$T_{deloc}^{typ} \sim T_c \left(1 - \frac{4\sigma}{q_0^2 \ln L} \right) \quad (15.21)$$

In conclusion, the strong disorder RG just described for the asymmetric case is a direct extension of the Imry-Ma argument based on rare events [150] given in section 15.3.1. It allows to characterize in details the delocalization transition via the explicit construction of polymer loops in each sample. Recent mathematical work [57] have obtained rigorous bound for the free-energy from this RG loop construction.

16 Asymmetric simple exclusion process with disorder

The asymmetric simple exclusion process (ASEP) is the paradigmatic example of a model for non-equilibrium transport. Moreover this model can be related via simple mappings to other problems of non-equilibrium statistical physics which include e.g. surface growth problems [21, 22]. For homogeneous transition rates the model has a detailed analytical solution, both for periodic and open boundary conditions. Disorder in this model can be introduced in two different ways. For particle-wise (pt) disorder[225, 132] each particle has specific

transition rates, which are the random variables. On the other hand for site-wise (st)disorder[342] the specific transition rates are assigned to lattice sites, rather than to particles. Our understanding about the random model is more complete for pt disorder, what we are going to consider first in the following.

16.1 ASEP with particle-wise disorder

To be concrete we consider here the ASEP on a periodic chain of N sites and with M particles. Particle i may hop to empty neighboring sites with rates p_i to the right and q_i to the left, where p_i and q_i are independent and identically distributed random variables. Representing a configuration by the number of empty sites n_i in front of the i th particle, the stationary weight of a configuration n_1, n_2, \dots, n_M is given by [334, 132]:

$$f_N(n_1, n_2, \dots, n_M) = \prod_{\mu=1}^M g_{\mu}^{n_{\mu}}, \quad (16.1)$$

where

$$g_{\mu} = \left[1 - \prod_{k=1}^M \frac{q_k}{p_k} \right]^{-1} \left[\sum_{i=0}^{M-1} \frac{1}{p_{\mu-i}} \prod_{j=\mu+1-i}^{\mu} \frac{q_j}{p_j} \right] \quad (16.2)$$

provided $p_i > 0$ for all particles. The stationary velocity is given by:

$$v = \frac{Z_{N-1,M}}{Z_{N,M}}, \quad Z_{N,M} = \sum_{n_1, n_2, \dots, n_M} f_N(\{n_{\mu}\}). \quad (16.3)$$

where in the summation $\sum_{\mu=1}^M n_{\mu} = N - M$. In the thermodynamic limit one can define a control parameter:

$$\delta = \frac{[\ln p]_{\text{av}} - [\ln q]_{\text{av}}}{\text{var}[\ln p] + \text{var}[\ln q]}, \quad (16.4)$$

so that for $\delta > 0$ ($\delta < 0$) the particles move to the right (left).

Depending on the form of disorder the stationary state can be of three different types. i) The stationary state has a homogeneous particle density and there is a finite velocity, $v > 0$. ii) The particle density in the stationary state is not homogeneous: there is a macroscopic hole before the slowest particle and $v > 0$. iii) The particle density in the stationary state is not homogeneous and the stationary velocity is $v = 0$. Here we shall consider the third case, which is realized in the partially asymmetric model, which means that i) both $p_i > 0$ and $q_i > 0$, and ii) there is a finite fraction of particles, for which $p_i > q_i$ and also $q_i > p_i$. The partially asymmetric model is conveniently studied by the strong disorder RG method[209], what is going to be described in the following.

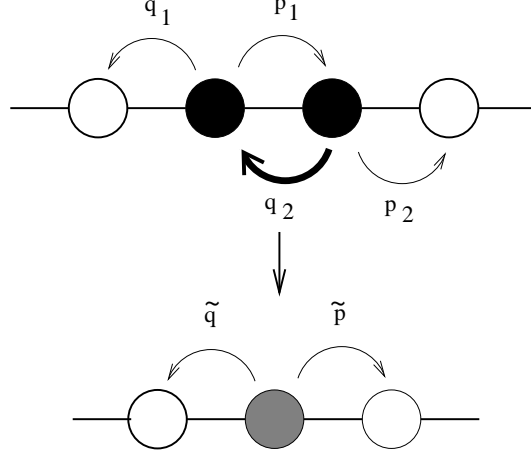


Figure 28: Renormalization scheme for particle clusters. If q_2 is the largest hopping rate in a time-scale, $\tau > 1/q_2$, the two-particle cluster moves coherently and the composite particle is characterized by the effective hopping rates \tilde{q} and \tilde{p} , respectively, see the text.[209]

16.1.1 RG rules

In the RG method one sorts the transition rates in descending order and the largest one sets the energy scale, $\Omega = \max(\{p_i\}, \{q_i\})$, which is related to the relevant time-scale, $\tau = \Omega^{-1}$. During renormalization the largest hopping rates are successively eliminated, thus the time-scale is increased. In a sufficiently large time-scale some cluster of particles moves coherently and form composite particles, which have new effective transition rates. To illustrate the decimation rules for the system (see Fig. 28) let us assume that the largest rate is associated to a left jump, say $\Omega = q_2$.

Typically, $q_2 \gg p_2$, and the same relation is assumed to hold with the transition rates of the particle to the left: $q_2 \gg q_1, p_1$. In a time-scale, $\tau > \Omega^{-1}$, the fastest jump with rate q_2 can not be observed and the two particles 1 and 2 form a composite particle. The composite particle has a left hopping rate $\tilde{q} = q_1$, since a jump of particle 1 is almost immediately followed by a jump of particle 2. The transition rate of the composite particle to the right, \tilde{p} , follows from the observation that, if the neighboring site to the right of particle 2 is empty it spends a small fraction of time: $r = p_2/(p_2 + q_2) \approx p_2/q_2$ on it. A jump of particle 1 to the right is possible only this period, thus $\tilde{p} = p_1 r \approx p_1 p_2 / q_2$. The renormalization rules can be obtained similarly for a large p decimation and can be summarized as:

$$\tilde{p} = \frac{p_1 p_2}{\Omega}, \quad \Omega = q_2; \quad \tilde{q} = \frac{q_1 q_2}{\Omega}, \quad \Omega = p_1. \quad (16.5)$$

16.1.2 Relation with the random XX -chain

The decimation equations in Eq.(16.5) are in a similar form as that of the random XX chain in Eq.(6.11). The correspondence properly holds for a chain with $2M$ sites having the exchange couplings: $J_{2i-1} = p_i$ and $J_{2i} = q_i$. Using the results of Sec. B.2 this mapping can be extended further for the RTFIC, too. Here we list the immediate consequences of these mappings.

Let us consider first the region with $\delta > 0$, which corresponds to the Griffiths phase of the RTFIC. Using the analogy with the solution to the RTFIC in Sec.4.3.2 we can state that during renormalization almost exclusively the left hopping rates are decimated out. After M -steps of decimation we are left with a single particle of mass, M , having effective hopping rates, \tilde{p} and \tilde{q} , so that $\tilde{q}/\tilde{p} \rightarrow 0$ for large M and $\tilde{p} \sim M^{-z}$, with a dynamical exponent given from Eqs. (4.27) and (4.33) as:

$$\left[(p/q)^{1/z} \right]_{av} = 1 . \quad (16.6)$$

This result indicates that in the stationary state of the partially asymmetric process i) there is a phase separation, with an occupied region, which corresponds to the effective particle and with a non-occupied region. ii) The stationary velocity v of the system vanishes in a large ring as:

$$v \sim N^{-z} , \quad (16.7)$$

provided $M/N = O(1)$. More precisely the accumulated distance traveled by the particles, x , in time, t , is given by

$$x \sim t^{1/z} . \quad (16.8)$$

This relation is very much similar to the behavior of a Brownian particle in a random potential in the anomalous diffusion regime with the correspondence $\mu = 1/z$ (see section 12).

This analogy can be made even closer by noting that motion of the macroscopically occupied region takes place in such a way that single and non-interacting holes diffuse into the opposite direction. The motion of the holes takes place in a position dependent random potential, the hopping rates of which, p_i and q_i , are generated by the particles. The average distance traveled by a hole is just the absolute value of the accumulated distance made by the ASEP.

At the critical point, $\delta = 0$, left and right hopping rates are decimated symmetrically and the system scales into an infinite disorder fixed point. After M -steps the remaining effective particle has a symmetric hopping probability: $\tilde{q} \sim \tilde{p} \sim \exp(-const M^{1/2})$. Thus the motion of the system is diffusive and ultra-slow, the appropriate scaling combination is given by: $(\ln v)M^{-1/2}$. Close to the critical point the correlation length in the system, ξ , which measures the width of the front, is given by $\xi \sim \delta^{-2}$, compare with Eq.(4.46) for the RTFIC.

Numerical results about the velocity distribution of a periodic system with $M/N = 1/2$ is presented in Figs.29 and 30, in the Griffiths phase and at the critical point, respectively. Here a bimodal distribution is used with $p_i q_i = r$,

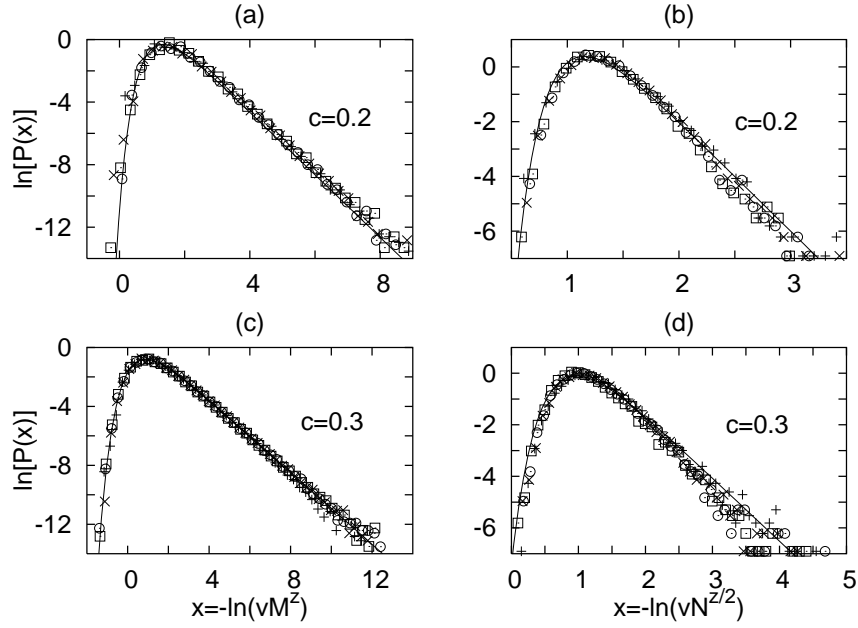


Figure 29: Scaling of the velocity distribution in the Griffiths phase at two concentrations ($c = 0.2$ and $c = 0.3$) for pt (a,c) and st (b,d) disorder. Data denoted by symbols $+$, \times , O , \square correspond to $M = 64, 128, 256, 512$ for (a,c) and $N = 64, 128, 256, 512$ for (b,d), respectively. The Fréchet distribution[149] with the dynamical exponent: $z = z_{pt}$, calculated from Eq.(16.6) and with $z_{st} = z_{pt}/2$, as given in Eq.(16.9) are indicated by a full line.[209]

for all i , and $P(p) = c\delta(p-1) + (1-c)\delta(p-r)$, with $r > 1$ and $0 < c \leq 1/2$. In this case the control-parameter is $\delta = (1-2c)/[2c(1-c)\ln r]$ and the dynamical exponent from Eq. (16.6) is $z = \ln r / \ln(c^{-1} - 1)$.

16.2 ASEP with site-wise disorder

For site-wise disorder, i.e. when the hopping rates are assigned to sites rather than to particles, the RG rules can not be simply generalized. Therefore our knowledge in this case is mainly based on numerical and scaling results. For st disorder and for the partially asymmetric process analytical and numerical results show the presence of macroscopic phase separation on a periodic chain. While for pt disorder the macroscopic occupied domains move with a stationary velocity given in Eq. (16.7), for st disorder the position of the domains are fixed in the stationary state. In this case the macroscopic transport is due to two symmetric processes: i) diffusion of holes in the ordered domains, and ii) diffusion of particles in the non-occupied domains. It is argued in Ref.[209] that for st disorder both diffusive particles and holes should overcome one-one independent large potential barriers, whereas for pt disorder just the holes should go over a large barrier. As a consequence the probability of occurrence of rare events with a characteristic time-scale, τ , in the two cases are related as: $p_{st}(\tau) = p_{pt}^2(\tau)$. Since the distribution of the relaxation times follows a power-law form, as $p_\alpha(\tau) \sim \tau^{-1/z_\alpha}$, where α stands for pt or st . From the above argument one obtains the relation:

$$z_{st} = \frac{z_{pt}}{2}, \quad (16.9)$$

which has been checked by numerical simulations, see Figs. 29 and 30. In particular at the critical point with $\delta = 0$ also with st disorder the dynamical exponent is formally infinity and the appropriate scaling combination is $(\ln v)M^{-1/2}$, although in this case it is supplemented by logarithmic corrections.

17 Reaction-diffusion models with disorder

17.1 Phase transition into an absorbing state

Stochastic many particle systems with a phase transition into an absorbing state are of wide interest in physics, chemistry and even biology [19]. Much recent work has focused on establishing a classification of possible universality classes for systems having this type of transition [20]. For models with a scalar order parameter, absence of conservation laws, and short range interactions, the critical behavior is conjectured to be that of directed percolation [157]. Well known models with a phase transition in this universality class are the contact process [164] and the Ziff-Gulari-Barshad model of catalytic reactions [368]. When there is a conservation law present, other universality classes can appear, the best known of which is the parity conserving class [82]. Quenched, i.e. time-independent, disorder is an inevitable feature of many real processes and could

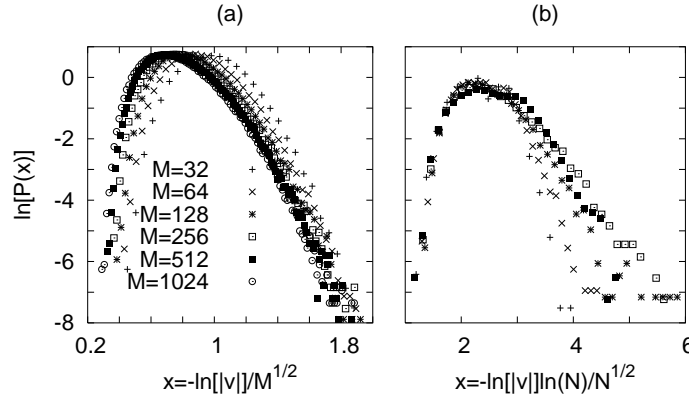


Figure 30: Scaling plot of the velocity distribution at the critical point for pt (a) and st (b) disorder. In the latter case a logarithmic correction term is included.[209]

play an important role in stochastic particle systems too. As an example, it has been argued that due to the presence of some form of disorder the directed percolation universality class has not yet been seen in real experiments[174], such as in catalytic reactions [368], in depinning transitions [23], and in the flow of granular matter [105] (for a review, see [174]). In stochastic particle systems, disorder is represented by position dependent reaction rates and its relevance can be expressed in a $(d+1)$ -dimensional system by a Harris-type criterion [291],

$$\nu_{\perp} < 2/d . \quad (17.1)$$

Here ν_{\perp} is the correlation length exponent in the spatial direction of the pure system, compare with Eq.(5.9) for isotropic systems. Indeed for directed percolation at any $d < 4$ dimensions the disorder is a relevant perturbation.

In the following we consider the random contact process and study the properties of the new random fixed point.

17.2 Random contact process

In the contact process each site of the lattice can be either vacant (\emptyset) or occupied by at most one particle (A), and thus can be characterized by an Ising-spin variable, $\sigma_i = 1$ for \emptyset and $\sigma_i = -1$ for A . The state of the system is then given by the vector $\mathbf{P}(\sigma, t)$ which gives the probability that the system is in the state $\sigma = \{\dots, \sigma_i, \dots\}$ at time t . A particle can be created at an empty site i with a rate $p\hat{\lambda}_i/p_0$, where $p(p_0)$ is the number of occupied neighbors (the coordination number of the lattice) and at an occupied site the particle is annihilated with a rate μ_i . The time evolution is governed by a master equation, which can be written into the form:

$$\frac{d\mathbf{P}(\sigma)}{dt} = -H_{CP}\mathbf{P}(\sigma) . \quad (17.2)$$

Here the generator H_{CP} of the Markov process is given by:

$$H_{CP} = \sum_i \mu_i M_i + \sum_{\langle ij \rangle} \frac{\hat{\lambda}_i}{p_0} (n_i Q_j + Q_i n_j) \quad (17.3)$$

in terms of the matrices:

$$M = \begin{pmatrix} 0 & -1 \\ 0 & 1 \end{pmatrix}, n = \begin{pmatrix} 0 & 0 \\ 0 & 1 \end{pmatrix}, Q = \begin{pmatrix} 1 & 0 \\ -1 & 0 \end{pmatrix}$$

and $\langle ij \rangle$ stands for nearest neighbors. It is well known[22] that the steady state probability distribution of a stochastic process coincides with the ground state of its generator (sometimes also called quantum Hamiltonian of the stochastic process) while relaxation properties can be determined from its low lying spectrum.

The average number of particles at site- i and time- t is given by $\langle n_i \rangle(t)$, which evolves to a constant in the stationary state. The order-parameter of the system is given by $\rho = 1/L \sum_i \langle n_i \rangle$, for surface sites, $i = 1$ and $i = L$, we obtain the surface order-parameter: $\rho_s = [\langle n_1 \rangle]_{av}$. In the thermodynamic limit in the active phase $\rho > 0$ and in the inactive phase $\rho = 0$. For non-random couplings the non-equilibrium phase transition, which separates the active and inactive phases, belongs to the universality class of directed percolation[20, 157]. Scaling in this transition point is governed by an anisotropic fixed point, as described in Sec.A.2, but here we use the convention $\nu = \nu_\perp$. In one dimension the transition is at $(\mu/\hat{\lambda})_c = 0.3032$ and the critical exponents are given by[21]: $\beta = 0.2765$, $\beta_s = 0.7337$, $\nu_\perp = 1.097$ and $z = 1.581$. In the following we often use the variable $\lambda = \hat{\lambda}/p_0$ to characterize the creation rate. The random contact process and related models are studied in a series of papers[291, 275, 203, 64, 79, 351] and unconventional critical properties are observed (logarithmically slow dynamical correlations, disorder dependent Griffiths-like effects, etc.). Recently, the system is studied by the strong disorder RG method[177], the results of which have provided possible explanations of the previous numerical results. In the following we describe the application of the strong disorder RG for this system.

17.2.1 RG rules

In the usual way the transition rates are put in descending order and the largest rate: $\Omega = \max(\{\lambda_i\}, \{\mu_i\})$ sets the energy scale in the system. Here one should use two different ways of decimation depending if the largest transition rate is a branching rate or it is an annihilation rate.

The largest term is a branching rate: $\Omega = \lambda_2$

In this case the two-site cluster, $(2, 3)$, having the largest branching rate, λ_2 , spends most of the time in the configurations AA or $\emptyset\emptyset$ and can be rarely found in one of the other two configurations, $A\emptyset$ and $\emptyset A$. Consequently for a large time-scale, $\tau \sim 1/\Omega$, the two sites behave as an effective cluster with a moment

of $\tilde{m} = 2$ and with an effective death rate, $\tilde{\mu}_2$, which can be obtained by the following simple reasoning. Let us start with the original representation, when the two-site cluster is in the occupied state, AA . In the effective decay process first the particle at site (2) should decay (with rate μ_2), which is then followed by the decay of the particle at (3). This second process has a very low probability of $pr(3) = \mu_3/(\lambda_2 + \mu_3) \approx \mu_3/\lambda_2$. Since the same processes can also occur with the role of (2) and (3) interchanged, we find that $\tilde{\mu} = pr(3)\mu(2) + pr(2)\mu(3)$, which is given by:

$$\tilde{\mu} = \frac{2\mu_2\mu_3}{\lambda_2} . \quad (17.4)$$

The renormalization equation in Eq.(17.4) should be extended by the renormalization of moments (i.e. the number of original sites in the cluster):

$$\tilde{m} = m_2 + m_3 , \quad (17.5)$$

where in the initial situation $m_2 = m_3 = 1$.

The largest term is a death rate: $\Omega = \mu_2$

In this case the site (2) is almost always empty, \emptyset , therefore it does not contribute to the fractal properties of the A cluster and can be decimated out. The effective branching rate, $\tilde{\lambda}$ between the remaining sites (1) and (3) can be obtained from the following reasoning. Let us have the configuration of the three-site cluster in the original representation as $A\emptyset\emptyset$. The effective branching rate between sites (1) and (3) is generated by a virtual process, in which first a particle is created at site (2) (rate λ_2), and then one at site 3 (probability $\lambda_3/(\lambda_3 + \mu_2)$). Hence, we get for strong disorder the effective branching rate as:

$$\tilde{\lambda} = \frac{\lambda_2\lambda_3}{\mu_2} . \quad (17.6)$$

The renormalization equations in Eqs.(17.4) and (17.6) can be transformed into a symmetric form in terms of the variable, $J = \lambda/\kappa = \hat{\lambda}/(p_0\kappa)$ with $\kappa = \sqrt{2}$ as

$$\tilde{\mu} = \kappa \frac{\mu\mu'}{J}, \quad \tilde{m} = m + m', \quad \tilde{J} = \kappa \frac{JJ'}{\mu} . \quad (17.7)$$

We note that the renormalization rules in Eqs.(17.4) and (17.6) can be obtained in the Hamiltonian formalism[177] with Eq.(17.3) in an analogous way as for the RTFIC in Sec.4.2.

17.2.2 Analysis of the RG equations

The decimation equations in Eq.(17.7) are very similar to that of the RTFIC in Eqs.(4.17) and (4.16), and a similar prefactor, $\kappa \neq 1$ can be found in the renormalization equations of random quantum spin chains with discrete symmetry in Sec.5, see Eq.(5.6). Using the same arguments as in Sec5 one expects that for strong enough initial disorder the RG flow is attracted by the infinite

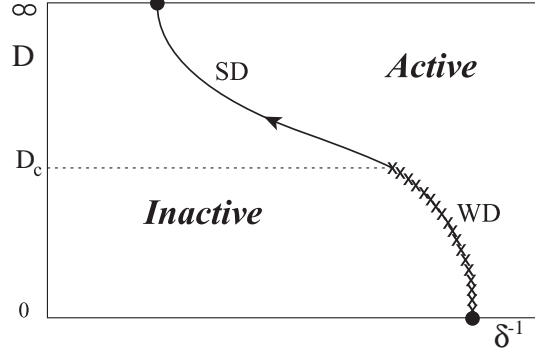


Figure 31: Schematic phase diagram of the random contact process as a function of the control parameter, δ , and the strength of disorder, D , (see text). The inactive and active phases are separated by a phase transition line, along which the critical exponents are D dependent for weaker disorder (WD, $D \leq D_c$), or are determined by an infinite disorder fixed point at $D = \infty$, for strong disorder (SD, $D > D_c$).

disorder fixed point of the RTFIC. For weaker disorder, however, the infinite disorder fixed point is not attractive. This is due to the prefactor, $\kappa = \sqrt{2} > 1$, in Eq.(17.7). As already argued in Sec.5 in this case the variation of the energy-scale during renormalization is not monotonic and the corresponding fixed point is different of that observed for strong disorder.

The control parameter of the model, δ , is defined as:

$$\delta = \frac{[\ln \mu]_{\text{av}} - [\ln J]_{\text{av}}}{\text{var}[\ln \mu] + \text{var}[\ln J]}. \quad (17.8)$$

Its value at the strong disorder fixed point is given by $\delta = 0$, which follows from duality of the RG equations in Eq.(17.7).

A schematic phase diagram of the model is presented in Fig.31 as a function of the control parameter δ and the strength of disorder, $D = \text{var}[\ln \mu] + \text{var}[\ln J]$. Note that along the phase transition line $\delta \geq 0$. According to numerical results[177] and analogies with random quantum spin chains in Sec.5 for strong enough disorder, $D > D_c$, the critical behavior is controlled by the strong disorder fixed point located at $D \rightarrow \infty$.

The critical exponents at the strong disorder fixed point are exactly known from the analysis of the RTFIC in Sec.4.4 and from the mapping between the two models. In the random contact process the average particle density in the bulk, ρ , and at the surface, ρ_s , corresponds to the bulk and surface magnetizations, respectively, of the RTFIC. They have a singular behavior, $\rho \sim (-\delta)^\beta$ and $\rho_s \sim (-\delta)^{\beta_s}$, $\delta \rightarrow 0^-$, respectively. At the strong disorder fixed point: $\beta^\infty = (3 - \sqrt{5})/2$ and $\beta_s^\infty = 1$. The particle-particle correlation function, $[\langle n_i n_j \rangle]_{\text{av}}$ of the random contact process is analogous to the spin-spin correlation function

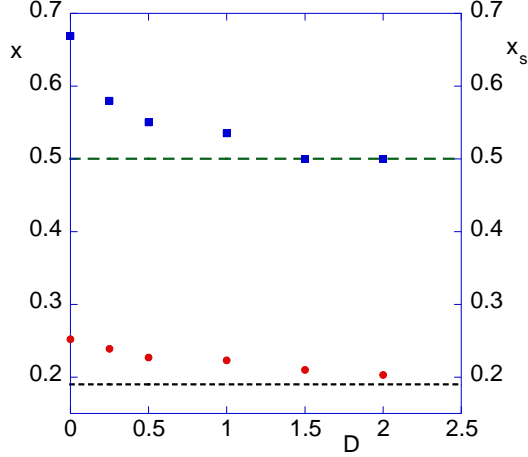


Figure 32: Numerical estimates of the exponents $x_m = \beta/\nu_\perp$ (circles) and x_m^s (squares). The broken lines indicate the value at the strong disorder fixed point. The errors are of the same order as the size of the symbols[177].

of the RTFIC, and the correlation length, $\xi_\perp \sim |\delta|^{-\nu_\perp}$, involves an exponent, ν_\perp , which at the infinite disorder fixed point is given by: $\nu_\perp^\infty = 2$. Finally, the correlation length in the parallel direction, ξ_\parallel , corresponds to the relaxation time of the RTFIC. At the strong disorder fixed point $\ln \xi_\parallel \sim \xi_\perp^\psi$, with $\psi = 1/2$.

17.2.3 Numerical results and scaling in the weak disorder regime

A systematic numerical study of the random contact process with varying strength of disorder is performed in Ref.[177]. The results of density matrix renormalization (DMRG) of the Hamiltonian version in Eq.(17.3) and that of Monte Carlo simulations are consistent with each other. For weak disorder, $D < D_0$, the order parameter exponents, $x_m = \beta/\nu_\perp$ and $x_m^s = \beta_s/\nu_\perp$ are found to be disorder dependent, which vary continuously between the values of the pure system and that of the infinite disorder fixed point. This is shown in Fig.32. Therefore we can conclude that in the weak disorder regime there is a line of random fixed points.

For the form of dynamical scaling in this regime two possible scenarios are proposed. It can be either i) conventional random scaling, see Sec.A.2 or ii) infinite disorder scaling, as in Sec.A.3. In the former case the dynamical exponent, z , is finite for $D < D_0$, but becomes divergent at $D = D_0$. We remind that this type of behavior is observed in random quantum spin chains, see Sec. 5 and 7. In the second scenario the dynamical exponent is formally infinity in the weak disorder regime, too, but the scaling exponent, ψ in Eq.(A.16) is disorder dependent, and approaches $\psi = 1/2$ at $D = D_0$. This infinite disorder scaling is noticed in numerical studies of the 2d random contact process[275].

For the random contact process in 1d it is difficult to decide between the two scenarios by numerical studies and there is still no final, definite answer. The reason of this is that for a finite system one can fit c.f. the autocorrelation function by both types of scaling forms. Conventional scaling with a large effective z has similar accuracy, as infinite disorder scaling with a small ψ . One should note, however, that the present numerical data can be interpreted with a slight preference of infinite disorder scaling.

17.3 Other types of reaction-diffusion models with quenched disorder

The Reggeon field-theory, which is the Hamiltonian version of directed percolation[74], has been studied by the strong disorder RG approach[177]. The decimation equations are found to be identical to that of the random contact process in Eq.(17.7), which is a consequence of an exact mapping[157], which exists between the two models. Therefore the random Reggeon field-theory has the same critical behavior as the random contact process. The presence of infinite disorder scaling for the directed percolation in $(1 + 1)$ -dimension is demonstrated in Ref.[177], for extreme strong disorder.

On the other hand the generalized contact process[173], which for homogeneous transitions rates belongs to the parity conserving universality class, in the presence of quenched disorder has conventional random scaling[177].

18 Classical models in $d \geq 2$

Quenched randomness could cause strong disorder effects in higher dimensional classical systems, too. However, not all the systems which have an infinite disorder fixed point in $d = 1$ have a similar one in $d \geq 2$. For example disorder is an irrelevant perturbation for the random walk in $d \geq 2$, (in $d = 2$ there are logarithmic corrections) as has been shown in[243]. On the contrary for reaction-diffusion models, such as the random contact process infinite disorder scaling is observed[275, 177] in higher dimensions, too. d -dimensional classical systems with layered randomness, such as the McCoy-Wu model[252], which are isomorph with random quantum spin chains, constitute examples of strong disorder scaling, too. Finally, one can ask the question, if an isotropic classical spin model can be constructed, which is isomorphic with the McCoy-Wu model, and thus with the RTFIC and therefore the critical properties are exactly known. A possible realization of this universality class is the random bond Potts model in the large- q limit[34]. We are going to review these developments in the following.

18.1 Random contact process in 2d

Renormalization of the random contact process, as shown in Sec.17.2, has many similarities with the random transverse-field Ising model. The RG rules in

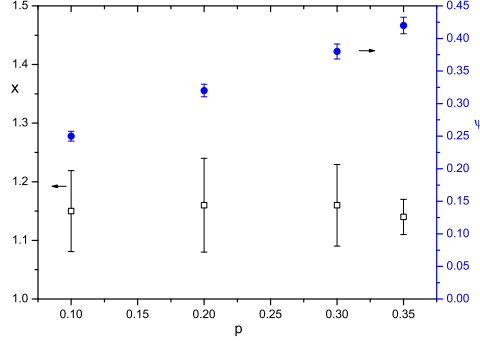


Figure 33: Exponents x_m (squares) and ψ (circles) in the random contact process in $d = 2$ as a function of dilution p assuming logarithmic scaling[177]. The values are calculated from the data given in Ref.[275].

Eq.(17.7) differ only by a prefactor, $\kappa = \sqrt{2}$ from the similar equations for the random transverse-field Ising model in Eqs. (4.17) and (4.16) and the topology of the lattice, even in higher dimensions, are analogous in the two cases. Therefore the conclusion obtained in Sec.17.2, which predicts for strong enough disorder isomorph infinite disorder fixed points for the two problems in $d = 1$, should be valid for $d \geq 2$, too. This conjecture has been checked in Ref[177] in which the numerical data of Ref.[275] about the strongly random contact process are compared to the critical parameters of the 2d random transverse-field Ising model, see Table 2. As seen in Fig.33 for strong dilution there is a satisfactory agreement. For weaker disorder the random contact process has an intermediate disorder regime[177], the properties of which are similar to that found in 1d, see in Sec.17.2.3.

18.2 Classical systems with layered randomness

Here we consider d -dimensional classical systems in which disorder in the couplings is strictly correlated in $d' < d$ dimension. For the general problem we mention field-theoretical investigations[63] and mean-field results[47]. In the following we restrict ourselves to two-dimensional systems with layered randomness ($d = 2$ and $d' = 1$), the prototype of which is the two-dimensional Ising model, which has been introduced and partially exactly solved by McCoy and Wu[252]. The McCoy-Wu model and the RTFIC are isomorph at their critical points and a similar relation is true between another classical strip-random models and the corresponding random quantum spin chains. As an example we mention the q -state Potts model the quantum version of which is studied in Sec.5. The Potts model in the $q \rightarrow 1$ limit corresponds to the percolation problem[214], which - in the presence of layered disorder - has been studied in[208].

18.2.1 The McCoy-Wu model and the RTFIC

The McCoy-Wu model is a square lattice Ising model with vertical, $K_1(i) = -J_1(i)/k_B T$, and horizontal bonds, $K_2(i) = -J_2(i)/k_B T$, the value of both may depend on the position in the horizontal direction, i . The row transfer matrix, T , which is used to transfer information in the vertical direction is given by[324]:

$$T = \exp \left[\sum_i K_1^*(i) \sigma_i^z \right] \exp \left[\sum_i K_2(i) \sigma_i^x \sigma_{i+1}^x \right] \quad (18.1)$$

in terms of the $\sigma_i^{x,z}$ Pauli matrices and the $K_1^*(i)$ dual couplings ($\tanh K_1^* = \exp(-2K_1)$). In the extreme anisotropic (or Hamiltonian) limit[224] there are strong vertical and weak horizontal bonds, so that $K_1^*(i)$ and $K_2(i)$ are both small and one can combine the exponentials to obtain

$$T = \exp(-\tau H_I) . \quad (18.2)$$

Here $\tau = K_1^*$ is a reference value, which measures the lattice spacing in the vertical direction and H_I is the Hamiltonian of the RTFIC as given in Eq.(4.1). This mapping, which works also in higher dimensions, constitutes a relation between the thermodynamic quantities of a d -dimensional classical system with layered randomness and the ground-state expectation values of a $(d-1)$ -dimensional random quantum spin system. According to the standard relations[224] the equivalent quantities are:

- transfer matrix \leftrightarrow Hamiltonian
- free-energy density \leftrightarrow ground-state energy density
- correlations in the horizontal direction \leftrightarrow equal-time correlations
- correlations in the vertical direction \leftrightarrow imaginary-time autocorrelations
- vertical correlation length (ξ_{\parallel}) \leftrightarrow relaxation time, inverse energy gap
- anisotropy exponent \leftrightarrow dynamical exponent

The McCoy-Wu model is solved analytically for the boundary spin magnetization [252] and for the typical correlations in the vertical direction[329]. Both agree with the strong disorder RG results, which gives further credit about the conjecture that the strong disorder RG calculation leads to asymptotically exact results.

18.2.2 Percolation in a random environment

In percolation the i -th bond (or site) of a regular lattice is occupied with a given probability, p_i , and one is interested in the properties of clusters, in particular in the vicinity of the percolation transition point[335]. Singularities at

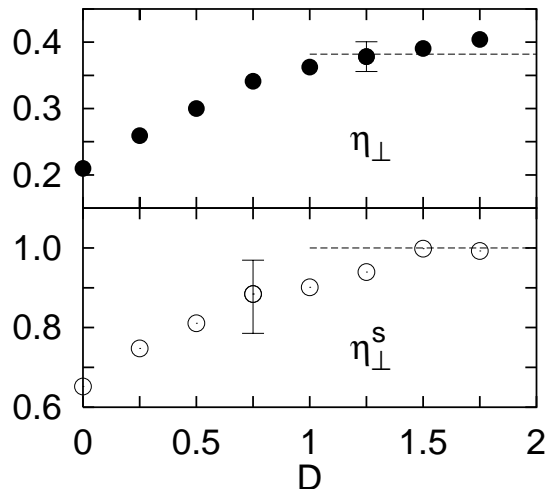


Figure 34: Bulk ($\eta_{\perp} = 2x_m$) and surface ($\eta_{\perp}^s = 2x_m^s$) decay exponents versus the strength of disorder for the $2d$ percolation with layered randomness. Values at the IDFP, as given in Table 1 are denoted by dashed lines[208].

the transition point are insensitive to homogeneous randomness in the values of p_i , which follows from the Harris criterion Eq.(5.9), since $\nu_0 > 2/d$ in any dimensions. Layered randomness in two-dimensions, however, is a relevant perturbation, since $\nu_0 = 4/3$ [335] and the critical behavior of this system is studied in Ref.[208].

In the MC simulation the distribution of the mass of clusters, the anisotropy exponent, z , and the critical bulk and surface correlations in the horizontal direction are measured for different strength of disorder, D . Disorder dependent critical behavior is found, and the scenario is analogous to that of random quantum spin chains, as described in Sec.5. For weak disorder, $D < D_{\infty}$, which corresponds to the *intermediate disorder regime* in Sec.5, the critical behavior of the system is controlled by a line of conventional random fixed points. Here the anisotropy exponent is finite, $1 < z < \infty$, and together with the order-parameter exponents monotonously increases with the strength of disorder, see Fig.34. In the *strong disorder regime*, $D > D_{\infty}$, the critical behavior of the system is controlled by the infinite disorder fixed point. Here the anisotropy exponent is formally infinity and the order-parameter exponents have the same values as for the RTFIC, see Table 2. This means that ordinary percolation and directed percolation (contact process, see Sec.17.2) in the presence of strong layered randomness have the same fixed point, so that the different type of anisotropy in the non-random models does not matter.

18.3 Random-bond Potts model in the large- q limit

The mapping presented in Sec.18.2.1 makes a relation between the RTFIC and an anisotropic random classical model, the McCoy-Wu model. It is interesting to ask the question if the RTFIC is isomorph with an *isotropic* random classical model? If yes, then the critical singularities of that classical random model should be known exactly from the properties of the RTFIC. In Ref.[34] it is argued that a possible candidate of this rôle is the random ferromagnetic-bond Potts model in the large- q limit, what we will describe in the following.

First we note that disorder has a rounding effect at first-order phase transitions[84]. In $2d$, according to rigorous results by Aizenman and Wehr[28] any amount of quenched disorder will turn a first-order phase transition into a second-order one. Numerical studies of the $2d$ random-bond Potts model[302, 83, 94, 294, 296] indicate that the magnetization exponent, x_m is q -dependent, and $x_m(q)$ seems to be saturated[202] in the large- q limit. Here we argue that this limiting value is universal and can be obtained from the strong disorder RG results of the RTFIC.

The partition function of the Potts-model is convenient to express in the random cluster representation[214]:

$$Z = \sum_{G \subseteq E} q^{c(G)} \prod_{ij \in G} [q^{\beta J_{ij}} - 1] \quad (18.3)$$

where the sum runs over all subset of bonds, $G \subseteq E$ and $c(G)$ stands for the number of connected components of G . The $J_{ij} > 0$ are nearest neighbor coupling constants, see Eq.(5.1), and $\beta = 1/(k_B T \ln q)$. In the large- q limit, where $q^{\beta J_{ij}} \gg 1$, the partition function can be written as

$$Z = \sum_{G \subseteq E} q^{\phi(G)}, \quad \phi(G) = c(G) + \beta \sum_{ij \in G} J_{ij} \quad (18.4)$$

which is dominated by the largest term, $\phi^* = \max_G \phi(G)$. Thermodynamic quantities are calculated from the free energy per site, $f = -\beta \phi^*/N$, and the scaling dimension of the magnetization, x_m , is obtained from the fractal dimension of the percolating cluster, d_f , as $x_m = d - d_f$. One important observation that for a given realization of disorder thermal fluctuations are irrelevant and disorder plays a completely dominant rôle, which is a property characteristic for infinite disorder fixed points, see Sec.2.1.

In a technical point of view solution of the random bond Potts model in the large- q limit is reduced to an optimization problem[207], which can be solved by a computer algorithm in polynomial time[33]. Numerical results in $2d$ [34] have given strong support to the conjecture, that the magnetization exponents, x_m and x_m^s , are the same as for the RTFIC in Table 1. This is illustrated in Fig.35. The correlation length exponent is conjectured to be $\nu = 1$, which is the half of the correlation length exponent of the RTFIC.

To explain this conjectured isomorphism we present two arguments. The first argument concerns the topological structure of the optimal set, which is

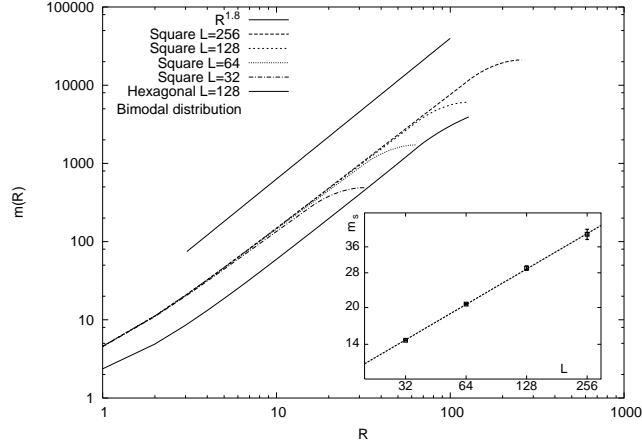


Figure 35: Average mass of the percolating cluster within a region of size R at the critical point, for the square and the hexagonal lattices. The conjectured asymptotic behavior is indicated by a straight line: $m(R) \sim R^{d_f}$ with $d_f = (5+\sqrt{5})/4 \approx 1.8$. Inset: average mass of surface points of the percolating cluster in the square lattice, $m_s(L) \sim L^{1-x_m^s}$ with the conjectured value $x_m^s = 1/2$. [34]

show in Fig.36 for a typical disorder configuration at the critical point [221]. The percolating cluster is self-similar, i.e. it is a fractal, and in a one-dimensional cut it has a connectivity structure, which can be brought in analogy with the strong disorder RG ground state of the RTFIC. If the connected parts are identified with spin clusters and the empty parts with (renormalized) bonds to each 1d cut corresponds an RG ground state of the RTFIC, for which a given set of random couplings and transverse fields can be identified. If in the two problems the statistics of the equivalent ground states is asymptotically similar the singularities of the average quantities are indeed simply related to each other.

In the second argument we consider the q -state Potts model with layered randomness, when the fractal structure of the dominant graph is the same, as for random percolation in the strong disorder region, see Sec.18.2.2. Therefore the mass of the giant cluster scales as: $M \sim L_{\parallel} L_{\perp}^{1-x_m}$. Now let the couplings to be random also in the vertical direction. In this way translational symmetry in the vertical direction is broken and in the originally homogeneous (occupied and non-occupied) strips connected and disconnected parts will appear. At the critical point, due to duality, these two (creation and destruction) processes are symmetric, therefore it is plausible to assume that the mass of the largest cluster stays invariant, i.e. $M \sim L^{d_f} \sim L^{2-x_m}$, which leads to the conjectured isomorphism.

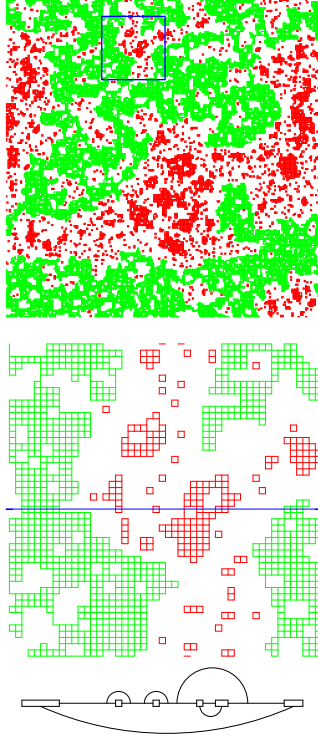


Figure 36: top: Optimal set for a typical disorder realization of the random bond Potts model: percolating and finite clusters are marked with gray (green) and dark (red) lines, respectively. middle: Enlargement of a square proportion in the upper-middle part to illustrate self-similarity. bottom: The connectivity structure of the optimal set along a line, which consists of six connected units (“spins”) and five open units (“bonds”). [34]

18.3.1 Numerical study in three-dimensions

In three-dimensions the first-order transition in the non-random model remains unaffected by weak disorder, however the thermodynamic quantities display essential singularities[258]. Only for strong enough disorder will the transition be softened into a second-order one, in which case the ordered phase becomes non-homogeneous at large scales, while the non-correlated sites percolate the sample. In the critical regime the critical exponents are found universal: $\beta/\nu = 0.60(2)$ and $\nu = 0.73(1)$. The 3d random bond Potts model and the 2d random transverse-field Ising model do not belong to the same infinite disorder universality class, in contrary to that found in 2d.

19 Summary and perspectives

In this review, we have described in details how strong disorder RG methods allows to study disordered systems in which space heterogeneities of the disorder dominate at large scale over quantum, thermal or stochastic fluctuations. We have explained how these methods could be applied to different types of random systems. In all cases, these methods have a very clear physical meaning, because the RG rules are defined in real space (or in energy space) and use some physical arguments to construct the degrees of freedom that are important at large scale:

(i) in quantum models, the RG rules allow to construct clusters of strongly correlated spins, such as singlets in the $S = 1/2$ antiferromagnetic chain, VBS clusters in the $S = 1$ antiferromagnetic chain, or ferromagnetic clusters in the Random Transverse Field Ising chain;

(ii) in random walks in random media, the RG rules allow to construct the finite-time metastable states, and are based on the time needed to cross over a potential barrier or to escape from a trap;

(iii) in classical random field models, like the random field Ising chain, or the heteropolymer near an interface, the RG rules can be considered as an extension of the Imry-Ma arguments based on the energy that can be gained by taking advantage of the fluctuations of the random fields in an interval.

(iv) in stochastic models of interacting particles, such as the simple exclusion process or the contact process, the RG rules allow to define effective clusters of strongly correlated particles.

In contrast with usual RG methods which treat space homogeneously, the strong disorder RG procedures are inhomogeneous in space to better adapt to the local realizations of the disorder. Moreover, it has been understood for many years that the probabilistic questions arising in disordered systems concern extremal statistics [124, 61]: the equilibrium at low temperature is controlled by the statistics of states of low energy [115, 124, 61, 89, 112], whereas dynamics at large time is controlled by the statistics of large barriers [134, 127, 40, 350]. From this point of view, the strong disorder RG rules give a new perspective. Indeed, following the Ma-Dasgupta idea, it is always the extreme value of a disorder variable which is decimated iteratively and which generates the RG flow of the corresponding probability distribution. In dimension $d = 1$, it turns out that this special structure makes it possible to obtain explicit solutions most of the time, whereas in higher dimension $d > 1$, the RG rules have to be implemented numerically. Whenever these methods can be applied, they give a very detailed description. Indeed, as the RG procedure is carried out sample by sample, it is possible to study many observables within the same framework, their distributions over the samples, and the influence of the rare events/rare regions on averaged quantities.

We now finish with a short list of perspectives that seem to us the most interesting presently

- *New fields of applications for strong disorder RG methods*

It would be of course very interesting to define and study strong disorder

der RG rules for other disordered systems than the ones that have been considered up to now. Indeed, considering a model from the point of view of strong disorder RG usually gives completely new insight and new predictions with respect to other methods.

More generally, the strong disorder RG methods show that an essential property of a disordered system is the relative importance of disorder inhomogeneities with respect quantum, thermal or stochastic fluctuations. A general classification of disordered systems with respect to this ratio ‘disorder/fluctuations’ would certainly be very helpful.

- *Numerical studies of strong disorder RG flows in $d > 1$*

The strong disorder RG method has provided several qualitative predictions about the singular behavior of higher dimensional systems, such as the isomorphism between spin glasses and random ferromagnets, or the absence of infinite disorder fixed point in Heisenberg antiferromagnets. Furthermore there are some numerical predictions by the method for the actual values of the critical exponents, c.f. for the random transverse-field Ising model or for the Heisenberg model with mixed ferromagnetic and antiferromagnetic interactions. Most of these RG results need a numerical verification. These future numerical investigations could also help to explore new problems having disorder dominated singularities.

- *Disorder induced cross-over effects*

For several systems considered in this review, such as for instance the $S = 1/2$ antiferromagnetic spin chain, or the symmetric Sinai walk, any amount of initial disorder drives the system towards an infinite disorder fixed point. However for other models, such as for instance the $S > 1/2$ antiferromagnetic spin chains, the quantum clock model or the contact process, the RG rules drive the system towards the infinite or strong disorder fixed points only if the initial disorder is larger than a threshold. In these cases, the disorder induced cross-over effects have not yet been explored in full details. A consistent treatment of the different regions of disorder would be of great importance.

- *Relations with other methods*

Exact calculations, not using the RG frame-work, are expected to reproduce the asymptotically exact results of the strong disorder RG method. For the Sinai model, some results obtained via strong disorder RG have now be proven by mathematicians [114, 97], and we believe that the mathematical proofs of other strong disorder RG should be similarly possible.

Another interesting questions concerns the relations of strong disorder RG with other methods widely used in disordered systems, such as the replica method [7], the supersymmetric method [130], and the dynamical method [62] : is it possible to recover some strong disorder RG results via these other methods which start by averaging over the disorder ?

Acknowledgements

It is a pleasure to thank our collaborators on strong disorder RG methods :

Ferenc Iglói wishes to thank J-C. Anglès d'Auriac, E. Carlon, B. Douçot, J. Hooyberghs, R. Juhász, D. Karevski, N. Kawashima, P. Lajkó, Y-C. Lin, R. Mélin, M.-T. Mercaldo, M. Preissmann, H. Rieger, L. Santen, A. Sebő, L. Turban and C. Vanderzande.

Cécile Monthus wishes to thank D.S. Fisher, O. Golinelli, Th. Jolicoeur and P. Le Doussal for their collaborations on strong disorder RG methods, as well as G. Biroli and T. Garel for useful comments on the manuscript.

The work of F.I. has been supported by the French-Hungarian cooperation programme Balaton (Ministère des Affaires Etrangères - OM), by a German-Hungarian exchange program (DAAD-MöB), the Hungarian National Research Fund under grant No OTKA TO34183, TO37323, TO48721, MO45596 and M36803. He thanks the SPhT Saclay for hospitality.

APPENDICES

A Scaling in random systems

Here we summarize different types of scaling behaviors observed in random systems and presented in context of specific systems in this review. Our aim is to give here a uniform description of singularities and list the known results. After setting the general notions we consider the different scaling types. For a detailed presentation of the theory of scaling in critical systems we refer to [145, 2, 1, 3] and in quantum systems to [5].

A.1 General notions

- Strength of disorder - D

We consider an interacting many-particle system, in which the interactions $\{\lambda_{i,j}\}$ are independent and identically distributed random variables. The strength of disorder, D , is related to the broadness of the distribution. One possibility is to identify D^2 with the variance of the distribution of the logarithmic couplings. In this case a generic distribution is given by:

$$P(\lambda) = D^{-1} \lambda^{-1+1/D} \quad (\text{A.1})$$

with $0 \leq \lambda \leq 1$. The $\lambda_{i,j}$ -s are couplings in spin models, transition probabilities in a random walk or in reaction-diffusion systems, etc.

- Length-scale - L , energy-scale - Ω , time-scale - t_r

The length-scale, L , can be most simply defined for a finite system by its linear extent. The corresponding energy-scale, Ω , is the typical excitation energy in such a finite system. More generally, in an infinite system for a given type of localized excitation of typical energy, Ω , the average distance between two such excitations is measured by L . The time-scale associated to such type of excitation is given by $t_r \sim \Omega^{-1}$.

- Control parameter - δ

In these systems there are deterministic fluctuations which are generally due to a (disordering) field, such as the temperature, T , a set of transverse-fields $\{h_i\}$, enforced dimerization, bias in a random walk or in a driven lattice gas, etc. The combined effect of interactions and fields (fluctuations) can be measured by an average quantity, which is called the control parameter, δ . Generally δ is defined in such a way that at $\delta = 0$ there is a singularity in the system which is associated to a phase transition. Examples for control parameters of different models can be found, c.f. in Eqs.(4.5),(6.27),(11.7) and (16.4).

- Dynamical variables - $\sigma_i(t)$

These are variables which enter into the definition of the model, c.f. operators in the Hamiltonian, site occupation variables in random walks or lattice gases, etc. Generally $\sigma_i(t)$ depends on the position, i , and time, t , and their average value is often related to the order in the system.

- Averaging procedure

For a physical observable, say, O , averaging in the presence of quenched disorder is made by the usual way[73, 6]. First, for a given realization of disorder one performs thermal averaging, which is denoted by $\langle O \rangle$, and this is followed by an average over disorder, for which we use the notations $O = \overline{\langle O \rangle}$ or $O = [\langle O \rangle]_{\text{av}}$.

- Equal time correlation function - $C(r) = \overline{\langle \sigma_i(0) \sigma_{i+r}(0) \rangle}$

Its long-distance limit:

$$\lim_{r \rightarrow \infty} C(r) = \begin{cases} m^2, & \delta < 0 \\ 0, & \delta > 0 \end{cases} \quad (\text{A.2})$$

is used to define the order-parameter, m , in the system. In the ordered phase, $\delta < 0$, one often uses the connected correlation function: $C^c(r) = C(r) - m^2$.

- Correlation lengths - ξ_{av} and ξ_{typ}

The correlation length is defined by:

$$\xi_{av}^{-1} = \lim_{r \rightarrow \infty} - \frac{\ln C(r)}{r}, \quad (\text{A.3})$$

in the paramagnetic phase, whereas in the ordered phase one uses the connected correlation function. The typical correlation length, ξ_{typ} , is defined by:

$$\xi_{typ}^{-1} = \lim_{r \rightarrow \infty} - \frac{\ln \overline{\langle \sigma_i(0) \sigma_{i+r}(0) \rangle}}{r}, \quad (\text{A.4})$$

In systems in which the correlation function is self-averaging $\xi_{av} = \xi_{typ}$, which is the case c.f. for the $d = 2$ random bond Ising model [305, 231].

In several systems, however, the correlation function is not self-averaging and therefore $\xi_{av} \neq \xi_{typ}$. Examples are the $d = 1$ Ising model[118], the random bond Potts models in $d = 2$ [294, 296, 299] and the RTFIC [138].

- Autocorrelation function - $G_i(t) = \overline{\langle \sigma_i(t) \sigma_i(0) \rangle}$

Its asymptotic limit is used to define the local order-parameter, m_i :

$$\lim_{t \rightarrow \infty} G_i(t) = \begin{cases} m_i^2, & \delta < 0 \\ 0, & \delta > 0 \end{cases} \quad (\text{A.5})$$

For surface sites it is the surface order-parameter, $m_1 \equiv m_s$.

- Singular points

Spatial and (or) dynamical correlations are quasi-long-ranged (i.e. they have a power-law asymptotic decay) at a critical (semi-critical) point.

- Critical point

At this point, which is generally located at $\delta = 0$, in an infinite system both the physical length scale, ξ , and the time scale, t_r , are divergent. In the vicinity of the critical point one has: $\xi \sim |\delta|^{-\nu}$.

- “Semi-critical” points

In a random system generally there is a line of semi-critical fixed points, in which - due to Griffiths singularities - the time scale is divergent, although ξ is finite.

- Relevant scaling fields - H , T , etc.

At a singular point one generally considers the behavior of different physical quantities as a function of relevant scaling fields, such as a small ordering field of strength, H , or in a quantum system as a function of a small temperature, T .

- Scaling transformation

At a singular point, static and (or) dynamical correlations transform covariantly under a scaling transformation, when lengths are rescaled by a factor, $b > 1$, i.e. $L' = L/b$. For example at the critical point the order-parameter correlation function behaves as[145]:

$$C(r) = b^{-2x_m} C(r/b) . \quad (\text{A.6})$$

Similarly, static and (or) dynamical densities, such as the local magnetization and (or) the local susceptibility obey scaling relations[145].

A.2 Conventional random critical scaling

In a conventional random critical point:

- dynamical scaling is anisotropic
- densities in large scale are homogeneous

The correlation length and the relaxation time are related as:

$$t_r \sim \xi^z , \quad (\text{A.7})$$

with a dynamical exponent, $1 \leq z < \infty$. From this follows that in a finite system the excitation energies are typically:

$$\Omega \sim L^{-z} , \quad (\text{A.8})$$

and are transformed as $\Omega' = \Omega b^z$. Distribution of the low-energy excitations, $P(\epsilon)$, ($\epsilon \sim \Omega$) is assumed to be in the form as given in Eq.(A.1). Under a scaling transformation the distribution function is expected to satisfy the relation:

$$P(\epsilon)d\epsilon = b^{-d}P(\epsilon')d\epsilon' = b^{-d+z/D}P(\epsilon)d\epsilon, \quad (\text{A.9})$$

provided the low-energy excitations are localized, thus their density is transformed by a factor of b^{-d} , where d is the dimension of the system. The fixed point of Eq.(A.9) is given by:

$$D = z/d, \quad (\text{A.10})$$

thus the strength of disorder is finite and proportional to the dynamical exponent.

The order-parameter (magnetization), $m(\delta, L)$, in a finite system satisfies the scaling relation:

$$m(\delta, L) = b^{-x_m}m(\delta b^{1/\nu}, L/b). \quad (\text{A.11})$$

Taking the scaling parameter $b = \delta^{-\nu}$ we have $m(\delta, L) = \delta^{x_m\nu}\tilde{m}(L\delta^\nu)$, where the scaling function in the limiting cases behaves as: $m(y) = \text{const}$, if $y \rightarrow \infty$ and $m(y) \sim y^{-x_m}$, if $y \rightarrow 0$. Thus in the thermodynamic limit, $L \rightarrow \infty$, $m(\delta) \sim \delta^\beta$ with $\beta = x_m\nu$. On the other hand at the critical point, $\delta = 0$, the finite-size scaling behavior is: $m(\delta = 0, L) \sim L^{-x_m}$. We note that for a surface spin x_m is replaced by the appropriate surface exponent, x_m^s .

The scaling law of the critical correlation function is given in Eq.(A.6), which is generalized outside the critical point:

$$C(\delta, r) = b^{-2x_m}C(\delta b^{1/\nu}, r/b). \quad (\text{A.12})$$

Here with $b = r$ we obtain $C(\delta, r) = r^{-2x_m}\tilde{C}(\delta r^{1/\nu})$, where the scaling function is $\tilde{C}(0) = \text{const}$ and $\tilde{C}(y) \sim \exp(-y^\nu)$ for $y \rightarrow \infty$.

The autocorrelation function transforms similarly to Eq.(A.6):

$$G(\delta, t) = b^{-2x_m}G(\delta b^{1/\nu}, t/b^z), \quad (\text{A.13})$$

and with $b = t^{1/z}$ we obtain $G(\delta, t) = t^{-2x_m/z}\tilde{G}(\delta t^{1/\nu z})$. Here the scaling function is $\tilde{G}(0) = \text{const}$, whereas $\tilde{G}(y)$ for large y has a decay, which is slower than $\exp(-y^{\nu z})$. Its proper form is determined by classical Griffiths singularities[158].

At a conventional random quantum critical point, which takes place at $T = 0$, the low-temperature behavior of singular quantities, such as the local susceptibility, $\chi(T)$, and the specific heat, $C_v(T)$, can be obtained from the consideration that the temperature sets an energy-scale, $\Omega \sim T$, which corresponds to a thermal length, $L_T \sim T^{-1/z}$. Taking the rescaling factor, $b = L_T$, we obtain for small T :

$$\chi(T) \sim T^{-\gamma/\nu z}, \quad C_v(T) \sim T^{-\alpha/\nu z}, \quad (\text{A.14})$$

where $\gamma = (d - 2x_m)\nu$ and $\alpha = 2 - d\nu$ are the standard susceptibility and specific heat exponents, respectively.

Similarly, for a (longitudinal) ordering field the energy-scale is given by $\Omega_H \sim H m L_H^d$, which is set a length-scale: $L_H \sim H^{-1/(d+z-x_m)}$. Taking the rescaling factor, $b = L_H$, we obtain for small H :

$$\chi(H) \sim H^{-\gamma/\nu(d+z-x_m)}, \quad C_v(H) \sim H^{-\alpha/\nu(d+z-x_m)}. \quad (\text{A.15})$$

A.3 Infinite disorder scaling

An infinite disorder fixed point has two important properties:

- activated scaling
- densities are non-homogeneous in large scales, average values are dominated by rare regions.

Activated scaling means that the log time-scale is related to the length-scale:

$$\ln t_r \sim \xi^\psi, \quad (\text{A.16})$$

thus in a finite system the excitation energies are typically:

$$|\ln \Omega| \sim L^\psi, \quad (\text{A.17})$$

and are transformed as $\ln \Omega' = \ln \Omega b^{-\psi}$.

Distribution of the log of the low-energy excitations is assumed to follow the transformation:

$$P(\ln \epsilon, L) = b^{-\psi} P(b^{-\psi} \ln \epsilon, L/b). \quad (\text{A.18})$$

As the length, $L \sim b$, increases the strength of disorder increases, too, and in the fixed point the disorder becomes infinitely strong. (Note the difference with Eq.(A.9) for conventional scaling.)

Scaling of a physical observable, O , which can be an average density or a correlation function, is dominated by rare regions (realizations) in which regions (samples) it has a value of $\langle O \rangle_{rare} = O(1)$, whereas in typical samples it is (exponentially) small, $\langle O \rangle_{typ} = O(\exp(-aL^\omega))$, $\omega = O(1)$. Explicit examples of rare events can be found in Sec.4.1.2 for the surface magnetization of the RTFIC and in Sec.11.1.2 for the persistence of the Sinai walk. The average value, $\overline{\langle O \rangle}$, has the same scaling properties as the fraction of rare events or the density of rare regions, ρ_O .

Scaling of the average order-parameter, m , follows from scaling of the density of locally ordered regions, ρ_m , which is given by:

$$\rho_m(\delta, L) = b^{-x_m} \rho_m(\delta b^{1/\nu}, L/b). \quad (\text{A.19})$$

Note, that this relation is in identical mathematical form as for conventional random critical scaling in Eq.(A.11), therefore m has the same properties in the two cases, see below Eq.(A.11). The same conclusion holds for the spatial correlation function, $C(r)$, too. In this case a rare event consists of two independent, locally ordered regions which are separated by a distance, r . The

density of rare regions of the correlation function, ρ_C , is given by $\rho_C \sim \rho_m^2$ and through $C \sim \rho_C$ we arrive to the scaling law in Eq.(A.12) and to the conclusion described below this equation.

In the strong disorder RG one often considers the global order parameter, $\mu = mL^d$, which is called the cluster moment. This obeys the scaling relation:

$$\mu(\delta, |\ln \Omega|) = b^{d_f} \mu(\delta b^{1/\nu}, |\ln \Omega| b^\psi), \quad (\text{A.20})$$

in which $d_f = d - x_m$ is the fractal dimension of the cluster. Taking the length-scale, $b = |\ln \Omega|^{1/\psi}$, we have at the critical point:

$$\mu(\delta = 0, |\ln \Omega|) \sim |\ln \Omega|^\phi, \quad \phi = (d - x_m)/\psi. \quad (\text{A.21})$$

We note that the typical correlation length at an infinite disorder fixed point is much smaller than the (true) correlation length and they are related as given in Eq.(9.4): $\xi_{typ} \sim \xi_{av}^{1-\psi}$.

To calculate the average autocorrelation function one should keep in mind that disorder in the time-direction is strictly correlated. Thus, if there is local order at a given rare region, say at site, i , at time 0, the order stays for any later time, t . Consequently the density of rare regions of G is given by: $\rho_G \sim \rho_m$, so that the average autocorrelation function satisfies the scaling relation:

$$G(\delta, \ln t) = b^{-x_m} G(\delta b^{1/\nu}, \ln t / b^\psi). \quad (\text{A.22})$$

Now taking $b = (\ln t)^{1/\psi}$ we obtain:

$$G(\delta, \ln t) = (\ln t)^{-x_m/\psi} \tilde{G}(\ln t \delta^{\nu\psi}), \quad (\text{A.23})$$

thus the decay of critical autocorrelations is ultra-slow, logarithmic in time. In the disordered phase the scaling function, $\tilde{G}(y)$ is expected to behave for large arguments as: $\ln \tilde{G}(y) \sim -y$. Thus the dominant decay of the average autocorrelation function in the disordered region is in a power-law form:

$$G(\delta, \ln t) \sim (\ln t)^{-x_m/\psi} t^{-\eta(\delta)}, \quad \delta > 0, \quad (\text{A.24})$$

which is supplemented by logarithmic corrections. This region is the disordered Griffiths phase in which the decay exponent, $\eta(\delta)$, depends on the control parameter. For $\delta \rightarrow 0$ it goes to zero as $\eta(\delta) \sim \delta^{\nu\psi}$.

The low-temperature singularities at a quantum critical point can be obtained by setting the length-scale $b = L_T \sim (\log T)^{1/\psi}$. For the specific heat the rare events are low-energy excitations which are separated by a distance, L_T , thus $C_v(T) \sim L_T^{-d}$. For the susceptibility the rare events bring a Curie-type contribution, thus we obtain in analogy with Eq.(A.14), $\chi(T) \sim L_T^{d-2x_m}/T$, thus:

$$\chi(T) \sim \frac{(\ln T)^{(d-2x_m)/\psi}}{T}, \quad C_v(T) \sim (\ln T)^{-d/\psi}. \quad (\text{A.25})$$

For a small ordering field, H , the thermal and magnetic energy-scales can be compared: $T \sim HmL_H^d \sim HL_H^{d-x_m}$, from which we have the relation: $H \sim$

$T(\ln T)^{d-x_m}$. Putting it into Eq.(A.25) we obtain the small H singularities at $T = 0$:

$$\chi(H) \sim \frac{(\ln H)^{-x_m/\psi}}{H}, \quad C_v(H) \sim (\ln H)^{d/\psi} . \quad (\text{A.26})$$

A.4 Scaling in the Griffiths phases

In the Griffiths-phase:

- the correlation length is finite, the relaxation time is divergent
- dynamical scaling (between L and t_r) is anisotropic
- densities are non-homogeneous in large scales, average values are dominated by rare regions.

The physical origin of the singular behavior of disordered systems outside the critical point is due to rare regions, in which strong fluctuations of the local couplings prefer the existence of the thermodynamically non-stable phase locally. Scaling in the ordered and disordered Griffiths phases is somewhat different, in particular for $d > 1$.

A.4.1 Disordered Griffiths phase

In the disordered phase a small region is locally ordered if the couplings there are larger than the average disordering field. To find such a rare region of linear size, l_c , is exponentially small, $p(l_c) \sim \exp(-\alpha l_c^d)$, however these regions are extremely stable against fluctuations and have a typical relaxation time, $t_r \sim \exp(\sigma l_c^d)$. Indeed the lowest gap of a finite, ordered system is given by $\epsilon \sim \exp(-\sigma l_c^d)$ and $t_r \sim \epsilon^{-1}$. Then the distribution of large relaxation times has an algebraic tail: $p(t_r) \sim t_r^{-d/z-1}$, with $d/z = \alpha/\sigma$, which is supplemented by a logarithmic correction factor, $(\ln t_r)^{-1+1/d}$. The leading behavior of the average autocorrelation function:

$$G(t) \sim \int dt_r p(t_r) \exp(-t/t_r) \sim t^{-d/z} \quad (\text{A.27})$$

is algebraic and the decay exponent is δ dependent. Comparing with the scaling form in Eq.(A.24) we obtain for small δ :

$$\frac{d}{z} \sim \delta^{\nu\psi} , \quad (\text{A.28})$$

see also Eq.(9.4).

From the distribution of the relaxation times one obtains for the distribution of the small gaps:

$$P(\epsilon) \sim \epsilon^{-1+d/z} , \quad (\text{A.29})$$

which is in the same form as in Eq.(A.1). Thus in the Griffiths-phase there is finite disorder the strength of which is given by $D = z/d$. Since the excitations

are localized the scaling transformation of $P(\epsilon)$ is the same as in Eq.(A.9) for conventional scaling. Consequently one has the relation:

$$\Omega \sim L^{-z} . \quad (\text{A.30})$$

The scaling form of the autocorrelation function follows from the observation that the density of rare regions in the Griffiths phase is just the density of the system which transforms as

$$G(t) = b^{-d} G(t/b^z) . \quad (\text{A.31})$$

Here with $b = t^{1/z}$ we recover the relation in Eq.(A.27).

The low-temperature singularities can be obtained by setting the length-scale, $b = L_T \sim T^{-1/z}$, and make use of the fact that the density of rare regions is the particle density, both for the specific heat, $C_v(T) \sim L_T^{-d}$, and for the susceptibility $\chi(T) \sim L_T^{-d}/T$, where in the latter case a Curie-type contribution per site is taken into account. We thus obtain:

$$\chi(T) \sim T^{-1+d/z}, \quad C_v(T) \sim T^{d/z} . \quad (\text{A.32})$$

The small H singularities at $T = 0$ are obtained by using the length-scale, $b = L_H \sim H^{-1/z}$. Note that in the disordered phase for $H \sim T$, $L_H \sim L_T$ and we obtain as in Eq.(A.32):

$$\chi(H) \sim H^{-1+d/z}, \quad C_v(H) \sim H^{d/z} . \quad (\text{A.33})$$

A.4.2 Ordered Griffiths phase

In the ordered Griffiths phase the relevant excitations are connected to such large ordered domains, which are isolated from the macroscopic ordered regions of the system. Therefore the probability of the existence of such an ordered domain of linear size, l_c , is generally smaller, than the similar expression in the disordered phase. In one dimension one needs l_c weak and consecutive l_c strong couplings, thus the corresponding probability is $p_o(l_c) \sim \exp(-\alpha 2l_c)$. Since the typical relaxation time stays the same as in the disordered phase, $t_r \sim \exp(\sigma l_c)$, the autocorrelation function in Eq.(A.27) involves the decay exponent, $2/z$. This is in agreement with the strong disorder RG calculation for the RTFIC in Eq.(4.67).

In $d > 1$, as argued in Sec.9.1.3 for a successful isolation of a cluster of l_c^d sites one needs a distance from the ordered domain at least, $l_o \sim l_c^d$. Consequently the probability of the existence of an isolated large cluster reads as $p(l_c) \sim \exp(-\alpha' l_o^d) \sim \exp(-\alpha l_c^{d^2})$. Now, with $t_r \sim \exp(\sigma l_c^d)$ we obtain from Eq.(A.27) an enhanced power-law form:

$$G(t) \sim \exp(-A |\ln t|^d) , \quad (\text{A.34})$$

as already presented in Eq.(9.7).

Relation between the length-scale, L , and the energy-scale, Ω , can be obtained in the following way. In a system of linear size, L , the typical size of the largest isolated cluster follows from extreme value statistics and given by: $l_c^{d^2} \sim \ln L$. On the other hand the excitation energy due to this cluster is $\Omega \sim 1/t_r \sim \exp(-\sigma l_c^d)$, consequently:

$$|\ln \Omega| \sim (\ln L)^{1/d} . \quad (\text{A.35})$$

The low-temperature singularities can be obtained as in the disordered phase however with a length-scale, $L_T \sim \exp[A|\ln T|^d]$. In this way we obtain:

$$\chi(T) \sim \frac{1}{T} \exp[-C|\ln T|^d], \quad C_v(T) \sim \exp[-C'|\ln T|^d] , \quad (\text{A.36})$$

and similarly for the small H dependence, by the substitution $H \sim T$.

A.5 Scaling in the large spin phase

This phase is observed in random Heisenberg models and characterized by

- a size-dependent effective spin
- anisotropic dynamical scaling
- often non-localized excitations.

The typical value of the large spin, S_{eff} , grows with the size as:

$$S_{eff} \sim L^{d\zeta} , \quad (\text{A.37})$$

where ζ is often equal to (or close to) $1/2$, see Sec.8.2. The energy- and length-scales are related as in the Griffiths-phase:

$$\Omega \sim L^{-z} , \quad (\text{A.38})$$

so that the relation between spin and energy, $S_{eff} \sim \Omega^{-\kappa}$, involves an exponent, $\kappa = d\zeta/z$. The gap exponent, ω , defined as $P(\epsilon) \sim \epsilon^\omega$, $\epsilon \rightarrow 0$, however, is generally not given by $\omega = -1 + d/z$, as in the Griffiths-phase, see Eq.(A.29), while the excitations are often non-localized.

The low-temperature singularities are given by:

$$\chi(T) \sim \frac{1}{T}, \quad C_v(T) \sim T^{2\zeta(\omega+1)} |\ln T| , \quad (\text{A.39})$$

whereas for a small ordering field the order parameter behaves as:

$$m(H) \sim H^{\zeta(\omega+1)/[1+\zeta(\omega+1)]} . \quad (\text{A.40})$$

B Mapping between different models

This Appendix describe the mapping between different models considered in this review.

B.1 The random RW and the RTFIC

Solution of the master equation for the RW in Eq.(11.4) necessitates the solution of the eigenvalue problem of the Fokker-Planck operator, $\underline{\underline{M}}$, the matrix elements of which take the form $(\underline{\underline{M}})_{i,j} = w_{i,j}$ for $i \neq j$ and $(\underline{\underline{M}})_{i,i} = -\sum_j w_{i,j}$. All the physical properties of the model can be expressed in terms of the left and right eigenvectors \underline{u}_q and \underline{v}_q , respectively, and the eigenvalues λ_q , which are non-positive. The eigenvalue problem in terms of the components of the right eigenvector $v_q(i)$ reads as:

$$w_{i-1,i} v_q(i-1) - (w_{i,i-1} + w_{i,i+1}) v_q(i) + w_{i+1,i} v_q(i+1) = \lambda_q v_q(i) . \quad (\text{B.1})$$

Here we consider a finite system of size L , i.e., we put $w_{0,1} = w_{L+1,L} = 0$. Then we introduce the new variables:

$$v(i) = \alpha_i \tilde{v}(i), \quad \alpha_{i+1} = \alpha_i \left(\frac{w_{i,i+1}}{w_{i+1,i}} \right)^{1/2} \alpha_1 \left(\prod_{j=1}^i \frac{w_{j,j+1}}{w_{j+1,j}} \right)^{1/2}, \quad (\text{B.2})$$

in terms of which the eigenvalue problem is transformed into:

$$(w_{i-1,i} w_{i,i-1})^{1/2} \tilde{v}_q(i-1) - (w_{i,i-1} + w_{i,i+1}) \tilde{v}_q(i) + (w_{i+1,i} w_{i,i+1})^{1/2} \tilde{v}_q(i+1) = \lambda_q \tilde{v}_q(i), \quad (\text{B.3})$$

which corresponds to a real symmetric eigenvalue problem $\sum_j S_{ij} \tilde{v}_q(j) = \lambda \tilde{v}_q(i)$ with $S_{ij} = S_{ji}$. Consequently the eigenvalues λ_q of the FP operator are real.

The symmetric matrix, $\underline{\underline{M}}$, can be compared with the square of the matrix, $\underline{\underline{T}}^2$, in Eq.(4.3), which appears in the eigenvalue problem of the free-fermion representation of the RTFIC. The two problems are equivalent, if we have the correspondences:

$$\begin{aligned} J_i &\Longleftrightarrow (w_{i+1,i})^{1/2} \\ h_i &\Longleftrightarrow (w_{i,i+1})^{1/2} \\ \epsilon_q^2 &\Longleftrightarrow -\lambda_q . \end{aligned} \quad (\text{B.4})$$

Thus there is a *mathematical equivalence* between the random RW and the RTFIC with the corresponding random couplings, as described in (B.4). The relation between the values of the low-energy excitations in Eq.(B.4), which leads to the exact result of the dynamical exponent of the RTFIC in Eq.(4.15) can be extended by a relation between the order-parameters:

$$[m_s(L)]^2 \Longleftrightarrow p_{per}(L) . \quad (\text{B.5})$$

The correspondence between the two models outlined in this section explains the presence of the same type of strong disorder fixed points in the two models. This mapping, however, does not establish relations between another fundamental observables, such as the bulk magnetization of the RTFIC.

B.2 The random XY chain and the RTFIC

The decimation equations in Eqs.(4.16) and (4.17) are very similar to the decimation equation for the XX chain in Eq.(6.11), in particular if dimerization is considered. This analogy is the consequence of an exact mapping between the XY model and the RTFIC, what we show here for an open XY chain of $L = \text{even}$ sites with open boundary conditions. In terms of the spin operators $S_j^{(x,y)}$, $j = 1, 2, \dots, L$ we introduce two sets of Pauli operators $\sigma_l^{(x,z)}, \tau_l^{(x,z)}$, $l = 1, 2, \dots, L/2$ as:

$$\begin{aligned}\sigma_i^x &= \prod_{j=1}^{2i-1} (2S_j^x), & \sigma_i^z &= 4S_{2i-1}^y S_{2i}^y \\ \tau_i^x &= \prod_{j=1}^{2i-1} (2S_j^y), & \tau_i^z &= 4S_{2i-1}^x S_{2i}^x.\end{aligned}\tag{B.6}$$

The original XY Hamiltonian, H_{XY} with L spins can be expressed as the sum of two TIM-s with variables $\sigma_l^{x,z}$ and $\tau_l^{x,z}$ each of which of $L/2$ spins as:

$$H_{XY} = H_{TIM}(\sigma) + H_{TIM}(\tau).\tag{B.7}$$

where the couplings and the transverse fields are given by:

$$\begin{aligned}J_l(\sigma) &= \frac{1}{4}J_{2l}^x, & h_l(\sigma) &= \frac{1}{4}J_{2l-1}^y \\ J_l(\tau) &= \frac{1}{4}J_{2l}^y, & h_l(\tau) &= \frac{1}{4}J_{2l-1}^x.\end{aligned}\tag{B.8}$$

Correlations in the two models are related as can be found in Refs.[139, 196].

C Kesten random variables : exact results versus strong disorder RG

Since Kesten random variables naturally appear in various models considered in this review, we first recall in this Appendix some important properties of these variables. We then explain how the strong disorder RG approach corresponds for these variables to a saddle-point approximation in each sample, that becomes asymptotically exact for large samples.

C.1 Discrete Kesten random variables

A Kesten random variable [218] has the following specific structure of a sum of products of random variables y_i

$$Z_L \equiv \sum_{i=1}^L \prod_{j=1}^i y_i\tag{C.1}$$

This type of random variables appears in the context of random walks in random media for various observables [332, 328, 116] (see Eq 11.5), in the surface magnetization (4.4) of the RTFIC [191, 126], as well as in the random field Ising chain via the formulation with 2×2 random transfer matrices [117, 80].

It is actually convenient to rewrite the Kesten random variable (C.1) with a varying left boundary

$$Z(a, b) = \sum_{i=a}^b \prod_{j=1}^i y_j \quad (\text{C.2})$$

The fundamental property of $Z(a, b)$ is the recurrence equation

$$Z(a, b) = y_a [1 + Z(a + 1, b)] \quad (\text{C.3})$$

where the random coefficient y_a appears multiplicatively : $Z(a, b)$ is thus a multiplicative stochastic process.

One of the main outcome of the studies on the random variable $Z(a, b)$ is that, in the limit of infinite length $L = b - a \rightarrow \infty$, there exists a limit distribution $P_\infty(Z)$ if

$$[\ln y]_{av} < 0 \quad (\text{C.4})$$

Moreover, the limit distribution then presents the algebraic tail [217, 218, 117, 80]

$$P_\infty(Z) \underset{Z \rightarrow \infty}{\sim} \frac{1}{Z^{1+\mu}} \quad (\text{C.5})$$

where the exponent μ is defined as the positive root $\mu > 0$ of the equation

$$[y^\mu]_{av} = 1 \quad (\text{C.6})$$

In the field of random walks in random media, this exponent μ is known to govern the anomalous diffusion behavior $x \sim t^\mu$ in the domain $0 < \mu < 1$ [218, 116, 14]. In the context of the RTFIC, the exponent μ defined by (C.6) has for analog the dynamical exponent $1/z$.

C.2 Continuous version of Kesten random variables

The continuous version of the Kesten random variable (C.2) is the exponential functional [14, 262]

$$Z[a, b] = \int_a^b dx e^{-\int_a^x dy F(y)} \quad (\text{C.7})$$

where $\{F(x)\}$ is the random process corresponding to the random variables $(-\ln y_i)$ in the continuous limit. The analog of the recurrence equation (C.3) is the stochastic differential equation

$$\partial_a Z[a, b] = F(a) Z[a, b] - 1 \quad (\text{C.8})$$

where the random process $F(x)$ appears multiplicatively, in contrast with usual Langevin equations where the noise appears additively. In the limit of infinite length $L = b - a \rightarrow \infty$, the condition (C.4) to have a limit distribution $P_\infty(Z)$ becomes a condition on the mean value of the process $F(x)$ that should be strictly positive

$$F_0 \equiv [F(x)]_{av} > 0 \quad (\text{C.9})$$

The exponent μ (C.5) is now determined as the root of the equation (C.6)

$$[e^{-\mu \int_0^x dy F(y)}]_{av} = 1 \quad (\text{C.10})$$

for arbitrary x as long as the process $F(x)$ has no correlation.

It is interesting to note that the exponential functional (C.7) actually determines the stationary flux J_L [262] that exists in a given Sinai sample $[0, L]$ between two fixed concentration c_0 and $c_N = 0$ (i.e. particles are injected via a reservoir at $x = 0$ and are removed when they arrive at the other boundary $x = N$) : it is simply given by the inverse of the variable $Z_L \equiv Z[0, L]$

$$J_L = \frac{c_0}{Z_L} \quad (\text{C.11})$$

In some sense, it is the simplest physical observable in the Sinai diffusion, as the surface magnetization is the simplest order parameter in the RTFIC : both can be expressed in a simple way in terms of the Kesten random variable of the sample.

The simplest process for $F(x)$ is of course the case where $F(x)$ is a biased Brownian motion

$$\langle F(x) \rangle = F_0 \quad (\text{C.12})$$

$$\langle F(x)F(x') \rangle - F_0^2 = 2\sigma\delta(x - x') \quad (\text{C.13})$$

In this case, the exponent μ solution of (C.10) reads [14, 262]

$$\mu = \frac{F_0}{\sigma} \quad (\text{C.14})$$

The Brownian process actually corresponds to the fixed point of the real-space renormalization approach and can thus be used to study the universal properties near the critical point. The probability distribution of the random variable Z_L (C.7) in the case where the process $\{F(x)\}$ is a Brownian motion (C.13) can be determined exactly by various methods [262, 99, 360, 271], and we refer to these articles for various detailed explicit results.

C.3 Meaning of the strong disorder RG

It turns out that the strong disorder RG for observables involving Kesten random variables actually corresponds to the following saddle-point analysis [271].

In the case of a Brownian process (C.13), the continuous version of the Kesten process (C.7) can be written as

$$Z_L = \int_0^L dx e^{-U(x)} \quad (\text{C.15})$$

where the potential $U(x) = \int_0^x dy F(y)$ is a random walk that presents fluctuations of order \sqrt{L} on the interval $[0, L]$. As a consequence, it seems natural to evaluate this integral in the large L limit by the saddle-point method

$$Z_L \underset{L \rightarrow \infty}{\propto} e^{E_L} \quad (\text{C.16})$$

where $(-E_L) < 0$ is defined as the minimum reached by the process $U(x)$ on the interval $[0, L]$. The scaling $E_L \sim \sqrt{L}$ shows that there will exist a limit distribution for $(\ln Z_L)/\sqrt{L}$, and that this limiting distribution is given by the limit distribution of E_L/\sqrt{L} . We refer the reader to [271] for a more detailed discussion along these lines.

In conclusion, the study of observables that have a closed expression in terms of the disorder variables, such as the surface magnetization in the RTFIC, shed light on the meaning of the strong disorder approach and of its asymptotic exactness: for these variables, the strong disorder approach amounts to perform a saddle-point analysis in each sample. More generally, for the other observables one may still consider that the strong disorder approach gives in some sense a direct access to an appropriate ‘saddle-point’, even if there is no closed exact expressions on which one could perform a usual saddle-point method.

D Extrema of 1D random potentials via RG

In the Sinai model where a particle diffuses in a 1D Brownian potential, we have seen that the strong disorder RG amounts to construct the extrema of the Brownian potential at large scale, where only barriers bigger than the RG scale Γ are kept. This construction of the extrema at large scale can actually be defined for arbitrary 1D potentials [233]. In particular, the RG procedure may be implemented numerically for correlated random potentials, which has been done in particular for logarithmic correlations [91].

On the analytical side, we explain in this Appendix what can be said in general for the case of Markovian potentials and some results that have been obtained for the specific example of a Brownian potential with quadratic confinement [233].

D.1 RG for Markovian potentials

For ‘Markovian’ random potentials $U(x)$, satisfying a local Langevin equation of the form

$$\frac{dU(x)}{dx} = F[U(x), X] + \eta(x) \quad (\text{D.1})$$

where $\eta(x)$ is a white noise, the measure of the renormalized landscape can be factorized in blocks which satisfy closed RG equations [233]. In the case of stationary landscapes, where the force F is independent of x

$$F[U, X] = F[U] = -\frac{dW[U]}{dU} \quad (\text{D.2})$$

(this case generalizes the pure Brownian landscape $F = 0$ and the biased Brownian landscape $F[U] = F > 0$), one obtains explicit solutions for the renormalization equations [233]. Other cases may also be explicitly solved, in particular the Brownian potential with quadratic confinement considered in details below, which corresponds to a force independent of U and linear in x

$$F[U(x), X] = F[x] = \mu X \quad (\text{D.3})$$

The measure of the renormalized landscape is then expressed in terms of Airy functions [233].

D.2 Results for the Brownian potential with quadratic confinement

D.2.1 Definition and properties of the model

Let us first briefly explain the physical interests of the so-called ‘toy model’

$$U_{\text{toy}}(x) = \frac{\mu}{2}x^2 + V(x) \quad (\text{D.4})$$

containing a deterministic quadratic term and a random Brownian term $V(x)$

$$\overline{(V(x) - V(y))^2} = 2|x - y| \quad (\text{D.5})$$

This model was introduced by Villain *et al.* as a ‘toy model’ for interfaces in the presence of random field [347]. In addition, within the field of random manifolds of internal dimension D living in a random medium of dimension $(N + D)$, the toy model is considered as the extreme simplest case $D = 0$ and $N = 1$ [259].

As a consequence of the quadratic containment, the absolute minimum of the potential (D.4) is finite and an Imry-Ma argument can be used to obtain its scaling : the balance between the elastic energy of order μx^2 and the random energy of order \sqrt{x} yields the scaling

$$x_{\min} \sim \mu^{-2/3} \quad (\text{D.6})$$

whereas the usual perturbation methods at all the orders [348] or of iteration [349] are unable to reproduce this scaling (D.6). Within the framework of the replica variational method, the result (D.6) requires a replica symmetry breaking [259, 131].

Another important property of the model is its ‘statistical tilt symmetry’ also present in other models with random fields. This symmetry implies remarkable identities [326] for disorder averaged of thermal cumulants of the position, that are summarize by

$$\overline{\ln \langle e^{-\lambda X} \rangle} = T \frac{\lambda^2}{2\mu} \quad (\text{D.7})$$

This identity on the generating function shows that the second cumulant is simply

$$\overline{\langle x^2 \rangle - \langle x \rangle^2} = \frac{T}{\mu} \quad (\text{D.8})$$

and that the disorder averages of all higher cumulants actually vanish! At low temperature, the result (D.8) implies that the thermal fluctuations are related to the presence of metastable states in rare samples [326]. The renormalization allows in particular to study this phenomenon quantitatively, as explained below.

D.2.2 Results on the statistics of the minima

At $T = 0$, the particle is at the minimum x_{min} of the random potential (D.4). The final state $\Gamma = \infty$ of the renormalization procedure [233] allows to find that the distribution of x_{min} over the samples is, in agreement with [159, 147]

$$P_{]-\infty, +\infty[}(x) = g(x)g(-x) \quad (\text{D.9})$$

and the auxiliary function

$$g(x) = \int_{-\infty}^{+\infty} \frac{d\lambda}{2\pi} \frac{e^{-I\lambda X}}{aAi(bI\lambda)} \quad (\text{D.10})$$

with the notations $a = (\mu/2)^{1/3}$ and $b = 1/a^2$.

The probability that a sample presents two almost degenerate minima, located at positions x_1 and x_2 , with an energy difference $\delta E = \epsilon \rightarrow 0$, can be written as

$$\mathcal{D}(\epsilon, x_1, x_2) = \epsilon g(-x_1)d(x_2 - x_1)g(x_2) + O(\epsilon^2) \quad (\text{D.11})$$

in terms of the function g (D.10) and the function

$$d(y) = a \int_{-\infty}^{+\infty} \frac{d\lambda}{2\pi} e^{i\lambda y} \frac{Ai'(iB\lambda)}{Ai(ib\lambda)} \quad (\text{D.12})$$

The probability of having two minima separated by a distance $y > 0$ is thus

$$D(y) = \int_{-\infty}^{+\infty} dx_1 \lim_{\epsilon \rightarrow 0} \left(\frac{\mathcal{D}(\epsilon, x_1, x_1 + y)}{\epsilon} \right) = Bd(y) \int_{-\infty}^{+\infty} \frac{d\lambda}{2\pi} \frac{e^{-i\lambda y}}{Ai^2(IB\lambda)} \quad (\text{D.13})$$

In particular, the computation of the second moment yields

$$\int_0^{+\infty} dy y^2 D(y) = \frac{1}{\mu} \quad (\text{D.14})$$

The contribution of the samples with two nearly degenerate minima to the second thermal cumulant of the position (D.8) can be estimated at first order in temperature as follows : the two minima have for respective Boltzmann weights $p = \frac{1}{1+e^{-\beta\epsilon}}$ and $(1-p) = \frac{e^{-\beta\epsilon}}{1+e^{-\beta\epsilon}}$. The variable $(x- < x >)$ is thus $(1-p)(x_1-x_2)$ with probability p and $p(x_2-x_1)$ with probability $(1-p)$. The average yields

$$\overline{< (x- < x >)^2 >} = \overline{p(1-p)(x_1-x_2)^2} \quad (\text{D.15})$$

$$\begin{aligned} &= \int_{-\infty}^{+\infty} dx_1 \int_{x_1}^{+\infty} dx_2 \int_{-\infty}^{+\infty} d\epsilon \mathcal{D}'(\epsilon=0, x_1, x_2) \frac{e^{-\epsilon/T}}{(1+e^{-\epsilon/T})^2} (x_2-x_1)^2 \\ &= T \int_0^{+\infty} dy D(y) \end{aligned} \quad (\text{D.16})$$

Using (D.14), one then obtains the exact result (D.8). This shows that the thermal fluctuations at low temperature are entirely due to the metastable states which exist in some rare samples. In particular, the susceptibility

$$\chi \equiv \frac{1}{T} (< x^2 > - < x >^2) \quad (\text{D.17})$$

has a finite average at zero temperature

$$\overline{\chi} = \frac{1}{\mu} \quad (\text{D.18})$$

but only the samples with two nearly degenerate minima actually contribute to this average value, because the typical samples with only one minimum have a susceptibility which vanish at zero temperature.

Similarly, the even moments of the relative position $(x- < x >)$ behaves in the following way at low temperature

$$\overline{< (x- < x >)^{2n} >} = \frac{T}{n} \int_0^{+\infty} y^{2n} D(y) + O(T^2) \quad (\text{D.19})$$

in term of the function $D(y)$ defined in (D.13). The comparison with the identity (D.7) shows that there are many terms which cancel in the disorder averages of thermal cumulants.

D.2.3 Results on the statistics of the largest barrier

The time t_{eq} necessary to reach equilibrium is directly related to the largest barrier $\Gamma_{max} = t \ln t_{eq}$ existing in the sample. More precisely, the probability

$\mathcal{P}(t_{eq} < t)$ that the system has already reached equilibrium at time t , corresponds to the probability that there remains only one renormalized valley at scale $\gamma = T \ln t$: it is a function of the scaling variable γ

$$\mathcal{P}(t_{eq} < t) = \Phi \left(\gamma \equiv \left(\frac{\mu}{2} \right)^{1/3} T \ln T \right) \quad (\text{D.20})$$

The function Φ has the following explicit expression in terms of Airy functions [233]

$$\begin{aligned} \Phi(\gamma) &= \int_{-\infty}^{+\infty} \frac{d\lambda}{2\pi} \frac{1}{Ai^2(i\lambda)} e^{-2 \int_0^{+\infty} df \tilde{\psi}_\gamma(f, \lambda)} \\ \tilde{\psi}_\gamma(f, \lambda) &= \frac{Ai(f + \gamma + i\lambda)}{\pi Ai(f + i\lambda) [Ai(f + i\lambda) Bi(f + \gamma + i\lambda) - Bi(f + i\lambda) Ai(f + \gamma + i\lambda)]} \end{aligned} \quad (\text{D.21})$$

This result yields directly by derivation the probability distribution of the scaling variable $\gamma = \left(\frac{\mu}{2} \right)^{1/3} \Gamma_{max}$ for the largest barrier Γ_{max} existing in the sample

$$P_{max}(\gamma) = \frac{d}{d\gamma} \Phi(\gamma) \quad (\text{D.22})$$

The asymptotic behaviors of this distribution are as follows

$$P_{max}(\gamma) \underset{\gamma \rightarrow \infty}{\simeq} \frac{9}{4} \sqrt{\frac{\pi}{2}} \gamma^{5/4} e^{-\frac{3}{2} \gamma^{3/2}} \quad (\text{D.23})$$

$$P_{max}(\gamma) \underset{\gamma \rightarrow 0}{\simeq} \frac{6\zeta(3)}{\gamma^4} e^{-2 \frac{\zeta(3)}{\gamma^3}} \quad (\text{D.24})$$

where $\zeta(n)$ is the Riemann zeta function.

E Comparison with some growth models without disorder

The strong disorder RG rules discussed in Section 3 have actually a close relationship with some growth models, which were introduced in a completely independent way. These geometrical growth models describe a collection of intervals on the line which evolve by an iterative transformation on the smallest interval remaining on the line. The various rules that have been considered are the following :

(i) in the “cut-in-two model” [121], the smallest interval is eliminated and gives one half of its length to each one of these two neighbors. This model thus introduces correlations between the neighboring intervals and has been studied numerically [121].

(ii) in the “paste-all model” [121], the smallest interval is eliminated and gives all its length randomly to the one of these two neighbors drawn in an

equiprobable way. This model does not introduce correlations between the neighboring intervals, and the invariant distribution of lengths has been computed [121].

(iii) in the “instantaneous collapse model” [315], the smallest interval is eliminated with its two neighbors to form one new interval $l = l_1 + l_2 + l_3$. This model actually describes the effective dynamics at large time of the unidimensional scalar field which evolves according to a Ginzburg-Landau equation at zero temperature [281, 315]. This model thus aroused a great interest as a soluble model of coarsening. The exact results concern the invariant distribution of the lengths [315], the persistence exponent [70] which characterizes the auxiliary variable $d' = d_1 + d_3$, the autocorrelation exponent [71] which characterizes the auxiliary variable $q' = q_1 - q_2 + q_3$ and finally the generalized persistence exponent [249] which characterizes the auxiliary variable $m' = m_1 + pm_2 + m_3$ with a parameter p . The only technical difference with the strong disorder RG rules presented before is that, in these growth models, it is the length which is the main variable that determines the renormalization, whereas in disordered models, the length is only an auxiliary variable, the main variable that defines the dynamics being a disorder variable. This explains the analytical differences between the solutions for the fixed points and the exponents in the two types of models.

From a physical point of view, this example shows that a dynamics without intrinsic disorder, starting from a random initial condition, can be controlled, in a certain sense, by an ‘infinite disorder’ fixed point. More recently, another pure dynamical model starting from a random initial condition involving diffusion and annihilation of multi-species was shown to be described also by some RG of the Ma-Dasgupta type [113].

References

BOOKS AND REVIEWS ON RELATED TOPICS

Phase transitions and Critical Phenomena

- [1] M.E. Fisher, in *Critical Phenomena*, edited by F.J.W. Hahne, Springer Lecture Notes in Physics, Vol. 186 (Heidelberg, 1983).
- [2] S.K. Ma, *Modern Theory of Critical Phenomena*, Benjamin (Reading, 1976).
- [3] J.L. Cardy, *Scaling and Renormalization in Statistical Physics*, Cambridge University Press (Cambridge, 1996).
- [4] K.G. Wilson, Rev. Mod. Phys. 47 , 773 (1975) “The renormalization group : critical phenomena and the Kondo problem”.

Quantum Phase Transitions :

- [5] S. Sachdev, *Quantum phase transitions*, Cambridge University Press (1999).

Disordered Systems :

- [6] K. Binder and A.P. Young, Rev. Mod. Phys. 58, 801 (1986)
“Spin-glasses - experimental facts, theoretical concepts, and open questions”
- [7] M. Mézard, G. Parisi, and M.A. Virasoro, *Spin Glass Theory and Beyond*, World Scientific (Singapore, 1987)
- [8] J.M. Luck, Aléa Saclay (1992),
Systèmes désordonnés unidimensionnels.
- [9] A. Crisanti, G. Paladin, A. Vulpiani, “Products of random matrices in statistical physics”, Springer Verlag (1993).
- [10] *Spin glasses and random fields* A. P. Young Ed., World Scientific (Singapore, 1998)
- [11] N. Kawashima, and H. Rieger, in *Frustrated Spin Systems* edited by H.T. Diep, World Scientific, (Singapore, 2004)
“Recent Progress in Spin Glasses”

Aging and glassy dynamics :

- [12] L. F. Cugliandolo, “Dynamics of glassy systems ” Lecture notes in Slow Relaxation and non equilibrium dynamics in condensed matter, Les Houches Session 77 July 2002.

- [13] A. Crisanti and F. Ritort J. Phys. A 36 (2003) R181
 “ Violation of the fluctuation-dissipation theorem in glassy systems: basic notions and the numerical evidence ”

Random walks in random media :

- [14] J.P. Bouchaud and A. Georges, Phys. Reports 195 (1990) 127
 “Anomalous diffusion in disordered media : statistical machanisms, models and physical applications” ;
- [15] J.W. Haus et K.W. Kehr Phys. Rep. 150 (1987) 263
 “Diffusion in regular and disordered lattices” .
- [16] S. Havlin and D. Ben Avraham, Adv. Phys. 36 (1987) 695
 “Diffusion in disordered media”;
 D. Ben-Avraham and S. Havlin, *Diffusion and reactions in fractals and disordered systems*, Cambridge University Press (2000)

Coarsening phenomena :

- [17] A. Bray, Adv.Phys. 43, 357 (1994)
 “Theory of phase ordering kinetics” .

Persistence :

- [18] S. Redner, *A guide to first-passage process* Cambridge University Press (Cambridge, 2001)

Stochastic models of interacting particles :

- [19] J. Marro and R. Dickman, *Nonequilibrium phase transitions in lattice models* (Cambridge University Press, Cambridge, 1996).
- [20] R. Dickman in *Nonequilibrium statistical mechanics in one dimension* edited by V. Privman , Cambridge University Press (1997).
- [21] H. Hinrichsen, Adv. Phys. **49**, 815 (2000)
 “Nonequilibrium critical phenomena and phase transitions into absorbing states”
- [22] G.M. Schütz, “Integrable Stochastic many-body systems” in *Phase Transitions and Critical Phenomena*, vol. 19, Eds. C. Domb and J.L. Lebowitz (Academic Press, San Diego, 2001).

Surface growth phenomena

- [23] A.L. Barabási and H.E. Stanley, *Fractal concepts in surface growth*, Cambridge University Press (Cambridge, 1995).

RESEARCH ARTICLES

- [24] M. Abramowitz and I.A. Stegun, *Handbook of Mathematical Functions*, (Dover, New York, 1964), p. 556.
- [25] I. Affleck, T. Kennedy, E. H. Lieb, and H. Tasaki, Phys. Rev. Lett. 59, 799 (1987)
“Rigorous results on valence-bond ground states in antiferromagnets”.
- [26] A. Aharony, Y. Imry and S.-K. Ma Phys. Rev. Lett. 37, 1364 (1976)
“Lowering of Dimensionality in Phase Transitions with Random Fields”.
- [27] A. Aharony, A.B. Harris and S. Wiseman, Phys. Rev. Lett. **81** (1998) 252
“Critical Disordered Systems with Constraints and the Inequality $\nu > 2/d$ ”.
- [28] M. Aizenman and J. Wehr, Phys. Rev. Lett. **62**, 2503 (1989); errata **64**, 1311 (1990)
“Rounding of 1st-order phase-transitions in systems with quenched disorder”
- [29] Y. Ajiro, T. Wakisaka, H. Itoh, K. Watanabe, H. Satoh, Y. Inagak, T. Asano, M. Mito, K. Takeda, H. Mitamura, and T. Goto,
Physica B **329**, 1004 (2003)
“Random quantum chain system: mixture of $S = 1/2$ antiferromagnetic chains with uniform and alternating couplings”.
- [30] S. Alexander, J. Bernasconi, W. Schneider and R. Orbach Rev. Mod. Phys. 53 (1981) 175
“Excitation dynamics in random one-dimensional systems”.
- [31] E. Altman, Y. Kafri, A. Polkovnikov and G. Refael, cond-mat/0402177
“Phase transition of one dimensional bosons with strong disorder”.
- [32] P.W. Anderson, Phys. Rev. **109**, 1492 (1958)
“Absence of diffusion in certain random lattices”
- [33] J-Ch. Anglès d’Auriac, F. Iglói, M. Preissmann and A. Sebő,
J. Phys. A **35**, 6973-83 (2002)
“Optimal cooperation and submodularity for computing Potts’ partition functions with a large number of states”
J.-Ch. Anglès d’Auriac, in *New Optimization Algorithms in Physics*, ed. A. K. Hartmann and H. Rieger (Wiley-VCH, Berlin 2004).
“Computing the Potts free energy and submodular functions”
- [34] J-Ch. Anglès d’Auriac and F. Iglói Phys. Rev. Lett. 90, 190601 (2003)
“Phase Transition in the 2D Random Potts Model in the Large-q Limit” ;
M. T. Mercaldo, J-Ch. Anglès d’Auriac, and F. Iglói Phys. Rev. E 69, 056112 (2004)
“Disorder-induced rounding of the phase transition in the large- q -state Potts model”

- [35] T. Arakawa, S. Todo and H. Takayama, cond-mat/0410755
“Randomness-driven quantum phase transition in bond-alternating Haldane chain”.
- [36] M. Arlego, W. Brenig, D.C. Cabra, F. Heidrich-Meisner, A. Honecker, and Rossini G,
Phys. Rev. B **70**, 014436 (2004)
“Bond-impurity-induced bound states in disordered spin-1/2 ladders”
- [37] J. Ashkin and E. Teller, Phys. Rev. **64**, 178 (1943)
“Statistics of two-dimensional lattices with four components”
M. Kohmoto, M. den Nijs and L.P. Kadanoff, Phys. Rev. B **24**, 5229 (1981)
“Hamiltonian studies of the d=2 Ashkin-Teller model”
- [38] C. Aslangul, M. Barthelemy, N. Pottier and D. Saint-James, J. Stat. Phys. **59**, 11 (1990)
“Dynamical exponents for one-dimensional random-random directed walks”.
- [39] M. Azuma, M. Takano, R.S. Eccleston, cond-mat/9706170
“Disappearance of the spin gap in a Zn doped 2-leg ladder compound $\text{Sr}(\text{Cu}_{1-x}\text{Zn}_x)_2\text{O}_3$ ”
- [40] L. Balents, J.P. Bouchaud and M. Mézard, J. Phys. I France **6** (1996) 1007
“The large scale energy landscape of randomly pinned objects”.
- [41] J.R. Banavar and A.J. Bray, Phys. Rev B **35** (1987) 8888
“Chaos in spin glasses: A renormalization-group study”.
- [42] A. Barrat, Phys. Rev. E **57**, 3629 (1998)
“Monte Carlo simulations of the violation of the fluctuation-dissipation theorem in domain growth processes”.
- [43] A. Barrat, J. Kurchan, V. Loreto and M. Sellitto, Phys. Rev. Lett. **85** 5034 (2000)
“Edwards Measures for Powders and Glasses”;
A. Barrat, J. Kurchan, V. Loreto and M. Sellitto, Phys. Rev. E **63** 51301 (2001)
“Edwards measures: A thermodynamic construction for dense granular media and glasses”.
- [44] R.J. Baxter, Ann. Phys. (N.Y.) **70**, 193 (1972)
“Partition function of the eight-vertex lattice model”
- [45] R.J. Baxter, J. Phys. C **6**, L445 (1973)
“Potts model at the critical temperature”
- [46] G. Ben-Arous, ICM, Beijing 2002, vol. 3, 3–14, math.PR/0304364
“Aging and spin-glass dynamics”.

- [47] B. Berche, P-E. Berche, F. Iglói and G. Palágyi, J. Phys. A **31**, 5193 (1998)
 “The McCoy-Wu model in the mean-field approximation”
 T. Vojta, J. Phys. A **38**, 10921 (2003)
 “Smearing of the phase transition in Ising systems with planar defects”
- [48] S. Bergkvist, P. Henelius, and A. Rosengren, Phys. Rev. B **66**, 134407 (2002)
 “Ground state of the random-bond spin-1 Heisenberg chain”.
- [49] K. Bernardet, F. Pazmandi and G. Batrouni, Phys. Rev. Lett. **84** (2000) 4477
 “Disorder Averaging and Finite-Size Scaling”.
- [50] L. Berthier, J.L. Barrat and J. Kurchan, Eur. Phys. J. B **11**, 635 (1999)
 “Response function of coarsening systems”.
- [51] E.M. Bertin and J.P. Bouchaud, Phys. Rev. E **67**, 026128 (2003)
 “Sub-diffusion and localization in the one dimensional trap model”.
- [52] E.M. Bertin and J.P. Bouchaud, Phys. Rev. E **67**, 065105(R) (2003)
 “Linear and non linear response in the aging regime of the one-dimensional trap model”.
- [53] E. Bertin, PhD Thesis, University Paris 7 (2003)
 “Dynamique vitreuse : de l’espace des phases à l’espace réel”.
- [54] R. N. Bhatt, in Ref.[10].
 “Quantum Spin Glasses”.
- [55] R. N. Bhatt and P. A. Lee, Phys. Rev. Lett. **48**, 344 (1982)
 “Scaling Studies of Highly Disordered Spin-1/2 Antiferromagnetic Systems”.
- [56] G. Biroli and J. Kurchan, Phys. Rev. E **64**, 016101 (2001)
 “Metastable states in glassy systems”.
- [57] T. Bodineau and G. Giacomin, J. Statist. Phys. **117** (2004) 17 “On the localization transition of random copolymers near selective interfaces”.
- [58] J.P. Bouchaud, A. Comtet, A. Georges and P. Le Doussal, Ann. Phys. **201**, 285 (1990)
 “Classical diffusion of a particle in a one-dimensional random force field”.
- [59] J.P. Bouchaud, J. Phys. I (France) **2** (1992) 1705
 “Weak ergodicity breaking and aging in disordered systems”;
 J.P. Bouchaud and D. Dean, J. Phys. I (France) **5** (1995) 265
 “Aging on Parisi’s tree”.
- [60] B. Boechat, A. Saguia, and M. A. Continentino, Solid State Comm. **98**, 411 (1996)
 “Random spin-1 quantum chains”

- [61] J.-P. Bouchaud and M. Mézard, J. Phys. A 30 (1997) 7997
“Universality classes for extreme-value statistics ”.
- [62] J.P. Bouchaud, L.F. Cugliandolo, J. Kurchan and M. Mézard, in “Spin glasses and random fields” A. P. Young Ed., World Scientific (1997)
“Out of equilibrium dynamics in spin-glasses and other glassy systems”.
- [63] D. Boyanovsky, and J.L. Cardy, Phys. Rev. B **26**, 154 (1982)
“Critical behavior of m-component magnets with correlated impurities”
- [64] M. Bramson, R. Durrett and R. H. Schonmann, Ann. Prob. **19**, 960 (1991)
“The contact process in a random environment”
- [65] A. J. Bray and S. Feng Phys. Rev. B 36, 8456 (1987)
“ Percolation of order in frustrated systems: The dilute J spin glass”.
- [66] A.J. Bray and M. A. Moore, J. Phys. C 17 (1984) L463
“Lower critical dimension of Ising spin glasses : a numerical study”.
- [67] A.J. Bray and M. A. Moore, “Scaling theory of the ordered phase of spin glasses” in Heidelberg Colloquium on glassy dynamics, (1986) Springer Verlag.
- [68] A.J. Bray and M. A. Moore, Phys. Rev. Lett. (1987) 57
“ Chaotic Nature of the Spin-Glass Phase”.
- [69] A.J. Bray, Phys. Rev. Lett. 59, 586 (1987)
“Nature of the Griffiths phase”;
A.J. Bray, Phys. Rev. Lett. 60, 720 (1988)
“Dynamics of dilute magnets above T_c ”.
- [70] A.J. Bray, B. Derrida and C. Godrèche, Europhys. Lett. 27, 175 (1994)
“Nontrivial algebraic decay in a soluble model of coarsening”.
- [71] A.J. Bray and B. Derrida Phys. Rev. E 51, R1633 (1995)
“Exact exponent λ of the autocorrelation function for a soluble model of coarsening”.
- [72] J. Bricmont and A. Kupiainen, Phys. Rev. Lett. 59, 1829 (1987)
“ Lower critical dimension for the random-field Ising model”.
- [73] R. Brout, Phys. Rev. **115**, 824 (1959)
“Statistical mechanical theory of a random ferromagnetic system”
- [74] R.C. Brower, M.R. Furman, and K. Subbarao, Phys. Rev. D **15**, 1756 (1977)
“Quantum spin model for Reggeon field-theory”
- [75] P. W. Brouwer, C. Mudry, B. D. Simons, and A. Altland, Phys. Rev. Lett. **81**, 862 (1998)
“Delocalization in coupled one-dimensional chains”

- [76] P. W. Brouwer, A. Furusaki, I. A. Gruzberg, and C. Mudry, Phys.Rev.Lett. **85**, 1064 (2000)
“Localization and delocalization in dirty superconducting wires”
- [77] P.W. Brouwer, A. Furusaki, and C. Mudry, Phys. Rev. B **67**, 014530 (2003)
“Universality of delocalization in unconventional dirty superconducting wires with broken spin-rotation symmetry”
- [78] T.W. Burkhardt and J.M.J. van Leeuwen, Topics in Current Physics 30, Springer (1982)
“Real Space renormalization”.
- [79] R. Cafiero, A. Gabrielli and M. A. Muñoz, Phys. Rev. E **57**, 5060 (1998)
“Disordered one-dimensional contact process”
- [80] C. Calan, J.M. Luck, T. Nieuwenhuizen and D. Petritis, J. Phys. A 18 (1985) 501
“On the distribution of a random variable occurring in 1D disordered systems”.
- [81] A. Caldeira and A. Leggett, Phys. Rev. Lett. **46**, 211 (1983)
“Influence of Dissipation on Quantum Tunneling in Macroscopic Systems”;
A. Caldeira and A. Leggett, Ann. Phys. **149**, 374 (1983)
”Quantum Tunnelling in a Dissipative System”
- [82] J. Cardy and U. C. Täuber, Phys. Rev. Lett. **77**, 4780 (1996);
“Theory of branching and annihilating random walks”
J. Cardy and U. C. Täuber, J. Stat. Phys. **90**, 1 (1998)
“Field theory of branching and annihilating random walks”
- [83] J.L. Cardy and J.L. Jacobsen, Phys. Rev. Lett. **79**, 4063 (1997)
“Critical behavior of random-bond Potts models”
J.L. Jacobsen and J.L. Cardy, Nucl. Phys. B **515**, 701 (1998)
“Critical behaviour of random-bond Potts models: a transfer matrix study”
- [84] J.L. Cardy, Physica A **263**, 215 (1999)
“Quenched randomness at first-order transitions”
- [85] E. Carlon, C. Chatelain, and B. Berche, Phys. Rev. B **60**, 12974 (1999)
“Critical behavior of the random Potts chain”
- [86] E. Carlon, P. Lajkó, and F. Iglói Phys. Rev. Lett. **87**, 277201 (2001) “
Disorder Induced Cross-Over Effects at Quantum Critical Points”.
- [87] E. Carlon, P. Lajkó, H. Rieger, and F. Iglói, Phys. Rev. B **69**, 144416 (2004)
“Disorder induced phases in higher spin antiferromagnetic Heisenberg chains”

- [88] D. Carpentier and P. Le Doussal Phys. Rev. Lett. 81, 2558 (1998)
“Disordered XY Models and Coulomb Gases: Renormalization via Traveling Waves”.
- [89] D. Carpentier and P. Le Doussal Phys. Rev. E 63, 026110 (2001)
“Glass transition of a particle in a random potential, front selection in nonlinear renormalization group, and entropic phenomena in Liouville and sinh-Gordon models”.
- [90] H. E. Castillo, C. Chamon, E. Fradkin, P. M. Goldbart, C. Mudry Phys. Rev. B 56, 10668 (1997)
“Exact calculation of multifractal exponents of the critical wave function of Dirac fermions in a random magnetic field”.
- [91] H. E. Castillo and P. Le Doussal Phys. Rev. Lett. 86, 4859 (2001)
“Freezing of Dynamical Exponents in Low Dimensional Random Media”.
- [92] A. H. Castro Neto, G. Castilla, and B. Jones, Phys. Rev. Lett. **81**, 3531 (1998)
“Non-fermi liquid behavior and Griffiths phase in f-electron compounds”
M.C. de Andrade, R. Chau, R.P. Dickey, N.R. Dilley, E.J. Freeman, D.A. Gajewski, and M.B. Maple, Phys. Rev. Lett. **81**, 5620 (1998)
“Evidence for a common physical description of non-Fermi-liquid behavior in chemically substituted f-electron systems”.
- [93] C. Chamon, C. Mudry, X.-G. Wen, Phys.Rev.Lett. 77 (1996) 4194
“Gaussian field theories, random Cantor sets and multifractality”.
- [94] Ch. Chatelain and B. Berche, Phys. Rev. Lett. **80**, 1670 (1998)
“Finite-size scaling study of the surface and bulk critical behavior in the random-bond eight-state Potts model”
Ch. Chatelain and B. Berche, Phys. Rev. E **58** R6899 (1998)
“Tests of conformal invariance in randomness-induced second-order phase transitions”
Ch. Chatelain and B. Berche, Phys. Rev. E **60**, 3853 (1999)
“Magnetic critical behavior of two-dimensional random-bond Potts ferromagnets in confined geometries”
- [95] J. Chave and E. Guitter J. Phys. A 32 (1999) 445
“Statistical and dynamical properties of the discrete Sinai model at finite times”.
- [96] J. T. Chayes, L. Chayes, D.S. Fisher and T. Spencer Phys. Rev. Lett. 57, 2999 (1986)
“Finite-Size Scaling and Correlation Lengths for Disordered Systems”.
- [97] D. Cheliotis, math.PR/0310306
“Diffusion in random environment and the renewal theorem ”.

- [98] A. Compte and J.P. Bouchaud, J. Phys. A 31 (1998) 6113
“Localization in one-dimensional random random walks”.
- [99] A. Comtet, C. Monthus and M. Yor, J. Appl. Prob. **35** (1998) 255 “Exponential functionals of Brownian motion and disordered systems ”.
- [100] J. Cook, B. Derrida, J. Stat. Phys. 57, 89 (1989)
“Polymers on disordered hierarchical lattices: a non-linear combination of random variables”
- [101] M.C. Cross and D.S. Fisher, Phys. Rev. B**19**, 402 (1979)
“New theory of the spin-Peierls transition with special relevance to the experiments on TTFCuBDT”
- [102] L. F. Cugliandolo and J. Kurchan Phys. Rev. Lett. 71, 173 (1993)
“ Analytical solution of the off-equilibrium dynamics of a long-range spin-glass model” ;
L. F. Cugliandolo and J. Kurchan J. Phys. A: Math. Gen. 27 (1994) 5749
“On the out-of-equilibrium relaxation of the Sherrington-Kirkpatrick model”.
- [103] L. F. Cugliandolo, J. Kurchan and L. Peliti, Phys. Rev. E 55 (1997) 3898
“Energy flow, partial equilibration, and effective temperatures in systems with slow dynamics ”.
- [104] L.F. Cugliandolo, G.S. Lozano, H. Lozza, cond-mat/0412638
“Static properties of the dissipative random quantum Ising ferromagnetic chain”
- [105] A. Daerr and S. Douady, Nature **399**, 241 (1999)
“Two types of avalanche behaviour in granular media”
H. Hinrichsen, A. Jimenez-Dalmaroni, Y. Rozov, E Domany, Phys. Rev. Lett 83, 4999 (1999)
“Flowing sand: A physical realization of directed percolation”
- [106] E. Dagotto, J. Riera and D.J. Scalapino, Phys. Rev. B **45**, 5744 (1992)
“Superconductivity in ladders and coupled planes”
- [107] E. Dagotto, and T.M. Rice, Science, **271**, 618 (1996)
“Surprises on the way from one- to two-dimensional quantum magnets: The ladder materials”
- [108] K. Damle, O. Motrunich, D.A. Huse, Phys. Rev. Lett. 84, 3434 (2000)
“ Dynamics and Transport in Random Antiferromagnetic Spin Chains” .
- [109] K. Damle, Phys. Rev. B 66, 104425 (2002)
“Griffiths effects in random Heisenberg antiferromagnetic S=1 chains”.
- [110] K. Damle and D. A. Huse Phys. Rev. Lett. 89, 277203 (2002)
“ Permutation-Symmetric Multicritical Points in Random Antiferromagnetic Spin Chains”.

- [111] R.A. Da Silveira and J.P. Bouchaud, cond-mat/0310706
“Temperature and disorder chaos in low dimensional directed paths”.
- [112] D. S. Dean and S. N. Majumdar, Phys. Rev. E 64, 046121 (2001)
“Extreme-value statistics of hierarchically correlated variables deviation from Gumbel statistics and anomalous persistence”.
S. N. Majumdar, P.L. Krapivsky, Physica A 318, 161 (2003)
“Extreme Value Statistics and Traveling Fronts: Various Applications”.
- [113] O. Deloubriere, H.J. Hilhorst and U. Tauber Phys. Rev. Lett. 89 (2002) 250601
“ Multi-species pair annihilation reactions”;
H.J. Hilhorst, O. Deloubriere, M.J. Washenberger, U.C. Tauber, cond-mat/0403246
“Segregation in diffusion-limited multispecies pair annihilation”.
- [114] A. Dembo, A. Guionnet and O. Zeitouni, math.PR/0105215
“ Aging properties of Sinai’s model of random walk in random environment”
in Lectures Notes of O. Zeitouni for the Saint Flour Summer School 2001, to appear in Lecture Notes in Mathematics, Springer (2004).
- [115] B. Derrida, Phys. Rev. Lett. 45, 79-82 (1980)
“ Random energy model: limit of a family of disordered models”;
B. Derrida, Phys. Rev. B 24, 2613-2626 (1981)
“The random energy model, an exactly solvable model of disordered systems” ;
B. Derrida, G. Toulouse, J. Physique Lett. 46, L223-L228 (1985)
“Sample to sample fluctuations in the random energy model” ;
E. Gardner, B. Derrida, J. Phys. A 22, 1975 (1989)
“The probability distribution of the partition function of the random energy model”.
- [116] B. Derrida, Y. Pomeau, Phys. Rev. Lett. 48 (1982) 627
“Classical diffusion on a random chain” ;
B. Derrida, J. Stat. Phys. 31 (1983) 433
“Velocity and diffusion constant of a periodic one-dimensional hopping model”.
- [117] B. Derrida and H.J. Hilhorst, J. Phys. A 16 (1983) 2641
“Singular behaviour of certain infinite products of random 2×2 matrices”.
- [118] B. Derrida, Physics Reports **103**, 29 (1984)
“Can disorder induce several phase transitions?”
- [119] B. Derrida and E. Gardner J. Phys. A 17 (1984) 3223
“ Renormalisation group study of a disordered model”.
- [120] B. Derrida and R.B. Griffiths, Europhys. Lett. 8, 111 (1989) “ Directed polymers on disordered hierarchical lattices ”.

- [121] B. Derrida, C. Godrèche and I. Yekutieli, *Europhys. Lett.* **12**, L385 (1990)
 “Stable distributions of growing and coalescing droplets” ;
 B. Derrida, C. Godrèche and I. Yekutieli, *Phys. Rev. A* **44**, 6241 (1991)
 “Scale-invariant regime in the one-dimensional models of growing and coalescing droplets” ;
 I. Yekutieli, C. Godrèche and B. Derrida, *Physica A* **185**, 240 (1992)
 “One-dimensional models of growing and coalescing droplets”.
- [122] B. Derrida, V. Hakim, J. Vannimenus, *J. Stat. Phys.* **66**, 1189 (1992)
 “Effect of disorder on two dimensional wetting”.
- [123] B. Derrida and R. Zeitak, *Phys. Rev. E* **54**, 2513 (1996)
 “Distribution of domain sizes in the zero temperature Glauber dynamics of the 1d Potts model”.
- [124] B. Derrida, *Physica D* **107**, 186 (1997)
 “From random walks to spin-glasses”.
- [125] G. De Smedt, C. Godrèche and J.M. Luck, *Eur. Phys. J. B* **27**, 363 (2002)
 “Jamming, freezing and metastability in one-dimensional spin systems ” ;
 G. De Smedt, C. Godrèche and J.M. Luck, *Eur. Phys. J. B* **32**, 215-225 (2003)
 “Metastable states of Ising chain with Kawasaki dynamics”.
- [126] A. Dhar and A.P. Young, *Phys. Rev. B* **68**, 134441 (2003)
 “Ensemble dependence in the random transverse-field Ising chain ”.
- [127] B. Drossel and M. Kardar *Phys. Rev. E* **52**, 4841-4852 (1995)
 “Scaling of energy barriers for flux lines and other random systems” ;
 L. V. Mikheev, B. Drossel, and M. Kardar *Phys. Rev. Lett.* **75**, 1170-1173 (1995)
 “Energy Barriers to Motion of Flux Lines in Random Media”.
- [128] J. M. Dumont, in *Number Theory and Physics*, Springer Proceedings in Physics, Vol. 47, edited by J. M. Luck, P. Moussa, and M. Waldschmidt (Springer, Berlin, 1990), p. 185.
- [129] F. Dyson, *Phys. Rev.* **92**, 1331 (1953)
 “The Dynamics of a Disordered Linear Chain”.
- [130] K.B. Efetov, “Supersymmetry in Disorder and chaos”, Cambridge University Press (1997).
- [131] A. Engel, *Nucl. Phys. B* **410**, 617 (1993)
 “Replica Symmetry breaking in zero dimension”.
- [132] M. R. Evans, *Europhys. Lett.* **36**, 13 (1996)
 “Bose-Einstein condensation in disordered exclusion models and relation to traffic flow”
 M. R. Evans, *J. Phys. A* **30**, 5669 (1997)

- “Exact steady states of disordered hopping particle models with parallel and ordered sequential dynamics”
- [133] M. Fabrizio, and R. Melin, Phys. Rev. Lett. **78**, 3382 (1997)
 “Coexistence of antiferromagnetism and dimerization in a disordered spin-Peierls model: Exact results”
 M. Fabrizio, and R. Melin, Phys. Rev. B. **56**, 5996 (1997)
 “Enhanced magnetic fluctuations in doped spin-Peierls systems: A single-chain model analysis”
 M. Fabrizio, and R. Melin, J. Phys. Condens. Matter **9**, 10429 (1997)
 “A single chain analysis of doped quasi one dimensional spin 1 compounds: paramagnetic versus spin 1/2 doping”
 M. Fabrizio, R. Melin, and J. Souletie, Eur. Phys. J. B. **10**, 607 (1999)
 “Phase diagram of doped spin-Peierls systems”
- [134] M.V. Feigelman and V.M. Vinokur, J. Phys. (France) **49** (1988) 1731
 “On the stochastic transport in disordered systems”.
- [135] S. Fielding and P. Sollich Phys. Rev. Lett. **88**, 050603 (2002)
 “Observable Dependence of Fluctuation-Dissipation Relations and Effective Temperatures ”;
 P. Sollich, J. Phys. A **36**, 10807 (2003)
 “Fluctuation-dissipation relations in trap models” ;
 F. Ritort, J. Phys. A **36**, 10791 (2003)
 “ Universal dependence of the fluctuation-dissipation ratio on the transition rates in trap models”.
- [136] D. S. Fisher, Phys. Rev. Lett. **56**, 1964 (1986)
 “ Interface Fluctuations in Disordered Systems: 5- epsilon Expansion and Failure of Dimensional Reduction”.
- [137] D.S. Fisher and D.A. Huse, Phys. Rev. Lett. **56**, 1601 (1986)
 “Ordered Phase of Short-Range Ising Spin-Glasses” ;
 D. S. Fisher and D. A. Huse, Phys. Rev. B **38**, 386 (1988)
 “Equilibrium behavior of the spin-glass ordered phase” ;
 D. S. Fisher and D. A. Huse, Phys. Rev. B **38**, 373 (1988)
 “Nonequilibrium dynamics of spin glasses”.
- [138] D. S. Fisher Phys. Rev. Lett. **69**, 534-537 (1992)
 “Random transverse field Ising spin chains” ;
 D. S. Fisher Phys. Rev. B **51**, 6411-6461 (1995)
 “Critical behavior of random transverse-field Ising spin chains”.
- [139] D. S. Fisher Phys. Rev. B **50**, 3799 (1994)
 “Random antiferromagnetic quantum spin chains”.
- [140] D.S. Fisher and A. P. Young, Phys. Rev. B **58**, 9131 (1998)
 “Distributions of gaps and end-to-end correlations in random transverse-field Ising spin chains”.

- [141] D. Fisher, P. Le Doussal and C. Monthus, Phys. Rev. Lett. 80 (1998) 3539
“Random Walks, Reaction-Diffusion, and Nonequilibrium Dynamics of Spin Chains in One-dimensional Random Environments”.
- [142] D. S. Fisher, P. Le Doussal and C. Monthus, Phys. Rev. E 59 (1999) 4795
“Random Walkers in One-dimensional Random Environments : Exact Renormalization Group Analysis”.
- [143] D.S. Fisher, Physica A 263 (1999) 222
“Phase transitions and singularities in random quantum systems”.
- [144] D. S. Fisher, P. Le Doussal and C. Monthus, Phys. Rev. E 64 (2001) 66107
“Nonequilibrium Dynamics of Random Field Ising Spin Chains : exact results via real space RG”.
- [145] M.E. Fisher, Rep. Progr. Phys. **38**, 615 (1967)
“The theory of equilibrium critical phenomena”.
- [146] L.R. Fontes, M. Isopi and C. Newman, math.PR/0009098
“Random walks with strongly inhomogeneous rates and singular diffusions : Convergence, localization and aging in one dimension” ;
G. Ben Arous and J. Cerny, math.PR/0210633
“Bouchaud’s model exhibits two aging regimes in dimension one”.
- [147] L. Frachebourg and P. A. Martin, J. Fluid. Mech. 417, 323 (2000)
“Exact statistical properties of the Burgers equation”.
- [148] R. Gade, Nucl. Phys. **B398**, 499 (1993)
“Anderson localization for sublattice models”
- [149] J. Galambos, *The Asymptotic Theory of Extreme Order Statistics* (John Wiley and Sons, New York, 1978).
- [150] T. Garel, D. Huse, S. Leibler et H. Orland, Europhys. Lett. 8, 9 (1989)
“Localization transition of random chains at interfaces”.
- [151] C. Godrèche and J.M. Luck, J. Phys. A 33, 1151 (2000)
“Response of non-equilibrium systems at criticality: Exact results for the Glauber-Ising chain”.
- [152] C. Godrèche and J.M. Luck, J. Phys. A 33, 9141 (2000)
“Response of non-equilibrium systems at criticality: Ferromagnetic models in dimension two and above”.
- [153] A.O. Gogolin, A.A. Nersesyan, M. Tsevlik and L. Yu, Nucl. Phys. B **540**, 705 (1999)
“Zero-modes and thermodynamics of disordered spin-1/2 ladders”
- [154] A.O. Golosov, Sov. Math. Dokl. 28 (1983) 18
“Limiting distributions for random walks in random environments”.

- [155] A.O. Golosov, Comm. Math. Phys. 92 (1984) 491
“Localization of random walks in one-dimensional random environments”.
- [156] A.O. Golosov, Russ. Math. Surv. 41 199
“On limiting distributions for a random walk in a critical one-dimensional random environment”.
- [157] P. Grassberger and A. de la Torre, Ann. Phys. (NY) **122**, 373 (1979)
“Reggeon field-theory (Schlogl 1st model) on a lattice - Monte-Carlo calculations of critical behavior”
- [158] R. B. Griffiths, Phys. Rev. Lett. 23, 17 (1969)
“Nonanalytic Behavior Above the Critical Point in a Random Ising Ferromagnet”.
- [159] P. Groeneboom, Prob. Theo. Rel. Fields 81 (1989) 79
“Brownian motion with a parabolic drift and Airy functions”.
- [160] M.Y. Guo, R.N. Bhatt, and D.A. Huse, Phys. Rev. Lett. **72**, 4137 (1994)
“Quantum critical behavior of a 3-dimensional Ising spin-glass in a transverse magnetic-field”
- [161] F.D.M. Haldane, Phys. Lett. **A93**, 464 (1983)
“Continuum dynamics of the 1d Heisenberg antiferromagnet - Identification with the O(3) non-linear sigma-model”
- [162] K. Hallberg, X.Q.G. Wang, P. Horsch, and A. Moreo, Phys. Rev. Lett. **76**, 4955 (1996). “Critical behavior of the $S = 3/2$ antiferromagnetic Heisenberg chain”
- [163] K. Hamacher, J. Stolze, and W. Wenzel, Phys. Rev. Lett. **89**, 127202 (2002)
“Disorder induced quantum phase transition in random-exchange spin-1/2 chains”
- [164] T. E. Harris, Ann. Prob. **2**, 969 (1974)
“Contact interactions on a lattice”
- [165] A. B. Harris, J. Phys. C **7**, 1671 (1974)
“Effect of random defects on the critical behaviour of Ising models”.
- [166] P. Henelius, and S.M. Girvin, Phys. Rev. **B57**, 11457 (1998)
“Numerical study of the random dimerized XX spin-1/2 chain”
- [167] J. Hermisson, U. Grimm, and M. Baake, J. Phys. **A30**, 7315 (1997)
“Aperiodic Ising quantum chains”
J. Hermisson, and U. Grimm, Phys. Rev. **B57**, R673 (1998)
“Surface properties of aperiodic Ising quantum chains”
- [168] J. Hermisson, J. Phys. **A33**, 57 (2000)
“Aperiodic and correlated disorder in XY chains: exact results”

- [169] K. Hida, Phys. Rev. Lett. **83**, 3297 (1999)
“DMRG study of the Haldane phase in random 1D antiferromagnets” .
- [170] K. Hida, J. Phys. Soc. Jp. **72**, 2627 (2003)
“Ground state and magnetization process of the mixture of bond-alternating and uniform $S=1/2$ antiferromagnetic Heisenberg chains”
- [171] K. Hida, Phys. Rev. Lett. **93**, 037205 (2004)
“New Universality Class in the $S=1/2$ Fibonacci Heisenberg Chains”
K. Hida, J. Phys. Soc. Jpn. **73** 2296-2304 (2004)
“Real Space Renormalization Group Study of the $S=1/2$ XXZ Chains with Fibonacci Exchange Modulation”
- [172] T. Hikihara, A. Furusaki, and M. Sigrist, Phys. Rev. **B60**, 12116 (1999)
“Numerical renormalization-group study of spin correlations in one-dimensional random spin chains”
- [173] H. Hinrichsen, Phys. Rev. **E55**, 219 (1997)
“Stochastic lattice models with several absorbing states”
- [174] H. Hinrichsen, Braz. J. Phys. **30**, 69-82 (2000)
“On possible experimental realizations of directed percolation”
- [175] J. E. Hirsch and J. V. Jose J. Phys. C **13** (1980) L53
“Low-temperature thermodynamic properties of a random Heisenberg antiferromagnetic chain ($S=1/2$)” ;
J. E. Hirsch and J. V. José Phys. Rev. B **22**, 5339 (1980)
“Singular thermodynamic properties in random magnetic chains” ;
J.E. Hirsch Phys. Rev. B **22**, 5355 (1980)
“Low-temperature thermodynamic properties of a random anisotropic antiferromagnetic chain”.
- [176] J. Hooyberghs, PhD thesis - Limburgs Universitair Centrum (2002)
“A renormalization group study of one-dimensional contact processes”
- [177] J. Hooyberghs, F. Iglói, and C. Vanderzande Phys. Rev. Lett. **90**, 100601 (2003)
“ Strong Disorder Fixed Point in Absorbing-State Phase Transitions” ;
J. Hooyberghs, F. Iglói, and C. Vanderzande, Phys. Rev. E **69**, 066140 (2004)
“Absorbing state phase transitions with quenched disorder”.
- [178] J.A. Hoyos and E. Miranda, Phys. Rev. B **69**, 214411 (2004)
“Phase diagrams and universality classes of random antiferromagnetic spin ladders”
- [179] J. A. Hoyos, and E. Miranda, Phys. Rev. B **70**, 180401 (2004)
“Random antiferromagnetic $SU(N)$ spin chains”

- [180] Y. Hu, Z. Shi and M. Yor, Trans. Am. Math. Soc. 351 3915 (1999)
“Rates of convergence of diffusions with drifted Brownian potentials ”
- [181] Y. Hu, Stoch. Proc. and Appl. 86 (2000) 81
“Tightness of localization and return time in random environment ”.
- [182] D. Huse, Phys. Rev. B **40**, 304 (1989)
“Remanent magnetization decay at the spin-glass critical point: A new dynamic critical exponent for nonequilibrium autocorrelations”
- [183] D.A. Huse, Phys. Rep. 348 (2001) 159
“Renormalizing systems with strong quenched randomness”.
- [184] T. Hwa, E. Marinari, K. Sneppen and L.H. Tang, cond-mat/0302603
“Localization of Denaturation Bubbles in Random DNA Sequences”.
- [185] R. A. Hyman, K. Yang, R. N. Bhatt, and S. M. Girvin Phys. Rev. Lett. 76, 839 (1996)
“Random Bonds and Topological Stability in Gapped Quantum Spin Chains”.
- [186] R. A. Hyman and K. Yang, Phys. Rev. Lett. 78, 1783 (1997)
“Impurity Driven Phase Transition in the Antiferromagnetic Spin-1 Chain”.
- [187] F. Iglói and L. Turban, Europhys. Lett. **27**, 91 (1994)
“Relevant Aperiodic Modulation in the Two-Dimensional Ising Model”
- [188] F. Iglói, and L. Turban, Phys. Rev. Lett **77**, 1206 (1996)
“Common trends in the critical behavior of the ising and directed walk models”
- [189] F. Iglói, L. Turban, D. Karevski and F. Szalma, Phys. Rev. B**56**, 11031 (1997)
“Exact renormalization group study of aperiodic ising quantum chains and directed walks”
- [190] F. Iglói, and H. Rieger, Phys. Rev. Lett. **78**, 2473 (1997)
“Density profiles in random quantum spin chains”
- [191] F. Iglói and H. Rieger. Phys. Rev. B **57** (1998) 11404
“Random transverse Ising spin chain and random walks”.
- [192] F. Iglói, D. Karevski and H. Rieger, European Physical Journal B**5**, 613 (1998)
“Comparative study of the critical behavior in one-dimensional random and aperiodic environments”
F. Iglói, D. Karevski and H. Rieger, European Physical Journal B**1**, 513 (1998)
“Random and aperiodic quantum spin chains: A comparative study”

- [193] F. Iglói and H. Rieger, Phys. Rev. E **58**, 4238 (1998)
“Anomalous diffusion in disordered media and random quantum spin chains”
- [194] F. Iglói, L. Turban and H. Rieger, Phys. Rev. E **59**, 1465 (1999)
“Anomalous diffusion in aperiodic environments”
- [195] F. Iglói, R. Juhász and H. Rieger, Phys. Rev. B **59**, 11308 (1999)
“Griffiths-McCoy singularities in the Random Transverse-Field Ising Spin Chain”
- [196] F. Iglói, R. Juhász and H. Rieger, Phys. Rev. B **61**, 11552-115568 (2000)
“Random antiferromagnetic quantum spin chains: Exact results from scaling of rare regions”
H. Rieger, R. Juhász and F. Iglói, Eur. Phys. J. B **13**, 409-412 (2000)
“Critical exponents of random XX and XY chains: Exact results via random walks”
- [197] F. Iglói, R. Juhász, and P. Lajkó Phys. Rev. Lett. **86**, 1343 (2001)
“Griffiths-McCoy Singularities in Random Quantum Spin Chains: Exact Results through Renormalization”.
- [198] F. Iglói Phys. Rev. B **65**, 064416 (2002)
“Exact renormalization of the random transverse-field Ising spin chain in the strongly ordered and strongly disordered Griffiths phases”.
- [199] J.Z. Imbrie, Phys. Rev. Lett. **53**, 1747 (1984) “Lower Critical Dimension of the Random-Field Ising Model”.
- [200] Y. Imry and S. K. Ma, Phys. Rev. Lett. **35**, 1399 (1975)
“Random-Field Instability of the Ordered State of Continuous Symmetry”.
- [201] Y. Imry, J. Stat. Phys. **34** 849 (1984)
“Random external fields”.
- [202] J.L. Jacobsen and M. Picco, Phys. Rev. E **61**, R13 (2000)
Large-q asymptotics of the random-bond Potts model
- [203] H.K. Janssen, Phys. Rev. E **55**, 6253 (1997)
“Renormalized field theory of the Gribov process with quenched disorder”
- [204] C. Jayaprakash, E. K. Riedel and M. Wortis, Phys. Rev. B **18**, 2244 (1978)
“Critical and thermodynamic properties of the randomly dilute Ising model”.
- [205] J. Jose, L. Kadanoff, S. Kirkpatrick, and D. R. Nelson, Phys. Rev. B **16**, 1217 (1977)
“Renormalization, vortices, and symmetry-breaking perturbations in the two-dimensional planar model”
S. Elitzur, R. Pearson, and J. Shigemitsu, Phys. Rev. D **19**, 3698 (1979)
“Phase structure of discrete Abelian spin and gauge systems”

- [206] A. Joshi and K. Yang, Phys. Rev. B **67**, 174403 (2003)
“Bond-randomness-induced Neel order in weakly coupled antiferromagnetic spin chains”
- [207] R. Juhász, H. Rieger and F. Iglói, Phys. Rev. E **64**, 056122 (2001)
“The random-bond Potts model in the large- q limit”
- [208] R. Juhász and F. Iglói Phys. Rev. E **66**, 056113 (2002)
“Percolation in a random environment”
- [209] R. Juhász, L. Santen and F. Iglói, Phys. Rev. Lett. cond-mat/0404575
“Partially asymmetric exclusion models with quenched disorder”.
- [210] I. Junier and J. Kurchan, J. Phys. A: Math. Gen., **37**, 3945 (2004)
“Microscopic realizations of the trap model”.
- [211] L.P. Kadanoff, Ann. Phys. **100** (1976) 743
“Notes on Migdal’s recursion formulas”.
- [212] D. Karevski, R. Juhász, L. Turban and F. Iglói, Phys. Rev. B **60**, 4195 (1999)
“Transverse-field Ising spin chain with inhomogeneous disorder”
- [213] D. Karevski, Y-C. Lin, H. Rieger, N. Kawashima and F. Iglói, Eur. Phys. J. B **20**, 267-276 (2001)
“Random quantum magnets with broad disorder distribution”
- [214] P.W. Kasteleyn and C.M. Fortuin, J. Phys. Soc. Jp. **26**, (Suppl) 11 (1969)
- [215] K. Kato, S. Todo, K. Harada, N. Kawashima, S. Miyashita, and H. Takayama, Phys. Rev. Lett. **84**, 4204 (2000)
“Quantum phase transition of the randomly diluted Heisenberg antiferromagnet on a square lattice”
- [216] M. Kaufman and R. B. Griffiths, Phys. Rev. B **24**, 496(1981)
“Exactly soluble Ising models on hierarchical lattices” ;
R. B. Griffiths and M. Kaufman, Phys. Rev. B **26**, 5022(1982)
“Spin systems on hierarchical lattices : Introduction and thermodynamic limit”.
- [217] H. Kesten, Acta Math. **131** (1973) 207
“Random difference equations and renewal theory for products of random matrices”.
- [218] H. Kesten, M. Koslov and F. Spitzer, Compositio Math. **30** (1975) 145
“A limit law for random walk in a random environment”.
- [219] H. Kesten, Physica **138 A** (1986) 299
“The limit distribution of Sinai’s random walk in random environment”.

- [220] E.H. Kim, G. Fáth, J. Sólyom, and D. Scalapino, Phys. Rev. B **62**, 14965 (2000)
“Phase transitions between topologically distinct gapped phases in isotropic spin ladders”
- [221] W. Kinzel and E. Domany Phys. Rev. B **23**, 3421 (1981)
“Critical properties of random Potts models”.
- [222] J. Kisker and A.P. Young, Phys. Rev. B **58**, 14397 (1998)
“Dynamical critical properties of the random transverse-field Ising spin chain”
- [223] I. Kogan, C. Mudry, A. M. Tsvelik, Phys.Rev.Lett. **77** (1996) 707
“The Liouville Theory as a Model for Prelocalized States in Disordered Conductors”.
- [224] J.B. Kogut, Rev. Mod. Phys. **51**, 659 (1979)
“Introduction to lattice gauge-theory and spin systems”
- [225] J. Krug and P. A. Ferrari, J. Phys. A **29**, L465 (1996)
Phase transitions in driven diffusive systems with random rates”
- [226] J. Kurchan, cond-mat/0209399
“Supersymmetry, replica and dynamic treatments of disordered systems: a parallel presentation”.
- [227] N. Laflorencie, and H. Rieger, Phys. Rev. Lett. **91**, 229701 (2003)
Comment on ”Disorder induced quantum phase transition in random-exchange spin-1/2 chains”
- [228] N. Laflorencie, and H. Rieger, Eur. Phys. J. B **40**, 201 (2004)
“Scaling of the spin stiffness in random spin-1/2 chains : Crossover from pure-metallic behaviour to random singlet-localized regime”
- [229] N. Laflorencie, and D. Poilblanc, cond-mat/0502369
“Confinement and critical regime in doped frustrated quasi-one dimensional magnets”
- [230] N. Laflorencie, A. Lauechli, H. Rieger, and S. Wessel, (unpublished)
- [231] P. Lajkó and F. Iglói, Phys. Rev. E **61**, 147-152 (2000)
“Correlation length - exponent relation for the two-dimensional random Ising model”
- [232] P. Le Doussal and C. Monthus, Phys. Rev. E **60** (1999) 1212
“Reaction Diffusion models in one dimension with disorder”.
- [233] P. Le Doussal and C. Monthus, Physica A **317** (2003) 140
“Exact solutions for the statistics of extrema of some random 1D landscapes, Application to the equilibrium and the dynamics of the toy model.”

- [234] P. Le Doussal and K. J. Wiese, Phys. Rev. Lett. 89, 125702 (2002)
“Functional Renormalization Group at Large N for Disordered Systems”.
- [235] E. Lieb, T. Schultz and D. Mattis, Ann. Phys. (N.Y.) **16**, 407 (1961)
“Two soluble models of an antiferromagnetic chain”
S. Katsura, Phys. Rev. **127**, 1508 (1962)
“Statistical mechanics of the anisotropic linear Heisenberg model” P. Pfeuty, Ann. Phys. (Paris) **57**, 79 (1970)
“The one-dimensional Ising model with a transverse field”
- [236] I.M. Lifshitz, Adv. Phys. 13 (1964) 483
“The energy spectrum of disordered systems ” ;
I.M. Lifshitz, Sov. Phys. Usp. 7 (1965) 549
“Energy spectrum and quantum states of disordered condensed systems”.
- [237] I.M. Lifshitz, S.A. Gredeskul and L.A. Pastur, John Wiley and Sons (1987)
“Introduction to the theory of disordered systems”.
- [238] Y.-C. Lin, N. Kawashima, F. Iglói and H. Rieger, Progress in Theor. Phys. (Suppl.) **138**, 479 (2000)
“Numerical renormalization group study of random transverse Ising models in one and two space dimensions”
- [239] Y.-C. Lin, R. Mélin, H. Rieger, and F. Iglói Phys. Rev. B 68, 024424 (2003) “Low-energy fixed points of random Heisenberg models”.
- [240] Y.-C. Lin, H. Rieger and F. Iglói, J. Phys. Soc. Jp. **73**, 1602 (2004)
“Antiferromagnetic spin chains with bond alternation and quenched disorder”
- [241] Y.-C. Lin, H. Rieger and F. Iglói, (unpublished)
“Effects of bond randomness on a double-layer $S = 1/2$ Heisenberg antiferromagnet with random dimer dilution”
- [242] D. K. Lubensky and D. R. Nelson Phys. Rev. Lett. 85 (2000) 1572
“Pulling Pinned Polymers and Unzipping DNA” ;
D. K. Lubensky and D. R. Nelson Phys. Rev. E 65, 031917 (2002)
“Single molecule statistics and the polynucleotide unzipping transition” ;
D. R. Nelson, cond-mat/0309559
“Statistical Physics of Unzipping DNA” ;
Y. Kafri, D. K. Lubensky, D. R. Nelson, cond-mat/0310455
“Dynamics of Molecular Motors and Polymer Translocation with Sequence Heterogeneity”.
- [243] J. M. Luck, Nucl. Phys. B**225**, 169 (1983)
“Diffusion in a random medium: A renormalization group approach”
D.S. Fisher, Phys. Rev. A**30**, 960 (1984)
“Random-walks in random-environments”

- [244] J.M. Luck, J. Stat. Phys. **72**, 417 (1993)
 “Critical-behavior of the aperiodic quantum Ising chain in a transverse magnetic-field”
 J.M. Luck, Europhys. Lett. **24**, 359 (1993)
 “A classification of critical phenomena on quasi-crystals and other periodic structures”
- [245] J. M. Luck, in *Fundamental Problems in Statistical Mechanics VIII*, edited by H. van Beijeren and M. H. Ernst (Elsevier, Amsterdam, 1994), p. 127;
 U. Grimm and M. Baake, in *The Mathematics of Aperiodic Order*, edited by R.V. Moody (Kluwer, Dordrecht, 1997), p. 199.
- [246] A. Luther and I. Peschel, Phys. Rev. **B12**, 3908 (1975)
 “Calculation of critical exponents in 2 dimensions from quantum field-theory in one dimension”
- [247] J. Machta, J. Phys. A **18** (1985) L531
 “Random walks on site disordered lattices”.
- [248] S.-K. Ma, C. Dasgupta, and C.-k. Hu, Phys. Rev. Lett. **43**, 1434 (1979)
 “Random Antiferromagnetic Chain”;
 C. Dasgupta and S.-K. Ma Phys. Rev. B **22**, 1305 (1980)
 “Low-temperature properties of the random Heisenberg antiferromagnetic chain”.
- [249] S. N. Majumdar and A. J. Bray, Phys. Rev. Lett. **81**, 2626 (1998)
 “Persistence with Partial Survival”.
- [250] M.A. Martin-Delgado, J. Dukelsky and G. Sierra, Phys. Lett. A **250**, 431 (1998)
 “Phase diagram of the 2-Leg Heisenberg ladder with alternating dimerization”
 N. Flocke, Phys. Rev. B **56**, 13673 (1997)
 “Exact diagonalization study on spin-1/2 ladders as a function of two coupling parameters using the symmetric group approach”
- [251] W.L. Mc Millan, J. Phys. C **17** (1984) 3179
 “Scaling theory of Ising spin glasses”
- [252] B. M. McCoy and T. T. Wu Phys. Rev. **176**, 631 (1968)
 “Theory of a Two-Dimensional Ising Model with Random Impurities I : Thermodynamics” ;
 B. M. McCoy and T. T. Wu Phys. Rev. **188**, 982 (1969)
 “Theory of a Two-Dimensional Ising Model with Random Impurities II : Spin Correlation Functions” ;
 B. M. McCoy Phys. Rev. **188**, 1014 (1969)
 “Theory of a Two-Dimensional Ising Model with Random Impurities III : Boundary Effects” ;
 B. M. McCoy Phys. Rev. B **2**, 2795 (1970)

- “Theory of a Two-Dimensional Ising Model with Random Impurities IV : Generalizations”.
- [253] S.R. McKay, A.N. Berker and S. Kirkpatrick, Phys. Rev. Lett. 48 (1982) 767
“Spin-Glass Behavior in Frustrated Ising Models with Chaotic Renormalization-Group Trajectories”.
 - [254] R.H. McKenzie, Phys. Rev. Lett. **77**, 4804 (1996)
“Exact results for quantum phase transitions in random XY spin chains”
 - [255] R. Mélin, Eur. Phys. J. B**16**, 261 (2000)
“Antiferromagnetism in a doped spin-Peierls model: Classical and quantum behaviors”
 - [256] R. Mélin, Y.-C. Lin, P. Lajkó, H. Rieger, and F. Iglói, Phys. Rev. B 65, 104415 (2002)
“Strongly disordered spin ladders”.
 - [257] R. Mélin, B. Douçot, and F. Iglói, cond-mat/0503269 ”Strong disorder renormalization group on fractal lattices: Heisenberg models and magnetoresistive effects in tight binding models”.
 - [258] M. T. Mercaldo, J-Ch. Anglès d’Auriac, and F. Iglói, cond-mat/0502035
“Disorder driven phase transitions of the large q -state Potts model in $3d$ ”
 - [259] M. Mézard and G. Parisi, J. Phys. I 2, 2231 (1992)
“Manifolds in random media : two extreme cases”.
 - [260] A.A. Migdal, Sov Phys. JETP 42 (1976) 743
“Phase transitions in gauge and spin-lattice systems”.
 - [261] T. Miyazaki, M. Troyer, M. Ogata, K. Ueda and D. Yoshioka, J. Phys. Soc. Jpn. **66**, 2580 (1997)
“Susceptibilities of $\text{Sr}(\text{Cu}_{1-x}\text{Zn}_x)_2\text{O}_3$ studied by quantum Monte Carlo simulation”
 - [262] C. Monthus and A. Comtet, J. Phys. I (France) 4 (1994) 635
“On the flux distribution in a one dimensional disordered system”.
 - [263] C. Monthus, O. Golinelli and Th. Jolicoeur, Phys. Rev. Lett. 79 (1997) 3254
“Percolation transition in the random antiferromagnetic spin-1 chain”;
C. Monthus, O. Golinelli and Th. Jolicoeur, Phys. Rev. B 58 (1998) 805
“Phases of random antiferromagnetic spin-1 chains”.
 - [264] C. Monthus, Eur. Phys. J. B 13 (2000) 111
“On the localization of random heteropolymers at the interface between two selective solvents”.

- [265] C. Monthus and P. Le Doussal, Phys. Rev. E 65 (2002) 66129
“Localization of thermal packets and metastable states in the Sinai model.”
- [266] C. Monthus and P. Le Doussal, Physica A 334 (2004) 78
“Energy dynamics in the Sinai model.”
- [267] C. Monthus, Phys. Rev. E 67 (2003) 046109
“Localization properties of the anomalous diffusion phase in the directed trap model and in the Sinai diffusion with bias.”
- [268] C. Monthus, Phys. Rev. E 68 (2003) 036114
“Anomalous diffusion, Localization, Aging and Sub-aging effects in trap models at very low temperature”.
- [269] C. Monthus, J. Phys. A 36 (2003) 11605
“On a non-linear Fluctuation Theorem for the aging dynamics of disordered trap models ”.
- [270] C. Monthus, Phys. Rev. E 69, 026103 (2004)
“Non-linear Response of the trap model in the aging regime: Exact results in the strong disorder limit”.
- [271] C. Monthus, Phys. Rev. B 69, 054431 (2004)
“Finite-size scaling properties of random transverse-field Ising chains : comparison between canonical and microcanonical ensembles for the disorder ”.
- [272] C. Monthus and P. Le Doussal, Eur. Phys. J. B 41, 535 (2004)
“Low-temperature properties of some disordered systems from the statistical properties of nearly degenerate two-level excitations”.
- [273] C. Monthus and T. Garel, cond-mat/0411191
“Spin-glass chain in a magnetic field : influence of the disorder distribution on ground state properties and low-energy excitations”.
- [274] M. A. Moore, H. Bokil, B. Drossel Phys. Rev. Lett. 81 (1998) 4252
“ Evidence for the droplet/scaling picture of spin glasses”;
H. Bokil, B. Drossel, and M. Moore, Phys. Rev. B 62, 946 (2000)
“ The influence of critical behavior on the spin glass phase”;
B. Drossel, H. Bokil, M.A. Moore, A.J. Bray, Eur. Phys. J. B 13, 369 (2000)
“ Link Overlap and Finite Size Effects in the 3D Ising Spin Glass” ;
B. Drossel and M.A. Moore, Eur. Phys. J. B 21, 589 (2001)
“ The +/- J Ising spin glass in Migdal-Kadanoff approximation”;
T. Aspelmeier, A. J. Bray, M. A. Moore Phys. Rev. Lett. 89, 197202 (2002)
“ Why temperature chaos in spin glasses is hard to observe”.
- [275] A. G. Moreira and R. Dickman, Phys. Rev. E 54, R3090 (1996)
“Critical dynamics of the contact process with quenched disorder”
R. Dickman and A.G. Moreira, Phys. Rev. E 57, 1263 (1998)
“Violation of scaling in the contact process with quenched disorder”

- [276] O. Motrunich, S.-C. Mau, D. A. Huse, and D. S. Fisher Phys. Rev. B **61**, 1160 (2000)
“Infinite-randomness quantum Ising critical fixed points”.
- [277] O. Motrunich, K. Damle and D.A. Huse, Phys. Rev. B **63** 134424 (2001)
“Dynamics and transport in random quantum systems governed by strong-randomness fixed points”.
- [278] O. Motrunich, K. Damle, and D. A. Huse, Phys. Rev. B **63**, 224204 (2001)
“Griffiths effects and quantum critical points in dirty superconductors without spin-rotation invariance: One-dimensional examples”
- [279] O. Motrunich, K. Damle, and D. A. Huse, Phys. Rev. B **65**, 064206 (2002)
“Particle-hole symmetric localization in two dimensions”
- [280] C. Mudry, S. Ryu, and A. Furusaki, Phys. Rev. B **67**, 064202 (2003)
“Density of states for the π -flux state with bipartite real random hopping only: A weak disorder approach”
- [281] T. Nagai and K. Kawasaki, Physica A **134**, 483 (1986)
“Statistical dynamics of interacting kinks”.
- [282] T. Nattermann, in Ref.[10].
“Theory of the random field Ising model”
- [283] Th. Niemeijer and J.M. J. van Leeuwen, in “Phase transitions and critical phenomena”, Ed. Domb and Green (1976)
“Renormalization theories for Ising spin systems”.
- [284] Th. M. Nieuwenhuizen and J. M. Luck, J. Phys. A **19** (1986) 1207
“Exactly soluble random field Ising models in one dimension”
J. M. Luck and Th. M. Nieuwenhuizen, J. Phys. A **22** (1989) 2151
“Correlation function of random-field Ising chains: is it Lorentzian or not?”
J. M. Luck, M. Funke and Th. M. Nieuwenhuizen, J. Phys. A **24** (1991) 4155
” Low-temperature thermodynamics of random-field Ising chains: exact results”.
- [285] Th. M. Nieuwenhuizen, Phys. Rev. Lett. **63**, 1760 (1989)
“ Griffiths singularities in two-dimensional random-bond Ising models: Relation with Lifshitz band tails”.
- [286] Th. M. Nieuwenhuizen and H. Orland, Phys. Rev. B **40**, 5094 (1989)
“ Thermodynamics of Ising models with layered randomness : exact solutions on square and triangular lattices”.
- [287] M. Nifle and H.J. Hilhorst, Phys. Rev. Lett. **68** (1992) 2992
“New critical-point exponent and new scaling laws for short-range Ising spin glasses”;
M. Ney-Nifle and H.J. Hilhorst, Physica A **193** (1993) 48

- “Chaos exponents in spin-glasses” ;
M. Ney-Nifle and H.J. Hilhorst, *Physica A* 194 (1993) 462
“Renormalization theory and chaos exponents in random systems”.
- [288] M. den Nijs and K. Rommelse, *Phys. Rev. B* 40, 4709 (1989) “Preroughening transitions in crystal surfaces and valence-bond phases in quantum spin chains”.
- [289] Y. Nishiyama, *Physica A* 252, 35 (1998)
“Numerical analysis of the random bond antiferromagnetic $S = 1$ Heisenberg chain”;
Erratum *Physica A* 258, 499 (1998).
- [290] Y. Nishiyama, *E.P.J. B* 6, 335 (1998)
“Stability of the Haldane state against the antiferromagnetic bond randomness”.
- [291] A. J. Noest, *Phys. Rev. Lett.* **57**, 90 (1986)
“New universality for spatially disordered cellular automata and directed percolation”
- [292] Y. Nonomura, and Y. Ozeki, *J. Phys. Soc. Jp.* **64**, 2710 (1995)
“Ground-state phase-diagrams of the 2-dimensional quantum Heisenberg spin-glass models”
- [293] J. Oitmaa, and O.P. Sushkov, *Phys. Rev. Lett.* **87**, 167206 (2001)
“Two-dimensional randomly frustrated spin-1/2 Heisenberg model”
- [294] T. Olson and A.P. Young, *Phys. Rev.* **B60**, 3428 (1999)
“Monte Carlo study of the critical behavior of random bond Potts models”
- [295] E. Orignac and T. Giamarchi, *Phys. Rev. B* **57**, 5812 (1997)
“Weakly disordered spin ladders”
- [296] G. Palágyi, Ch. Chatelain, B. Berche, and F. Iglói, *Eur. Phys. J.* **B13**, 357 (2000)
“Boundary critical behaviour of two-dimensional random Potts models”
- [297] T. Papenbrock, T. Barnes, D.J. Dean, M.V. Stoitsov, and M.R. Strayer, *Phys. Rev. B* **68** 024416 (2003)
“Density matrix renormalization group study of critical behavior of the spin-1/2 alternating Heisenberg chain”
- [298] G. Parisi and N. Sourlas, *Phys. Rev. Lett.* 43, 744 (1979)
“Random Magnetic Fields, Supersymmetry, and Negative Dimensions”.
- [299] G. Parisi, M. Picco, and N. Sourlas, *Europhys. Lett.* **66**, 465 (2004)
“Scale Invariance and Self-averaging in disordered systems”

- [300] F. Pazmandi, R. Scalettar and G. Zimanyi, Phys. Rev. Lett. **79** (1997) 5130 “Revisiting the Theory of Finite Size Scaling in Disordered Systems: ν can be less than $2/d$ ”.
- [301] I. Peschel, Phys. Rev. B **30**, 6783 (1984)
“Surface magnetization in inhomogeneous two-dimensional Ising lattices”
- [302] M. Picco, Phys. Rev. Lett. **79**, 2998 (1997)
“Weak randomness for large q-state potts models in two dimensions”
- [303] C. Pich, A.P. Young, H. Rieger, and N. Kawashima, Phys. Rev. Lett. **81**, 5916 (1998)
“Critical behavior and Griffiths-McCoy singularities in the two-dimensional random quantum ising ferromagnet”
- [304] M. Queffélec, in *Substitutional Dynamical Systems-Spectral Analysis*, Lecture Notes in Mathematics, Vol. 1294, edited by A. Dold and B. Eckmann (Springer, Berlin, 1987).
- [305] S. L. A. de Queiroz and R. B. Stinchcombe, Phys. Rev. E **54**, 190 (1996)
“Correlation functions in the two-dimensional random-bond Ising model”
- [306] M. Randeria, J. P. Sethna and R. G. Palmer Phys. Rev. Lett. **54**, 1321 (1985)
“Low-Frequency Relaxation in Ising Spin-Glasses”.
- [307] T.G. Rappoport, B. Boechat, A. Saguia, M. A. Continentino, Europhysics Lett. **61**, 831 (2003)
“Griffiths phases in the strongly disordered Kondo necklace model”
- [308] G. Refael, S. Kehrein and D. S. Fisher Phys. Rev. B **66**, 060402 (2002)
“ Spin reduction transition in spin-3/2 random Heisenberg chains”.
- [309] G. Refael, and D. S. Fisher, Phys. Rev. B **70**, 064409 (2004)
“Energy correlations in random transverse field Ising spin chains”.
- [310] G. Refael, J. E. Moore, cond-mat/0406737
“Entanglement entropy of random quantum critical points in one dimension”.
- [311] H. Rieger and A.P. Young, Phys. Rev. Lett. **72**, 4141 (1994)
“Zero-temperature quantum phase-transition of a 2-dimensional Ising spin-glass”
- [312] H. Rieger, and F. Iglói, Europhys. Lett. **39**, 135 (1997)
“Quantum critical dynamics of the random transverse-field Ising spin chain”
- [313] H. Rieger, and F. Iglói, Europhys. Lett. **45**, 673 (1999)
“Average persistence of random walks“

- [314] H. Rieger and F. Iglói, Phys. Rev. Lett. **83**, 3741 (1999)
“Random quantum magnets with long-range correlated disorder:
Enhancement of critical and Griffiths-McCoy singularities”
- [315] A. D. Rutenberg and A. J. Bray, Phys. Rev. E **50**, 1900 (1994)
“Phase-ordering kinetics of one-dimensional nonconserved scalar systems”.
- [316] A. Saguia, B. Boechat and M.A. Continento, PRL **89**, 117202 (2002)
“Phase diagram of the random Heisenberg antiferromagnetic spin-1 chain”.
- [317] A. Saguia, B. Boechat, and M.A. Continentino, Phys. Rev B **68**, 020403 (2003)
“Spin-3/2 random quantum antiferromagnetic chains “
- [318] A.W. Sandvik, Phys. Rev. B **66**, 024418 (2002)
“Classical percolation transition in the diluted two-dimensional S=1/2 Heisenberg antiferromagnet”
- [319] A.W. Sandvik, Phys. Rev. Lett. **89**, 177201 (2002)
“Multicritical Point in a Diluted Bilayer Heisenberg Quantum Antiferromagnet”
- [320] A.W. Sandvik, (unpublished),
see [http : //online.itp.ucsb.edu/online/exotic04/sandvik/](http://online.itp.ucsb.edu/online/exotic04/sandvik/)
- [321] M. Sasaki and O. C. Martin, Phys. Rev. Lett. **91**, 97201 (2003)
“ Temperature chaos, rejuvenation and memory in Migdal-Kadanoff spin glasses”.
- [322] H. Schmidt, Phys. Rev. **105**, 425 (1957)
“Disordered One-Dimensional Crystals”.
- [323] G. Schröder, T. Knetter, M.J. Alava and H. Rieger, E.P.J. B **24**, 101 (2001)
“Ground states versus low-temperature equilibria in random field Ising chains”.
- [324] T.D. Schultz, D.C. Mattis, and E.H. Lieb, Rev. Mod. Phys. **36**, 856 (1964)
“Two-dimensional Ising model as a soluble problem of many fermions”
- [325] H. J. Schulz, Phys. Rev. B **34**, 6372 (1986)
“Phase diagrams and correlation exponents for quantum spin chains of arbitrary spin quantum number”
I. Affleck and F. D. M. Haldane, Phys. Rev. B **36**, 5291 (1987)
“Critical theory of quantum spin chains”
I. Affleck, D. Gepner, H. J. Schulz and T. Ziman, J. Phys. A **22**, 511 (1989)
“Critical behaviour of spin-s Heisenberg antiferromagnetic chains: analytic and numerical results”

- [326] U. Schulz, J. Villain, E. Brézin et H. Orland, J. Stat. Phys. 51, 1 (1988)
“Thermal fluctuations in some random field models”.
- [327] T. Senthil and S. N. Majumdar Phys. Rev. Lett. 76, 3001 (1996) “ Critical
Properties of Random Quantum Potts and Clock Models”.
- [328] Y.A.G. Sinai, Theor. Prob. Appl. 27 (1982) 256
“The limiting behavior of a one-dimensional random walk in a random
medium”.
- [329] R. Shankar and G. Murthy Phys. Rev. B 36, 536 (1987)
“Nearest-neighbor frustrated random-bond model in d=2: Some exact re-
sults”.
- [330] Z. Shi, Panoramas et synthèses, 12 (2001) 53, Soc. Math. de France
“Sinai’s walk via stochastic calculus”.
- [331] R. Sknepnek, Th. Vojta, and M. Vojta, Phys. Rev. Lett. **93**, 097201 (2004)
“Exotic vs. conventional scaling and universality in a disordered bilayer
quantum Heisenberg antiferromagnet”
- [332] F. Solomon, Ann. Prob. 3 (1975) 1
“Random walks in random environment”.
- [333] J. Sólyom and P. Pfeuty, Phys. Rev. B**24**, 218 (1981)
“Renormalization-group study of the Hamiltonian version of the Potts
model”
- [334] F. Spitzer (1970) Advances in Math. **5** 246. “Interaction of Markov pro-
cesses”
- [335] D. Stauffer and A. Aharony, Taylor and Francis, London and Philadelphia,
(1992)
“Introduction to percolation theory”.
- [336] S. Tanase-Nicola and J. Kurchan, cond-mat/0311273
“Metastable states, transitions, bassins and borders at finite temperatures”.
- [337] L.-H. Tang and H. Chaté Phys. Rev. Lett. 86, 830 (2001)
“Rare-Event Induced Binding Transition of Heteropolymers”.
- [338] M.J. Thill and D.A. Huse, Physica (Amsterdam) **15A**, 321 (1995)
“Equilibrium behavior of quantum Ising spin-glass”
- [339] M.J. Thill and H.J. Hilhorst, J. Phys. I 6 (1996) 67
“Theory of the critical state of low-dimensional spin-glass”.
- [340] M. Titov, P. W. Brouwer, A. Furusaki, and C. Mudry, Phys. Rev. B **63**,
235318 (2001)
“Fokker-Planck equations and density of states in disordered quantum
wires”

- [341] S. Todo, K. Kato, and H. Takayama, J. Phys. Soc. Jpn. Suppl. 69A, 355 (2000) “Quantum Monte Carlo Study of S=1 Random Antiferromagnetic Heisenberg Chain”.
- [342] G. Tripathy and M. Barma, Phys. Rev. Lett. **78**, 3039 (1997)
 “Steady state and dynamics of driven diffusive systems with quenched disorder”
 G. Tripathy and M. Barma, Phys. Rev. E **58**, 1911 (1998.)
 “Driven lattice gases with quenched disorder: Exact results and different macroscopic regimes”
- [343] L. Turban, F. Igloi and B. Berche, Phys. Rev. B **49**, 13239 (1994)
 “Surface magnetization and critical behavior of aperiodic Ising quantum chains”
- [344] L. Turban, D. Karevski and F. Igloi, J. Phys. A **32**, 3907 (1999)
 “Extended surface disorder in the quantum Ising chain”
- [345] O. P. Vajk and M. Greven, Phys. Rev. Lett. **89**, 177202 (2002)
 “Quantum Versus Geometric Disorder in a Two-Dimensional Heisenberg Antiferromagnet”
- [346] A. P. Vieira, cond-mat/0403635
 “Low-energy properties of aperiodic quantum spin chains”
- [347] J. Villain, B. Séméria, F. Lançon and L. Billard, J. Phys. C **16**, 6153 (1983)
 ‘A controversial problem : modified Ising model in a random field’.
- [348] J. Villain, J. Phys. A **21** L1099 (1988)
 ‘Failure of perturbation theory in random field models’.
- [349] J. Villain and B. Séméria, J. Phys. Lett. **44** L889 (1983)
 “The danger of iteration methods”.
- [350] V. Vinokur, C. Marchetti and L. Chen, Phys. Rev. Lett. **77** (1996) 1845,
 “Glassy Motion of Elastic Manifolds”.
- [351] I. Webman, D. Ben-Avraham, A. Cohen, S. Havlin, Phil. Mag. B **77**, 1401 (1998)
 “Dynamical phase transitions in a random environment”
- [352] A. Weinrib and B. I. Halperin, Phys. Rev. B **27**, 413 (1983)
 “Critical phenomena in systems with long-range-correlated quenched disorder”
 A. Weinrib, Phys. Rev. B **29**, 387 (1984)
 “Long-range correlated percolation”

- [353] E. Westerberg, A. Furusaki, M. Sigrist, and P.A. Lee, Phys. Rev. Lett. **75** 4302 (1995)
 “Random quantum spin chains - a real-space renormalization-group study”
 E. Westerberg, A. Furusaki, M. Sigrist, and P.A. Lee, Phys. Rev. B **55**, 12578 (1997)
 “Low-energy fixed points of random quantum spin chains”
- [354] K. J. Wiese, cond-mat/0302322
 “The Functional Renormalization Group Treatment of Disordered Systems: a Review”.
- [355] A.P. Wilkinson, A.K. Cheetham, W. Kunman, and A. Kvik, Eur. J. Solid State Inorg. Chem. **28**, 453 (1991)
 “The synthesis and structure of Sr₃CuPtO₆ [strontium copper platinum oxide] and its relationship to Sr₄PtO₆”
- [356] S. Wiseman and E. Domany, Phys. Rev. Lett. **81** (1998) 22
 “Finite-Size Scaling and Lack of Self-Averaging in Critical Disordered Systems”;
 S. Wiseman and E. Domany Phys Rev E **58** (1998) 2938
 “Self-averaging, distribution of pseudocritical temperatures, and finite size scaling in critical disordered systems”.
- [357] F.Y. Wu, Rev. Mod. Phys. **54**, 235 (1982)
 “The Potts model”
- [358] K. Yang and R. A. Hyman, Phys. Rev. Lett. **84**, 2044 (2000); comment on [169]
 Reply to comment : K. Hida, Phys. Rev. Lett. **84**, 2045 (2000).
- [359] K. Yang and R. N. Bhatt., Phys. Rev. Lett. **80**, 4562 (1998)
 “Generation of large moments in a spin-1 chain with random antiferromagnetic couplings”
- [360] M. Yor, Springer (2001)
 “Exponential functionals of Brownian motion and related processes”.
- [361] A. P. Young and R. B. Stinchcombe, J. Phys. C **9** (1976) 4419
 “Real-space renormalization group calculations for spin glasses and dilute magnets” ;
 B. W. Southern and A. P. Young J. Phys. C **10** (1977) 2179
 “Real space rescaling study of spin glass behaviour in three dimensions ”
- [362] A.P. Young and H. Rieger, Phys. Rev. B **53**, 8486 (1996)
 “Numerical study of the random transverse-field Ising spin chain”
- [363] A.P. Young, Phys. Rev. B **56**, 11691 (1997)
 “Finite-temperature and dynamical properties of the random transverse-field Ising spin chain”

- [364] E. Yusuf, and K. Yang, Phys. Rev. B **65**, 224428 (2002)
“Thermodynamics of strongly disordered spin ladders”
- [365] E. Yusuf, and K. Yang, Phys. Rev. B **67**, 144409 (2003)
“Large moment formation and thermodynamic properties of disordered spin ladders with site dilution”
- [366] E. Yusuf and K. Yang Phys. Rev. B 68, 024425 (2003) “Random antiferromagnetic spin-1 / 2 chains with competing interactions”.
- [367] E. Yusuf and K. Yang, cond-mat/0502530
“Dynamics of weakly coupled random antiferromagnetic quantum spin chains”
- [368] R.M. Ziff, E. Gulari, and Y. Barshad, Phys. Rev. Lett. **56**, 2553 (1986)
“Kinetic phase transitions in an irreversible surface-reaction model”